VACUUM REFINING OF COPPER

by

© Engin Ozberk

A Thesis Submitted to the Faculty of Graduate Studies and Research in Partial Fulfilment of the Requirements for the Degree of Master of Engineering in Metallurgical Engineering, McGill University, Montreal.

March 1980

ABSTRACT

An experimental investigation of the removal of impurities (bismuth, lead, arsenic and antimony) from baths of molten copper (blister, anode, and cathode type copper) under vacuum was carried out. A pilot scale 150 kilogram vacuum induction melting facility was used for these tests.

The effects of vacuum levels of 60-300 μHg, melt temperatures of 1150-1350°C, melt surface area to volume ratios of 6-10 m^{-1} and the effect of water cooled condensers placed within a two centimeter distance above the melt surface, were studied.

Kinetic data were obtained for evaluating the potential of a full scale vacuum melting facility. A mathematical model was also developed for the proper interpretation of the experimental results.

In the absence of oxygen and sulphur it was found that bismuth and lead could be eliminated by up to 80% and 90% respectively, while removal of arsenic and antimony was negligible.

The rate of removal of bismuth and lead increased as the chamber pressure was lowered and the melt temperature increased. The melt surface area to volume ratio and the distance of the condenser to melt surface did not have significant effects on the rate constants governing the rate of removal of impurities.

The rate of elimination of bismuth and lead over the range of 1150-1350°C and 300-60 μHg, followed first order kinetics. Removal rates were largely controlled by mass transport in the gas phase.

A comparative study has shown that the rates of elimination of impurities in the present pilot plant scale equipment were significantly lower than previously published laboratory scale tests.

RESUME

Une étude experimentale de l'élimination des impuretés (bismuth, plomb, arsenic et antimoine) des bains de cuivre fondu sous vide (cuivre "Blister", cathode et anode en cuivre) a été réalisée. Une installation pilote de fusion par induction sous vide, pouvant traiter une charge de 150 kilogrammes a été utilisée.

Les effets de la qualité du vide, variant de 60 à 300 µHg, de la température du bain, comprise entre 1150 et 1350°C, du rapport surface sur volume (de 6 à 10 m^{-1}) ainsi que l'effet de condenseurs refroidis à l'eau et placés à une distance de deux centimetres au-dessus du bain, ont été étudiés.

Des données sur la cinétique de réaction ont été obtenues dans le but d'évaluer les possibilités d'une installation sous vide industrielle. Un modèle mathématique a été développé afin d'interpréter les résultats expérimentaux.

En l'abscence d'oxygène et de soufre il a été trouvé que l'élimination du bismuth et du plomb peut atteindre respectivement 80 et 90% alors que celle de l'arsenic et de l'antimoine est négligeable.

La vitesse d'élimination du bismuth et du plomb augmente quand la pression diminue et la temperature du bain croit. Le rapport surface sur volume et la distance condenseurs-bain n'ont pas d'effet significatif.

La vitesse d'élimination du bismuth et du plomb suit une cinétique de premier ordre dans le domaine 1150-1350°C et

300-60 µHg. Elle est largement controlée par le transfert de masse dans la phase gaseuse.

Une étude comparative a montré que les vitesses d'élimination des impuretés dans l'installation pilote présente étaient notablement plus basses que celles publiées précédemment et prouvenant d'essais de laboratoire.

ACKNOWLEDGEMENTS

Every graduate student owes a great deal to others and I am no exception. I would like to acknowledge the intellectual, patient and helpful guidance and support I have received from Professor R.I.L. Guthrie throughout my three years at McGill University.

I would also like to recognize all the members of the Metallurgical Engineering Department with whom I have collaborated on the technical, academic, administrative and friendship level. The years at McGill University have been a very pleasant period in my life.

I must also thank Karen Rivett for typing this somewhat lengthy text with a patient, understanding and cheerful attitude.

TABLE OF CONTENTS

LIST OF TABLES

LIST OF FIGURES

NOMENCLATURE

A	melt surface area	cm^2
a	activity	
B	bulk	
C_i^B	bulk concentration of solute i	$g \cdot mole\ cm^{-3}$
C_i^*	surface concentration of solute i	$g \cdot mole\ cm^{-3}$
D_i	diffusivity of solute i	$cm^2 s^{-1}$
D_o	diffusion constant	
ΔE	activation energy for diffusion	$cal\ g \cdot mole^{-1}$
i	solute (or impurity)	
K	overall rate constant	$cm\ s^{-1}$
K_E	evaporation mass transfer coefficient	$cm\ s^{-1}$
K_{Ei_2}	evaporation mass transfer coefficient for diatomic gases	$cm\ s^{-1}$
K_G	gas phase mass transport coefficient	$cm\ s^{-1}$
K_{G°	gas phase mass transport coefficient characteristic of the system	$cm\ s^{-1}$
K_L	liquid phase mass transport coefficient	$cm\ s^{-1}$
K_U	term containing gas phase mass transport coefficient	
K_e	equilibrium coefficient	
K_B	Boltzman constant, 1.38062×10^{-23}	$joule\ K^{-1}$
L,l	liquid	
M,MO	metal, metal oxide	
M_{Cu}	molecular weight of copper	$g \cdot mole^{-1}$

M_i	molecular weight of solute i	$g \cdot mole^{-1}$
$\dot{N}'''_i$	rate of elimination of solute i	$g \cdot mole\ cm^{-3}s^{-1}$
$\dot{N}''_i$	overall flux of solute i	$g \cdot mole\ cm^{-2}s^{-1}$
$\dot{N}''_{i,ev}$	maximum evaporative flux of solute i	$g \cdot mole\ cm^{-2}s^{-1}$
$\dot{N}''_{i,gas}$	flux of solute i in gas phase	$g \cdot mole\ cm^{-2}s^{-1}$
$\dot{N}''_{i,liq}$	flux of solute it in liquid phase	$g \cdot mole\ cm^{-2}s^{-1}$
P	ambient pressure in chamber	pascal
P_i^b	vapour pressure of solute i at condenser surface	pascal
P_i^*	actual partial pressure of solute i at the interface or in the gas phase	pascal
P_i°	vapour pressure of pure solute i	pascal
P_i^+	equilibrium vapour pressure of solute i	pascal
R	gas constant, 8.31432×10^7	$gmole \cdot g \cdot cm^2s^{-2}K^{-1}$
r	radius of crucible	cm
r_A	radius of solute molecule	Å, 10^{-8}cm
s	solid	
T	melt temperature	K
t	time	s
U_i	mean surface velocity of solute i	$cm\ s^{-1}$
V	volume of melt	cm^3
wt%i	weight percent of solute i	
X	mole fraction	
X_i^*	mole fraction of solute i at interface	

α	relative volatility coefficient	
γ	activity coefficient	
ε	molecular diameter	cm
θ_i	life time of volume solute i moving along interface	s
λ	mean free path	cm
μ_B	liquid solvent viscosity	poise
ρ_{Cu}	density of copper	g cm^{-3}

CHAPTER I

INTRODUCTION

I-1. MINOR ELEMENTS IN COPPER

Copper ores invariably contain significant quantities of elements other than copper and some of these report with copper in the copper concentrate. A number of these impurities (e.g. arsenic, antimony, bismuth, lead, tin and zinc) are considered deleterious in that they tend to decrease the quality of the final product, copper-wire, following electrolytic refining[1]. Conversely, impurities such as gold, silver, selenium and telerium are classified as being valuable and are readily recovered in the electrolytic refining stage[2].

For such reasons, the behaviour of minor elements commonly present in copper concentrates represents an important technical, as well as economic consideration in any copper smelting operation.

I-1.A Production of Copper

Figure 1 summarizes the current major processes used in the pyrometallurgical production of copper from copper sulphide ores. These ores account for approximately 90% of the world's primary copper[3].

Sulphide ores are generally treated by beneficiation processes (comminution and flotation) so as to produce

copper concentrates (Figure 1). Matte, (a mixture of copper and iron sulphides containing 30-55% Cu) is smelted from concentrate either by conventional processes (blast or reverberatory or electric furnace) or by new processes (flash furnaces). Also, in recent years, the Noranda Continuous Copper Making Reactor has been employed to produce very high grade mattes containing 60-70% Cu. Both matte and high grade mattes are then converted into blister copper containing about 1% sulphur in Pierce-Smith converters.

Today, blister coppers (or rather a type of copper similar to conventional blister copper) can be produced directly from concentrates by the Mitsubishi and Noranda continuous processes. These molten blister coppers are then fire-refined and cast into anodes. This latter step is followed by electro-refining, enabling 99.99+% copper to be produced.

I-1.B Behaviour of Minor Elements in the Production of Copper

While high quality copper results from the controlled elimination of minor elements during the course of smelting and electro-refining operations (Figure 1), studies of conventional processes show that very little elimination of deleterious impurities occurs[4], during fire-refining in the anode furnace. In this latter operation any slag remaining from the converters is first skimmed off. The copper is then desulfurized, deoxidized and held for anode casting[5].

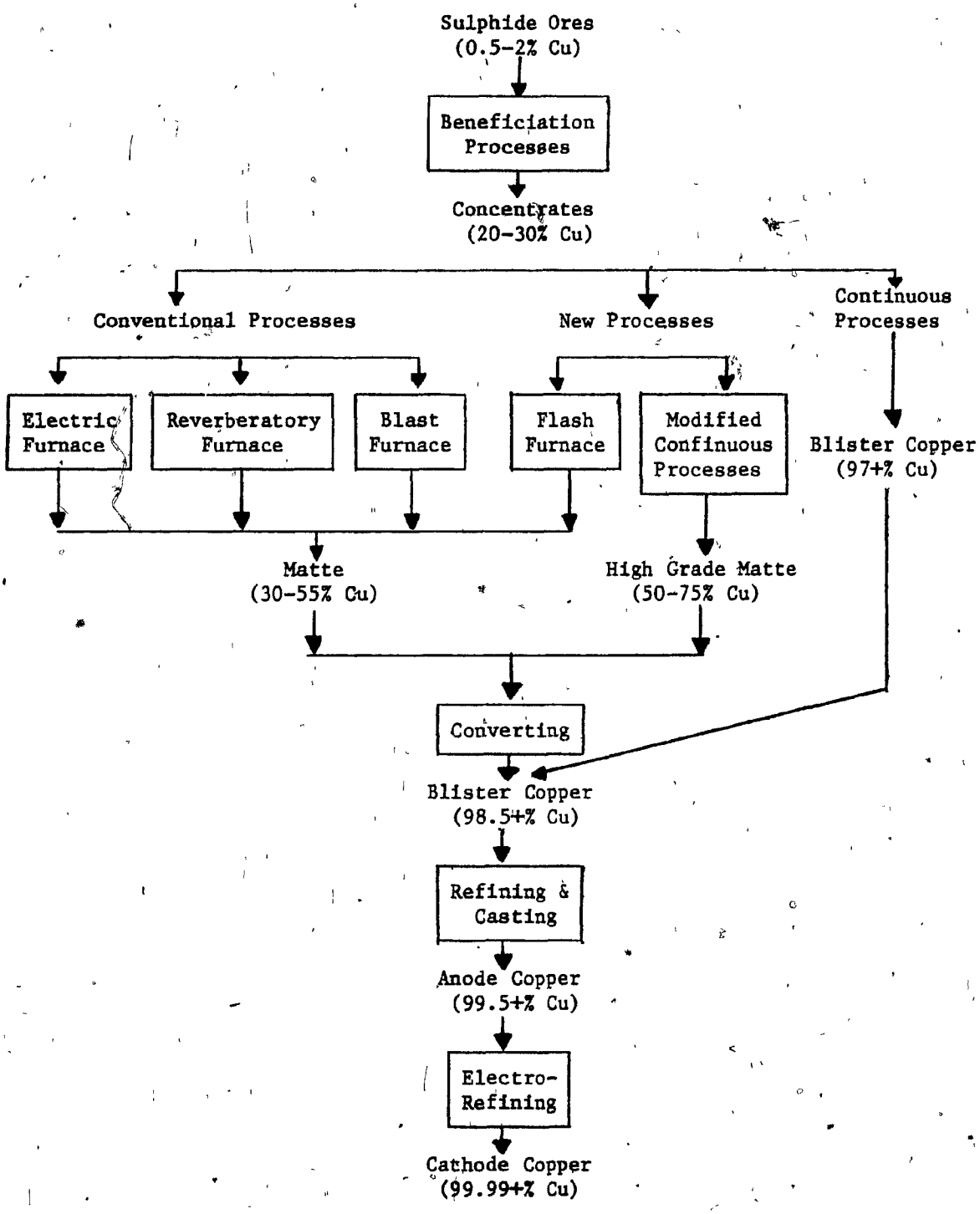

Figure 1. Combined process flow diagrams for the extraction of copper from sulphide ores.

However, any high impurity contents of other elements in the blister copper charged to the anode furnace, tend to remain and proceed on through to the electrolytic refining stage. This causes the following problems[3]:

1) Contamination of electrolyte, making electrolytic purification more difficult and costly.

2) Contamination of cathode copper, leading to inferior electrical and mechanical properties of the final product, copper-wire bar.

3) Contamination of anode slimes, leading to a more difficult and costly separation of valuable by-products.

It is clear that the removal of all deleterious impurities during matte smelting and converting stages and prior to the fire refining or electro-refining steps would be ideal. Similarly, the concentration of all valuable impurities in the blister copper and subsequently in the anode copper, would be ideal since they are easily recovered during the electrolytic refining stage.

Provided deleterious impurities in a matte are present below certain concentration levels, they can be eliminated adequately during the matte smelting and converting stages (Table 1). In these conventional processes, the elimination occurs by two mechanisms, slagging and volatilization, the overall elimination of each element being determined in an interplay of thermodynamic, kinetic and process factors. At the same time, conventional processes provide high recoveries

TABLE 1. Representative Analysis[1], weight %.

	Cu	Fe	S	O	As	Bi	Pb	Sb	Zn	Au	Ag
Matte	30–55	30–45	20–25	2–3	0–0.5	0–0.1	0–5	0–1	0–5	0– 15×10^{-4}	0–0.1
Blister Copper	98.5–99.5	0.1	0.02–0.1	0.5–0.8	0–0.3	0–0.01	0–0.1	0–0.3	0.005	0–100×10^{-4}	0–0.1
Anode Copper	99.4–99.8	0.002–0.03	0.001–0.003	0.1–0.3	0–0.3	0–0.01	0–0.1	0–0.3	--	0 – 0.005	trace–0.1
Cathode Copper	99.99+	0.0002–0.0006	0.0004–0.0007	n.i.[2]	trace–0.0001	trace–0.0003	trace–0.0005	trace–0.0002	--	0– 0.00001	0.0005–0.001

1. Conventional processes[3]
2. Not included in analysis

of valuable by-products such as gold, silver, selenium and telerium[6,7].

Over the years, the composition of ores has not remained uniform, copper contents tending to decrease and deleterious impurity elements tending to increase. As a direct reflection, levels of impurity contents in the blister copper have also generally risen[8].

Opposed to these trends, the demand for higher purity copper has increased substantially, in conjunction with technical advances achieved in the electronics industry.

Publications dealing with continuous processes (i.e. Noranda and Mitsubishi) introduced in the last decade, indicate that the processes tend to produce blister copper of higher impurity contents than that produced by conventional processes[9-15].

I-1.C Difficulties Related to Impurity Content of Copper and Possible Technical Solutions

One can summarize the present situation in copper production with respect to impurity contents as follows:

1) The demand for higher quality copper has increased.
2) The trend towards an increase in the impurity contents of copper ores will continue.
3) The recent continuous copper production processes result in blister copper of higher impurity levels than produced using the more conventional pyrometallurgical processes.

4) Current electro-refining processes are incapable of dealing with high levels of deleterious elements.

5) The existing fire refining process is totally inadequate for eliminating deleterious impurities.

A literature survey on research addressing itself to these difficulties of impurity removal from copper and possible solutions was carried out and is summarized below:

i) Chlorination of Copper: The removal of various impurities from liquid copper using chlorides (e.g. sodium, calcium, magnesium and ammonium chlorides) has been investigated in laboratory scale experiments[16]. It was concluded that the proposed process would not be feasible.

ii) Flux Additions and Oxidation of Copper: The idea of making flux additions and oxidizing the impure copper has been investigated extensively in both laboratory and industrial scale experiments[17-20]. The process involves the addition of various compositions and amounts of fluxes to blister copper contained in anode type furnaces with the simultaneous injection of air and/or oxygen enriched air into the melt.

The removal of an impurity by oxidation can be examined on the basis of the following equilibrium relation[7]:

$$Cu_2O_{(l)} + M_{(l)} = 2\,Cu_{(l)} + MO_{(l,s)} \qquad (1)$$

$$k_e = \frac{a^2_{Cu} \times a_{MO}}{a_{Cu_2O} \times a_M} \qquad (2)$$

M = impurity metal

MO = impurity metal oxide

k_e = equilibrium coefficient

a = activity

l,s = liquid and solid

To determine the upper limits of impurity removal through oxidation, one can consider the molten copper to be saturated with oxygen, in which case the equation for ke reduces to:

$$ke = \frac{A_{MO}}{A_M} = \frac{\gamma_{MO} \times X_{MO}}{\gamma_M \times X_M} \qquad (3)$$

γ = activity coefficient

X = mole fraction

where γ_M is that in an infinitely dilute solution.

For high impurity removal, it is clearly desirable to have small values of γ_{MO} and X_{MO}, and large values of γ_M and k_e. The addition of fluxes to form a slag, together with slag skimming promotes the removal of impurities as metal oxides, MO.

The experimental studies reported problems with high copper losses to the slag and low levels of bismuth elimination.

iii) Vacuum Refining of Copper: Vacuum refining is a comparatively new process for the copper pyrometallurgist even though it is well established in the production and refining of steel, zinc, mercury, etc. However, it has

potential with respect to the elimination of the more volatile impurities in liquid copper and is the subject of this thesis. In the following section, the technology of vacuum metallurgy will be discussed briefly and then its potential application to copper refining will be considered.

I-2. VACUUM METALLURGY PROCESSES

Vacuum is rapidly becoming an essential feature in a wide variety of metallurgical operations. An overall review of the vacuum metallurgy processes and where they are being applied is given below[21-24]:

i) Extractive Metallurgy
   - a - The beneficiation of ores; filtration, briquetting, etc.
   - b - The reduction of compounds; Mg and Ca production.

ii) Vacuum Melting Processes (for refining of crude metal, alloy preparations, remelting, etc.)
   - a - Induction melting
   - b - Arc melting
   - c - Electron beam techniques
   - d - Cold crucible and levitation melting techniques
   - e - Zone refining

iii) Vacuum Degassing of Liquid Steel
   - a - Stream degassing
   - b - Ladle degassing

c - Dortmund Horder (DH) degassing

d - Rheinstahl (RH) degassing

iv) Casting of Various Shaped Products

v) Heat Treatment

vi) Testing of Metals and Alloys

vii) Joining

viii) Surface Treatment

ix) Powder Metallurgy

x) Mechanical Working of Metals in Vacuum

Among these processes, vacuum induction melting is one possibility being considered for the refining of molten copper.

I-2.A Vacuum Induction Melting and Refining

Vacuum induction melting can provide close control of melt composition and temperature while simultaneously preventing undesired contamination by reactive gases such as oxygen[25]. Similarly through the use of low pressures (below 300 μHg ≈ 40 pascals) and inductive stirring, the rate of refining reactions can be improved and purification processes which would not take place at atmospheric pressures can be carried out.

Vacuum refining in induction melting units is achieved through evaporation of volatile impurities into the gas phase above the melt.

Two important features necessary for the success of a vacuum refining process are that 1) the rate of evaporation from the melt surface must exceed its rate of condensation back onto the metal surface and that 2) the rate of evaporation of impurities should be faster than that of the base metal. Of these, the first feature depends on the vacuum created above the melt surface while the second is fundamentally controlled by the equilibrium pressure of the impurity relative to that of the base metal.

In 1963, Kameda and Yazawa[26] in some laboratory scale experiments confirmed that the refining of copper by vacuum induction melting is possible. They also discussed the evaporation of impurities from a thermodynamic standpoint.

Since that time, numerous studies, all of laboratory scale, have been carried out in Europe and Japan.

I-3. PURPOSE OF PRESENT STUDY

The present study was undertaken to investigate the general feasibility of impurity elimination from blister or anode type of copper and to determine the main factors controlling the kinetics of vacuum induction melting at the pilot scale level.

Since all data reported in the literature has been obtained using laboratory scale equipment, the present study aimed at determining the effects of scaling-up to pilot-plant level.

CHAPTER II

REVIEW OF THEORY AND PREVIOUS EXPERIMENTAL WORK

II-1. INTRODUCTION TO VACUUM TECHNOLOGY

Although the latin word vacuum means "empty", it is useful to note that at the lowest pressures which can be obtained by modern pumping methods there are still hundreds of molecules in each cubic centimeter of evacuated space[27].

According to the definition of the American Vacuum Society (1958) the term "vacuum" refers to a given space filled with a gas at pressures below atmospheric, i.e. having a density of molecules less than about 2.5×10^{19} mole/cc.

The general term "vacuum" includes about 19 orders of magnitude of pressure (or densities) below that corresponding to the standard atmosphere. The lower limit of the range is continuously decreasing, as vacuum technology improves its pumping and measuring techniques.

Measuring a system's absolute pressure is the traditional way to classify the degree of vacuum: Thus, one can speak of low, medium, high and ultra-high vacuum corresponding to regions of lower and lower pressures as the levels indicated in Figure 2.

The list of applications of Vacuum Technology includes a large number of items which have become symbols of

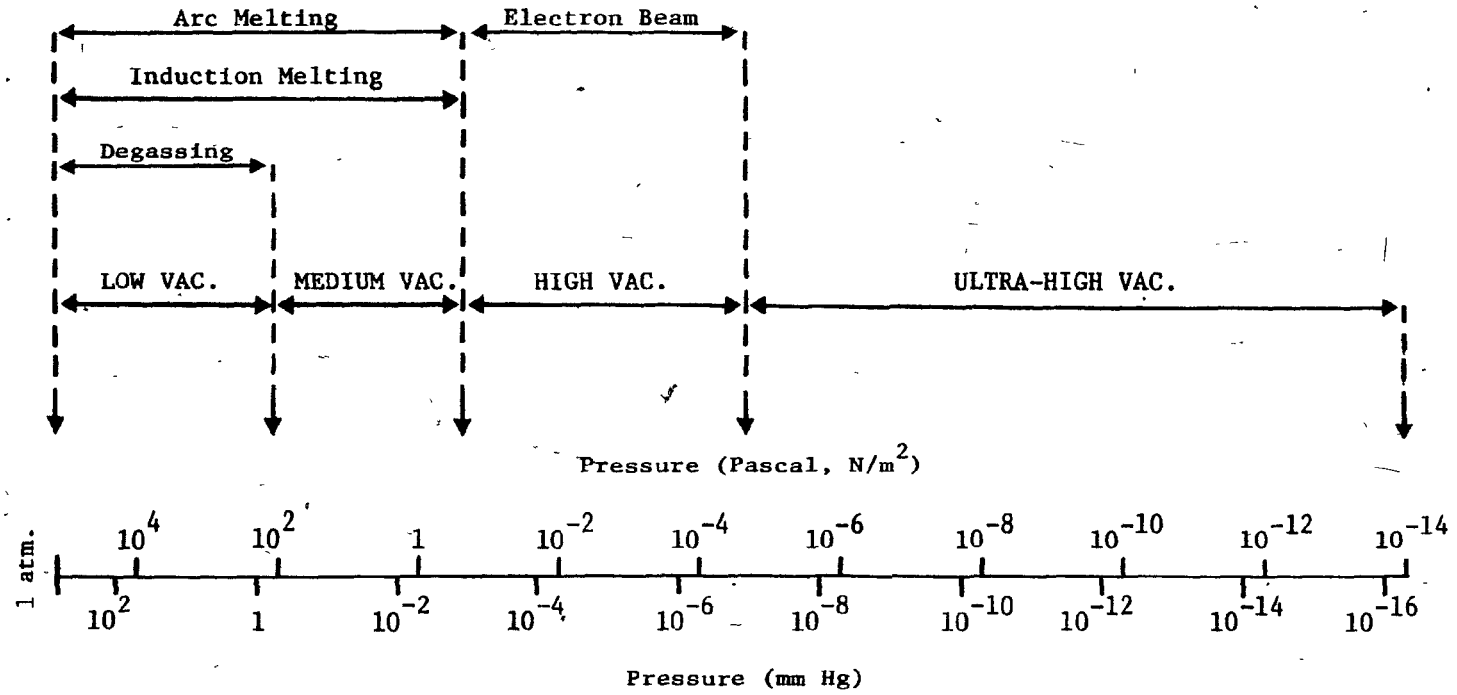

Figure 2. Degree of vacuum and pressure ranges of vacuum metallurgy processes.

technological progress. Its area of application ranges from vacuum holding, vacuum lifting, vacuum cleaning and electric lights to drying, distillation and insulation.

In this large field of vacuum technology Vacuum Metallurgy has gained an important place particularly during the last century with the introduction of several different types of processes.

II-2. HISTORY OF VACUUM METALLURGY

The effect of reduced pressures on metallurgical reactions was recognized towards the end of the 19th century as being important. In 1866 T. Graham carried out experiments under reduced pressure to show that hydrogen can diffuse through the walls of a platinum tube[28]. A United States patent was granted around 1867 for a vacuum furnace complete with vacuum locks, and other patents were granted in the 1890's for furnaces[25], as well as for a degassification technique (Aitken, 1882)[28]. There is no record of a practical furnace until that developed by Arsen in 1907, which became the first usable tool for studying metallurgical reactions in the molten state under vacuum. By 1921, it was found that resistance heated furnaces were not satisfactory for large scale vacuum melting. Accordingly, Heraeus G.m.b.H. built a 300 kilogram low frequency furnace in 1921 under the directions of Rohn. The size and the number of furnaces were increased during the 1920's after induction

melting was incorporated, and beginning in 1939, 5 ton heats were being produced. Since pressures less than 267 pascals (2 mm Hg) could not be maintained at that time, processes could not be carried out at full efficiency.

Meanwhile, vacuum arc melting found application in the Siemens works between 1903 and 1912 for the production of high quality tantalum for the electric lamp industry. Then Moore, in 1923, and W.J. Krall in 1940 further improved the vacuum arc melting applications[28].

The real breakthrough for vacuum melting came towards the end of the 1950's with new improved industrial pumping systems. The size of the furnaces were concurrently enlarged. For steel degassing and special alloy preparation purposes, furnaces well above 50 ton capacity started being built. For instance, in 1975 in Japan, twenty-nine units with a maximum capacity of 340 tons were in operation yielding about 6×10^6 tons/year of vacuum refined steel. This figure amounts to 10% of specialty steel products and 5% of common steel[29].

Vacuum melting processes also started being applied to zinc, cadmium, tin and titanium productions[30-32].

II-3. THEORY OF MASS TRANSPORT IN VACUUM

The investigation of evaporation phenomena began in 1873 by Stefan almost at the same time as vacuum technology began to be studied[33]. His first experiments were carried out with the evaporation of mercury into a vacuum. Over the

years the potentially advantageous applications that vacuum metallurgical processes offered in the production of high quality metals, resulted in a large number of basic studies being carried out on the kinetics of evaporation of metals under vacuum. These investigations included the evaporation of tungsten under vacuum[33], the vacuum refining of steel[33] and the separation of zinc and lead by distillation[34-36] etc.

However, the majority of recent theoretical information available on the kinetics of vacuum refining is based on experiments carried out with steel melts.

As mentioned earlier the application of vacuum metallurgy to copper is relatively new: the earliest literature available dates back only to the late 1940's[37]. Kinetic studies began during the last twenty years.

II-3.A Thermodynamics in Relation to Vacuum Metallurgy

As will be shown in Chapter III, any understanding of the kinetics of evaporation of impurities from a liquid metal bath held under vacuum first requires information on the thermodynamics of the system involved. Therefore in order to analyze the kinetics of evaporation under vacuum consideration of the vapour pressure of the constituents above the melt is a prerequisite. Unfortunately, very little data are available with respect to the vapour pressure of elements above their dilute solutions in liquid metals. However, vapour pressures of pure elements are more or less precisely known and a plot of these versus temperature may be used as

a rough guide for determining which elements will exhibit preferential evaporation. In Figure 3, the change in vapour pressure of the pure elements relevant to this study is plotted against temperature[38]. In Appendix I, the equations for the vapour pressure of elements appropriate to this study are included.

Figure 3 shows these elements with higher vapour pressure than copper that can be evaporated.

If the vapour pressure of the pure element is known, the equilibrium partial pressure of that element in a metallic solution can be computed, provided its activity coefficient is known, using Henry's relation:

$$P_i^+ = P_i^\circ \gamma_i X_i \qquad (4)$$

where

P_i^+ = equilibrium vapour pressure of solute i, pascal

P_i° = vapour pressure of pure solute at the known temperature, pascal

γ_i = Raoultian activity coefficient of the solute i, in an infinitely dilute solution

X_i = mole fraction of solute i

However, since solute vapour pressures are potentially dependent on the presence and amounts of other dissolved components, vapour pressures based on binary solution data does not in itself, guarantee the ease of a component's separation from multi-component solutions[39].

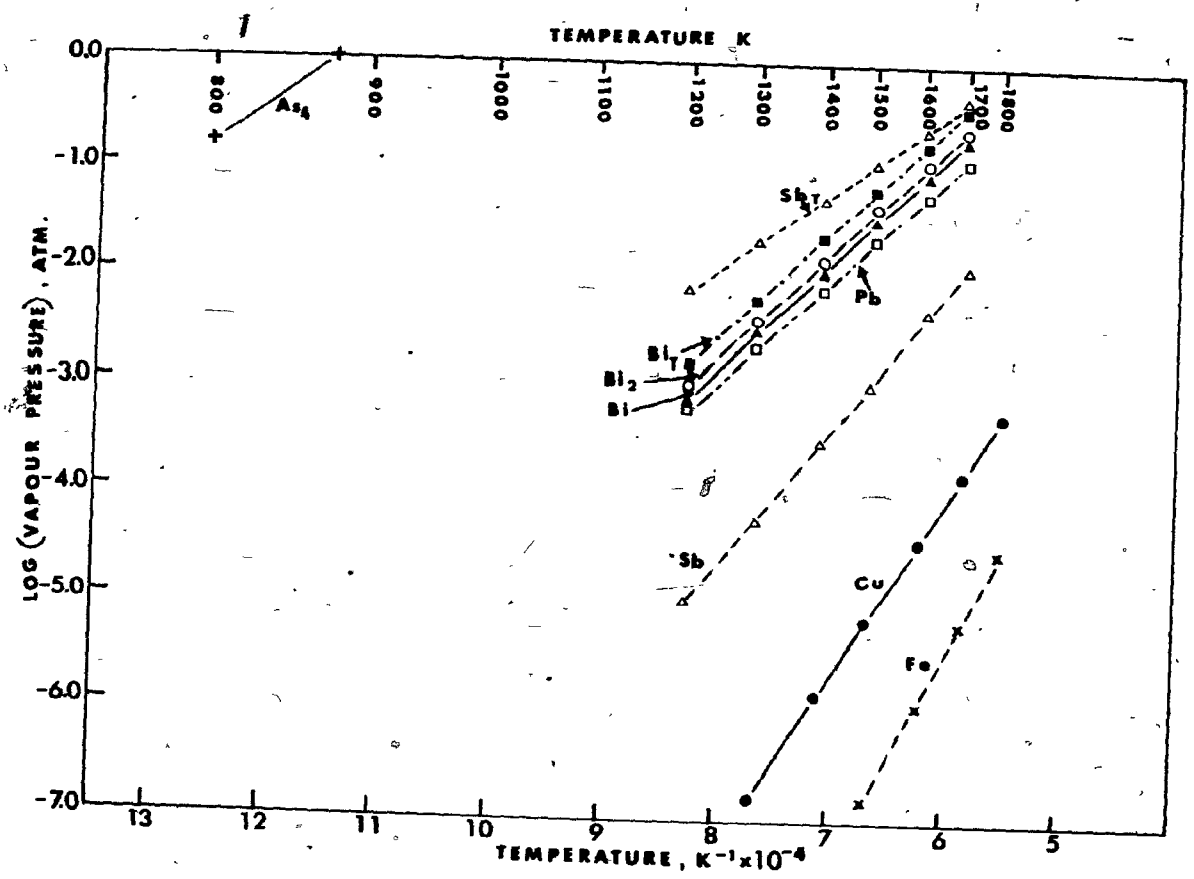

Figure 3. Vapour pressure of some pure elements plotted as a function of temperature.

II-3.B Relative Volatility Coefficient (Evaporation Coefficient)

The term relative volatility is used to compare the vapour pressure of one pure substance with another. Under conditions of molecular evaporation, as defined by Langmuir, the influence of the molecular weights of the components on the molar rate of evaporation must be considered[39-41]. Thus, for evaporation from copper baths, the relative volatility coefficient, α, as defined by Olette[39] is:

$$\alpha = \frac{\gamma_i}{\gamma_{Cu}} \left(\frac{P^\circ_i}{P^\circ_{Cu}}\right)\sqrt{\frac{M_{Cu}}{M_i}} \qquad (5)$$

where

M_{Cu} = molecular weight of copper, $g \cdot mole^{-1}$

M_i = molecular weight of solute, $g \cdot mole^{-1}$

In a dilute solution, copper (the solvent) will follow Raoult's law and hence, γ_{Cu} is unity. Also, the impurity i (the solute) at sufficiently low concentrations will follow Henry's law. Discounting solute-solute interactions, the activity coefficient γ_i, can be taken equal to γ°_i. Under such conditions, α then becomes:

$$\alpha = \gamma^\circ_i \left(\frac{P^\circ_i}{P^\circ_{Cu}}\right)\sqrt{\frac{M_{Cu}}{M_i}} \qquad (6)$$

By using the data given in Appendix I values of α were calculated for bismuth, lead, arsenic and antimony at three different temperatures and these are given in Table 2.

TABLE 2. Relative Volatility Coefficient Values[1].

Element	α Values		
	Temperature, K		
	1423	1523	1623
Bi	15057	5715	2477
Bi_2	9901	3454	1380
Pb	25387	8873	3579
As_T	-		35[2].
Sb	-		3[2].
Sb_2	-		47[2].

1. Calculated from the data given in Appendix I.

2. At 1573 K

If α is unity, no preferential separation is possible, since the concentration of the two components in the vapour will be the same as in the condensed phase. Substances that can be readily separated must show either large or small values of α (i.e. α should not approach unity).

II-3.C Overall Mass Transport Rate

Ward[42,43] has studied the vaporization of impurities, e.g. manganese, copper and chromium, from iron. Ten kilogram melts were heated and stirred inductively, and the molten metal surface exposed to an inert gas phase. The pressure ranged from 0.13 to 13.3 $\times 10^4$ pascal (1-10^6 μm). He showed that the relation between the loss of evaporating solute molecules i and the time of vacuum melting followed first order kinetics. As such the overall mass transport rate was given by:

$$\dot{N}_i''' = K \frac{A}{V} C_i^B \qquad (7)$$

or

$$\frac{-d(wt\%i)}{dt} = K \frac{A}{V} (wt\%i) \qquad (8)$$

which in integral form:

$$\int_0^t \frac{d(wt\%i)}{(wt\%i)} = -K \frac{A}{V} \int_0^t dt \qquad (9)$$

yields

$$2.303 \log_{10} \frac{(wt\%i)_t}{(wt\%i)_0} = -K \frac{A}{V} (t-t_0) \qquad (10)$$

where

N_i''' = rate of elimination of the impurity element (solute) i, g·mole $cm^{-3}s^{-1}$

C_i^B = bulk concentration of solute i, g·mole cm^{-3}

K = overall rate constant, cm s^{-1}

A = melt surface area, cm^2

V = volume of melt, cm^3

wt%i = weight percent of solute i

t = time, s

Equation 10 enables the overall rate constant K, to be calculated from the slope of the curve resulting from a plot of $\log_{10}$ wt%i versus time.

The mechanism of solute removal through evaporation occurs in a series of steps starting in the liquid metal and ending at the condenser.

Ward[42] considered six steps for the transfer of impurity atoms from the bulk liquid metal to a condenser surface. These were:

(i) Solute transport in the bulk liquid metal to the neighbourhood of the melt/vacuum boundary,

(ii) Transport through the melt boundary to the melt/vacuum interface,

(iii) Evaporation,

(iv) Transport of the solute vapour through the gas phase away from the clean melt/vacuum interface,

(v) Transport of the solute vapour through the bulk gas phase towards the condenser,

(vi) Condensation.

These steps would be more complicated and difficult to analyse when one considers (a) the possible existence of the surface active elements at the interface, (b) reaction of the vapour phase solute metal atoms with other gas molecules which may be present in the vacuum, e.g. oxygen.

A decade later, Ohno[44] considered the three limiting transport steps as:

(i) Transport of molecules through the bulk liquid metal to the metal/vacuum interface,

(ii) Evaporation,

(iii) Transport of molecules through the gas phase to the condenser surface.

Figure 4 shows these steps in schematic form. Of these, the mechanism of liquid phase mass transport rate and evaporation can be reasonably well quantified on the basis of work by previous researchers. However, mass transport mechanisms through the vacuum space between the melt surfaces and the chamber and pumping systems are, as yet, less clearly defined and understood.

The various mass transport steps are discussed in the following sections and the effect of each step on the overall mass transport coefficient is considered.

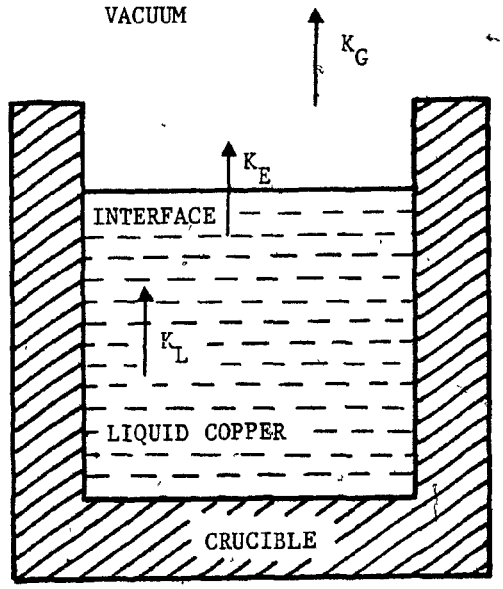

Figure 4. Stages of mass transport in vacuum induction melting.

II-3.D Mass Transport in Liquid Metal

The basis of solute mass transport through a liquid melt typically involves the two processes of diffusion and convection.

Transport process theory can take both mechanisms into account[45]. Danckwert's surface renewal theory, Kraus's natural convection model or Machlin's rigid flow model[46] can be used to describe transport phenomena in inductively stirred melts reasonably well[47]. The applicability of the latter model was shown in a recent study by Irons et al.[48].

The Machlin model supposes that flow across the surface of an inductively stirred melt may be considered to be free streamline slug flow with no shearing velocity gradients present within the transferring surface layer. As such, the volatile solute is supplied to the surface solely by diffusion from within this surface layer. The flux of atoms to the surface is then given by a modified form of the standard Penetration Theory first developed by R. Higbie[49].

$$\dot{N}''_{i,liq} = K_L \, (C_i^B - C_i^*) \tag{11}$$

where K_L is given as,

$$K_L = \sqrt{\frac{4D_i}{\pi\theta_i}} \tag{12}$$

taking

$$\theta_i = \frac{r}{2U_i} \tag{13}$$

then

$$K_L = \sqrt{\frac{8D_i U_i}{\pi r}} \tag{14}$$

$\dot{N}''_{i,liq}$ = flux of solute i in liquid phase, g·mole $cm^{-2}s^{-1}$

K_L = liquid phase mass transport coefficient, cm s^{-1}

C_i^B = bulk concentration of solute i, g·mole cm^{-3}

C_i^* = surface concentration of solute i, g·mole cm^{-3}

D_i = diffusivity of solute i, cm^2 s^{-1}

θ_i = life time of volume solute i moving along interface, s

r = radius of crucible, cm

U_i = mean surface velocity of solute i, cm s^{-1}

II-3.E Mass Transport at Melt Surface-Evaporation

In many metallurgical vacuum refining operations, particularly those carried out under conditions of high vacuum, the rate of elimination may be limited by the rate of evaporation of impurity atoms from the surface of the melt. As a result, equilibrium is not necessarily maintained between liquid and gas phase solute concentrations at the liquid/vapour interface. Under such conditions of hard vacuum Langmuir[50,51] has derived on the basis of the kinetic theory of gases, an expression for the maximum rate of evaporation of a solute from a surface.

$$\dot{N}''_{i,ev} = \frac{\alpha P_i^+}{\sqrt{2\pi RTM_i}} \qquad (15)$$

where, for the dilute case

$$P_i^+ = P_i^\circ \gamma_i X_i^* \tag{16}$$

and

$$X_i^* = \frac{M_{Cu}}{\rho_{Cu}} C_i^* \tag{17}$$

Equation 15 then takes the form of

$$\dot{N}''_{i,ev} = \frac{\alpha P_i^\circ \gamma_i M_{Cu}}{\rho_{Cu}\sqrt{2\pi RT M_i}} C_i^* \tag{18}$$

or

$$\dot{N}''_{i,ev} = K_E C_i^* \tag{19}$$

where

$$K_E = \frac{\alpha P_i^\circ \gamma_i M_{Cu}}{\rho_{Cu}\sqrt{2\pi RT M_i}} \tag{20}$$

$\dot{N}''_{i,ev}$ = maximum evaporative flux of solute i, g·mole cm^{-2} s^{-1}

α = evaporative coefficient ($\alpha \simeq 1$)

P_i^+ = equilibrium vapour pressure of solute i at the interface, pascal

P_i° = vapour pressure of pure solute i, pascal

γ_i = Raoultian activity coefficient of solute i

X_i^* = mole fraction of solute i at interface

M_{Cu} = molecular weight of copper, $g \cdot mole^{-1}$

ρ_{Cu} = density of copper, g cm^{-3}

C_i^* = surface concentration of solute i, g·mole cm^{-3}

R = gas constant, 8.31432 x 10^7 g $cm^2 s^{-2} K^{-1}$ g·mole

T = melt temperature, K

M_i = molecular weight of solute i, g·mole cm^{-3}

K_E = evaporation mass transfer coefficient, cm s^{-1}

Equation 15 is only valid when a perfect vacuum is attained, and all molecules evaporating are subsequently removed or condensed. In the latter case, the distance between the evaporating and condensing surfaces must be less than the mean free path of the evaporating molecule or partial recondensation on the surface of the liquid metal bath will occur (mean free path estimates for the impurity elements considered in this study are given in Appendix II). When the partial pressure of the impurity element i is not zero in the vacuum assembly, its rate of evaporation is reduced according to the Langmuir-Knudsen equation[40,52].

$$\dot{N}''_{i,ev} = \frac{\alpha\ (P_i^+ - P_i^*)}{\sqrt{2\pi RT\ M_i}} \qquad (21)$$

P_i^* = actual partial pressure of solute i (at the interface or in the gas phase), pascal

II-3.F Mass Transport in Gas Phase

In vacuum refining processes, the rate of elimination of impurity elements may also be affected by the rate of transport

of solute vapour away from the melt surface. This rate of transport is not as easy to predict as the other two mass transport rates mentioned above. Factors which must be considered are: (a) pressure gradient of vapour, (b) effective pressure of permanent gas in the vacuum system, (c) hydrodynamic factors and physical parameters of the system[40].

One can describe the rate of solute mass transport through the gas away from the melt surface with the following equation[52,53].

$$\dot{N}''_{i,gas} = \frac{K_G}{RT} (P_i^* - P_i^b) \qquad (22)$$

where,

$\dot{N}''_{i,gas}$ = flux of solute i in gas phase, g·mole cm^{-2} s^{-1}

K_G = gas phase mass transport coefficient, cm s^{-1}

P_i^b = vapour pressure of solute i at condenser surface ($P_i^b = 0$), pascal

Based on the set of equations given above, both Richardson[52] and Ohno[54,55] developed mathematical models to describe the kinetics of impurity elimination by vacuum induction melting. An equivalent model has been used in the present work. A critical analysis of the parameters chosen is included in Chapter III.

Salomon-de-Friedberg[56] also developed a model for the case of elimination of copper from steel melts. Mass transport rates in the liquid phase and evaporation rates at the interface were described on the basis of Machlin's and Langmuir's equations.

Mass transport rates in the gas phase were postulated to be directly dependent on the pumping rate of gas from the vacuum chamber. An implicit assumption that vapourized molecules were evacuated from the equipment in gaseous form was made.

II-4. PREVIOUS EXPERIMENTAL WORK

Numerous laboratory investigations into copper refining by vacuum treatment have been carried out since the 1940's. These studies were performed both with the aim of eliminating deleterious impurities down to marketable grades of copper and of decreasing ingot porosity so as to improve the mechanical and electrical properties. The effect of variables such as oxygen and/or sulphur levels in the melt, melt temperature, vacuum level, melt surface area to melt volume ratio, etc. were studied.

The information currently available on vacuum refining has been collected and reported in the following sections. Based on the type of copper treated, the information has been separated into three groups dealing with blister copper, anode and/or cathode copper and copper matte respectively.

In addition, a patent survey was carried out and this also is reported in the last section of the chapter.

II-4.A Treatment of Blister Copper (or Crude Copper)

Kameda and Yazawa[26] carried out some experiments on the refining of copper by vacuum induction melting on 30 gram melts* and discussed on the basis of thermodynamic arguments the evaporation of more than ten impurities. The average eliminations of bismuth, lead, arsenic and antimony were 80-95%, >90%, 30-70% and 30-50%, respectively, for the various initial solute concentrations. The results indicated that bismuth and lead eliminations depended very much on increasing temperature and decreasing pressure, while arsenic eliminations could be increased significantly by increased dissolved oxygen level in copper.

Table 3 summarizes the impurity elimination levels reported by previous workers.

Using the studies of Yazawa[26] as a basis, R. Ohno[54,55,57] was the first to investigate the kinetic factors involved in the evaporation of impurities from copper. Copper-silver, copper-lead, copper-bismuth, copper-silver-oxygen, copper-bismuth-oxygen and copper-bismuth-sulphur alloys were melted in the range of 0.1-1.0 pascal (0.75 - 7.5 μHg) pressure at either 1200°C or 1300°C, while being stirred either inductively or mechanically by a rotating molybdenum disk operating at various levels of intensity.

Both bismuth and lead eliminations were more than 95% (Table 3). The evaporation of silver and bismuth from copper at

---

*The chamber pressures in these experiments were not specified, but from the data given a pressure of 100 μHg (13.3 pa) would seem to have been typical.

TABLE 3. Summary of the Results Available in Literature

Source	Copper Weight kg	Pres. μ Hg	Temp. °C	Time Min	A/V m^{-1}	Elimination, wt%				$K(10^{-3}$ cm/s)		Ref. #
						Bi	Pb	As	Sb	Bi	Pb	
Kameda	0.03	100	1100	60	-	50-80	+90	10-30	50-55	-	-	26
Kameda	0.03	100	1200	60	-	+90	+95	40-70	30-40	-	-	26
Ohno	0.15	1-8	1200-1300	5-20	60	+95	+95	-	-	8-30	10-30	54
Bryan	0.02	80	1170	60	-	99	-	-	-	-	-	58
Bryan[1]	4.00	20-200	1200-1300	50-60	-	80-95[2]	-	-	-	-	-	58
Komorova	0.03	10	1200	120	-	50-80	50-90	50-80	50-75	-	-	59
Golovko	-	100-500	1200	5-15	-	93	100	20	20	-	-	62
Kim	-	-	-	-	-	-	75	30-50	40	-	-	60
Kametani	0.6-6.0	1000-2000	1200	Vacuum Lift Refining		10	60-80	10-20	20	-	-	29
Taubenblat	25	<0.1	1150-1300	30	-	≤50	≤50	-	-	Cathode Copper		89

1. Overall rate constants were reported in different unit.

2. Estimated from the graphs.

both temperatures of 1200°C and 1300°C in evacuated systems were found to follow first order kinetics. However, lead proved to be anomalous in this respect. The presence of oxygen in the melt (0.05-0.13%) decreased the rates of evaporation of silver and bismuth. Sulphur (0.11-0.12%) also decreased rates of evaporation of bismuth, although to a lesser extent than oxygen. While the rate of evaporation of these impurities seemed to be dependent on the induction stirring rate of the melt, they seemed to be totally insensitive to the rotational speed of the stirrer. It was also concluded that for the experimental conditions studied liquid phase transport was not rate determining but that the gas phase mass transport determined the overall mass transport rate.

Bryan et al.[58] studied the removal of only bismuth from 0.02 and 4.0 kilogram copper melts in a vacuum furnace over a range of 5-1000 μHg pressures. They concluded that the rate determining step changed from gas phase transport at pressures in excess of 200 μHg, and approached surface evaporation control at pressures of 10 μHg. It is not possible to compare their results with Ohno's results since they used the unit of "rate constant/$cm^{-2}sec^{-1}$" for mass transport without giving melt surface area or melt volume. Similarly percentage eliminations for 4 kilogram melts were not reported. They found with 0.02 kilogram melts at 1170°C and 80 μHg pressure that 99% bismuth elimination could be obtained within 60 minutes. They also found that oxygen and sulphur had a negligible effect on the transport rate in conflict with Ohno's results.

L. Komorova[59], using 20-30 gram samples, studied the behaviour of arsenic, antimony, bismuth, lead, zinc and tin during the vacuum (10^{-2} mm Hg) refining of the blister copper at 1200°C. It was concluded that the elimination of metallic vapours would increase in the sequence Sn-As-Sb-Pb-Bi-Zn. It was also suggested that arsenic and antimony would be evaporated more easily in the form of oxides as these oxides are easily formed at 1200°C. Although tin will also form oxides at these temperatures, the degree of tin elimination was found to be low. The amounts of elimination obtained are summarized in Table 3.

Between 1960 and 1965, Russian investigators, on the basis of results obtained in laboratory scale experiments[60-62], reported that the vacuum treatment of copper held significant promise. The behaviour of arsenic, antimony, bismuth, lead and zinc were studied and the improvement in the properties of copper as a result of higher purity was discussed. The results of these studies are included in Table 3.

H. Kametani and C. Yamauchi used a somewhat different experimental approach which they referred to as the 'vacuum lift' method of refining blister copper[63-65]. Experiments on the 'vacuum lift' refining of molten blister copper were carried out under reduced pressures of 1-2 mm Hg at 1200°C using copper samples of 0.6 and 6 kilograms. The fundamentals of the vacuum lift refining process were studied, experiments being carried out using a batchwise vacuum lift apparatus. The vacuum vessel was equipped with an oxygen concentration cell (of the lime stabilized zirconia type), and a small crystal microphone for measuring

oxygen potentials and detecting the evolution of SO_2 gas bubbles in the lifted melt. Following vacuum lifts of 4, 14 and 25 times, the average eliminations were:

oxygen (80%), sulphur (50-80%), arsenic (<20%), antimony (20%), bismuth (10%), lead (60-80%) and zinc (30-50%).

The merit claimed for the vacuum lifting technique is that by maintaining turbulent conditions in the melt, a large surface area is constantly exposed to vacuum. Consequently outgassing to low concentrations can be achieved rapidly because gaseous products are continually pumped away and steady-state equilibrium conditions are never attained. The vacuum lift principle is also utilized in the stream degassing of steel and in the R-H (Ruhrstahl-Heraus) and D-H (Dortmunt-Hoerder) steel processes. However, in the studies of Kametani and Yamauchi[63-65] not much success could be achieved in the removal of impurities other than sulphur and oxygen as the above mentioned elimination percentages indicate.

II-4.B Treatment of Anode and/or Cathode Type Copper

Vaquum refining of anode copper and especially cathode copper for the elimination of gaseous impurities (O,S) and metallic impurities has been a prime concern to many metallurgists over the past 40 years. This interest has been prompted by the rapid advance in electrical technology requiring improved electrical and mechanical properties. At the beginning of the 1960's, a product called oxygen-free high conductivity copper (OFHC copper) of extremely high purity (>99.99% Cu) was manufactured by the

United State Metal Refining Co.[66] It was found to be of higher quality than other OFHC copper which had been commercially available since the beginning of the 1930's.

Generally OFHC copper is produced by melting selected copper cathodes in contact with carbon in an electric furnace under a protective atmosphere of carbon monoxide and nitrogen, followed by casting under the same protective atmosphere[67]. In some OFHC copper producing plants, deoxidant metals were also used[68,69]. Since the advent in 1930's of the conventional OFHC copper process, alternative vacuum processes have been considered[66-85]. The common aim in these studies has been to decrease the contents of the gaseous (oxygen, sulphur and hydrogen) or metallic (arsenic, antimony, bismuth, lead, tin, zinc) impurities in copper thereby decreasing porosity and electrical resistance and increasing density, ultimate tensile strength, relative elongation and electrical conductivity. In studying ways to produce copper of superior quality to OFHC copper, more than 20 studies[66-85] have been carried out; temperatures ranging between 1180°C and 1460°C, and vacuum pressures as high as 300 mm Hg and as low as 10^{-5} mm Hg have been tried for holding time of 10 minutes to 7-8 hours.

Since these studies were very similar only a few of the more salient features are mentioned below.

Thus, in 1948, construction of a vacuum furnace to conduct tests on up to 180 kilogram melts of copper was reported[68]. A series of experiments were carried out with cathode copper at

1200°C - 1370°C under 5-10 μHg (0.005 - 0.010 mm Hg) pressure with holding time of 3 hours. Promising results were obtained and copper with lower impurity contents and better electrical and mechanical properties could be produced. The analyses of vacuum cast copper in comparison with OFHC copper produced by conventional methods is given in Table 4.

V. K. Gupta et al.[67] claimed that refining 2-3 kilogram charges of cathode copper at 1200°C for 10 minutes at below 10^{-3} mm Hg vacuum was adequate for producing certified grades of OFHC copper[66,70]. Further, using higher temperatures and longer holding times, copper of superior quality could be produced. This copper had oxygen contents of <1 ppm, three times less than that for OFHC copper. The study also claimed that it was possible to produce OFHC copper directly from fire refined copper provided the initial nickel content was low.

Taubenblat et al.[85] studied the effects of time, pressure and melt temperature on the properties of cathode copper, melted and cast in 20-25 kilogram amounts, under a range of 0.1-1000 μHg pressures. It was found that the concentrations of sulphur, lead, bismuth, tin and manganese could be decreased. Also, relative to copper cast under protective atmosphere conditions but not under vacuum, better resistance to grain boundary cracking during oxidation and higher elimination of porosity could be obtained.

In addition to these investigations on vacuum induction melting of copper, the castability of copper and copper alloys in vacuum[86] have been studied as well as a continuous vacuum pouring ladle[87]. Similarly, electron beam[78,80] and electric

TABLE 4. Analysis of Vacuum Cast Copper[18]

Element	% in OFHC	% in Vacuum Copper
Hydrogen	0.00012	0.000008
Oxygen	0.00045	0.00004
Sulfur	0.0023	0.0001
Selenium	0.00013	0.00005
Tellurium	0.0001	0.00005
Lead	0.0005	0.0001

arc[78,80,88] melting of copper were investigated. Even though copper with comparable qualities to induction melting could be produced, it was concluded by F. N. Strel'tsov et al.[78,80] and P. G. Clites[88] that electron beam and vacuum arc melting as methods of refining copper free of gas have no special advantages over induction melting. Further, there are disadvantages owing to difficulties with melt temperature control and over-cooling of the melt as a result of excessive heat conduction through the surrounding frozen scull of copper.

II-4.C Treatment of Copper Matte

Very little experimental work has been performed in this area.

Bryan et al.[58] reported that bismuth removal from copper sulphide was found to be considerably slower than from copper but no quantitative results were given.

In a laboratory scale vacuum furnace and vacuum lift apparatus (analogous to the D-H process) H. Kametani, C. Yamauchi et al.[89-93] investigated the removal of impurities from white metal and mattes using samples of 100 gram and 4 kilogram for a vacuum furnace and a vacuum lift apparatus respectively, under reduced pressures of 0.5-1.0 mm Hg at 1200°C. Holding times of one hour were employed for vacuum furnace melting, whereas 20 vacuum lifts were applied in the vacuum lift apparatus. In vacuum furnace melting, the elimination of impurities from the sulphide melt began to take place at pressures below about 10 mm Hg. The evaporation of impurities was increased at a pressure of ≈0.5 mm Hg,

and nearly all the impurities in the mattes were reduced below 0.1% after treatment periods of one hour. The range of eliminations were 65-90% arsenic, 50-95% antimony, 60-95% bismuth and 100% lead. In the vacuum lift refining of matte average eliminations were in the range of 85% arsenic, 60% antimony, 80% bismuth, 90% lead and 50% zinc[91].

Experimental results for a series of studies on the vacuum lift refining of matte and white metal were further discussed comparing the D-H process in steel making and a tentative mass transfer model was proposed by the same authors[92,93].

In more recent work, R. L. Player[94] studied the kinetics of removal of lead and arsenic from copper matte in laboratory (8-20 kilogram matte) and pilot plant (2 tonne matte) experiments. In laboratory experiments at pressures of 0.1 - 1.0 mm Hg and 1150°C average rate constant results varied in the range of 3-26 x 10^{-3} cm/s for lead and 5-17 x 10^{-3} cm/s for arsenic. Similarly, in the pilot plant experiments at pressures of 0.3-1.0 mm Hg and temperatures of 990-1070°C rate constant results were in the range of 4-25 cm/s for lead and 25-216 cm/s for arsenic.

Results obtained for matte and white metal were more promising than for blister copper.

II-4.D Patent Survey

In order to complete this investigation on the present state of the art regarding vacuum treatment of copper, existing patents have been studied:

An apparatus for the vacuum treatment of copper (or other metals) in which a conveying gas is introduced into the recirculating melt to improve the mixing of the melt and therefore to improve the vaporization of the impurities has been patented[95]. The process is similar to the R-H process used for steel refining[96]. The apparatus contained a melting chamber and two concentrically arranged, separately evacuable, degassing chambers in which liquid metal is circulated by a differential pressure and the action of a conveying gas. It was claimed that in 3 steps using first oxidizing gas (air and/or oxygen) then reducing gas (hydrogen, carbon monoxide, hydrocarbon compounds, or chlorine compounds) and finally an inert gas, it would be possible to eliminate arsenic, antimony, lead, selenium, telerium, sulphur and oxygen to amounts less than one ppm. A detailed explanation of the apparatus is included but experimental data and the specific kind of copper used were not given.

Thomas G. Hart developed a glass (!) and graphite apparatus and from this a process for the treatment of electrolytic refined copper (cathode copper). This is covered in 3 separate patents[97-99]. He claimed that the removal of oxygen, sulphur, hydrogen, lead, telerium and bismuth were tried by melting the copper in an excess of hydrogen and then exposing thin streams of the copper to vacuum, prior to casting. Several forms of suitable apparatus both simple and complex are described in detail with diagrams. No chemical or quantitative data are disclosed as to the results obtained with the described apparatus and the process.

A Japanese patent[100] specifies that treatment of tough pitch copper (cathode copper) in a vacuum arc furnace could provide decrease of oxygen content from 10-30 to 8 ppm.

It was claimed in a Russian patent[101] that copper can be refined by melting and holding it at 10^{-1} mm Hg at 1400-1450°C and then holding it at 10^{-3} mm Hg pressure. Similar to this a Czechoslovakian patent[102] claimed that at 10^{-4} - 5 x 10^{-5} mm Hg pressure passing hydrogen or hydrogen and carbon monoxide mixture under the surface of the copper melt for 1-2 hours could eliminate gasses from copper. No quantitative data is given for these three patents either.

The International Nickel Company patented a process for refining of cement copper by a two-stage vacuum treatment[103]. Copper (containing 5% iron, 1.0% sulphur and 10% oxygen) precipitated from solution is melted in an induction furnace in air to slag iron and to form a copper bath containing sulphur and oxygen. The oxygen content is maintained at least in excess of the sulphur content but not so much as to produce a separate cuprous oxide phase. After removing the slag from the copper bath, nitrogen or a mixture of nitrogen and hydrogen is passed through the melt at 0.76 mm Hg pressure so as to lower the sulphur content to less than about 0.001% and the oxygen content to about 0.1%. The pressure is then decreased to 0.075 - 0.15 mm Hg at 1200-1400°C. After holding for 1-2 hours and deoxidizing, the melt is cast. It is claimed that copper containing 0.1% arsenic, 0.1% bismuth, 0.1% lead, 0.01% selenium, 0.01% telerium, 0.1% tin and 0.1% zinc

can be treated by this process and the residual content of arsenic, bismuth, lead, tin and zinc can be lowered to less than about 0.001% while selenium and telerium can be at least halved. The final copper contained < 1 ppm sulphur and < 25 ppm oxygen.

In addition to these patents, processes for vacuum treatment of copper-nickel scrap[104] and copper-chrome alloys[105] to eliminate impurities such as lead, tin and zinc were also patented.

A process for vacuum treatment of copper matte (or white matte or speiss) has been patented by Japanese[106]. In the process, 100-300 grams of matte samples were treated at 1200-1250°C and pressures of 0.01-30 mm Hg and eliminations were as follows: Arsenic >80%, antimony ; 50-80%, bismuth ; 70-90%, lead ; 100% and zinc ; 75-99%.

As mentioned above, only two of the patents give detailed quantitative data[103,106]. Also the industrial scale application of the processes and specifically the treatment of copper produced by continuous processes are not mentioned in any of them.

II-4.E Summary of Previous Experimental Work

The results of this study on the state of art in the vacuum treatment of copper can be summarized as follows:

1. It is shown theoretically and experimentally that it is possible to eliminate gaseous or metallic impurities from copper by vacuum treatment at pressures of < 1 mm Hg and temperatures of 1150-1400°C. Better results with bismuth, lead and zinc could be obtained compared to arsenic, antimony and tin under neutral conditions.

2. Even though some doubt as to mechanisms exist, a kinetic model to explain the system of evaporation of impurities from copper is available and it is shown that under vacuum, the evaporation of metallic impurities are gas phase controlled. Ohno[49,50] and Bryan et al. were the only ones who attempted to do kinetic studies of the process both at laboratory scale.

3. Improvement in the quality of copper produced by vacuum treatment will depend mainly on higher temperatures (up to 1400°C) and lower pressures (<100 μHg).

4. It is possible to improve mechanical and electrical properties of copper by vacuum casting.

5. The possible effect of holding a water cooled condenser close to melt surface has not yet been studied.

6. Most of the work carried out on vacuum refining of copper has been laboratory scale, except for the two reports, mentioned above[68,74].

7. There are no known commercial installations currently in use for vacuum refining of copper.

8. Vacuum refining of copper produced by the continuous processes (such as the Noranda or Mitsubishi processes) have not been studied and reported in the scientific literature, nor does it seem likely that any such work is covered by patents, at the present time.

9. Higher percentages of impurity evaporation are obtained with copper mattes compared with copper melts. This indicates that it may be worthwhile to carry out studies on the vacuum treatment of high grade matte.

10. The vacuum treatment of other metals such as steel and lead is well established.

CHAPTER III

DEVELOPMENT OF MATHEMATICAL MODEL AND A CRITICAL ANALYSIS OF PARAMETERS, USED

III-1. DEVELOPMENT OF MODEL

As shown in the previous chapter, the elimination of impurities in vacuum induction melting generally follows first order kinetics. As a result, the overall mass transport rate can be described by an equation of the form:

$$2.303 \log \frac{(wt\%i)_t}{(wt\%i)_0} = -K \frac{A}{V} (t-t_0) \qquad (10)$$

Here, the overall mass transfer coefficient, K, will be a function of the liquid phase mass transport coefficient, K_L, the evaporation mass transfer coefficient, K_E, the gas phase mass transport coefficient, K_G, as well as being potentially dependent upon the presence of oxygen and/or sulphur and other reactive elements either dissolved in melt or present in the gas phase.[43,46,52]

Liquid phase mass transport and evaporation can be described with reasonable accuracy on the basis of the Machlin[46] and Langmuir-Knudsen equations[50] respectively. Mass transport of impurities through the gaseous phase can be interpreted on the basis of the theory of molecular resistance to diffusion in gases and related to the above mentioned rate equations.[40,52,53]

When the partial vapour pressure of the impurity element is not equal to zero at the interface, its rate of evaporation is less than its limiting maximum value, and is given by Equation 21.

$$\dot{N}''_{i,ev} = \frac{\alpha(P_i^+ - P_i^*)}{\sqrt{2\pi RTM_i}} \quad g\cdot mole\ cm^{-2}s^{-1} \tag{21}$$

Similarly, the rate of mass transport in the gas phase away from the melt surface can be represented in terms of Equation 22.

$$\dot{N}''_{i,gas} = \frac{K_G}{RT}(P_i^* - P_i^b)\ g\cdot mole\ cm^{-2}s^{-1} \tag{22}$$

Taking the vapour pressure of the impurity element at the condensing surface away from the melt as zero, one may substitute the value of P_i^* into Equation 22 from Equation 21, yielding

$$\dot{N}''_i\left(\frac{\sqrt{2\pi RTM_i}}{\alpha} + \frac{RT}{K_G}\right) = P_i^+ \tag{23}$$

The equilibrium vapour pressure of the impurity element, P_i^+, is given by Equations 16 and 17, i.e.

$$P^+ = P_i^\circ\ \gamma_i\ \frac{M_{Cu}}{\rho_{Cu}}\ C_i^* \tag{24}$$

so that,

$$\dot{N}''_i\left(\frac{\rho_{Cu}\sqrt{2\pi RTM_i}}{\alpha\ P_i^\circ\ \gamma_i\ M_{Cu}} + \frac{\rho_{Cu}RT}{P_i^\circ\ \gamma_i\ M_{Cu}\ K_G}\right) = C_i^* \tag{25}$$

The molar flux of impurity i through the liquid to the melt interface is given by

$$\dot{N}''_{i,liq} = K_L(C_i^B - C_i^*) \tag{11}$$

Combining Equations 25 and 11 to eliminate C_i^*:

$$\dot{N}''_i \left(\frac{1}{K_L} + \frac{\rho_{Cu}\sqrt{2\pi RTM_i}}{\alpha P_i^\circ \gamma_i M_{Cu}} + \frac{\rho_{Cu} RT}{P_i^\circ \gamma_i M_{Cu} K_G} \right) = C_i^B \tag{26}$$

Defining K_E as:

$$K_E = \frac{\alpha P_i^\circ \gamma_i M_{Cu}}{\rho_{Cu}\sqrt{2\pi RTM_i}} \tag{20}$$

and rearranging Equation 26, yields

$$\dot{N}''_i \left(\frac{1}{K_L} + \frac{1}{K_E} + \frac{\rho_{Cu} RT}{P_i^\circ \gamma_i M_{Cu} K_G} \right) = C_i^B \tag{27}$$

Similarly, defining K_U as

$$K_U = \frac{K_G M_{Cu} P_i^\circ \gamma_i}{RT \rho_{Cu}} \tag{28}$$

Then

$$\dot{N}''_i = \left(\frac{1}{\frac{1}{K_L} + \frac{1}{K_E} + \frac{1}{K_U}} \right) C_i^B \tag{29}$$

Which is equivalent to the mass transport equation

$$\dot{N}''_i = K\, C_i^B \text{ g·mole } s^{-1} \tag{30}$$

Thus, the overall mass transfer coefficient, K, is related to the assumed three resistive steps, in the liquid, interface, and gas phases according to

$$\frac{1}{K} = \frac{1}{K_L} + \frac{1}{K_E} + \frac{1}{K_U} \tag{31}$$

For simplicity, the overall rate of mass transport can be rearranged in terms of weight percent. Thus, for dilute solutions

$$C_i^B = \frac{\rho_{Cu}}{100\ M_i}\ wt\%i \tag{32}$$

Consequently, for a well stirred batch system of volume, V and melt surface area, A, one may write on the basis of the continuity equation for species, i, that

$$\frac{-d(wt\%i)}{dt} = \frac{A}{V} K\ (wt\%i) \tag{8}$$

In equation 8, K can be obtained from experiments while K_L and K_E can be estimated from the empirical equations provided necessary thermodynamic and kinetic data are available. Taking,

$$K_L = \sqrt{\frac{8D_iU_i}{\pi r}} \tag{14}$$

and

$$K_E = \frac{\alpha\ P_i^\circ\ \gamma_i\ M_{Cu}}{\rho_{Cu}\sqrt{2\pi RTM_i}} \tag{20}$$

Then by difference from Equation 32, K_U can be determined and finally K_G can be deduced.

In the following sections, the terms forming K_L and K_G will be discussed in more detail. K_E is not included in this discussion, since the terms in the equaiton are self-explanatory.

III-2. ANALYSIS OF PARAMETERS IN LIQUID PHASE MASS TRANSPORT COEFFICIENT

Diffusivity, D_i:

A thorough literature survey revealed the absence of published data relating to the diffusivity of the impurity elements arsenic, antimony, bismuth, lead etc. in liquid copper[107-109]. As a result, theories on the diffusivity of solute atoms in dilute solutions had to be reviewed and adopted to estimate the diffusivity of these impurity elements in liquid copper[47,52,109-111].

Using equations of Walls and Upthegrove, Stokes and Einstein and Sutherland[52], diffusivities of bismuth and lead in liquid copper were estimated (as shown in Appendix III, Table III-1) at temperatures of 1150, 1250 and 1350°C. The values obtained fell in the range of 1-3 x 10^{-5} cm^2/s for both elements. Since experimentally none of the theoretical equations are necessarily found to be more accurate, D_{Bi} or D_{Pb} were somewhat arbitrarily taken as being 1 x 10^{-5} cm^2/s at 1150°C. Similarly using the general Arrhenius Equation* and choosing typical activation energies of 15-30 Kcals/g·mole, values of D_{1250} and D_{1350} were

---

* Arrhenius Equation[52]: $D = D_o^{-\Delta E/RT}$

estimated as 2.0×10^{-5} cm^2/s and 3.7×10^{-5} cm^2/s, respectively. Similar procedures were adopted for estimated diffusivities at 1423 and 1523 K, the values being included in Table III-3 in Appendix III.

A summary of the calculations of diffusivity values and the formulas used are included in Appendix III.

Mean Surface Velocity of Melt, $\bar{u}$

On the basis of visual estimates, for a variety of induction melting furnaces ranging from 0.1 kilogram to 908.0 kilogram, Machlin[46] found melt surface velocities to be ≈10 cm/s (within an order of magnitude). These estimates were based on radial motion of particles floating across the top of the melts. Using the same method, Irons et al.[48] obtained a value of about 20 cm/s in 55 kilogram pig iron melts.

Similarly in much bigger size steel melts (0.3-45.0 tonnes) Szekely and Chang[112] measured the mean velocity as 15-40 cm/s. Tarapore and Evans in mercury pools weighing up to 275 kilogram obtained values of 2-8 cm/s[113,114].

For the present vacuum induction system, a mean surface velocity of 10 cm/s was taken as being a representative of the mean surface velocity of the molten copper bath.

Liquid phase mass transport coefficients were calculated at different temperatures following Equation 14 and the reasoning outlined above. These are included in Appendix III.

III-3. ANALYSIS OF GAS PHASE MASS TRANSPORT COEFFICIENT

As mentioned earlier, the gas phase mass transport coefficient is not readily accessible to quantitative evaluation. It is difficult to determine the partial pressure gradient of impurity vapour as well as its bulk value in the vacuum system. It is also known that the vapour pressure is difficult to treat analytically in a gas stream whose molecules are moving predominantly in one direction. Thermodynamic quantities are defined for systems at equilibrium and cannot be used rigorously under other conditions[40].

K_G, the gas phase mass transport coefficient, is considered to be proportional to a power of the diffusion in the gas phase ranging from unity to fractional values depending on the convection currents generated in the vacuum chamber.

Based on an early work by Sherwood and Cooke[53], Richardson[52] defined K_G as being inversely proportional to vacuum pressure.

$$K_G = \frac{K_G^\circ}{P}$$

K_G° = Gas phase mass transport coefficient characteristic of the system,

P = Ambient pressure in chamber

This relation would also hold true for the overall mass transfer coefficient, K, provided the gas phase resistance,

$1/K_G$, dominates[53], and this would tend to occur at higher chamber pressures. Ward[42] mentioned that with steel melts, evaporation of impurity elements became independent of pressure below 10 pascals, but was pressure dependent above 10 pascals.

The pressure level for a given system naturally depends on the pumping rates, melt composition and temperature. Similarly, the gas phase mass transport coefficient can be effected by the presence of oxygen, or other active components in the gas phase[115-118]. Heat transfer on the condenser surface may also effect K_G[119]. These effects have not been modelled in the present analysis.

III-4. VAPOUR MOLECULES CONTAINING MORE THAN ONE ATOM (DIATOMIC/COMPOUND GAS SPECIES)

The mass transport equations given in the previous sections referred all to monoatomic vapour molecules. However, bismuth, arsenic and antimony can form the following molecules:

Bi, Bi_2

As, As_2, As_3, As_4

Sb, Sb_2, Sb_4

The equilibrium vapour pressure of the impurity element (Equation 16) for molecules containing more than one atom is:

$$P_i^+ = P_i^\circ \ (\gamma_i \cdot X_i^*)^x \qquad (34)$$

where

$$x = 2,3,4.$$

For the case of diatomic molecules;

$$P^{+}_{i_2} = P^{\circ}_{i_2} (\gamma_{i_2} \cdot X^{*}_{i_2})^2 \tag{35}$$

or, since it is in dilute form:

$$P^{+}_{i_2} = P^{\circ}_{i_2} \left(\gamma_{i_2} \frac{M_{Cu}}{\rho_{Cu}} C^{*}_{i_2}\right)^2 \tag{36}$$

Rewriting Equation 15 taking the new value of P^{+},

$$\dot{N}''_{i,ev} = \frac{\alpha P^{\circ}_{i_2}}{\sqrt{2\pi RTM_{i_2}}} \left(\frac{\gamma_{i_2} \cdot M_{Cu}}{\rho_{Cu}}\right)^2 (C^{*}_{i_2})^2 \tag{37}$$

Converting concentrations into weight percent,

$$\frac{d(wt\%i_2)}{dt} = \frac{A}{V} \frac{P^{\circ}_{i_2}}{\sqrt{2\pi RTM_{i_2}}} \frac{\gamma^2_{i_2} M^2_{Cu}}{\rho_{Cu}\ 100 M_{i_2}} (wt\%i_2)^2 \tag{38}$$

The evaporation mass transfer coefficient then takes the following form for diatomic gases:

$$K_{Ei_2} = \frac{P^{\circ}_{i_2}}{\sqrt{2\pi RTM_{i_2}}} \frac{\gamma^2_{i_2} M^2_{Cu}}{\rho_{Cu}\ 100\ M_{i_2}} \tag{39}$$

III-5. VARIABLES AFFECTING OVERALL MASS TRANSPORT COEFFICIENT

For the experimental program, it was considered that the overall mass transfer coefficient for the removal of impurities from blister and/or anode copper could be effected by the following parameters:

1 - Melt temperature

2 - Vacuum pressure

3 - Melt surface area/melt volume

4 - Distance of condenser to melt surface

5 - Time span of vacuum treatment - processing time

6 - Type of crucible material used - reaction with refractories

7 - Oxygen content in the melt

8 - Sulphur content in the melt

In this study the first six parameters were studied and are discussed in detail in the following sections.

III-6. COMPUTER PROGRAM

A computer program was written in FORTRAN, and compiled and executed on an IBM system 370 model 158 computer.

The program was based on the equations given in the previous sections. Certain simplifying assumptions were necessary for applying the formulae and techniques of the model. The most important ones were that the melt surface was clean, that interactions between evaporating species were negligible, and that possible chemical effects (i.e. oxidation) above the melt surface

were either unimportant, or insensitive to changes in melt temperature and degree of vacuum.

A copy of the computer program appears in Appendix VI. For each experiment, the program carried out the plotting of the logarithm of the relative change in concentration of the impurity element versus time, calculation of the slopes following regression analysis, calculation of the correlation coefficients and determination of K, K_L, K_E, K_U and K_G respectively.

CHAPTER IV

EXPERIMENTAL WORK

IV-1. EXPERIMENTAL PROGRAM

The experimental program consisted of four parts involving a total of 20 experiments. The first three sections dealt with the removal of bismuth and lead from copper, while in Part IV studies on the simultaneous removal of bismuth, lead, arsenic and antimony were considered.

As mentioned in Section III-5, it was decided, in the present study, to investigate the effects of six variables (vacuum pressure, melt temperature, melt surface area to volume ratio, distance of condenser from melt surface, type of crucible material and processing time) on the overall rate constant, K, for the removal of impurities from copper. Four of these six variables (vacuum pressure, melt temperature, melt surface area to volume ratio and distance of condenser from melt surface) were chosen for study in Part I and II. (The remaining two were studied in Part III.)

In Part I, a 2^{4-1}-level fractional factorial test design was utilized for the purpose of screening these four variables so as to determine those most significantly affecting the rate of removal of bismuth and lead from copper[120]. Altogether eight experiments were carried out.

Once the results of Part I were known (vacuum pressure and melt temperature were found to be the most effective variables), Part II experiments were planned. Six experiments were then

carried out to obtain a relationship in between the overall rate constant, K, and vacuum pressure and melt temperature.

The effects of different crucible material and processing time together with reproducibility of the experimental results were investigated in four experiments in Part III.

In Part IV, the removal of bismuth, lead, arsenic and antimony were studied in two experiments.

IV-2. APPARATUS

IV-2.A Induction Furnace and Vacuum Chamber

Experiments were carried out in a 150 kW, 3000 hertz Tocco* induction furnace enclosed in a 2.25 cubic meter vacuum chamber, shown in Figure 5. The system was constructed by Deltec** Systems Inc. The chamber dimensions were 1.5 meter in diameter and 1.8 meter in length. The induction furnace contained within the vacuum chamber was connected to four flexible insulated leads which provided both power and cooling water. These flexible power connections permitted furnace tilting for casting out the melt.

The coil diameter was 35 centimeter and maximum steel melting capacity was 180 kilogram. Power was supplied by a 3000 hertz, 150 kW, 800 V, 188A Tocco Motor Generator.***

---

* Manufactured by Inductotherm Inc., Rancocas, N.J.

** Deltec Systems Inc., Primrose, PA.

*** Manufactured by Reliance Electrical, Cleveland, Ohio.

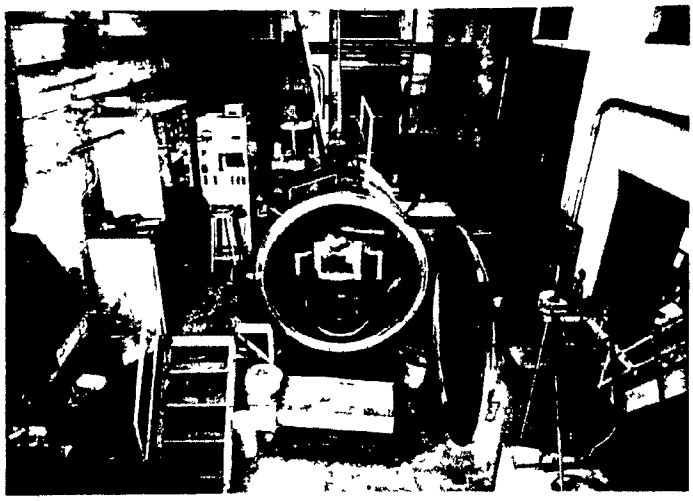

Figure 5. Vacuum induction furnace and the control system.

Auxiliary equipment on the vacuum chamber (Figure 6) included an alloy addition chute, four view ports (one for an optical pyrometer), three sampling probes, one temperature measurement probe (for dip tip thermocouple) and a water cooled condenser designed specifically for this study. The condenser, cylindrical in shape, with the dimensions of 15 centimeter diameter and 4 centimeter depth was fabricated in steel. It was designed for lateral and vertical movement (Figure 7-a and 7-b).

IV-2.B Pumping System

The vacuum chamber was evacuated by means of a two-stage pumping system consisting of a Stokes mechanical pump (nominal capacity = 0.142 m^3s^{-1}) and a Roots' Blower (nominal capacity = 0.614 m^3s^{-1}). The blower was set to start automatically at pressures below 2500 pascal (Figure 8).

IV-2.C Pressure and Temperature Control

In all experiments pressure was measured using a standard McLeod Gauge* which was accurate to within 10% at pressures below 300 pascal. At higher pressures two electrical resistance vacuum gauges (one functioning below 2700 pascal and the other below 150 pascal) were also used.

Melt temperature in all experiments were measured with Pt/Pt - 13% Rh thermocouple contained in a pure alumina (>99.8%) sheath. They remained continuously immersed in the bath during

* Supplied by The Virtis Company, Gardiner, N.Y.

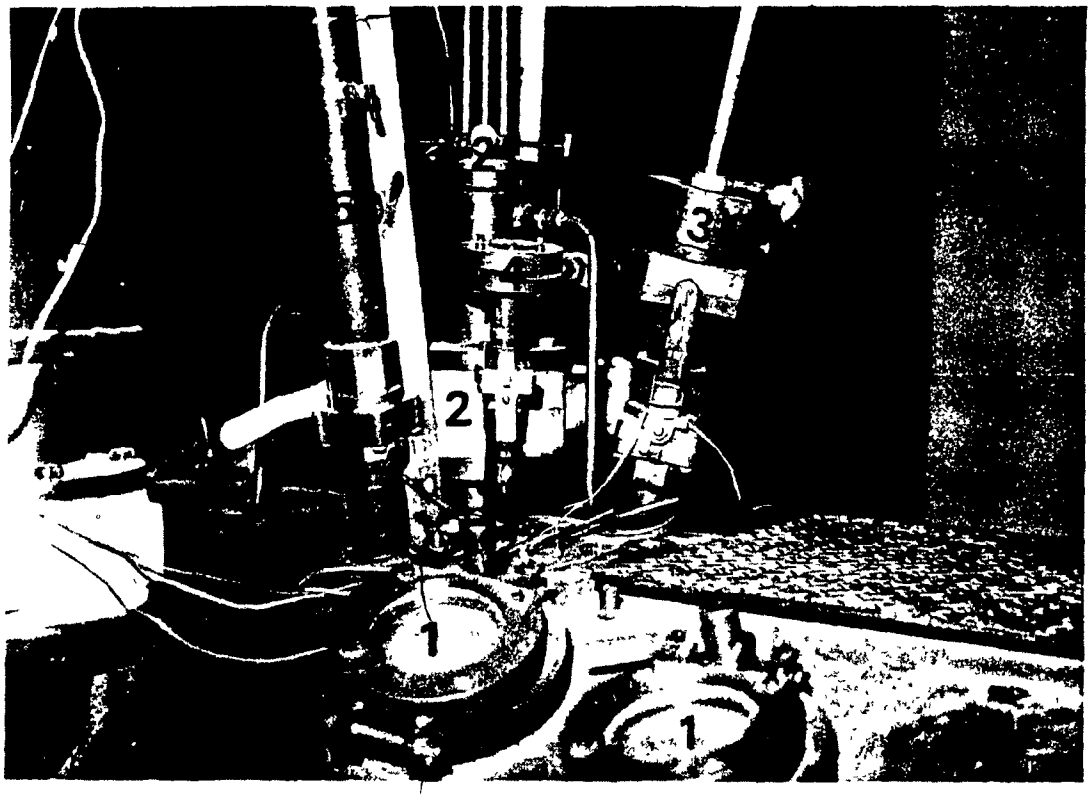

Figure 6. Various components.
1. Viewing ports, 2. Sampling and Dip-tip thermocouple rods,
3. Bridge breaker, 4. Optical pyrometer port,
5. Melt lancing port.

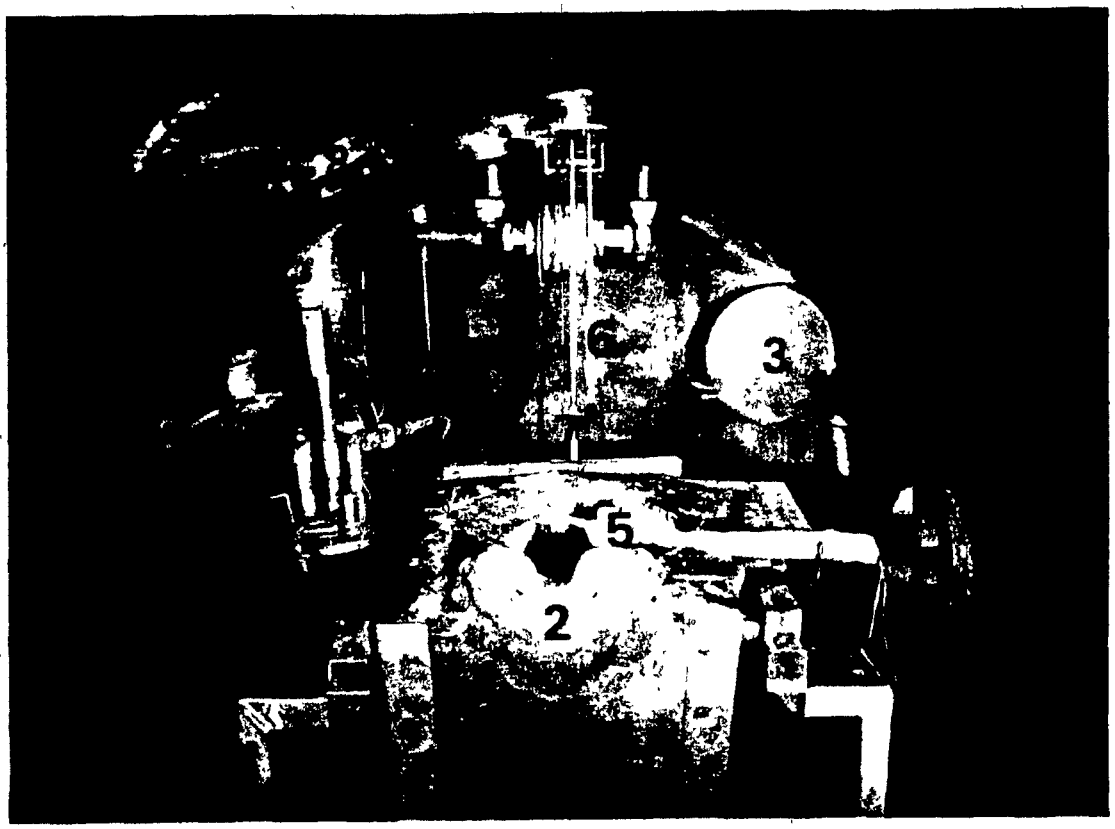

Figure 7-a. Inside view of the vacuum chamber. (Condenser on the side). 1. Condenser, 2. Induction furnace, 3. Filter to the pumps, 4. Chamber surface, 5. Pt-Pt 13% Rh thermocouple, 6. Dip-tip thermocouple, 7. Sampling rod and the graphite cup, 8. Viewing ports.

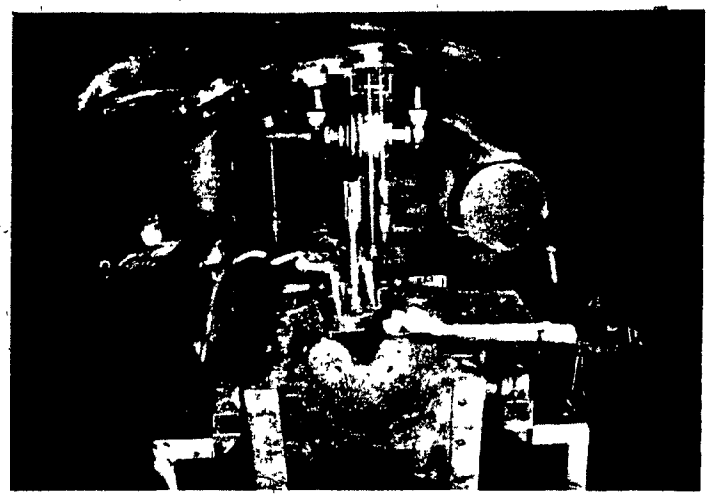

Figure 7-b. Inside view of the vacuum chamber. (Condenser in its position).

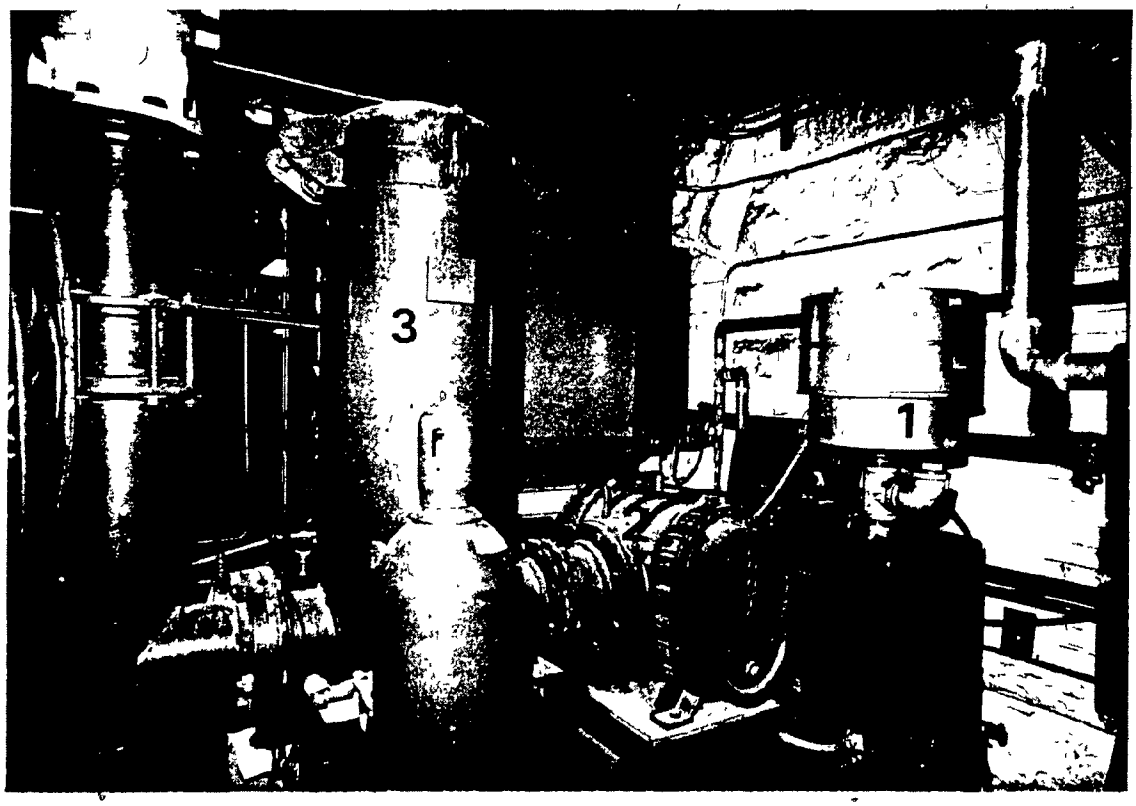

Figure 8. The pumping system.
1. Roots blower, 2. Stokes mechanical pump, 3. Filter.

experiments (±< 1.0% accuracy). As a second means of temperature control, Pt/Pt - 13% Rh, Dip-Tip Type R* thermocouples mounted on the temperature measurement probe were also used from time to time during experiments. Both of these thermocouples were connected to a 0-200 mV range digital voltmeter.**

Pressure was controlled by injecting nitrogen into the chamber while running the pumps at full capacity. The gas injection point was located in the center of the back wall of the chamber.

At times, minimization of air inleakage into the vacuum chamber could be difficult, especially at low operating pressures. Due to the complex structure of the chamber, the location and repair of leaks proved difficult. This caused serious problems in earlier studies carried out with this equipment[121,122]. The chamber and pumping system were regularly leak-checked using a helium leak detector. Testing and subsequent repair of leaks lowered the minimum operating pressure (that is the pressure at which the pumping capacity equals the rate of inleakage) to 4-5 pascal[122].

Melt temperature was controlled manually by adjusting the power input to the furnace.

---

* Supplied by Leeds and Northrup, Elliport, PA.

** Supplied by John Fluke Mfg. Co. Inc., Mississauga, Ontario.

IV-2.D Crucibles

In all the experiments which were labelled with "F", Tercod* - carbon bonded silicon carbide and graphite crucible - crucibles were used. Similarly, in the experiments which were labelled with "A", Hycor Alumina** crucibles were utilized.

Two different dimensions of Tercod crucibles were used:

i) #30 Tercod, ID = 19.0 cm, H = 25 cm

ii) #50 Tercod, ID = 24.0 cm, H = 25 cm

The dimensions of the Hycor Alumina crucibles were ID = 20 cm and H = 36 cm.

Chemical analysis of these crucibles are included in Tables 5-a and 5-b.

IV-3. SAMPLING AND CHEMICAL ANALYSES

Samples of the melt were taken in all the experiments using graphite cups at 30 minute intervals. A sampling probe with a graphite cup attached was lowered through the sampling port. The cup was immersed into the melt a few times in order to ensure complete filling. This procedure had minimal effect on vacuum levels, since double vacuum seals were incorporated in the furnace sampling facility. Similarly, power supply to the furnace remained uninterrupted during sampling providing excellent temperature stability.

---

* Supplied by Ferro Electro, Buffalo, N.Y.

** Supplied by Engineering Ceramics Co., Gilberts, Ill.

TABLE 5-a. Chemical Analysis of Tercod Crucibles; wt%

Compound	wt%	Compound	wt%
SiC	44-52	Al_2O_3	5.0
C	28-36	Fe_2O_3	0.7
SiO_2	11	glaze	3.0

TABLE 5-b. Chemical Analysis of Hycor Alumina Crucibles, wt%

Compound	wt%	Compound	wt%
Al_2O_3	88.3	TiO_2	0.10
SiO_2	11.2	K_2O	0.03
Fe_2O_3	0.15	MgO	0.03
Na_2O	0.12	CaO	0.02

The dimensions of the graphite cup (Figure 9) were: inside diameter = 2 centimeter, height = 5 centimeter, with a capacity of providing 20-30 gram copper samples.

After selected experiments, samples of condensate from the condenser and other locations inside the chamber were collected by scraping the powder from the surfaces. In addition, samples of the metallic accumulations above the melt level on the inside surface of the crucibles were taken for chemical analysis.

Samples taken by graphite cups were first separated from the graphite by hammering and then cut into small chips. Two to three gram portions of these chips would be dissolved in nitric acid and analysed for bismuth, lead, arsenic or antimony using atomic absorption spectrometric techniques.

Samples of condensate and metallic accumulations were analysed similarly.

IV-4. MATERIALS USED

The following materials were used in the experiments: copper as the melt; bismuth, lead, arsenic and antimony as alloying elements; graphite for sampling cups and nitrogen to provide an inert atmosphere.

Copper: Electrolytic tough pitch copper with the trade name of F-1100 copper off-cuts.* Nominal composition was +99.9% copper by weight.

---

* Supplied by Noranda Metal Industries Ltd., Montreal, P.Q.

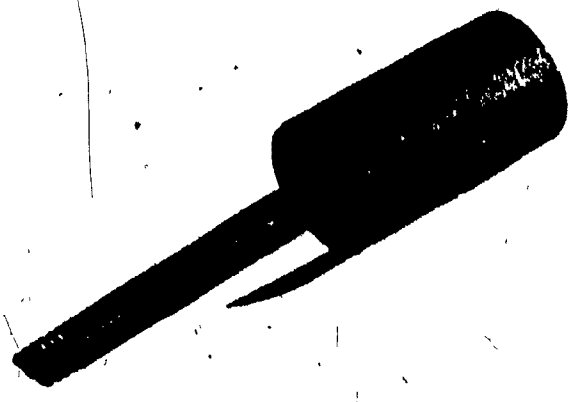

Figure 9. Graphite sampling cup.

Alloying Elements (bismuth, lead, arsenic, antimony): These were all pure grade lumps with nominal compositions of 99.9% by weight.*

Graphite: Commercial grade graphite rods, machined to specification.**

Nitrogen: Commercial grade in cylinders; capacity, $7m^3$, 298 K, 1 atm.***

IV-5. EXPERIMENTAL PROCEDURE

The following procedures were followed during the preparation and conduction of an experiment:

1) The selected crucible was placed in the furnace. The bath thermocouple was then assembled and inserted in one-end closed alumina insulating tube and then placed inside the crucible. Thirty-four kilogram of copper and a preselected quantity of alloying elements were then placed in the crucible. In some experiments, alloying elements were also added into the liquid copper following completion of charge melt down. In all experiments, the alloying elements were wrapped in a copper foil to ensure precise recoveries.

2) The vacuum chamber was cleaned, lubricated and closed. After all the ports had been closed, the chamber was subjected

---

* Supplied by American Chemicals Ltd. and Anachemia Chemicals Ltd., Montreal, P.Q.

** Supplied by Union Carbide Ltd., Lachine, P.Q.

*** Supplied by Welding Products Ltd., Montreal, P.Q.

to vacuum, pumping being carried out at full capacity for 30-40 minutes. Provided the minimum operating pressure had been obtained and stabilized, the experiment proceeded. If not, the experiment was aborted, the system checked for leaks, and any necessary maintenance carried out.

3) Once the desired pressure had been obtained, pumping stopped and nitrogen was injected into the chamber until the pressure reached 40,000 pascal. The purpose of this back filling operation was to eliminate possible splashing during melt down and to provide better control of the melt surface area to volume ratio.

4) Induction heating of the charge began toward the end of nitrogen injection. Heating up and melting usually required some two hours.

5) Following charge melt down, pumping was again started and continued until a minimum stable pressure had been attained. After approximately 30 minutes for complete degassing, the pressure was adjusted to the desired level by leaking nitrogen into the chamber.

6) Over this period, the melt temperature was adjusted manually by changing the level of power input to the furnace.

7) In the case of the condenser being used, it would then be relocated above the melt at this time. (Samples and temperature measurements were possible with the condenser in its operating position.)

8) The first sample was taken once the experiment temperature and pressure had stabilized and this was taken as the starting point of the experiment (time = t_0).

9) Pressure and temperature were monitored continuously during the experiment and deviations from set values minimized.

10) Samples were taken every 30 minutes.

11) On completion of an experiment, the condenser, if present, was removed; pumping was stopped and the valve opened to allow air into the chamber.

12) The door of the vacuum chamber was opened and the melt was cast into the iron mold.

13) Finally, all samples taken during the experiment as well as the cast of copper, were weighed.

14) After collecting the condensate samples, the chamber was cleaned and prepared for the next experiment.

IV-6. CRITICAL ANALYSIS OF THE EXPERIMENTAL TECHNIQUE AND AN ESTIMATE OF ERRORS

Generally, it was possible in all the experiments, to control variables within close limits of the set values without encountering any difficulties.

In the preliminary experiments, it was observed that new Tercod crucibles (sometimes) caused bubbling* during the course of an experiment, making the melt surface area to volume ratio

* It is possible that bubbling occurred due to reaction of a surface coating on the crucible with air leaking into the system.

value questionable. After two to three melts using the same crucible the bubbling phenomenon ceased. As the same crucible could be used for 8-10 melts, bubbling was avoided by using the same crucible after making two to three dummy melts. This problem did not occur with Hycor Alumina crucibles.

During sampling and casting the melt, some splashing occurred but this was not in excessive amounts (always less than 200 gram copper) and was therefore treated as being negliglble in terms of melt charge weight.

Similarly, in all the experiments, the melt surface was mirror like in appearance and apparently clean of any contaminating surface films.

The minimum stable pressure which could be attained was 60 μHg (8 pascal), the air leak rate into the system being in the range of 5-15 $cm^3 s^{-1}$, under standard conditions.[122]

Melt temperature, melt surface area to volume ratio, the distance of condenser from the melt surface, sampling time and location and chemical analyses were all held in close control during these experiments.

The reproducibility of the sampling, chemical analyses and experiments themselves were investigated using statistical analyses. The numerical results obtained are included in the following chapter.

For each experiment, correlation coefficients were calculated, so as to determine the significance of the overall mass transfer coefficient, K, used in the kinetic analysis.

Estimate of Error: The following accuracy limits were estimated for the variables listed below:

Pressure: ±5%

Temperature: ±0.5%

A/V: ±1.0%

Distance of Condenser: ±0.5 cm

Chemical Analyses: ±10%

CHAPTER V

RESULTS

V-1. PRELIMINARY WORK

At the beginning of the experimental work, three preliminary experiments were carried out to investigate melting and casting procedures, melt attack and crucible endurance, techniques for controlling experimental variables and sampling.

Preliminary studies indicated that the duration of each vacuum test should not be less than 120 minutes in order to observe the full effect of the conditions being applied. This required that each experimental test take about 4-5 hours. The selection of four variables to study, in conjunction with these extended time periods and experimental costs, necessitated that a statistical test design be carried out, thereby reducing the total number of experiments required. To this end, a 2^{4-1} fractional factorial test design was utilized[120]. This design facilitates screening the most influential factor or factors effecting the overall rate constant, K, for bismuth and lead removal from copper.

V-2. TWO-LEVEL FRACTIONAL FACTORIAL TEST DESIGN

The purpose of a fractional factorial test design is to obtain information on the main factors and interactions using a smaller number of observations than would be required by a complete factorial test design. With the help of this test design, the best combination of experimental treatment conditions for maximum elimination of solute impurities can be determined. Similarly, the methods of evaluation can allow one to estimate the influence of those interactions which are neglected, and at the same time to assess any potential (but unanticipated) importance they might have.

In this design, all four main effects are clear of two-factor interactions, but two-factor interactions are confused, one with another. That is, this method gives the main effects and, at most, three two-factor interactions, while all other interactions are assumed to be zero or at least negligible.

Fractional factorial test design involves first determining the number of variables and levels required. A table of variables and levels is then set, indicating the required conditions to be applied for each successive experiment (Table 6). After all the experiments are carried out, the results are tabulated (as in Table 7). From this table, by using Yates' Method[120], values for the total effect and sum of squares are calculated (Appendix IV,

TABLE 6. Design of Four Factors in Eight Observations

Experiment Number	Factors and the Levels Selected for the Factors				Treatment Combination	Effects Measured,[1] Aliases
	A Pressure 100μ(-) 300μ(+)	B Temperature 1150°C(-) 1250°C(+)	C A/V $6.70m^{-1}$(-) $10.20m^{-1}$(+)	D Condenser Dist. <0.02m(-) >0.65m(+)		
F-2	-	-	-	-	(I)	-
F-1	+	-	-	+	ad	A,BCD
F-3	-	+	-	+	bd	B,ACD
F-4	+	+	-	-	ab	AB,CD
F-5	-	-	+	+	cd	C,ABD
F-6	+	-	+	-	ac	AC,BD
F-7	-	+	+	-	bc	BC,AD
F-8	+	+	+	+	abcd	ABC,D

1. A,B,C,D (D = +ABC) main effects,
AB,CD,AC,BD,BC,AD interaction effects,
ABC = ABD = BCD = ACD = 0 by assumption.

TABLE 7. Experimental Conditions[1] and the Results for Part I Experiments (2^{4-1} Fractional Factorial Test Design)

Experiment Number	Level of Factors				Responses			
	A Pressure 100μ(-) 300μ(+)	B Temperature 1150°C(-) 1250°C(+)	C A/V $6.70m^{-1}$(-) $10.20m^{-1}$(+)	D Condenser Dist. 0.02m(-) >0.65m(+)	Elim'n, wt.%		$K(10^{-3}cm/s)$	
					Bi	Pb	Bi	Pb
F-2	-	-	-	-	46	61	1.127	1.795
F-1	+	-	-	+	24	29	0.611	0.707
F-3	-	+	-	+	49	66	1.337	2.215
F-4	+	+	-	-	46	54	1.108	1.432
F-5	-	-	+	+	38	58	0.652	1.116
F-6	+	-	+	-	22	32	0.389	0.590
F-7	-	+	+	-	75	85	1.794	2.521
F-8	+	+	+	+	53	71	0.991	1.656

1. Copper weight = 34 kg, time = 120 min.

Tables IV-1 and IV-2). Then, by using the experimental error variance and an F-test, the effects measured are compared with each other and the significantly different one (or ones) is selected. Finally, the best combination of experimental conditions are defined.

As mentioned earlier, the four factors (variables) chosen were vacuum pressure, melt temperature, ratio of melt surface area to melt volume and the distance of condenser from the melt surface.

The levels of factors were selected based on the results of preliminary experiments and theoretical studies. These levels and the combination of conditions for each test are tabulated in Table 6. This table represents one half of a 2^4 factorial design and it is therefore a half replicate.

If fractional factorial test design is used more than once for a certain experimental study, using the same set of variables and similar levels, experimental error variance can be determined directly from a comparison of the replicate set of test designs. However, if the fractional factorial test design is being applied for the first time to a certain experimental study (as was the case in the present study), then the experimental error variance can be estimated through indirect methods. Thus, in the present study, two methods were used for determining the variance in experimental error:

a) using arithmetic means of the two-factor interaction mean squares;

b) using the variance obtained from the duplication of a few randomly selected experiments from the test design.

Details of these calculations and the procedure followed for the evaluation of the results of 2^{4-1}-level fractional factorial test design are included in Appendix IV. A summary of the results obtained are included in the following section.

V-3. PART I EXPERIMENTS

In the eight experiments carried out for the fractional factorial test design, the weight percent elimination and the overall mass transfer coefficient values were obtained for the removal of bismuth and lead from copper. These are tabulated in Table 7.

In these series of experiments, the logarithm of the relative change in solute content with time has been plotted and these are shown in Figures 10 to 17 inclusive. With each figure, data on the change of bismuth or lead concentration (in weight percent) with time are reported together with the weight of total copper losses. In Tables 8 and 9 the results of K, K_L, K_E, K_U, K_{GAS}, initial wt%i, final wt%i and elimination wt%i, together with computed correlation coefficient, have been tabulated for bismuth and lead respectively.

In all these experiments it was observed that K_{Pb} was higher than K_{Bi}. It was confirmed that both bismuth and

TABLE 8. Summary of Results for Bismuth Removal, Part-I Experiments

Test No.	Corr. Coeff.	$K(10^{-3})$ cm/s)	$K_L(10^{-3}$ cm/s)	$K_E(10^{-3}$ cm/s)	$K_U(10^{-3}$ cm/s)	K_G (cm/s)	Initial wt%	Final wt%	Elim'n wt%
F-2	0.940	1.13	5.15	28.44	1.52	507	0.090	0.046	46
F-1	0.979	0.61	5.15	28.44	0.71	237	0.037	0.028	24
F-3	0.974	1.34	7.30	62.90	1.68	262	0.039	0.020	49
F-4	0.958	1.11	7.30	62.90	1.33	208	0.060	0.033	46
F-5	0.916	0.65	4.65	28.44	0.78	260	0.050	0.031	38
F-6	0.967	0.39	4.65	28.44	0.43	144	0.032	0.025	22
F-7	0.963	1.79	6.59	62.90	2.57	400	0.044	0.011	75
F-8	0.968	0.99	6.59	62.90	1.19	186	0.017	0.008	46

TABLE 9. Summary of Results for Lead Removal, Part I Experiments

Test No.	Corr. Coeff.	$K(10^{-3}$ cm/s)	$K_L(10^{-3}$ cm/s)	$K_E(10^{-3}$ cm/s)	$K_U(10^{-3}$ cm/s)	K_G (cm/s)	Initial wt%	Final wt%	Elim'n wt%
F-2	0.973	1.80	5.15	47.92	2.92	581	0.333	0.130	61
F-1	0.985	0.71	5.15	47.92	0.83	166	0.099	0.070	29
F-3	0.979	2.22	7.30	97.53	3.29	332	0.125	0.043	66
F-4	0.943	1.43	7.30	97.53	1.81	183	0.215	0.098	54
F-5	0.986	1.12	4.65	47.92	1.52	301	0.222	0.093	58
F-6	0.973	0.59	4.65	47.92	0.69	136	0.080	0.054	32
F-7	0.965	2.52	6.59	97.53	4.26	431	0.126	0.019	85
F-8	0.979	1.66	6.59	97.53	2.26	229	0.035	0.010	71

FIGURE 10

Rate of removal of bismuth and lead from copper, Test F-2.*

	Bi	Pb
K($\times 10^{-3}$ cm.s^{-1}):	1.127	1.795
Elim'n, wt.%:	46	61

time (min.)	wt.% Bi	wt.% Pb
0	0.090	0.333
30	0.063	0.212
60	0.060	0.198
90	0.054	0.162
120	0.049	0.130

Total copper loss** = 170 gr.

*The order of appearance of the figures follows the order in Table 7.

**Includes the splashes and the amount evaporated.

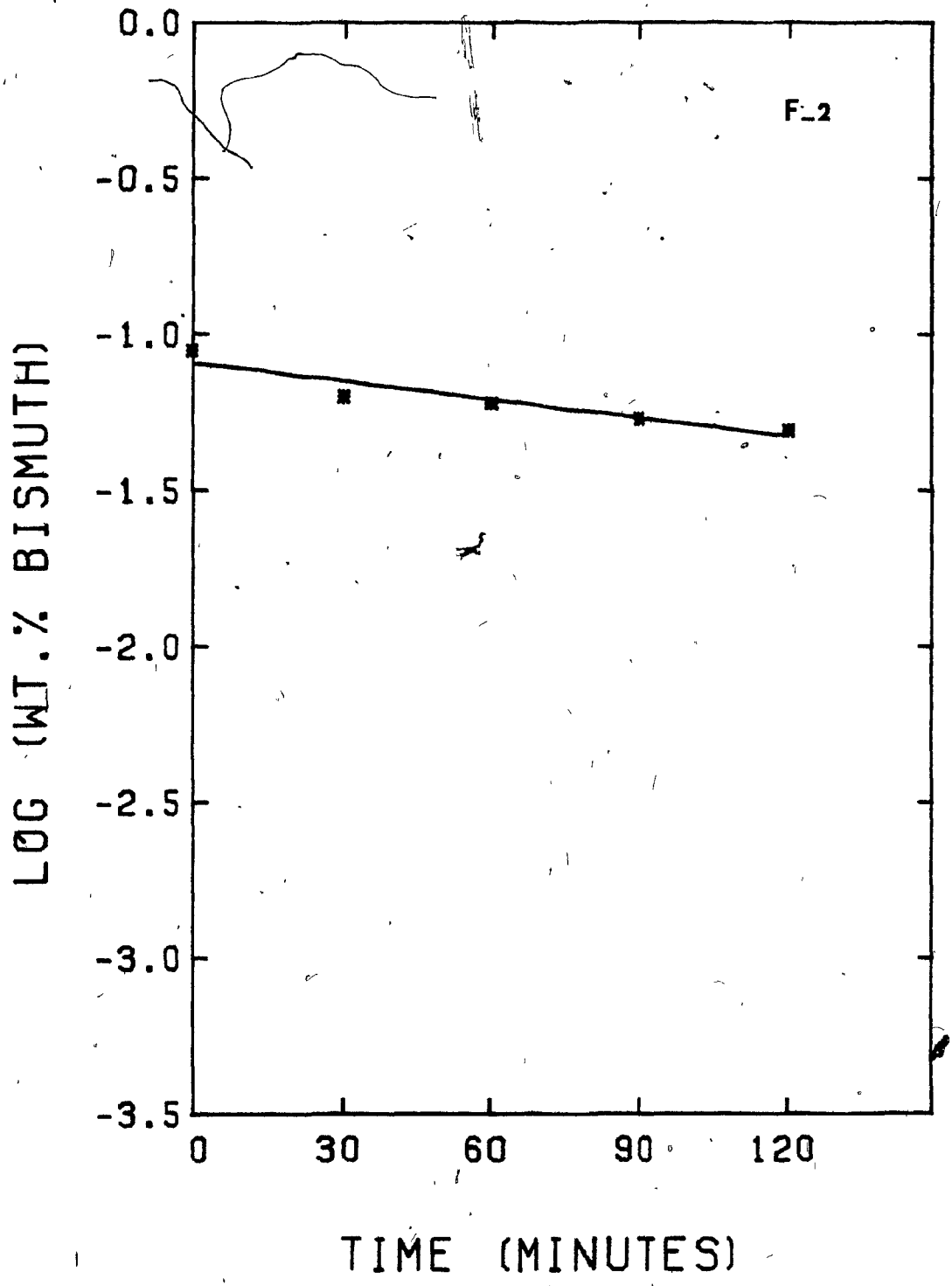
F_2
0.0
-0.5
-1.0
-1.5
-2.0
-2.5
-3.0
-3.5
LOG (WT.% BISMUTH)
0
30
60
90
120
TIME (MINUTES)

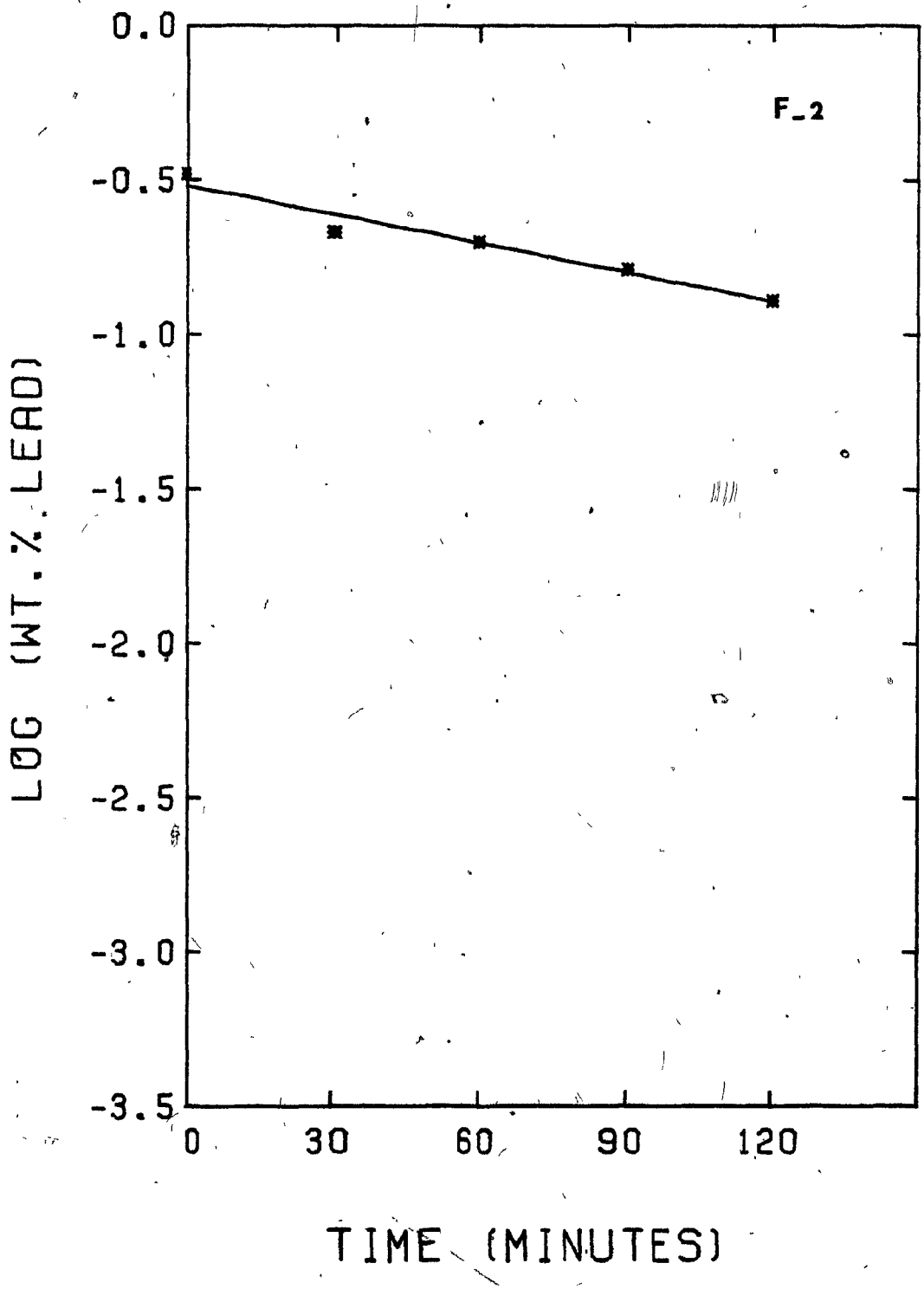
F_2
0.0
-0.5
-1.0
-1.5
-2.0
-2.5
-3.0
-3.5
LOG (WT.% LEAD)
0
30
60
90
120
TIME (MINUTES)

FIGURE 11

Rate of removal of bismuth and lead from copper, Test F-1.

	Bi	Pb
$K(\times 10^{-3}$ cm.s$^{-1})$:	0.611	0.707
Elim'n, wt.%:	24	29

time (min.)	wt.% Bi	wt.% Pb
0	0.037	0.099
30	0.036	0.095
60	0.034	0.088
90	0.030	0.082
120	0.028	0.070

Total copper loss = 110 gr.

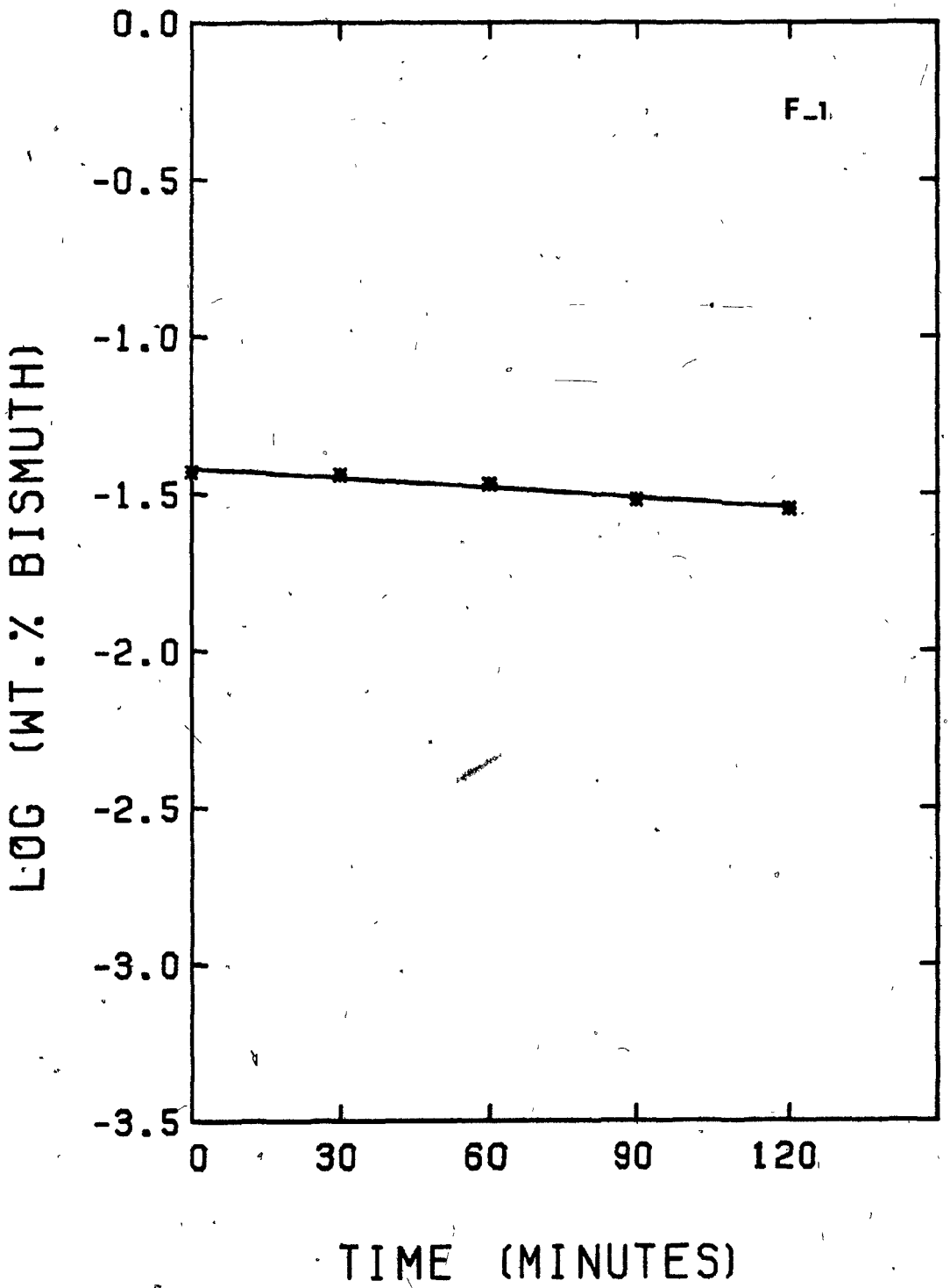
0.0
-0.5
-1.0
-1.5
-2.0
-2.5
-3.0
-3.5
F_1
LOG (WT.% BISMUTH)
0
30
60
90
120
TIME (MINUTES)

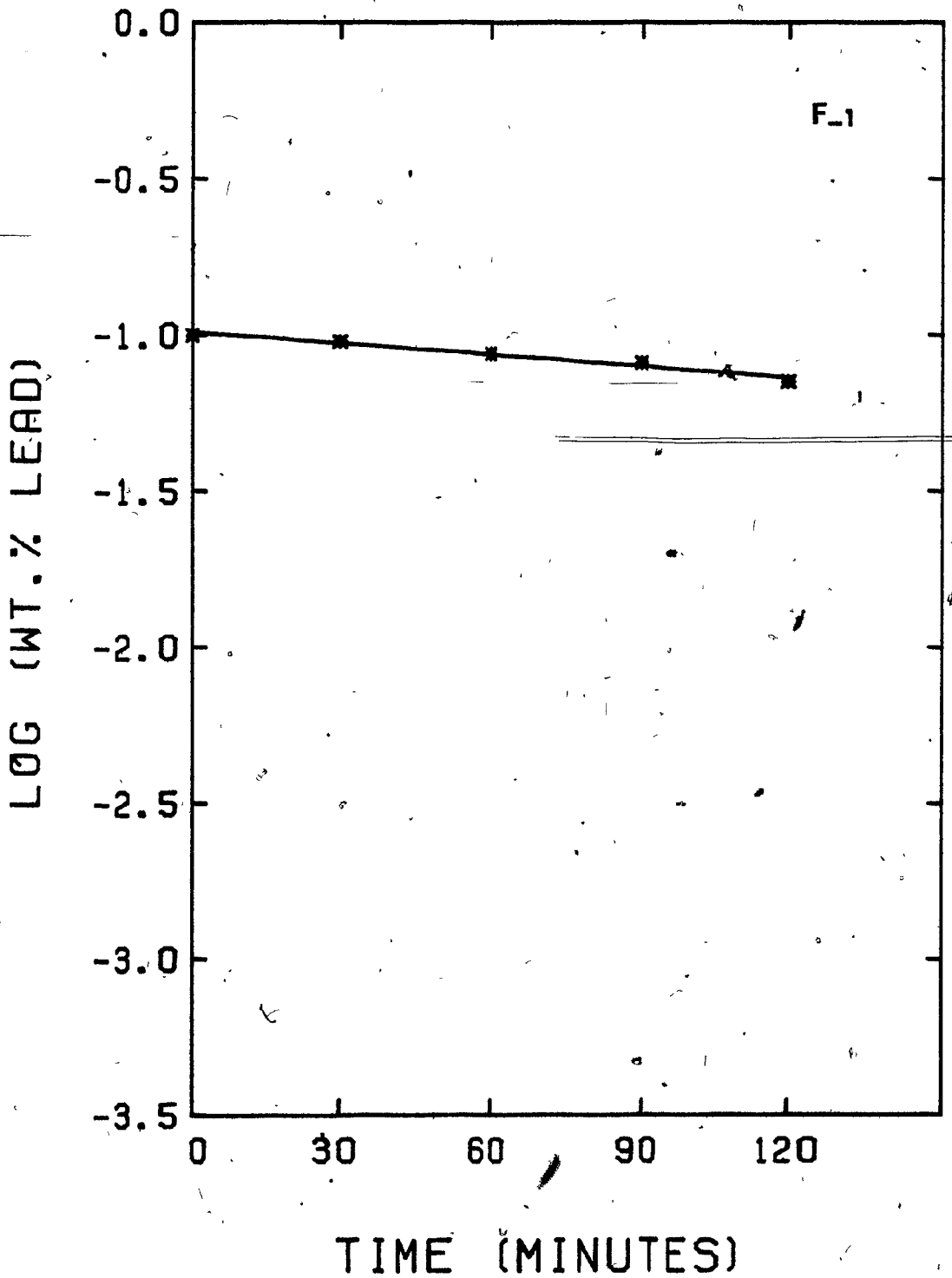
0.0
-0.5
-1.0
-1.5
-2.0
-2.5
-3.0
-3.5
F_1
LOG (WT.% LEAD)
0
30
60
90
120
TIME (MINUTES)

FIGURE 12

Rate of removal of bismuth and lead from copper, Test F-3.

	Bi	Pb
K($\times 10^{-3}$ cm.s^{-1}):	1.337	2.215
Elim'n, wt.%:	49	66

time (min.)	wt.% Bi	wt.% Pb
0	0.039	0.125
30	0.029	0.080
60	0.025	0.066
90	0.022	0.048
120	0.020	0.043

Total copper loss = 200 gr.

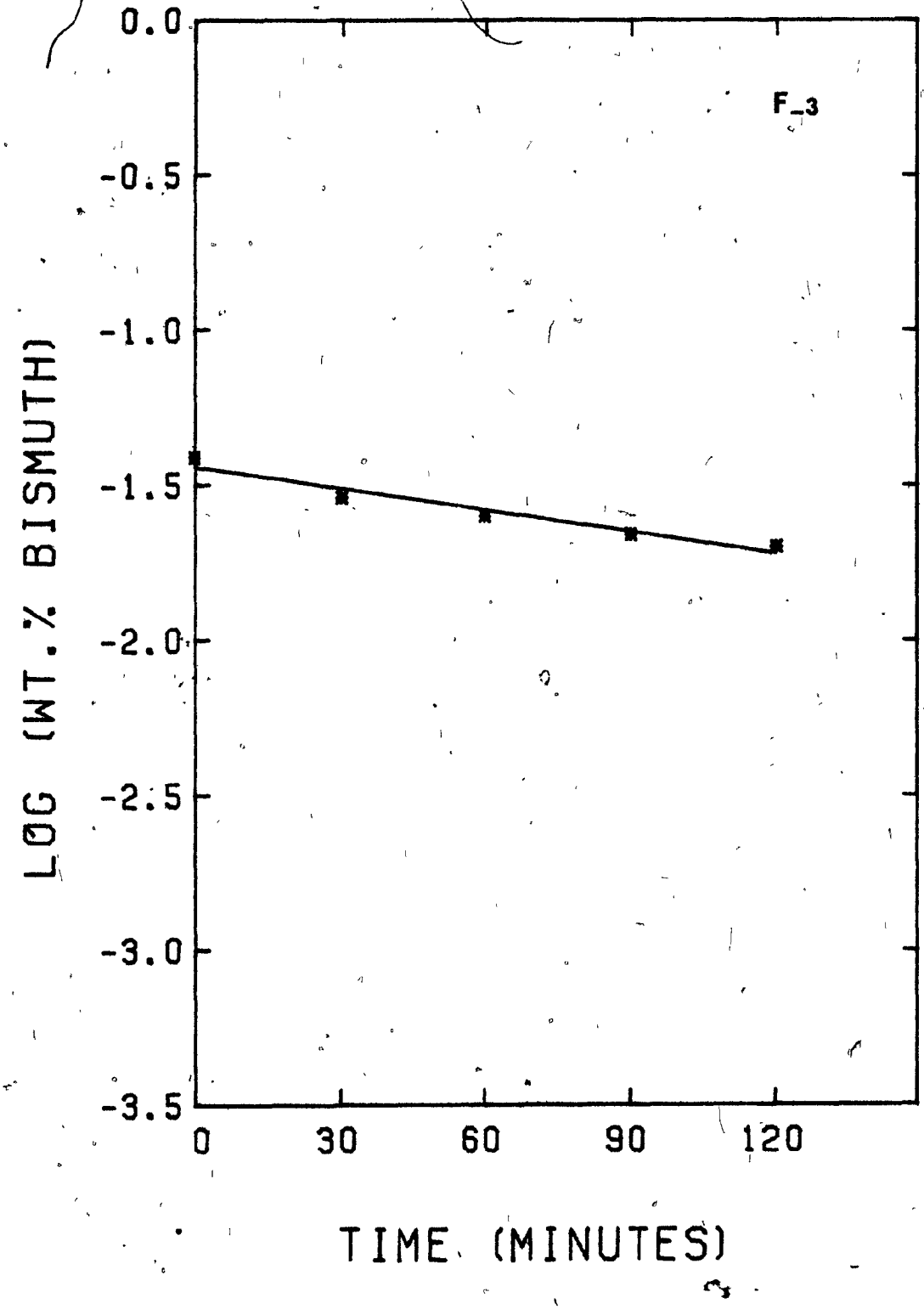
F_3
0.0
-0.5
-1.0
-1.5
-2.0
-2.5
-3.0
-3.5
LOG (WT.% BISMUTH)
0
30
60
90
120
TIME (MINUTES)

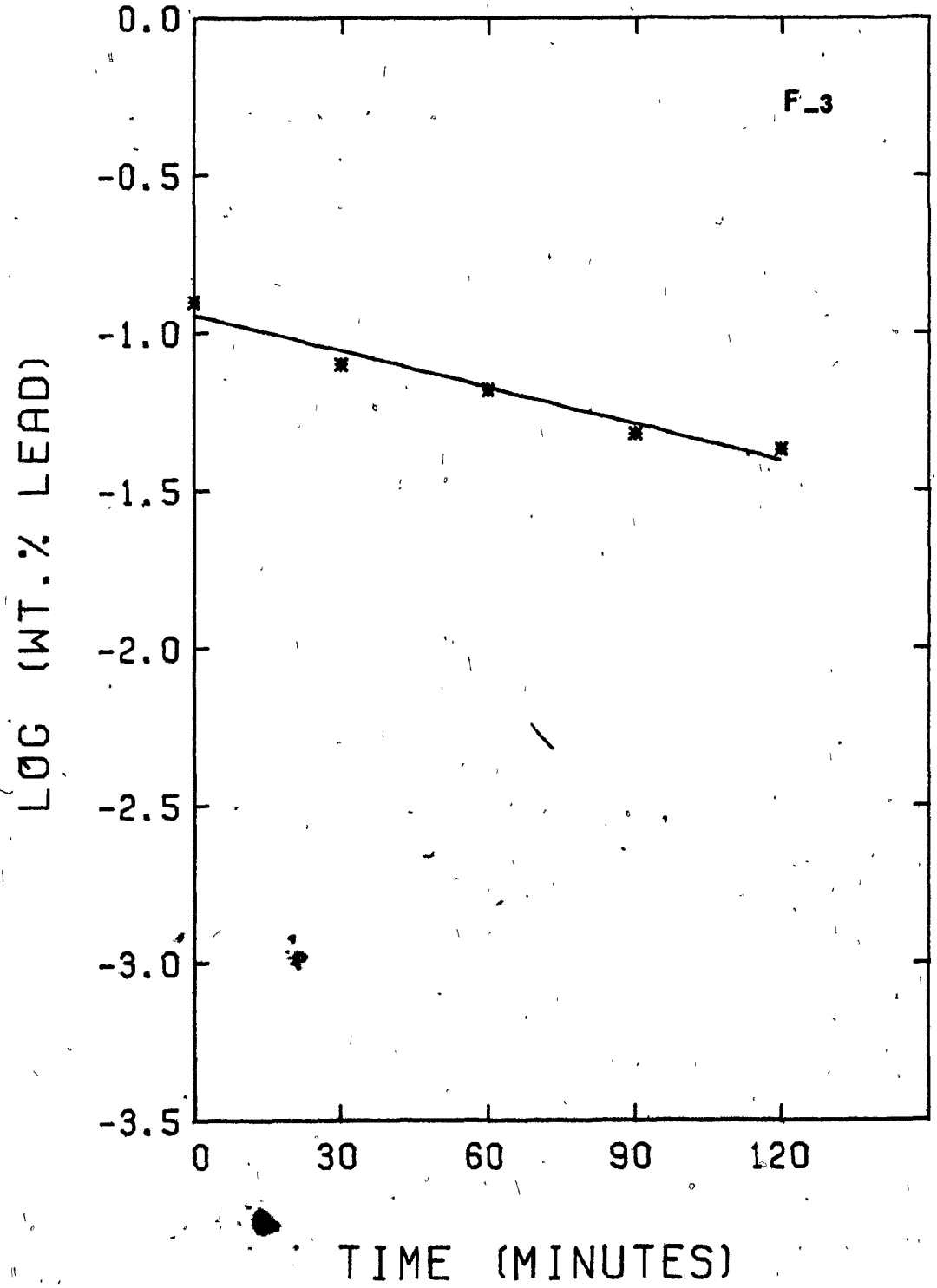
F_3
0.0
-0.5
-1.0
-1.5
-2.0
-2.5
-3.0
-3.5
LOG (WT.% LEAD)
0
30
60
90
120
TIME (MINUTES)

FIGURE 13

Rate of removal of bismuth and lead from copper, Test F-4.

	Bi	Pb
K($\times 10^{-3}$ cm.s^{-1}):	1.108	1.432
Elim'n, wt.%:	46	54

time (min.)	wt.% Bi	wt.% Pb
0	0.060	0.215
30	0.045	0.138
60	0.042	0.136
90	0.039	0.118
120	0.033	0.098

Total copper loss = 170 gr.

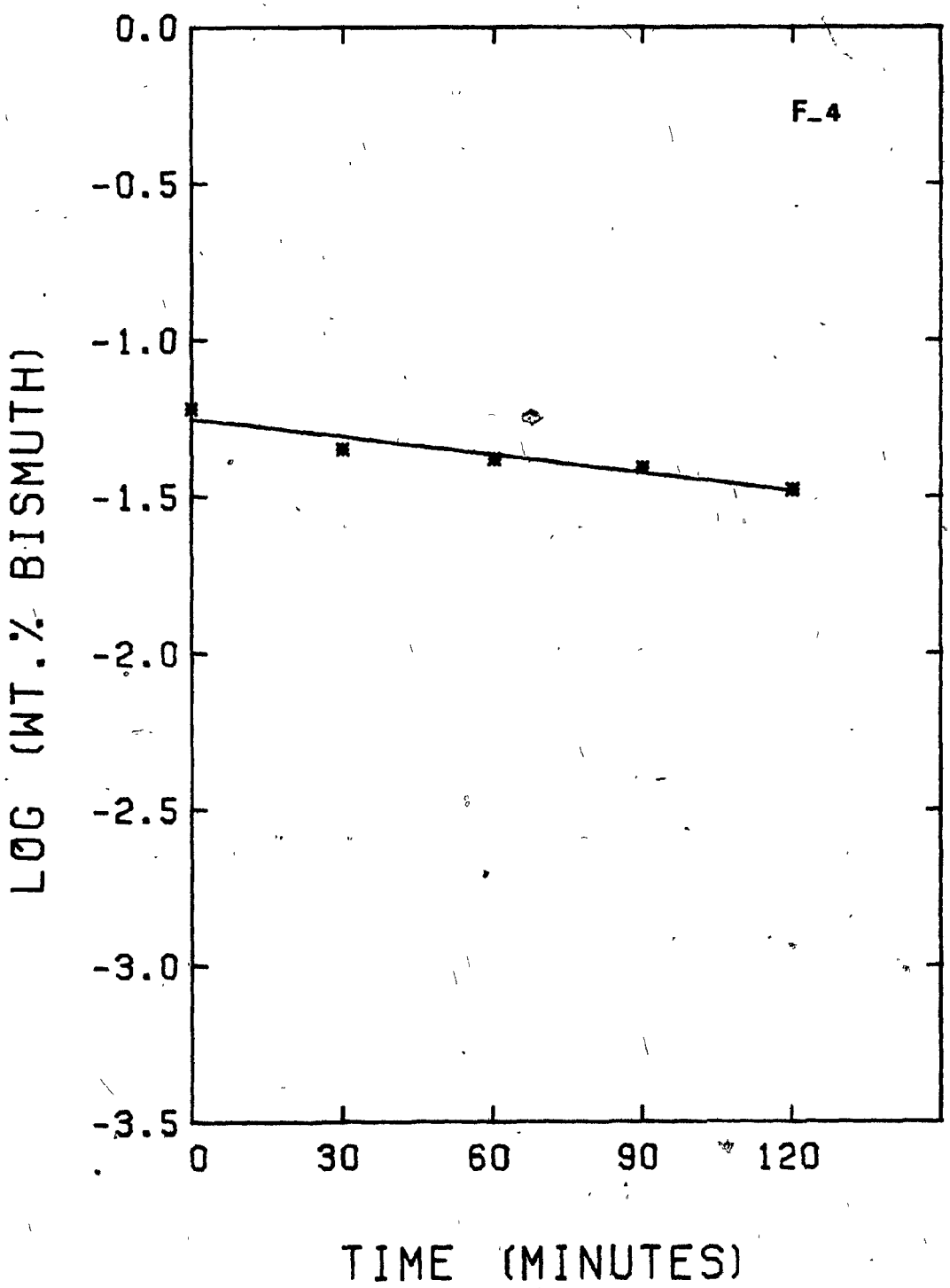
F_4
0.0
-0.5
-1.0
-1.5
-2.0
-2.5
-3.0
-3.5
LOG (WT.% BISMUTH)
0
30
60
90
120
TIME (MINUTES)

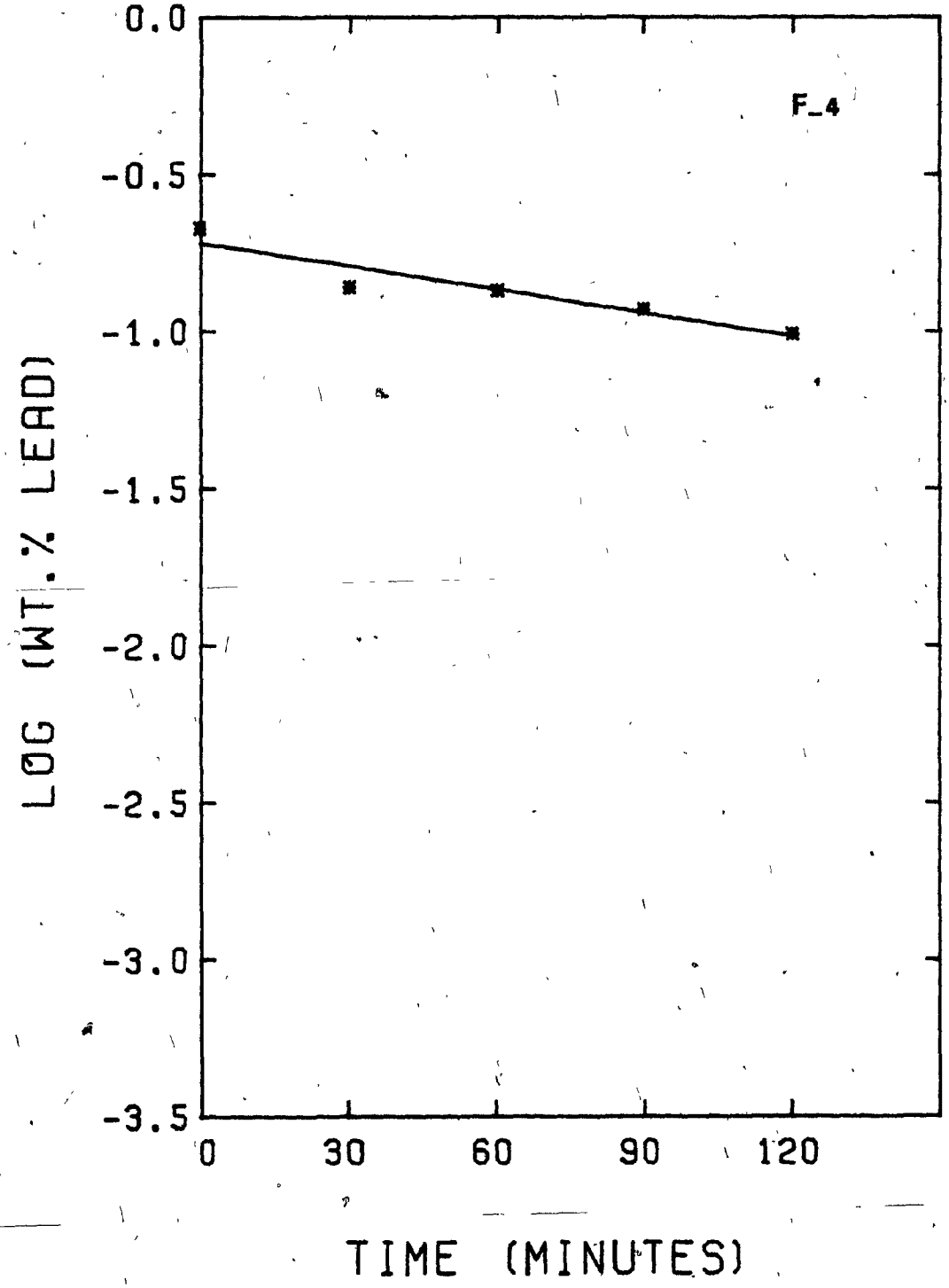
F_4
0.0
-0.5
-1.0
-1.5
-2.0
-2.5
-3.0
-3.5
LOG (WT.% LEAD)
0
30
60
90
120
TIME (MINUTES)

FIGURE 14

Rate of removal of bismuth and lead from copper, Test F-5.

	Bi	Pb
$K(\times 10^{-3}$ cm.s$^{-1})$:	0.652	1.116
Elim'n, wt.%:	38	58

time (min.)	wt.% Bi	wt.% Pb
0	0.050	0.222
30	0.049	0.167
60	0.048	0.156
90	0.039	0.122
120	0.031	0.093

Total copper loss = 130 gr.

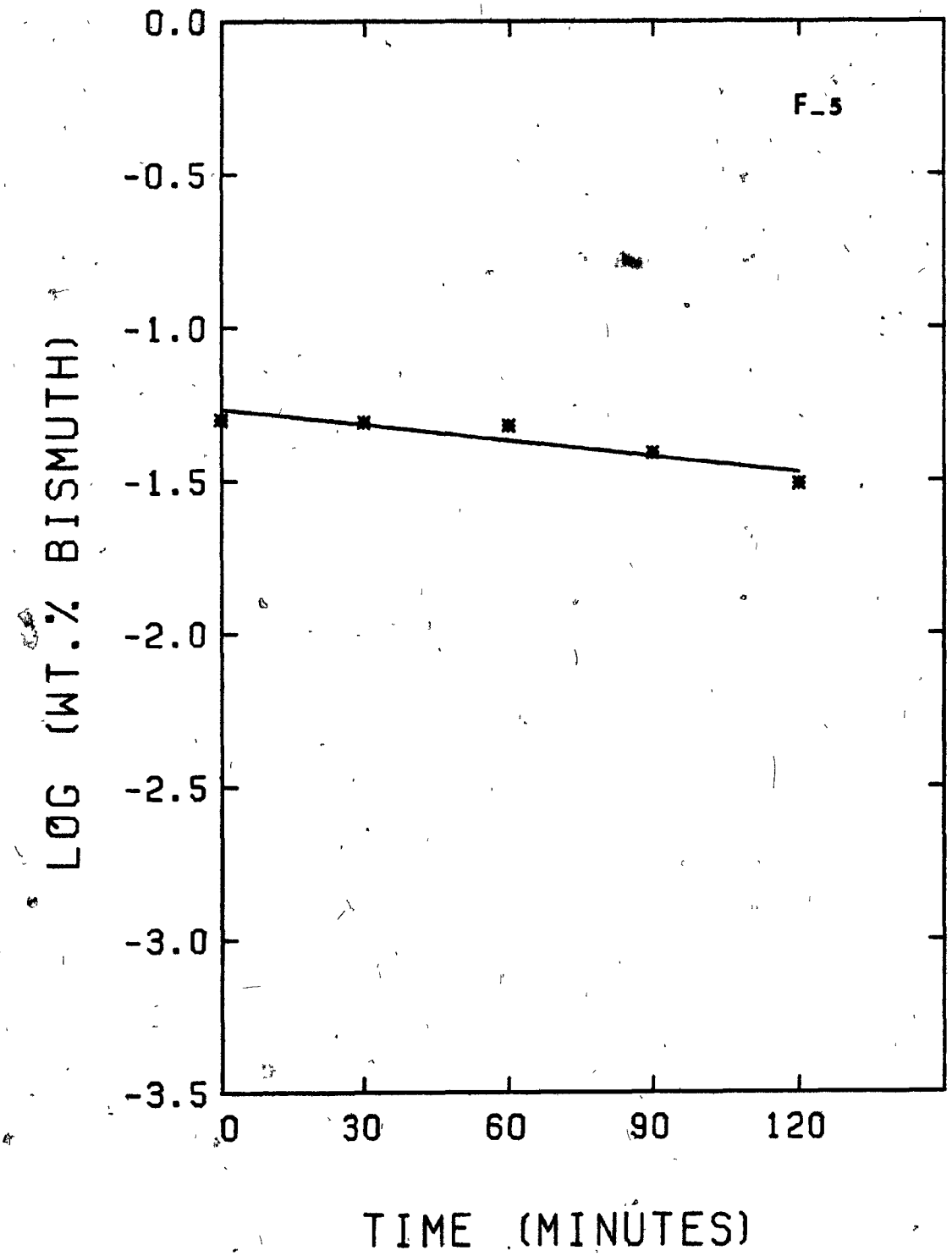
F_5
0.0
-0.5
-1.0
-1.5
-2.0
-2.5
-3.0
-3.5
LOG (WT.% BISMUTH)
0
30
60
90
120
TIME (MINUTES)

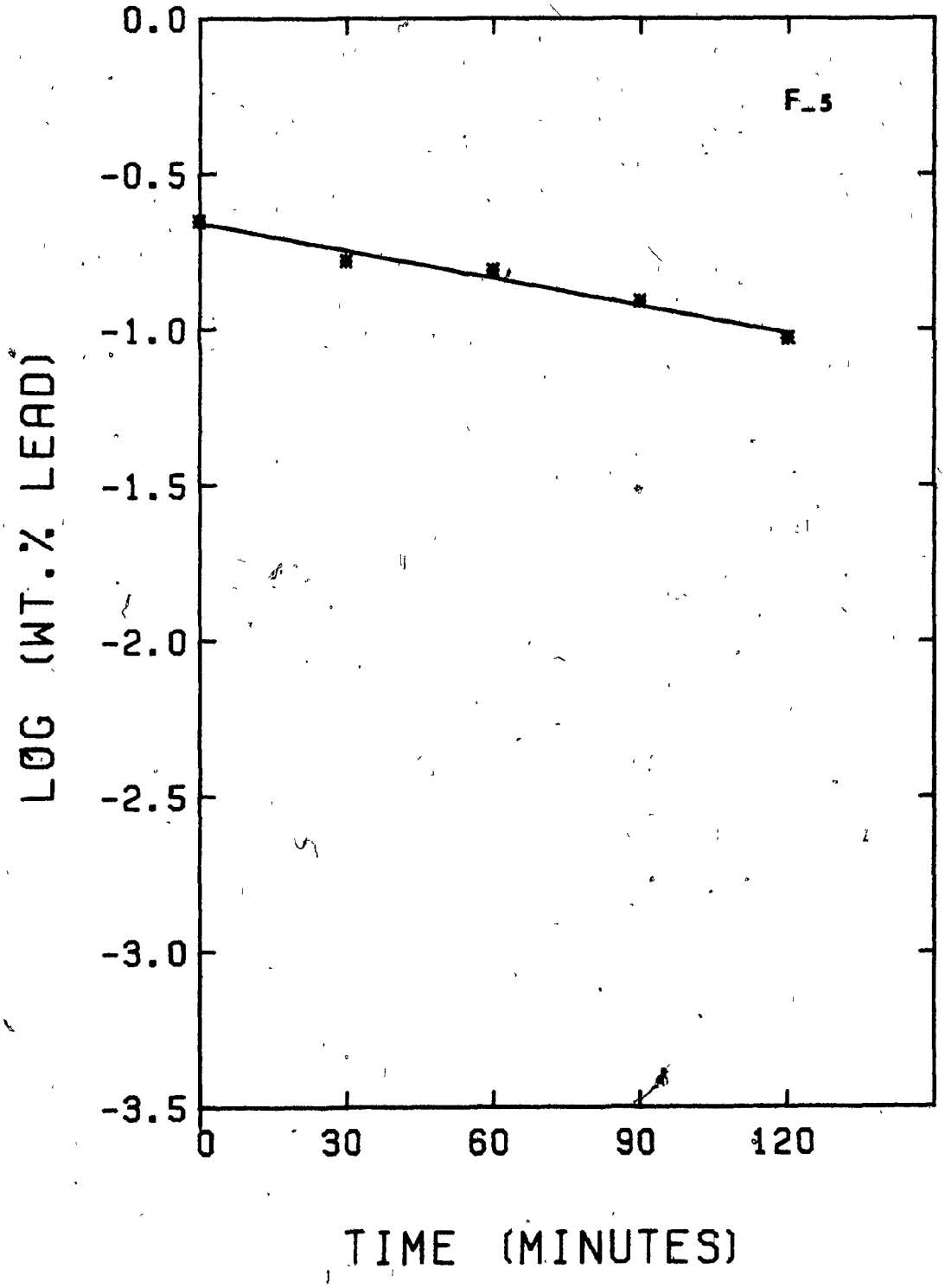
F_5
0.0
-0.5
-1.0
-1.5
-2.0
-2.5
-3.0
-3.5
LOG (WT.% LEAD)
0
30
60
90
120
TIME (MINUTES)

FIGURE 15

Rate of removal of bismuth and lead from copper, Test F-6.

	Bi	Pb
$K(\times 10^{-3}$ cm.s$^{-1})$:	0.389	0.590
Elim'n, wt.%:	22	32

time (min.)	wt.% Bi	wt.% Pb
0	0.032	0.080
30	0.031	0.079
60	0.029	0.066
90	0.025	0.059
120	0.025	0.054

Total copper loss = 100 gr.

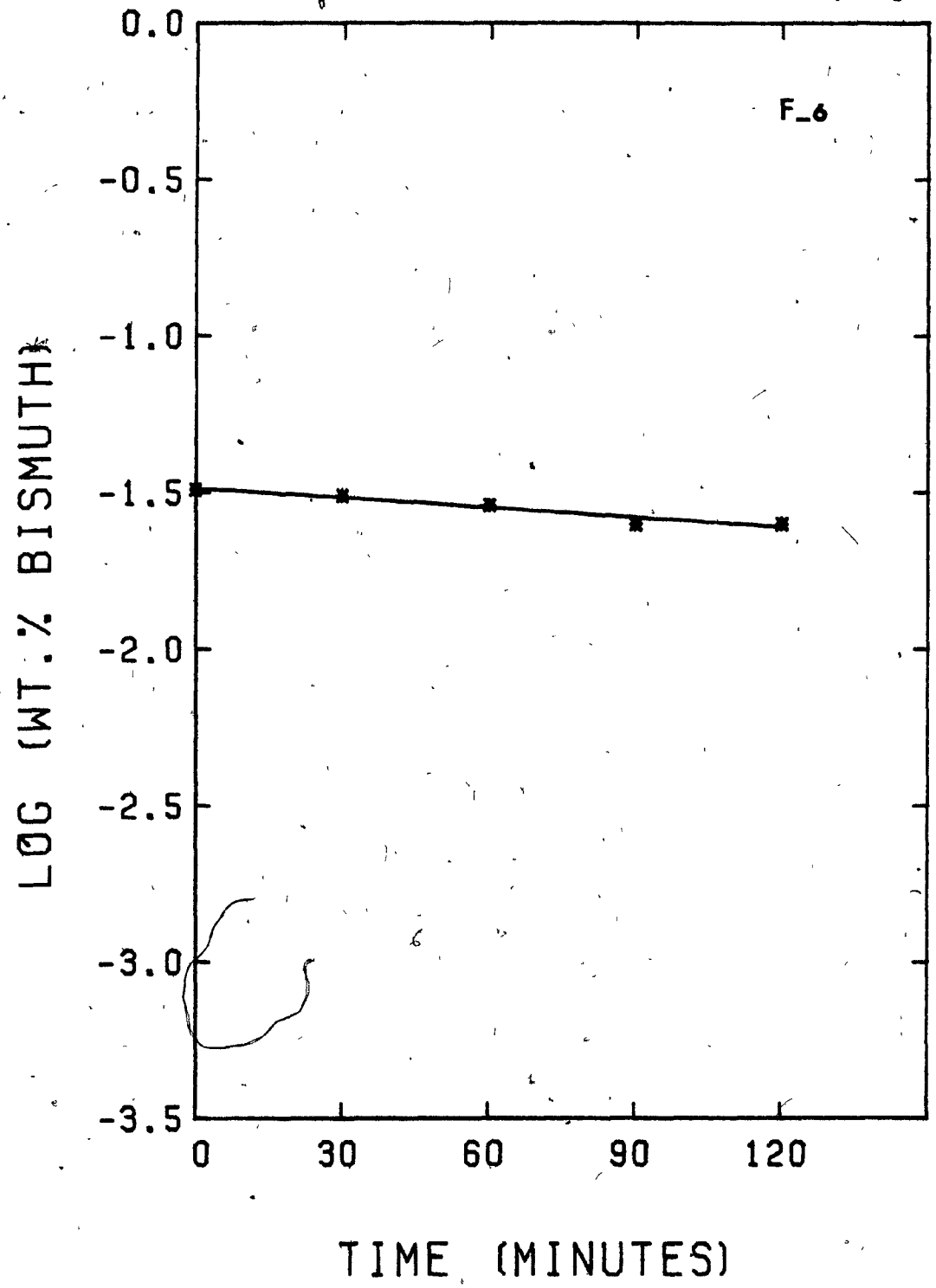
F_6
0.0
-0.5
-1.0
-1.5
-2.0
-2.5
-3.0
-3.5
LOG (WT.% BISMUTH)
0
30
60
90
120
TIME (MINUTES)

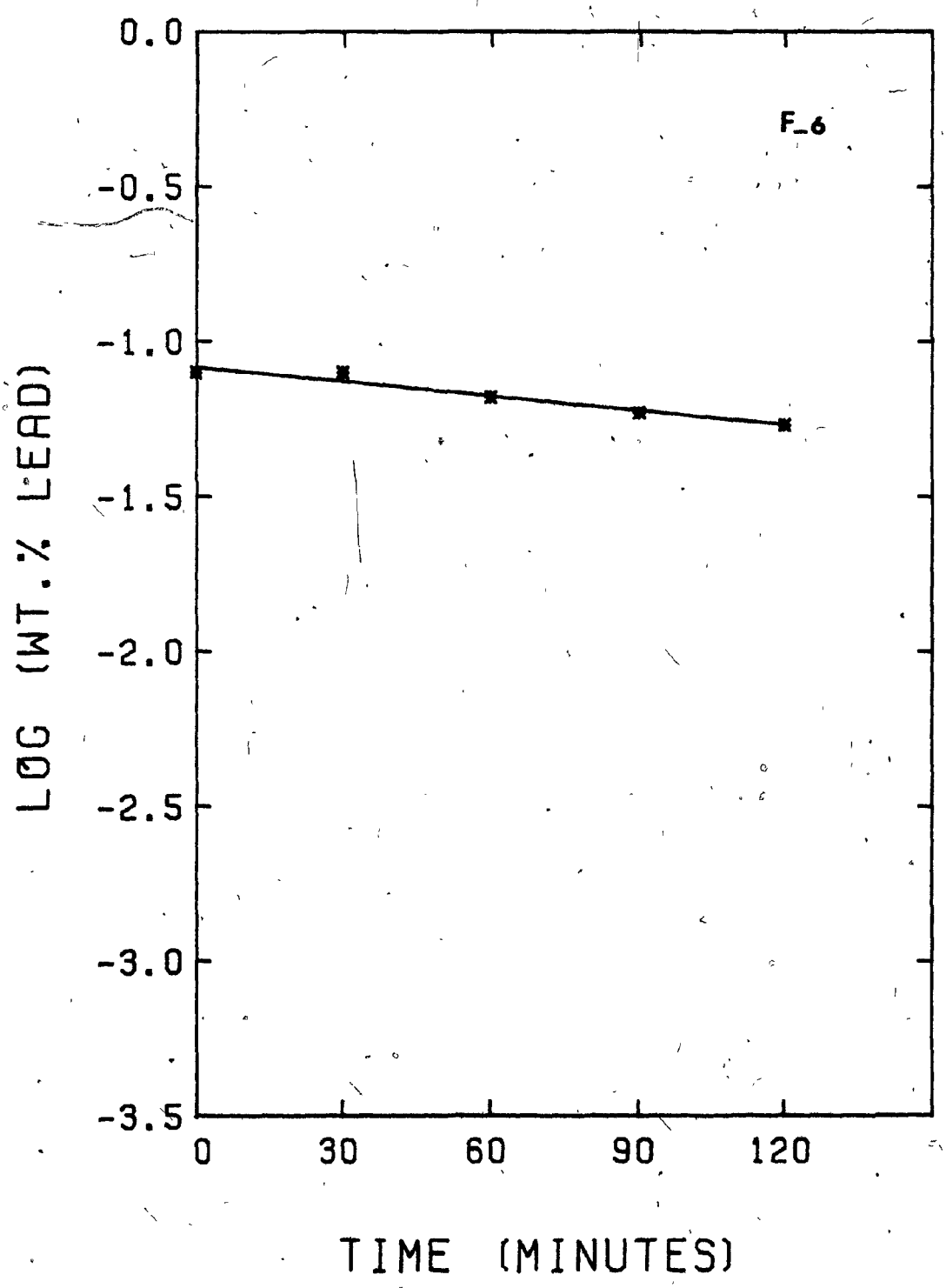
F_6
0.0
-0.5
-1.0
-1.5
-2.0
-2.5
-3.0
-3.5
LOG (WT.% LEAD)
0
30
60
90
120
TIME (MINUTES)

FIGURE 16

Rate of removal of bismuth and lead from copper, Test F-7.

	Bi	Pb
$K(\times 10^{-3}$ cm.s$^{-1})$:	1.794	2.521
Elim'n, wt.%:	75	85

time (min.)	wt.% Bi	wt.% Pb
0	0.044	0.126
30	0.037	0.107
60	0.023	0.049
90	0.022	0.046
120	0.011	0.019

Total copper loss = 290 gr.

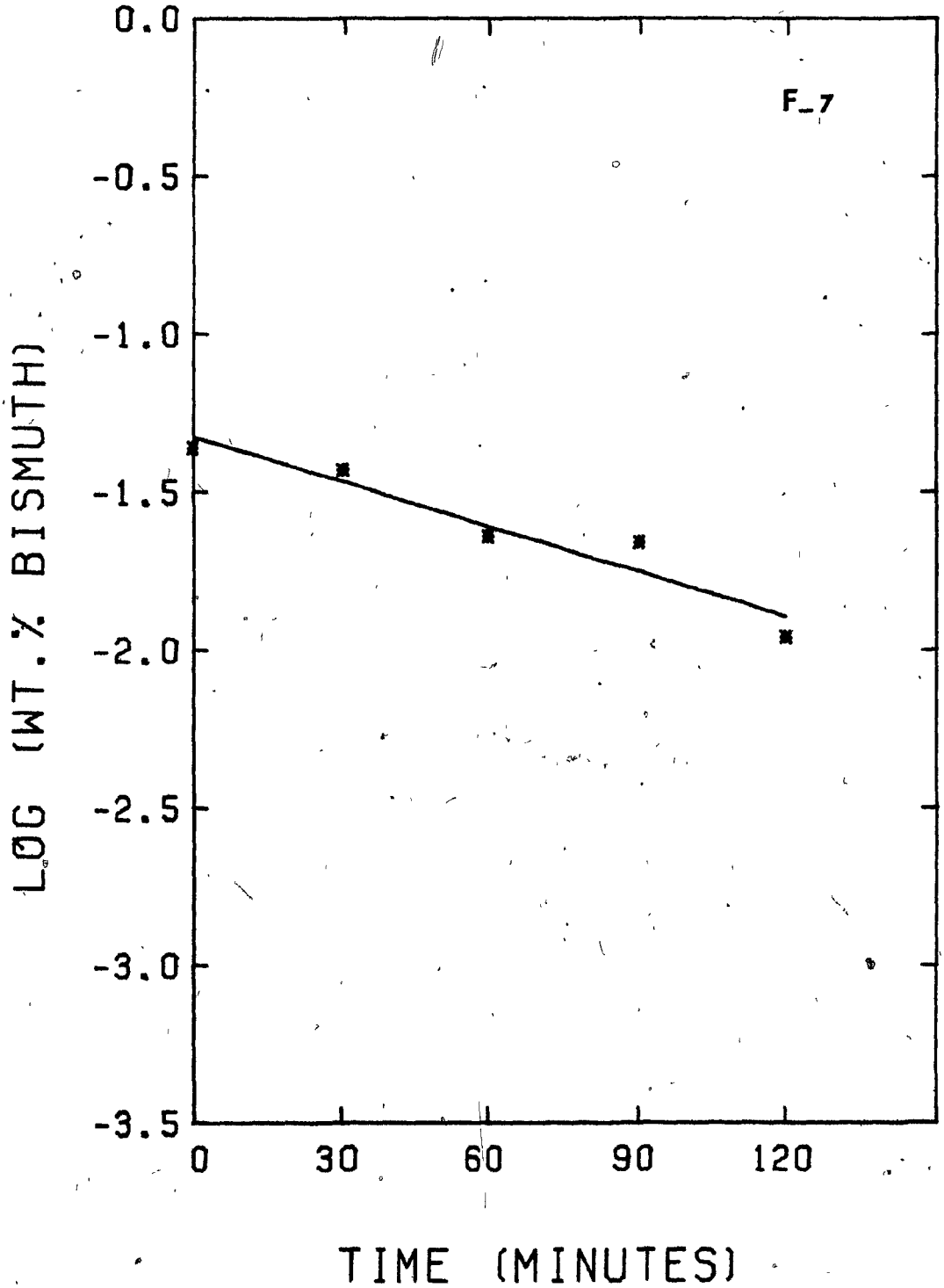
F_7
0.0
-0.5
-1.0
-1.5
-2.0
-2.5
-3.0
-3.5
LØG (WT.% BISMUTH)
0
30
60
90
120
TIME (MINUTES)

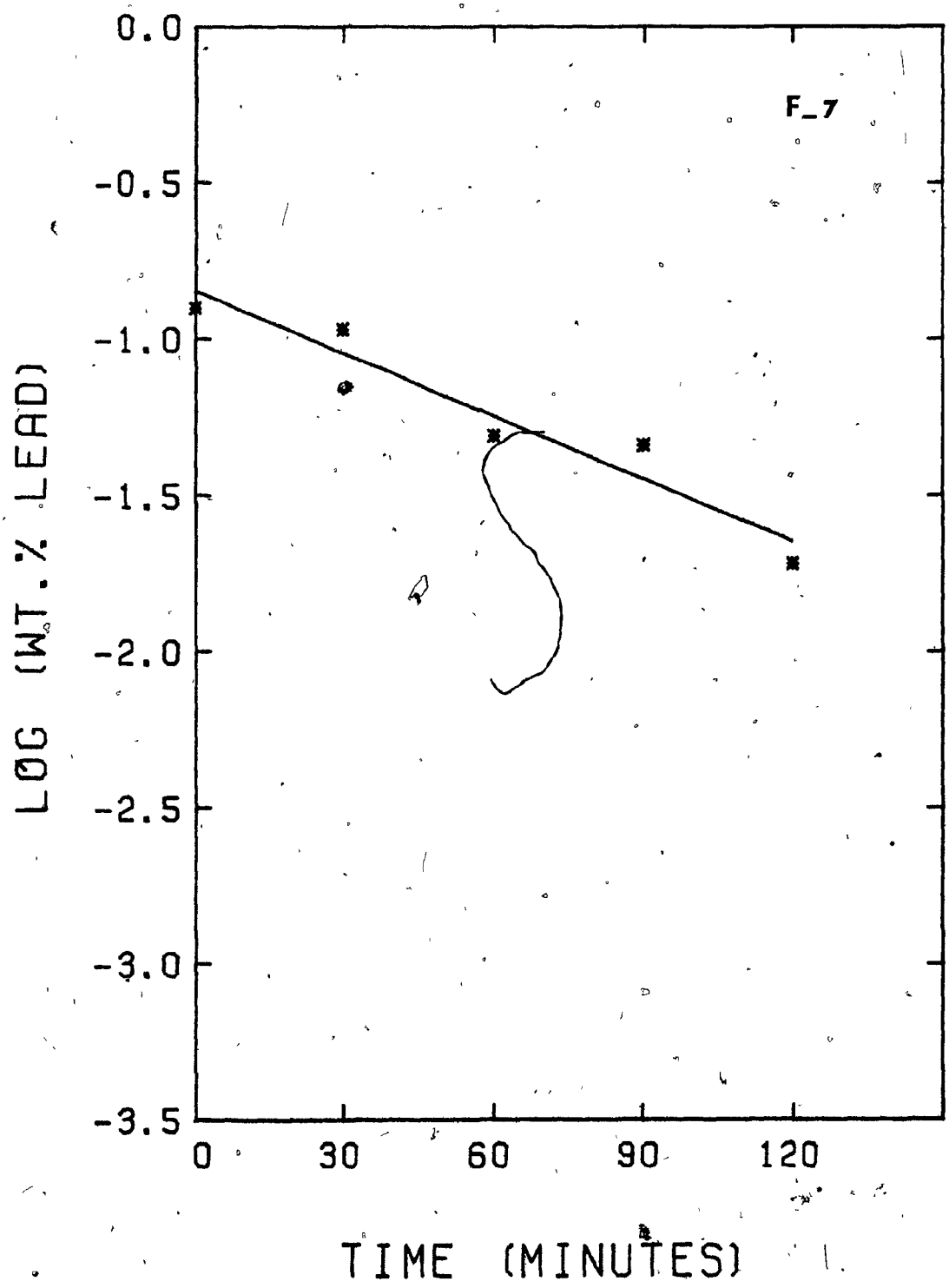
F_7
0.0
-0.5
-1.0
-1.5
-2.0
-2.5
-3.0
-3.5
LOG (WT.% LEAD)
0
30
60
90
120
TIME (MINUTES)

FIGURE 17

Rate of removal of bismuth and lead from copper, Test F-8.

	Bi	Pb
$K(\times 10^{-3}$ cm.s$^{-1})$:	0.991	1.656
Elim'n, wt.%:	53	71

time (min.)	wt.% Bi	wt.% Pb
0	0.017	0.035
30	0.012	0.021
60	0.010	0.015
90	0.009	0.012
120	0.008	0.010

Total copper loss = 240 gr.

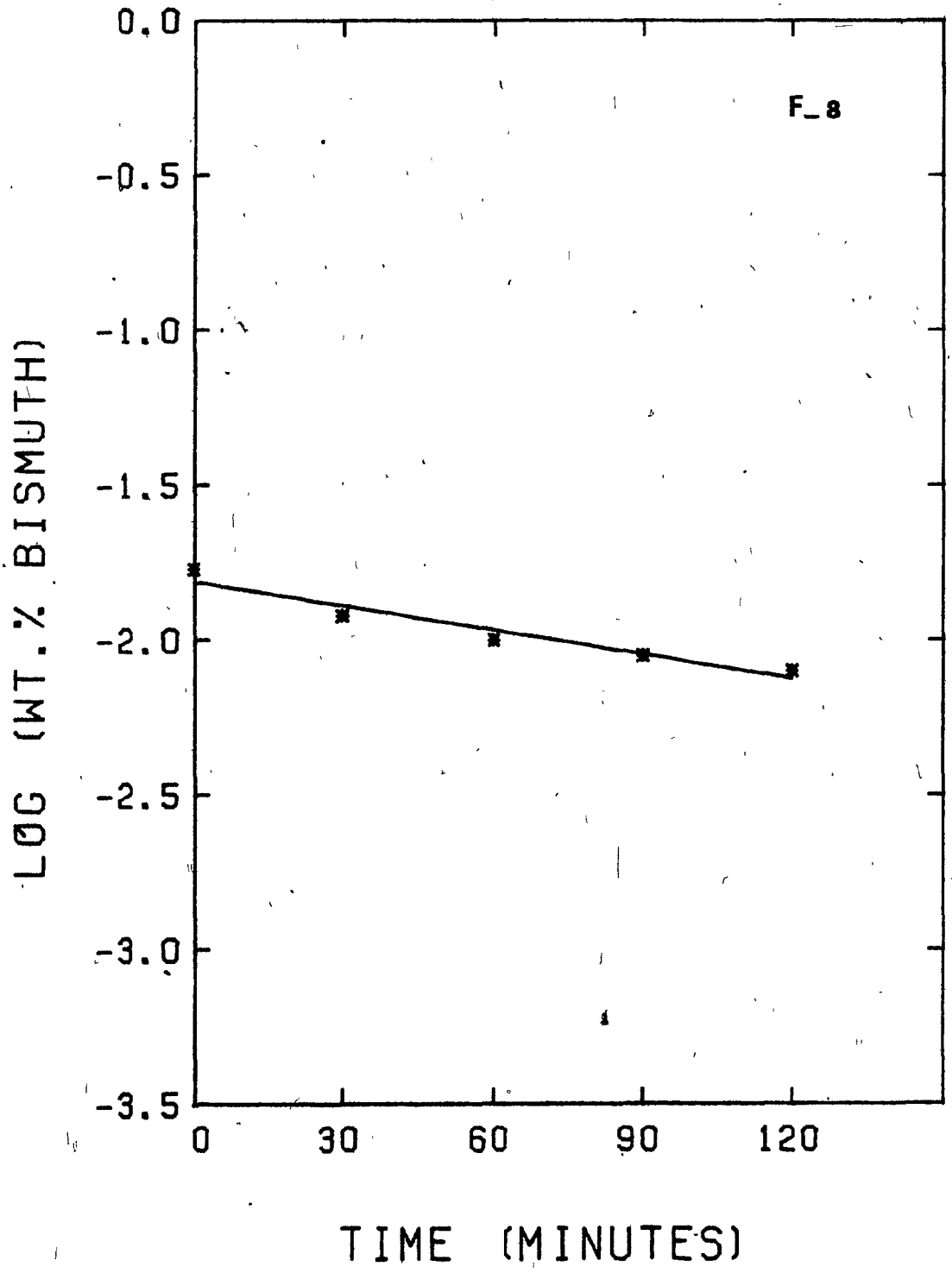
F_8
0.0
-0.5
-1.0
-1.5
-2.0
-2.5
-3.0
-3.5
LOG (WT.% BISMUTH)
0
30
60
90
120
TIME (MINUTES)

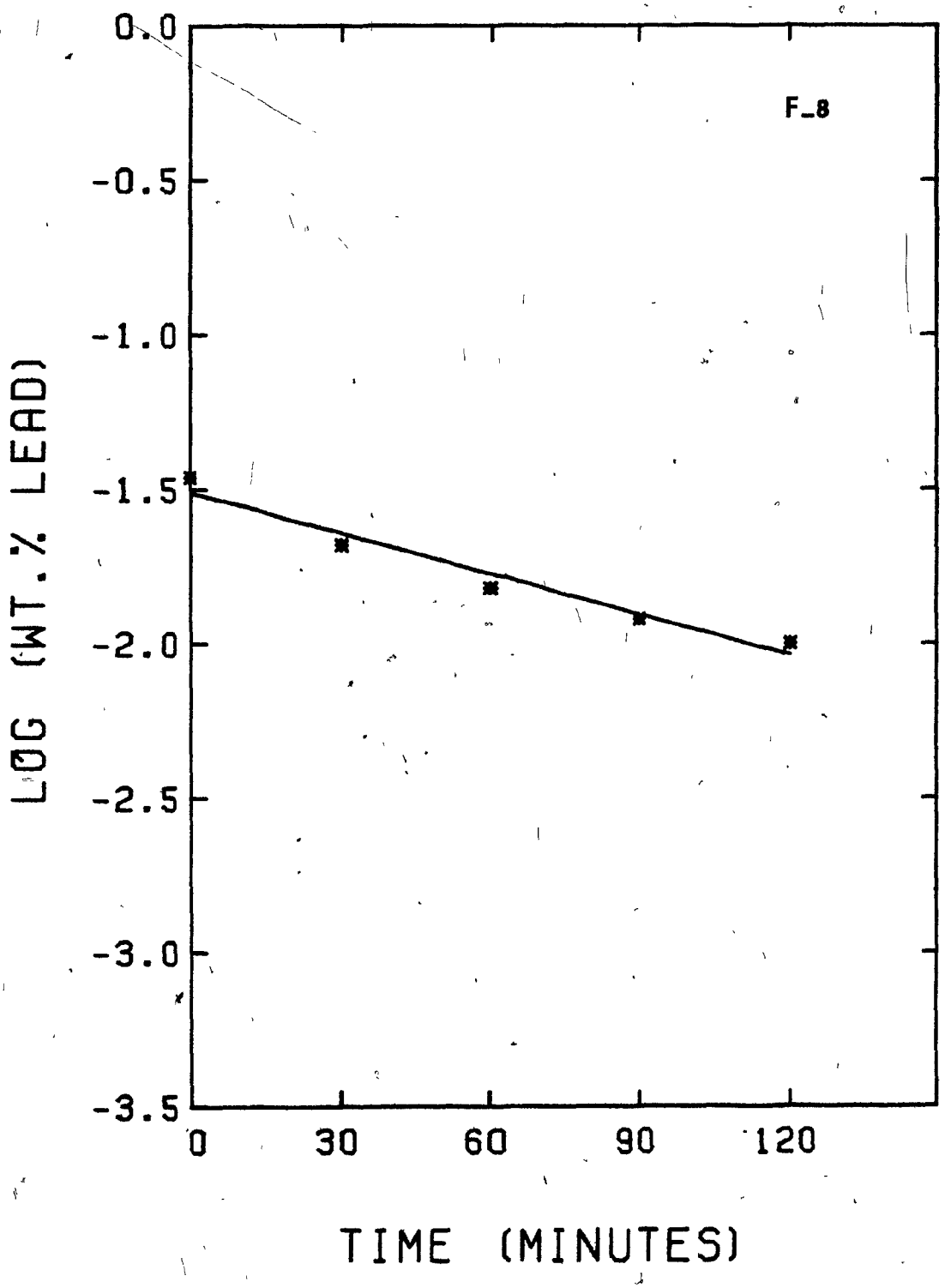
F_8
0.0
-0.5
-1.0
-1.5
-2.0
-2.5
-3.0
-3.5
LOG (WT.% LEAD)
0
30
60
90
120
TIME (MINUTES)

lead followed first order kinetics very closely, the correlation coefficient never dropping below 0.916 for bismuth or 0.943 for lead.

The results of the 2^{4-1} fractional factorial test design evaluation were as follows:

Method (a): By estimating the mean square(error variance) from two-factor interactions with one and three degrees of freedom (Appendix IV, Table IV-3-a) and using 5 and 10% levels of f-test, melt temperature and vacuum pressure were shown to be significantly effective on the overall mass transfer coefficient of both bismuth and lead compared to the effects of melt surface area to volume ratio and the distance of the condenser to melt surface (Appendix IV, Table IV-3-b).

Method (b): In the second method, by estimating the error variance from the variance obtained from duplication of two experiments (Appendix IV, Table IV-4-a), similar results were obtained. Melt temperature and vacuum pressure were highly significant at 1% level of f-test with one and two degrees of freedom for the error variance obtained from duplication of tests f-1 and f-3 (Appendix IV, Table IV-4-b). In addition, at 5 and 10% levels of f-test with one and two degrees of freedom, it was determined that the interaction effects of BC and AD (that is combined effects of melt temperature and A/V and the combined effects of vacuum pressure and the condenser distance to the melt surface) were

also significant for both bismuth and lead (Appendix IV, Table IV-4-b). Further analysis of the effects of interactions with a two-way table of total effects (Appendix IV, Table IV-5) showed very little difference in between AD and BC. As a consequence it was not possible to determine which set was the most significant. However, a tendency for the overall mass transfer coefficient to increase with decreasing levels of A and D (pressure and condenser distance) or with increasing levels of B and C (temperature and A/V) is apparent.

Summarizing, overall mass transfer coefficients for both bismuth and lead increase significantly with:

a - increasing melt temperature

b - decreasing vacuum pressure

They also increase slightly with the combined effects of:

c - decreasing vacuum pressure - decreasing distance of condenser to melt surface

d - increasing melt temperature - increasing A/V.

V-4. PART II EXPERIMENTS

In order to obtain a quantitative relationship between the overall mass transfer coefficient K, and the variables melt temperature and vacuum pressure, further experimental investigations were needed. Thus, the experiments in Part II were mainly concerned with the effect of vacuum pressure and melt temperature on K_{Bi} and K_{Pb} .

A total of six experiments were carried out at three different temperatures 1150°-1250°-1350°C and two different pressures 100 - 60 μHg. The melt surface area to volume ratio was kept constant at 7.1 m^{-1} and again the treatment time was 120 minutes in all experiments. The water cooled condenser was not used in these set of experiments. A summary of all the results obtained, together with the experimental conditions involved, are provided in Table 10 for bismuth and lead. The logarithm of the relative impurity weight change (in percent) with time was plotted in the same way as Part I and these are given in figures 18-23 inclusive.

Consistent with the previous results, it was observed that K_{Pb} was always higher than K_{Bi}. The rate of removal of both bismuth and lead exhibited definite first order kinetics (correlation coefficient was never below 0.971 for bismuth nor 0.965 for lead).

By increasing the temperature from 1150°C to 1350°C and decreasing the pressure from 100 μHg to 60 μHg, it was possible to increase K_{Bi} from 1.05×10^{-3} cms^{-1} to 3.15×10^{-3} cms^{-1} and K_{Pb} from 1.84×10^{-3} cms^{-1} to 4.70×10^{-3} cms^{-1}.

The results of Part I and II experiments showed that bismuth and lead can be removed from copper melts under vacuum and that lower vacuum pressures and higher melt temperatures were the key factors in increasing their rate

TABLE 10a. Summary of Experimental Conditions[1] and Results, Part II Experiments, Bismuth

				BISMUTH							
Test No	Press. μHg	Temp. °C	$K_L(10^{-3}$ cm/s)	Corr. Coeff.	$K(10^{-3}$ cm/s)	$K_E(10^{-3}$ cm/s)	$K_U(10^{-3}$ cm/s)	K_G (cm/s)	Initial wt%	Final wt%	Elim'n wt%
A-6	60	1150	5.09	0.986	1.32	28.44	1.89	631	0.030	0.015	50
A-3	60	1250	7.21	0.996	2.76	62.90	4.81	750	0.038	0.010	74
A-5	60	1350	9.78	0.990	3.15	125.40	4.84	391	0.030	0.006	80
A-1	100	1150	5.09	0.971	1.05	28.44	1.38	460	0.038	0.022	42
A-2	100	1250	7.21	0.986	1.86	62.90	2.60	406	0.020	0.008	60
A-4	100	1350	9.78	0.996	2.33	125.40	3.13	252	0.020	0.006	70

1. Copper weight = 34 kilogram, A/V = 7.1 m^{-1}, Condenser Distance > 65 cm, time = 120 minutes.

TABLE 10b. Summary of Experimental Conditions[1] and Results, Part II Experiments, Lead

				LEAD							
Test No	Press. μHg	Temp. °C	$K_L(10^{-3}$ cm/s)	Corr. Coeff.	$K(10^{-3}$ cm/s)	$K_E(10^{-3}$ cm/s)	$K_U(10^{-3}$ cm/s)	K_G (cm/s)	Initial wt%	Final wt%	Elim'n wt%
A-6	60	1150	5.09	0.965	2.00	47.92	3.54	704	0.071	0.025	65
A-3	60	1250	7.21	0.979	4.04	97.53	10.13	1024	0.059	0.006	90
A-5	60	1350	9.78	0.993	4.70	180.99	9.54	536	0.059	0.006	90
A-1	100	1150	5.09	0.988	1.84	47.92	3.06	609	0.096	0.038	60
A-2	100	1250	7.21	0.997	2.52	97.53	4.04	409	0.028	0.007	75
A-4	100	1350	9.78	0.994	3.93	180.99	6.81	383	0.027	0.004	85

1. Copper weight = 34 kilogram, A/V = 7.1 m^{-1}, Condenser Distance > 65 cm, time = 120 minutes.

FIGURE 18

Rate of removal of bismuth and lead from copper, Test A-6.*

	Bi	Pb
K($\times 10^{-3}$ cm.s^{-1}):	1.316	2.000
Elim'n, wt.%:	50	65

time (min.)	wt.% Bi	wt.% Pb
0	0.030	0.071
30	0.026	0.060
60	0.020	0.055
90	0.019	0.037
120	0.015	0.025

Total copper loss = 200 gr.

*The order of appearance of the figures follows the order in Table 10.

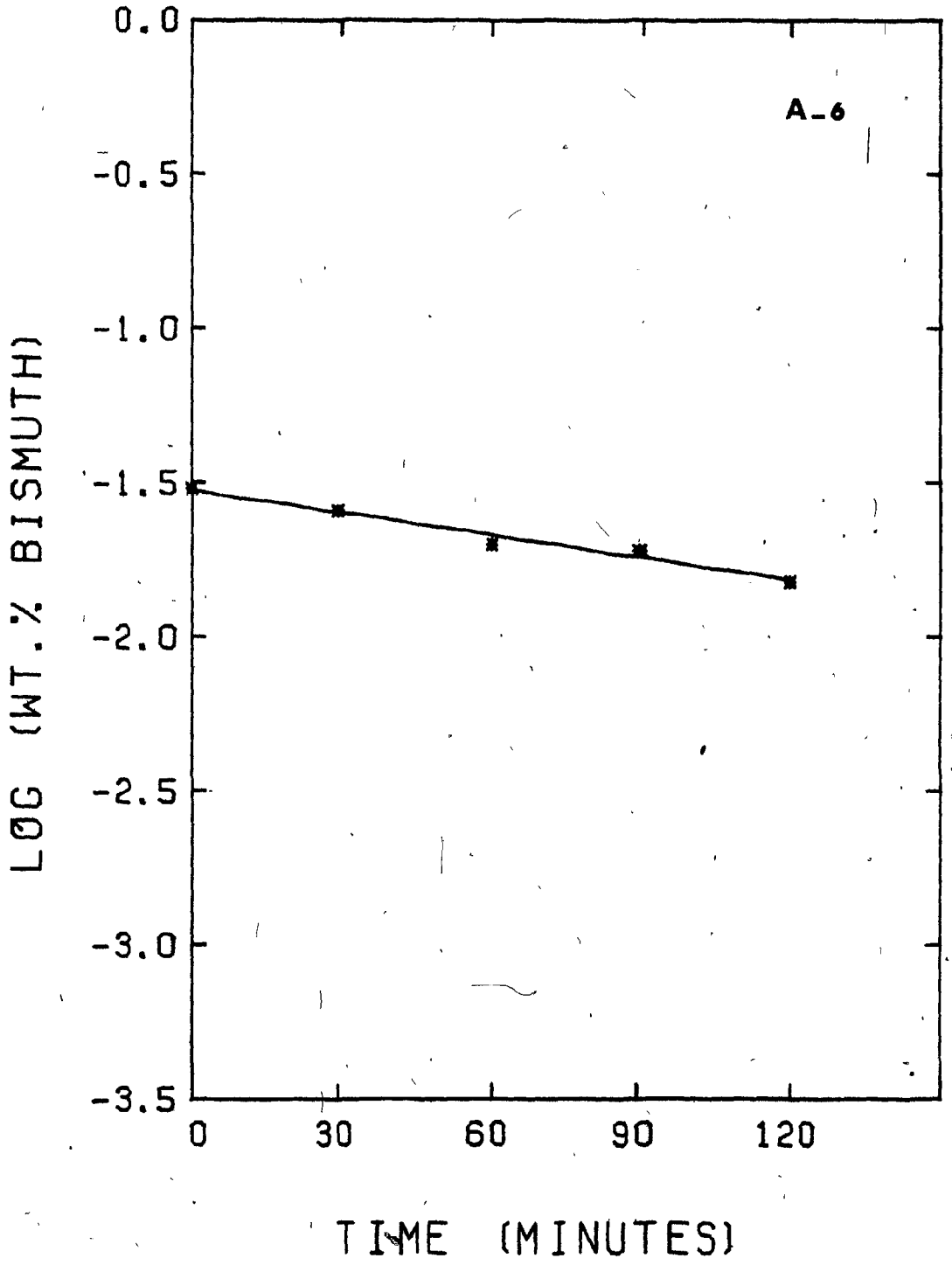
A-6
0.0
-0.5
-1.0
-1.5
-2.0
-2.5
-3.0
-3.5
LOG (WT.% BISMUTH)
0
30
60
90
120
TIME (MINUTES)

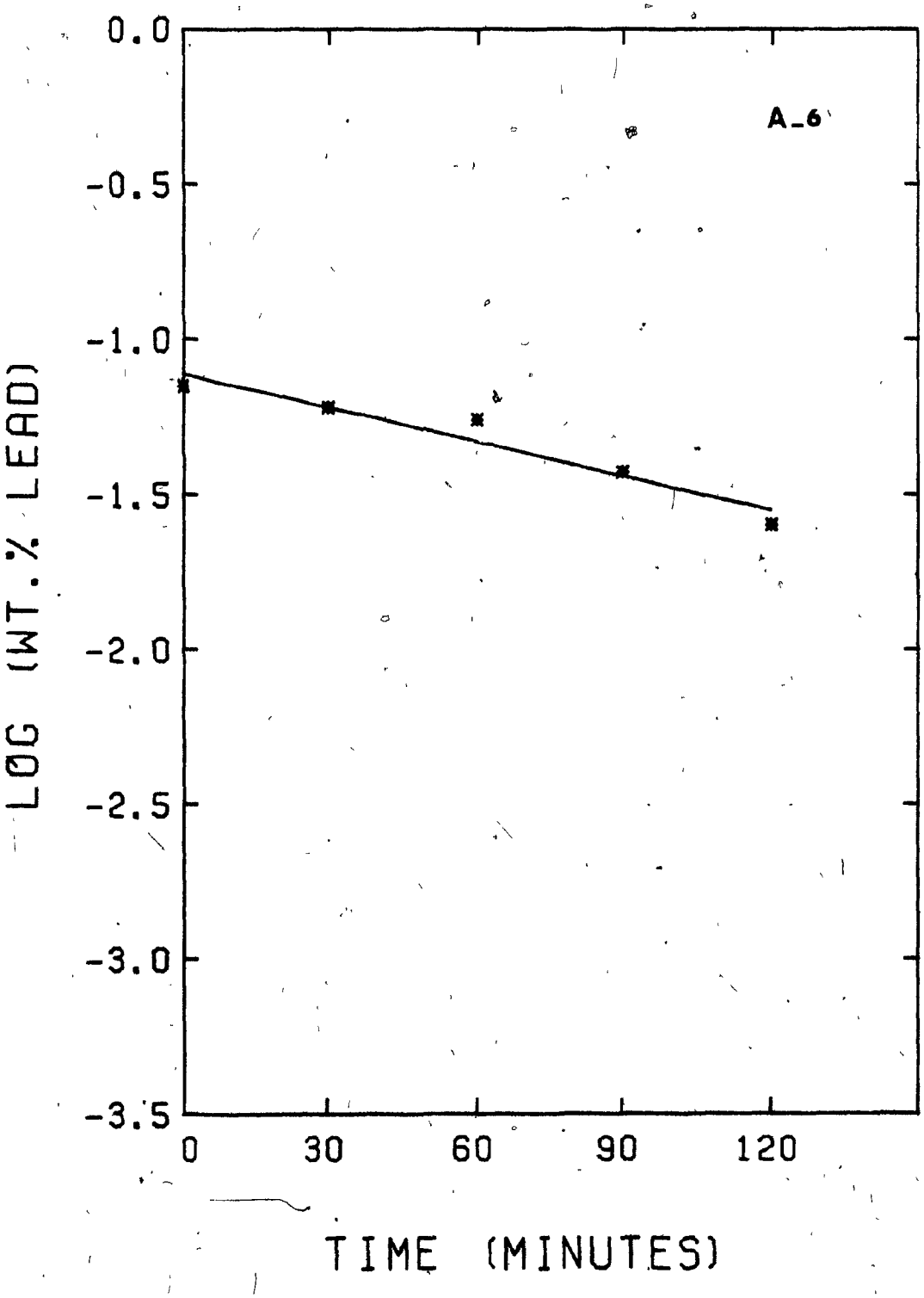
A_6
0.0
-0.5
-1.0
-1.5
-2.0
-2.5
-3.0
-3.5
LOG (WT.% LEAD)
0
30
60
90
120
TIME (MINUTES)

FIGURE 19

Rate of removal of bismuth and lead from copper, Test A-3.

	Bi	Pb
$K(\times 10^{-3}$ cm.s$^{-1})$:	2.757	4.037
Elim'n, wt.%:	74	90

time (min.)	wt.% Bi	wt.% Pb
0	0.038	0.059
30	0.030	0.026
60	0.021	0.019
90	0.013	0.014
120	0.010	0.006

Total copper loss = 280 gr.

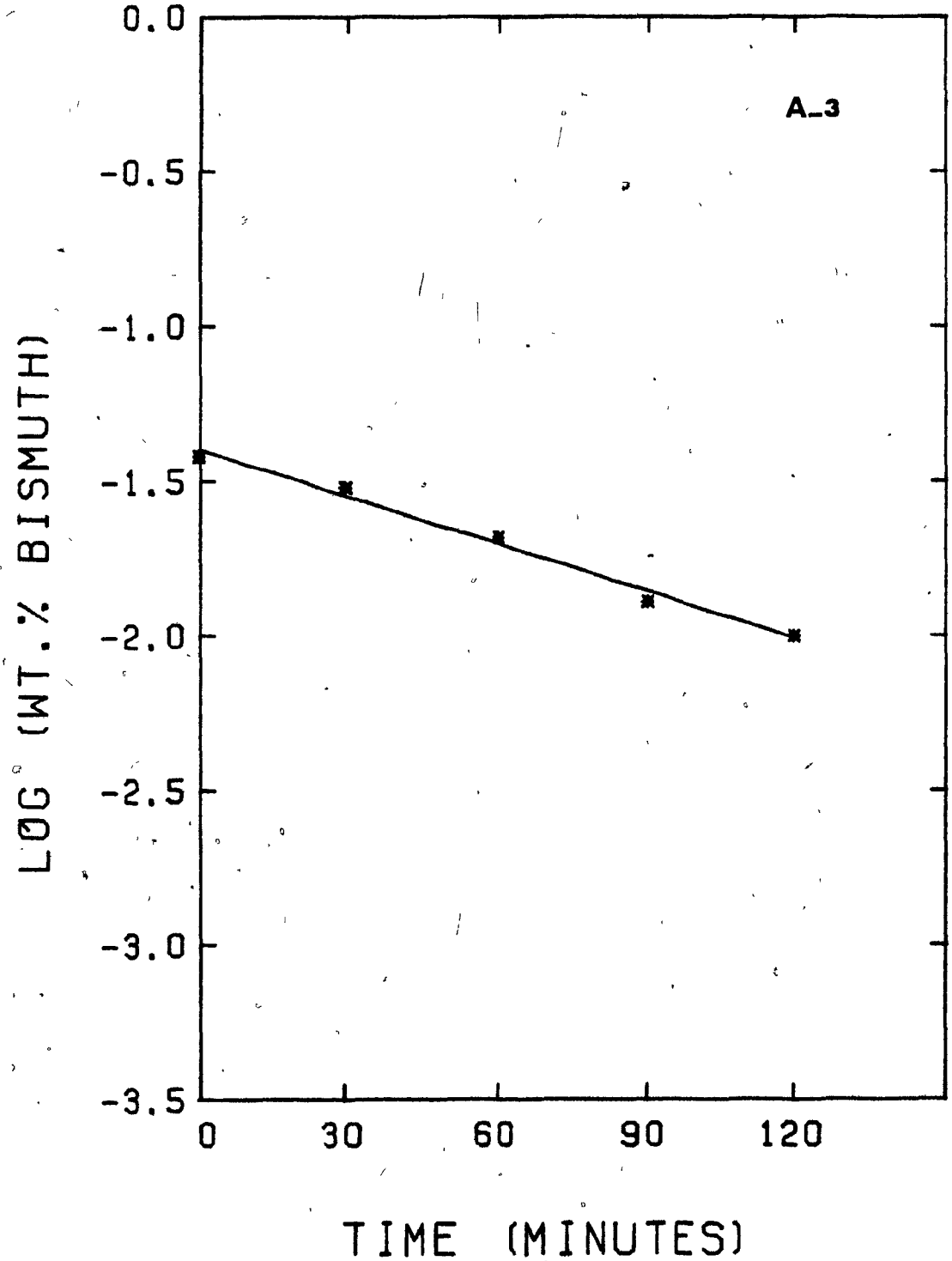
A_3
0.0
-0.5
-1.0
-1.5
-2.0
-2.5
-3.0
-3.5
LOG (WT.% BISMUTH)
0
30
60
90
120
TIME (MINUTES)

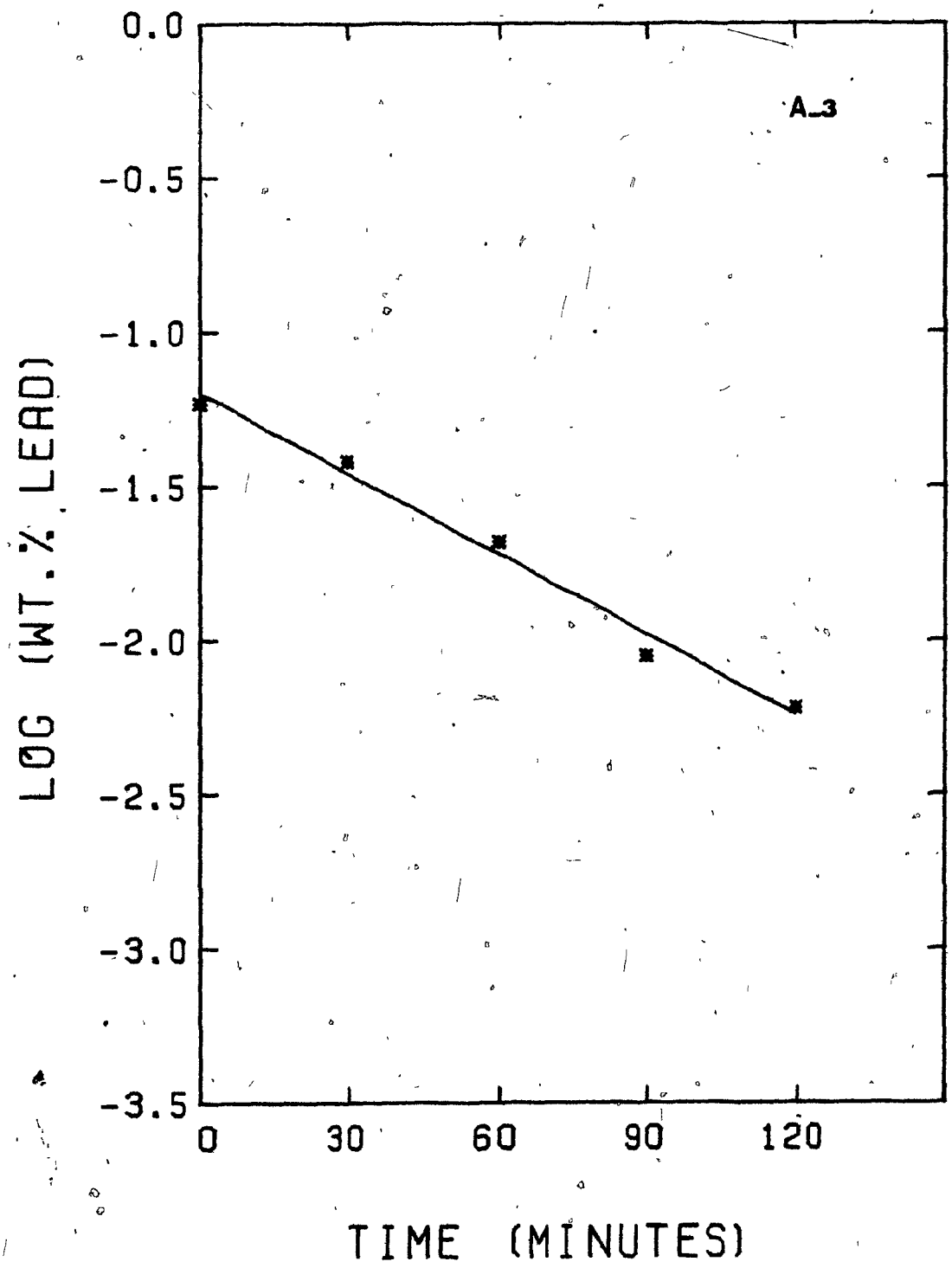
A_3
0.0
-0.5
-1.0
-1.5
-2.0
-2.5
-3.0
-3.5
LOG (WT.% LEAD)
0
30
60
90
120
TIME (MINUTES)

FIGURE 20

Rate of removal of bismuth and lead from copper, Test A-5.

	Bi	Pb
$K(\times 10^{-3}$ cm.s$^{-1})$:	3.154	4.703
Elim'n, wt.%:	80	90

time (min.)	wt.% Bi	wt.% Pb
0	0.030	0.059
30	0.020	0.038
60	0.011	0.021
90	0.009	0.009
120	0.006	0.006

Total copper loss = 300 gr.

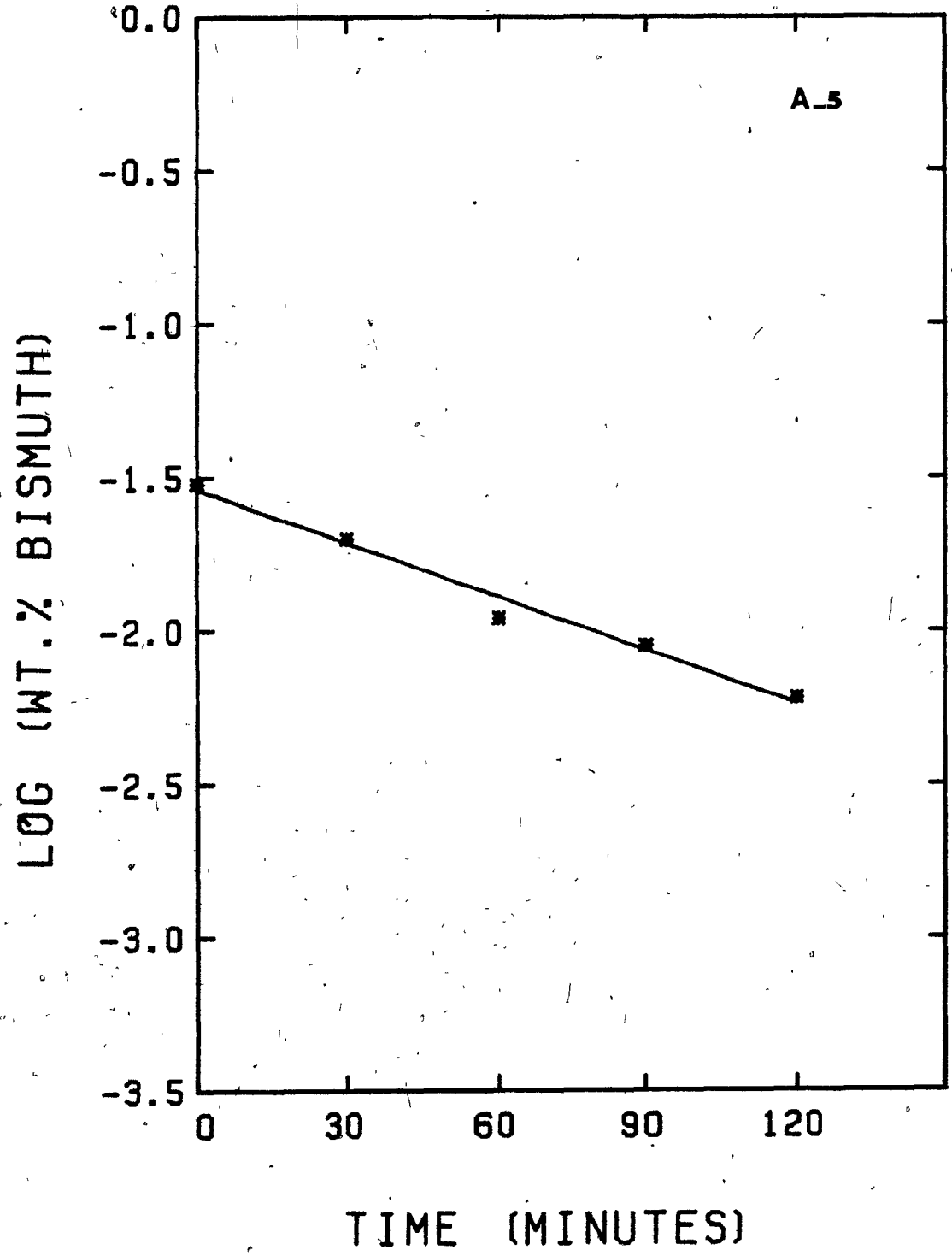
0.0
-0.5
-1.0
-1.5
-2.0
-2.5
-3.0
-3.5
A_5
LOG (WT.% BISMUTH)
0
30
60
90
120
TIME (MINUTES)

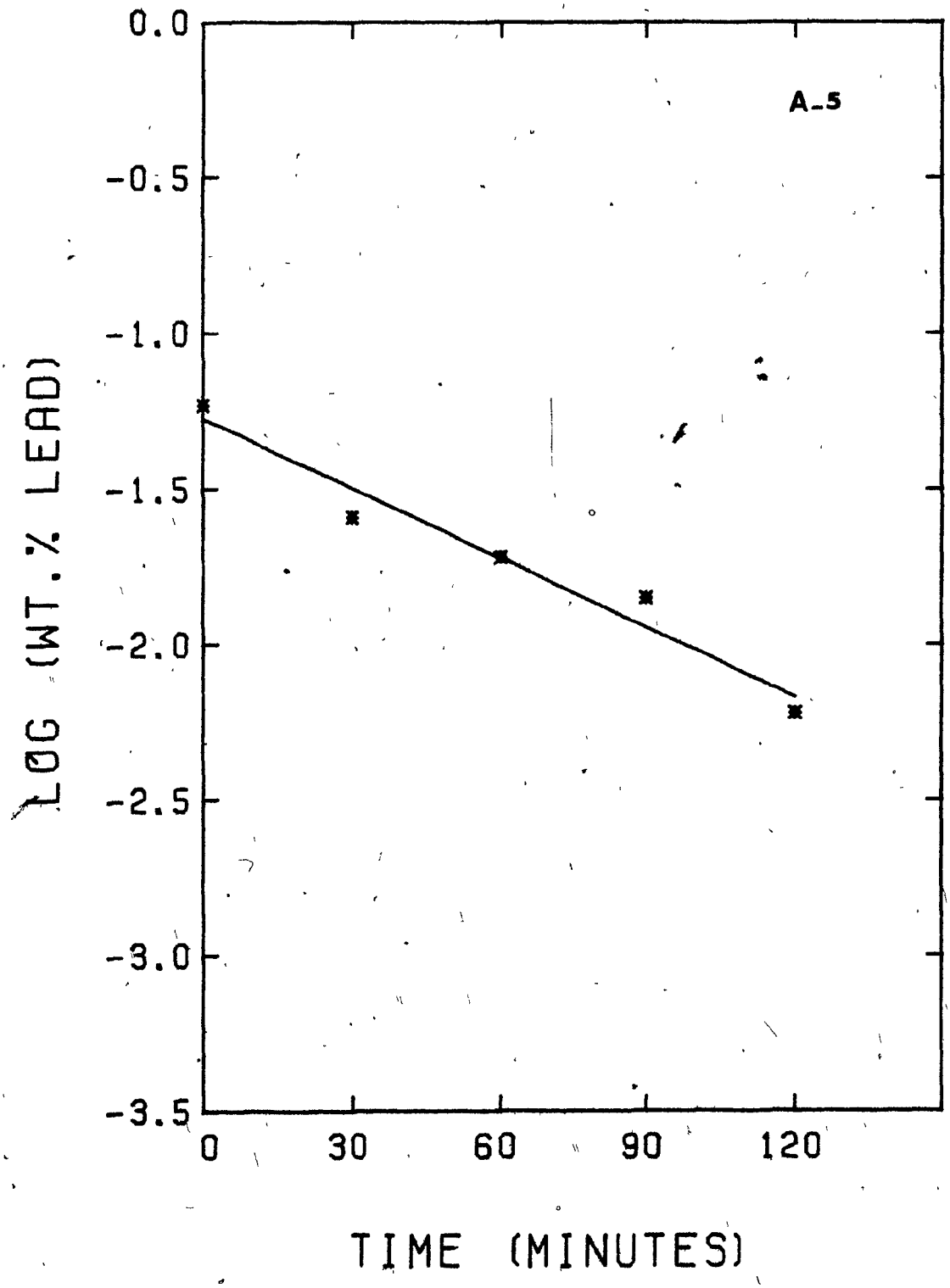
A-5
0.0
-0.5
-1.0
-1.5
-2.0
-2.5
-3.0
-3.5
LOG (WT.% LEAD)
0
30
60
90
120
TIME (MINUTES)

FIGURE 21

Rate of removal of bismuth and lead from copper, Test A-1.

	Bi	Pb
$K(\times 10^{-3}$ cm.s$^{-1})$:	1.045	1.838
Elim'n, wt.%:	42	60

time (min.)	wt.% Bi	wt.% Pb
0	0.038	0.096
30	0.030	0.071
60	0.026	0.054
90	0.024	0.043
120	0.022	0.038

Total copper loss = 180 gr.

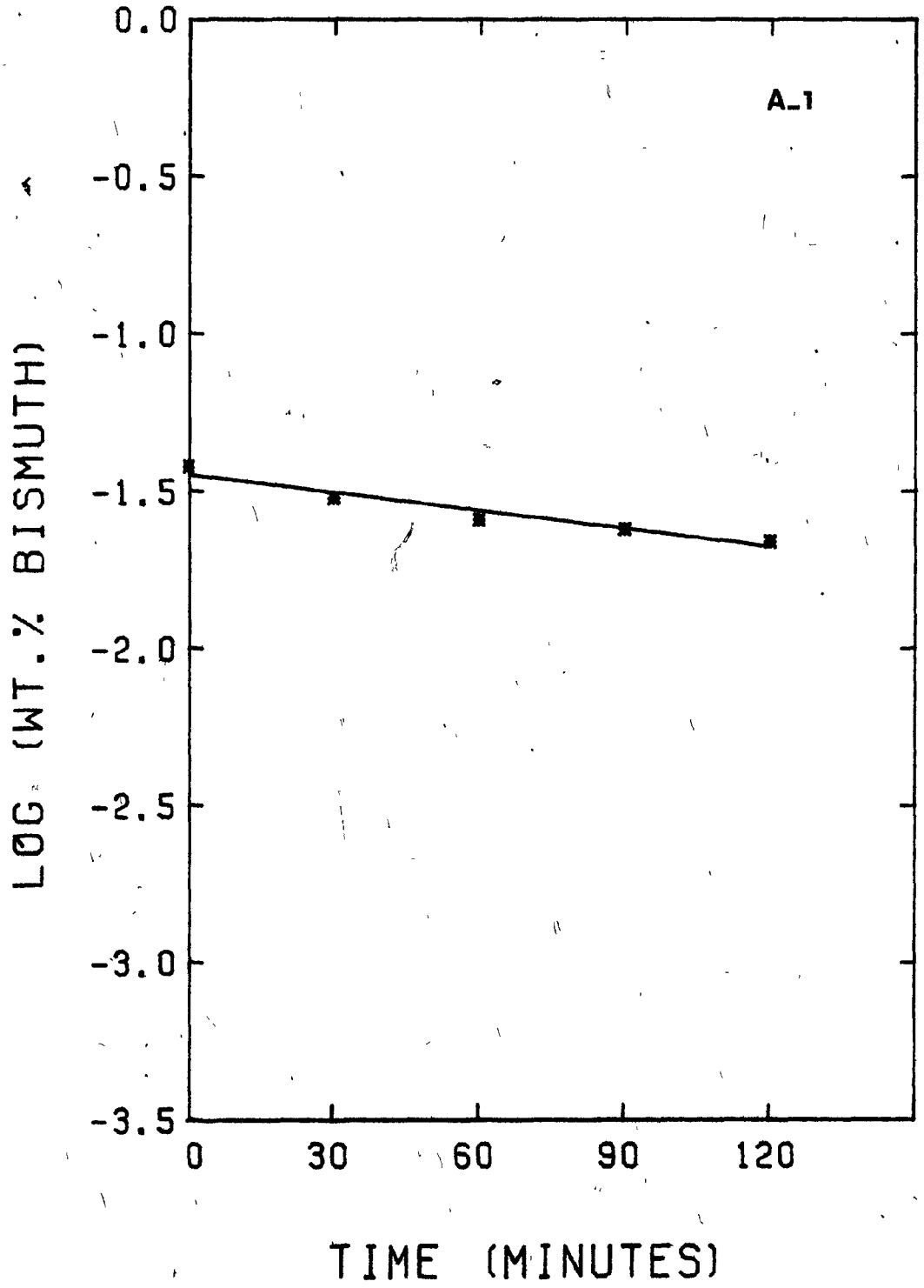
A_1
0.0
-0.5
-1.0
-1.5
-2.0
-2.5
-3.0
-3.5
0
30
60
90
120
LOG (WT.% BISMUTH)
TIME (MINUTES)

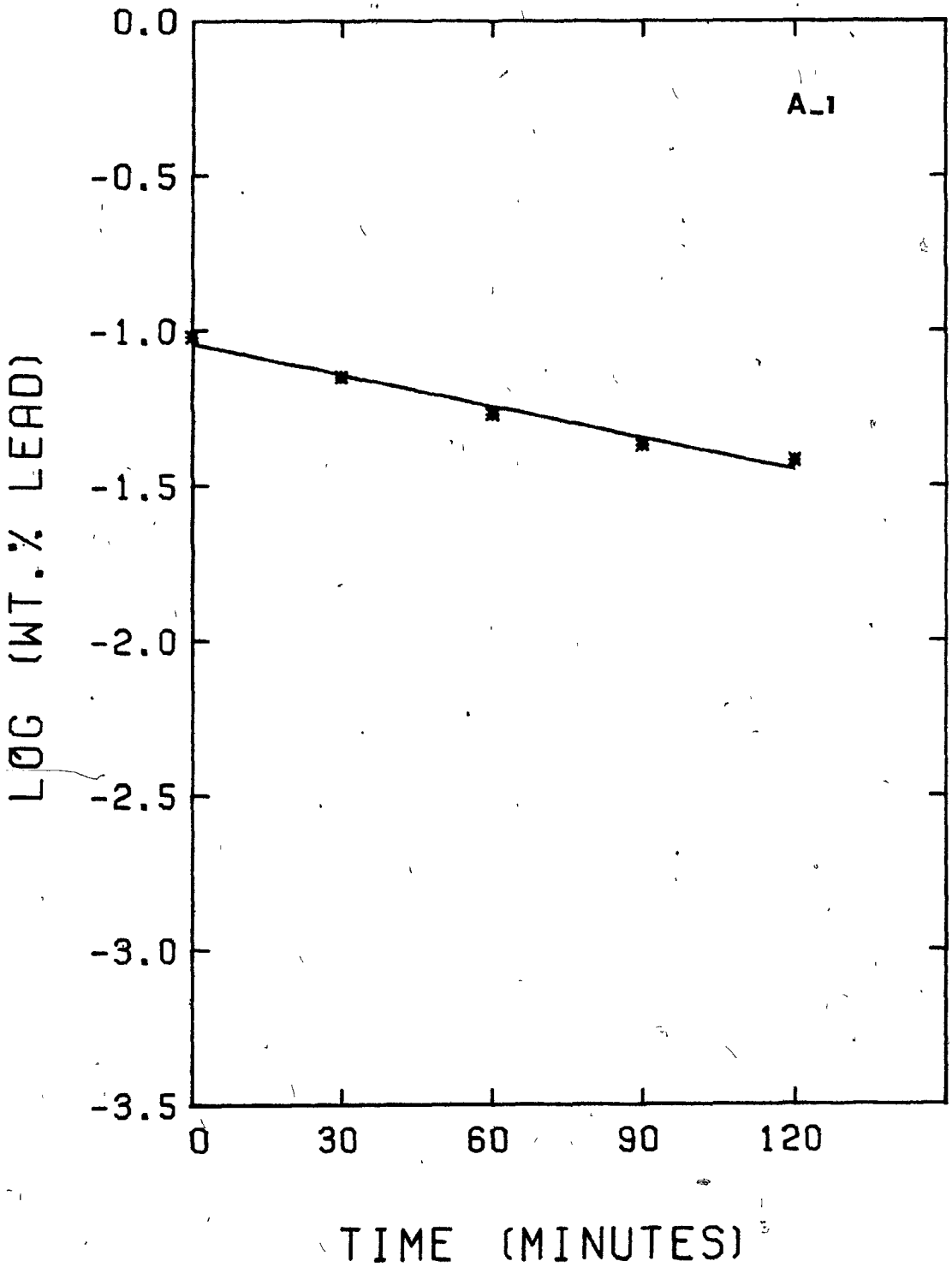
A_1
0.0
-0.5
-1.0
-1.5
-2.0
-2.5
-3.0
-3.5
LOG (WT.% LEAD)
0
30
60
90
120
TIME (MINUTES)

FIGURE 22

Rate of removal of bismuth and lead from copper, Test A-2.

	Bi	Pb
$K(\times 10^{-3}$ cm.$s^{-1})$:	1.856	2.523
Elim'n, wt.%:	60	75

time (min.)	wt.% Bi	wt.% Pb
0	0.020	0.028
30	0.015	0.020
60	0.011	0.014
90	0.009	0.010
120	0.008	0.008

Total copper loss = 220 gr.

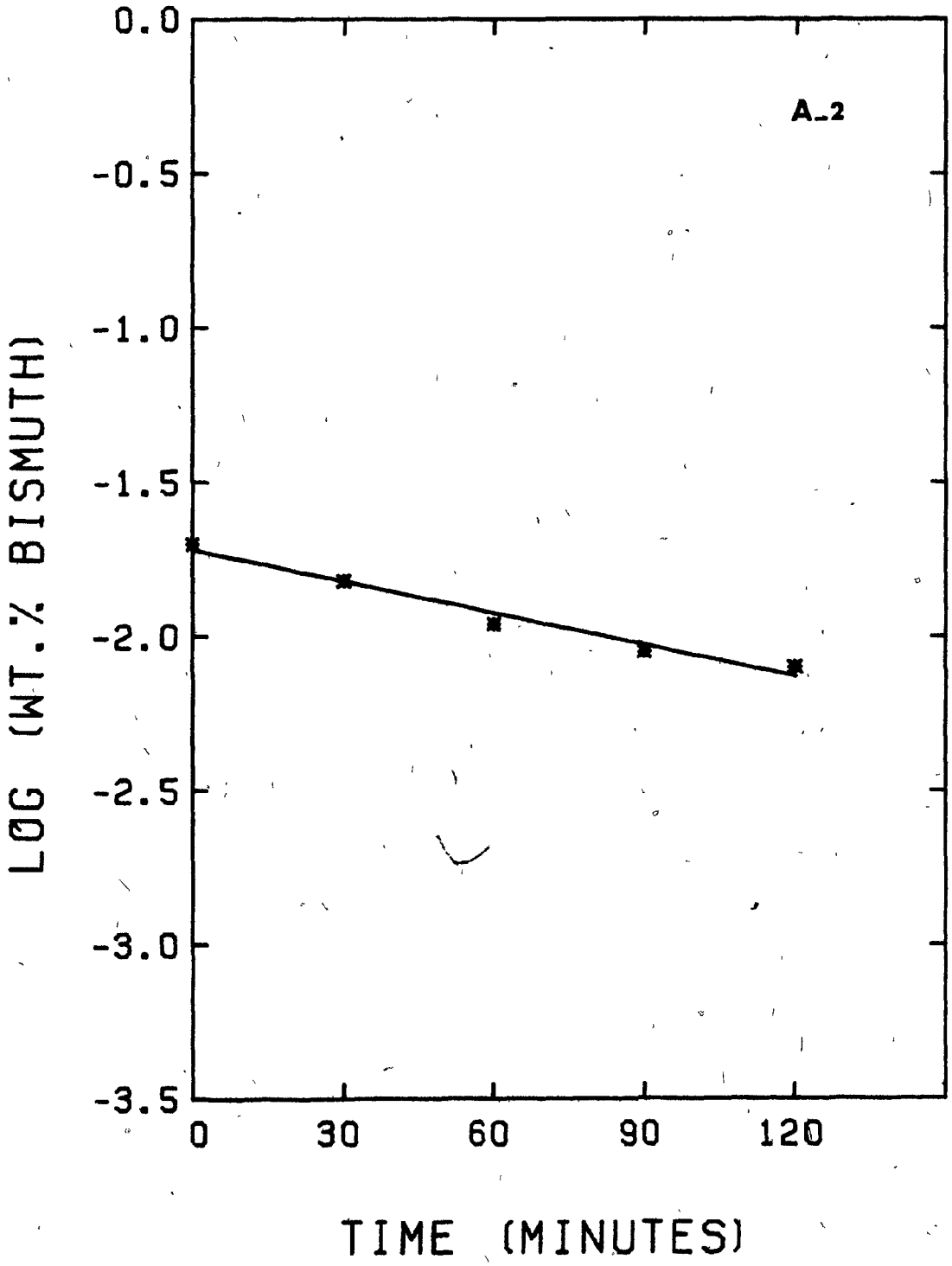
A_2
0.0
-0.5
-1.0
-1.5
-2.0
-2.5
-3.0
-3.5
LOG (WT.% BISMUTH)
0
30
60
90
120
TIME (MINUTES)

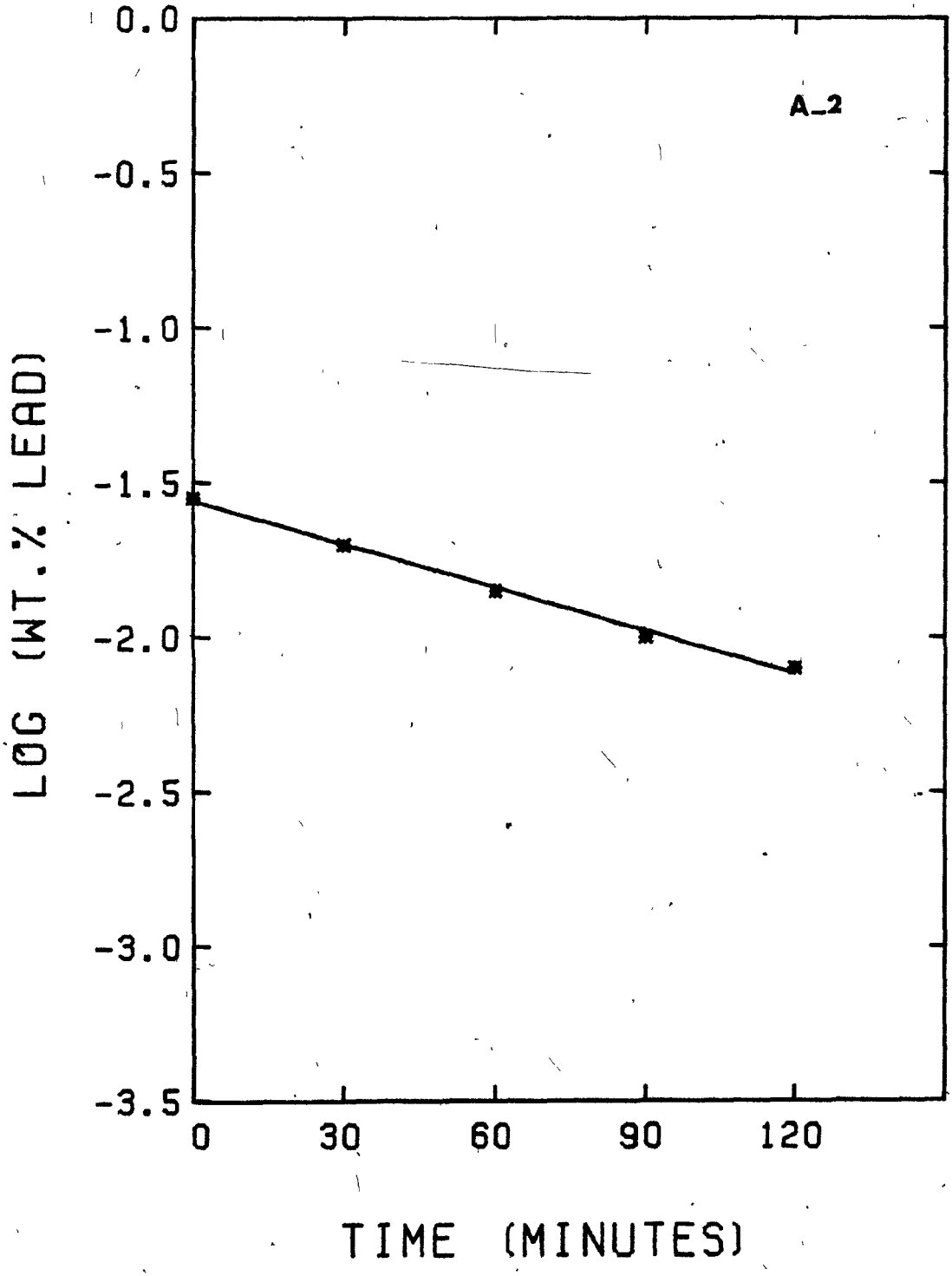
A_2
0.0
-0.5
-1.0
-1.5
-2.0
-2.5
-3.0
-3.5
LOG (WT.% LEAD)
0
30
60
90
120
TIME (MINUTES)

FIGURE 23

Rate of removal of bismuth and lead from copper, Test A-4.

	Bi	Pb
$K(\times 10^{-3}$ cm.s$^{-1})$:	2.325	3.928
Elim'n, wt.%:	70	85

time (min.)	wt.% Bi	wt.% Pb
0	0.020	0.027
30	0.016	0.020
60	0.011	0.010
90	0.009	0.006
120	0.006	0.004

Total copper loss = 250 gr.

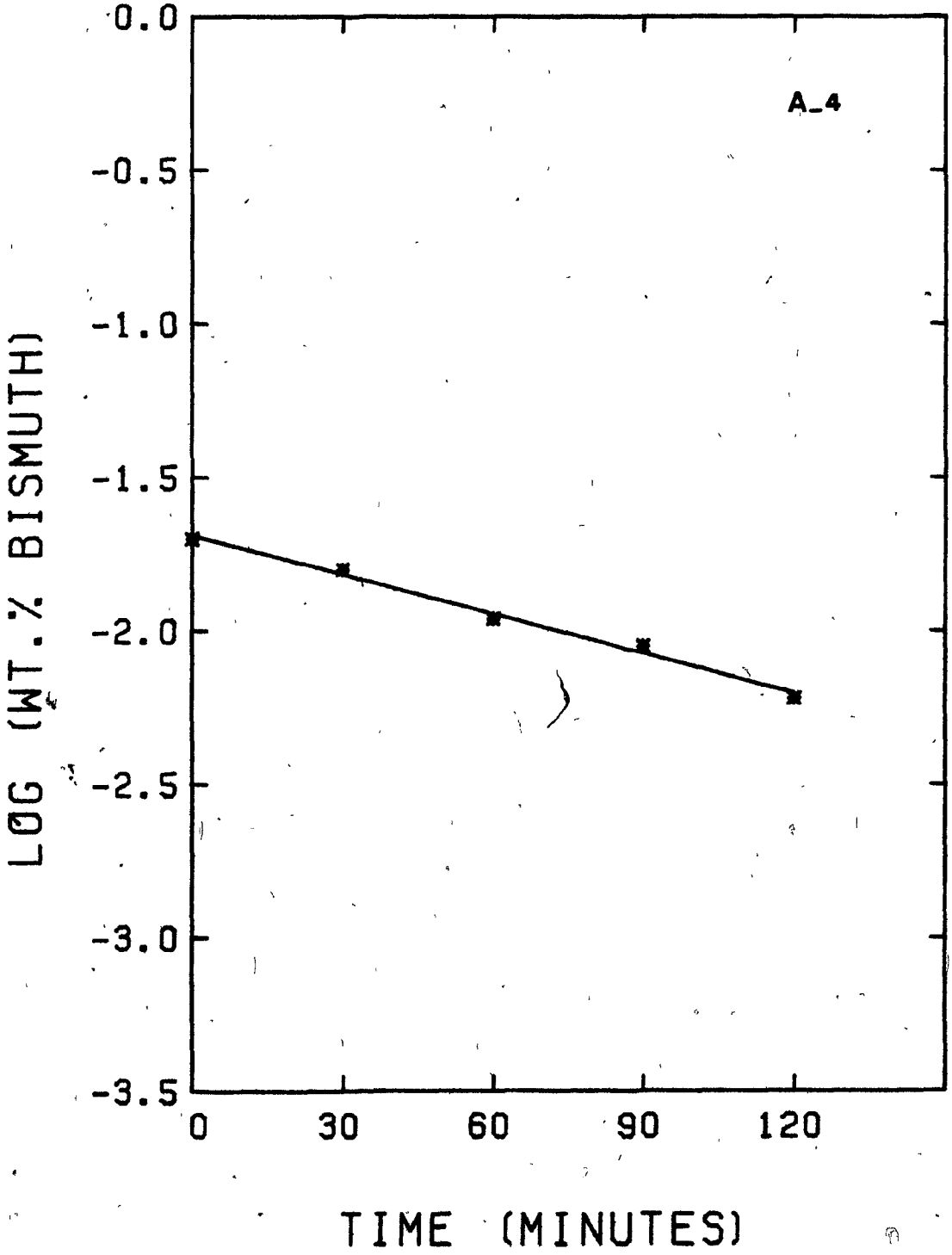
A_4
0.0
-0.5
-1.0
-1.5
-2.0
-2.5
-3.0
-3.5
LOG (WT.% BISMUTH)
0
30
60
90
120
TIME (MINUTES)

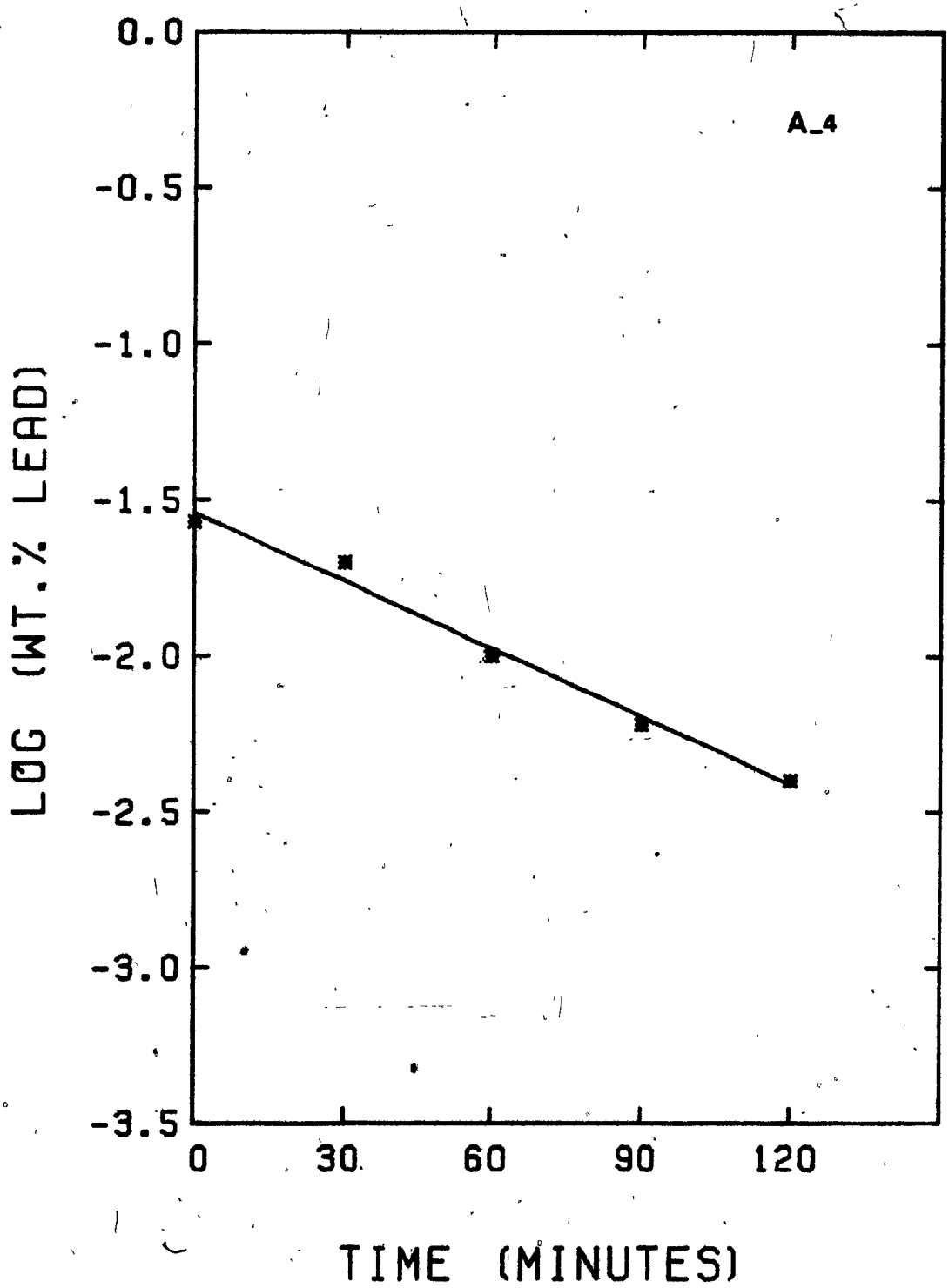
A_4
0.0
-0.5
-1.0
-1.5
-2.0
-2.5
-3.0
-3.5
LOG (WT.% LEAD)
0
30
60
90
120
TIME (MINUTES)

of removal. Based on these results, it was decided to carry on the research further, so as to investigate any effects of longer process time, or different crucible materials and to test the experimental reproducibility of the results.

V-5. PART III EXPERIMENTS

Four experiments were carried out in Part III, the aim being to maximize the amount of information possible with a minimum number of experiments.

Test F-1-X was carried out strictly for the purpose of duplicating test F-1. In the remaining three experiments, the refining time was doubled to 240 minutes. In experiments F-9 and A-7, conditions were selected so that the results of the first 120 minutes could be used as duplicates of the randomly selected experiments carried out in Parts I and II. In the last experiment, F-10, the results of the first 120 minutes was reported as F-7 in Part I. The only difference between F-9-X and F-3 are the A/V ratios.

A summary of all the results and experimental conditions are reported in Tables 11, 12 and 13. As in the previous parts, the logarithm of the change in weight percent of impurity with time was plotted, and these are shown in Figures 24-30 inclusive.

TABLE 11. Summary of Experimental Conditions[1] and Results, Part III Experiments

Test No.	Press. μ Hg	Temp. °C	A/V m^{-1}	Condenser Distance cm	Time min.	Type of Crucible	Elim'n, wt% Bi	Elim'n, wt% Pb	K(10^{-3} cm/s) Bi	K(10^{-3} cm/s) Pb
F-1-X[2]	300	1150	6.7	>65.0	120	Tercod #30	21	24	0.56	0.68
F-9-X[2]	100	1250	10.2	>65.0	120	Tercod #50	60	77	1.24	1.99
F-7[3] (F-10)	100	1250	10.2	<2.0	120	Tercod #50	75	85	1.79	2.52
A-7-X[2]	100	1250	7.1	>65.0	120	Hycor Alumina	60	75	1.87	2.51
F-9	100	1250	10.2	>65.0	240	Tercod #50	70	92	0.75	1.63
F-10	100	1250	10.2	<2.0	240	Tercod #50	89	98	1.62	2.84
A-7	100	1250	7.1	>65.0	240	Hycor Alumina	76	94	1.36	2.45

1. Copper weight = 34. kilogram

2. Duplications = F-1 and F-1-X, F-3 and F-9-X, A-2 and A-7-X.
F-9-X and A-7-X are first 120 minutes of tests F-9 and A-7.

3. First 120 minutes of test F-10 was reported as test F-7.

TABLE 12. Summary of Kinetic Results for Bismuth Removal, Part III Experiments[1].

Test No.	Corr. Coeff.	$K(10^{-3}$ cm/s)	$K_L(10^{-3}$ cm/s)	$K_E(10^{-3}$ cm/s)	$K_U(10^{-3}$ cm/s)	K_G (cm/s)	Initial wt%	Final wt%	Elim'n wt%
F-1-X[2]	0.969	0.56	5.15	28.44	0.56	187	0.043	0.034	21
F-9-X[2]	0.964	1.24	6.59	62.90	1.41	221	0.020	0.008	60
F-7[3] (F-10)	0.963	1.79	6.59	62.90	2.57	400	0.044	0.011	75
A-7-X[2]	0.987	1.87	7.21	62.90	2.64	412	0.025	0.010	60
F-9	0.951	0.75	6.59	62.90	0.86	134	0.020	0.006	70
F-10	0.986	1.62	6.59	62.90	2.22	346	0.044	0.005	89
A-7	0.972	1.36	7.21	62.90	1.71	267	0.025	0.006	76

1. Copper weight = 34. kilogram

2. Duplications: F-1 and F-1-X, F-3 and F-9-X, A-2 and A-7-X.

3. First 120 minutes of test F-10 was reported as test F-7.

TABLE 13. Summary of Kinetic Results for Lead Removal, Part III Experiments[1].

Test No.	Corr. Coeff.	$K(10^{-3}$ cm/s)	$K_L(10^{-3}$ cm/s)	$K_E(10^{-3}$ cm/s)	$K_U(10^{-3}$ cm/s)	K_G (cm/s)	Initial wt%	Final wt%	Elim'n wt%
F-1-X[2].	0.982	0.68	5.15	47.92	0.73	145	0.126	0.096	24
F-9-X[2].	0.954	1.99	6.59	97.53	2.81	284	0.048	0.011	77
F-7[3]. (F-10)	0.965	2.52	6.59	97.53	4.26	431	0.126	0.019	85
A-7-X[2].	0.927	2.51	7.21	97.53	4.00	404	0.047	0.012	75
F-9	0.982	1.63	6.59	97.53	2.22	224	0.048	0.004	92
F-10	0.985	2.84	6.59	97.53	5.27	532	0.126	0.003	98
A-7	0.985	2.45	7.21	97.53	3.85	389	0.047	0.003	94

1. Copper weight = 34. kilogram

2. Duplications = F-1 and F-1-X, F-3 and F-9-X, A-2 and A-7-X.

3. First 120 minutes of test F-10 was reported as test F-7.

FIGURE 24

Rate of removal of bismuth and lead from copper, Test F-1-X.

	Bi	Pb
$K(\times 10^{-3}$ cm.s$^{-1})$:	0.563	0.680
Elim'n, wt.%:	21	24

time (min.)	wt.% Bi	wt.% Pb
0	0.043	0.126
30	0.043	0.123
60	0.039	0.110
90	0.037	0.099
120	0.034	0.096

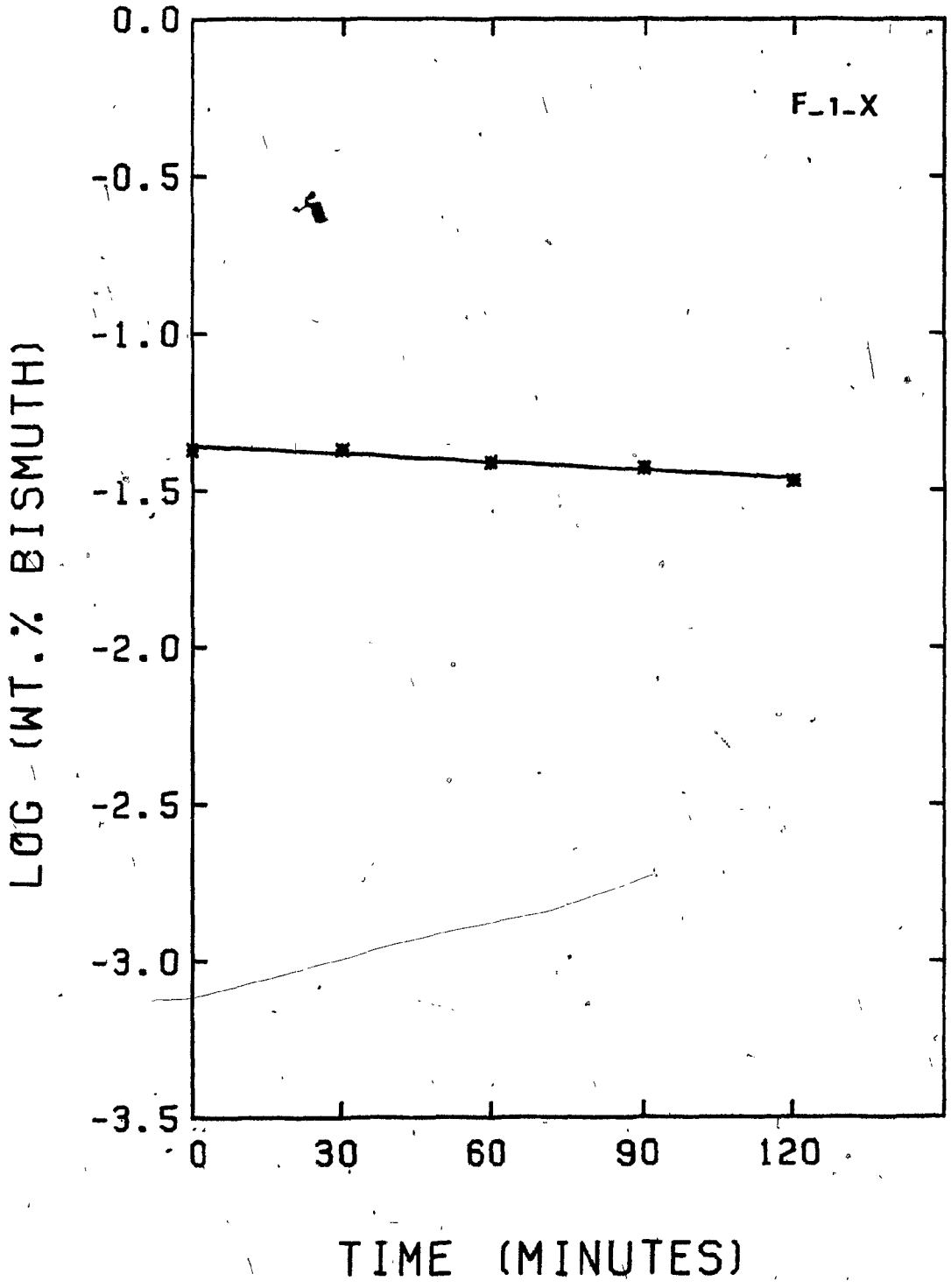
F_1_X
0.0
-0.5
-1.0
-1.5
-2.0
-2.5
-3.0
-3.5
LOG (WT.% BISMUTH)
0
30
60
90
120
TIME (MINUTES)

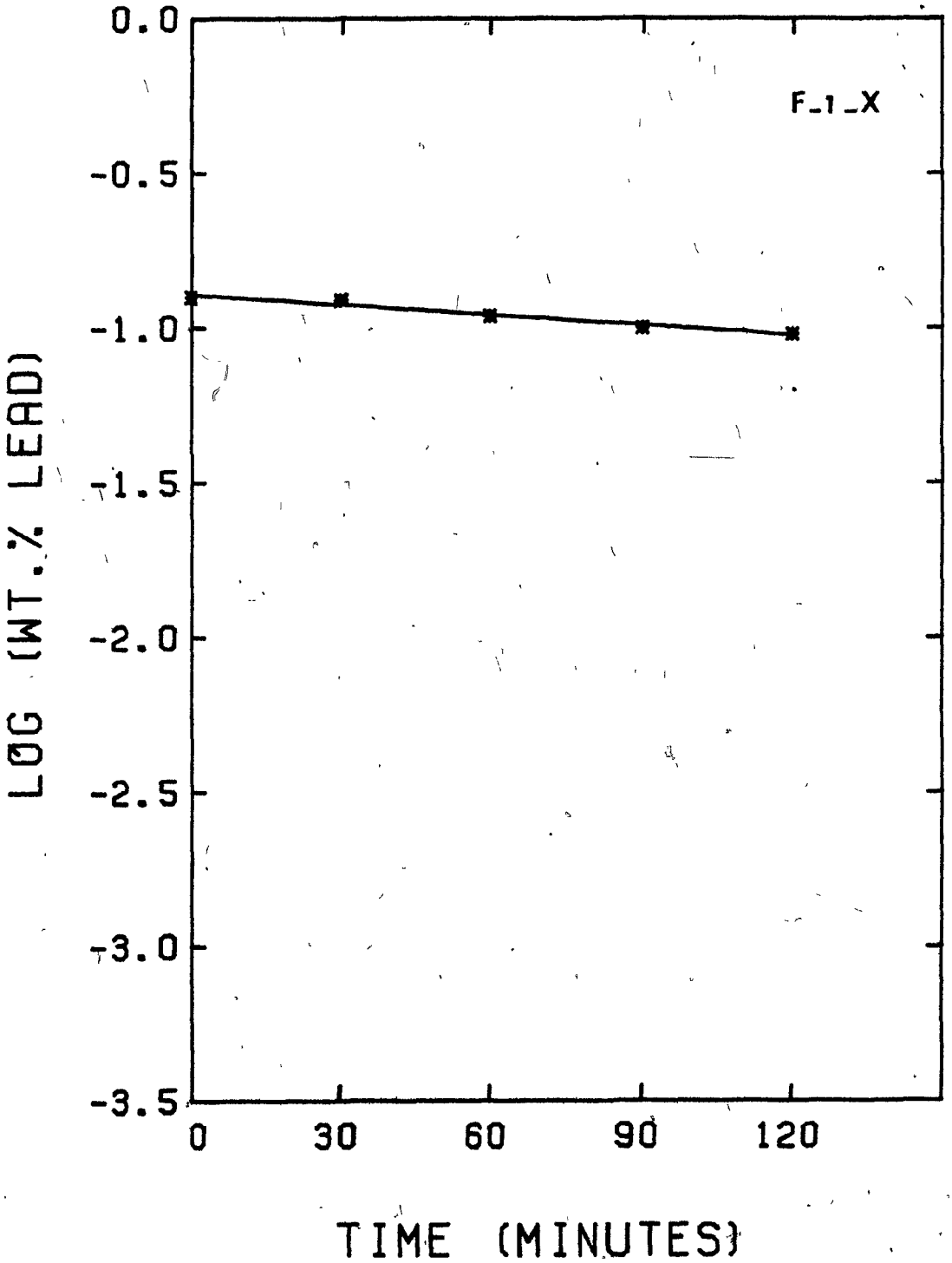
F_1_X
0.0
-0.5
-1.0
-1.5
-2.0
-2.5
-3.0
-3.5
LOG (WT.% LEAD)
0
30
60
90
120
TIME (MINUTES)

FIGURE 25

Rate of removal of bismuth and lead from copper, Test F-9-X.

	Bi	Pb
$K(\times 10^{-3}$ cm.s$^{-1})$:	1.242	1.992
Elim'n, wt.%:	60	77

time (min.)	wt.% Bi	wt.% Pb
0	0.020	0.048
30	0.013	0.026
60	0.011	0.015
90	0.010	0.014
120	0.008	0.011

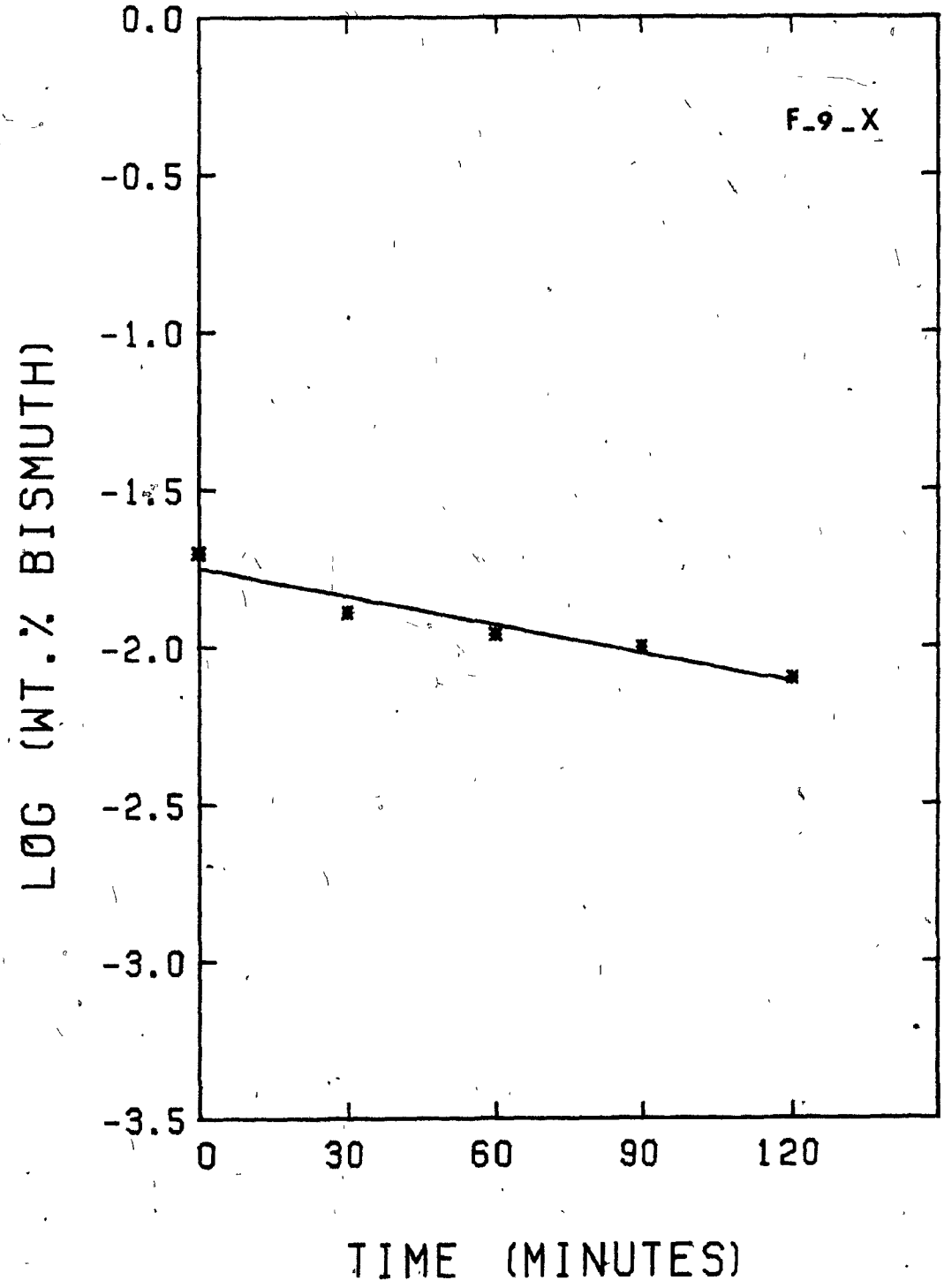
F_9_X
0.0
-0.5
-1.0
-1.5
-2.0
-2.5
-3.0
-3.5
LOG (WT.% BISMUTH)
0
30
60
90
120
TIME (MINUTES)

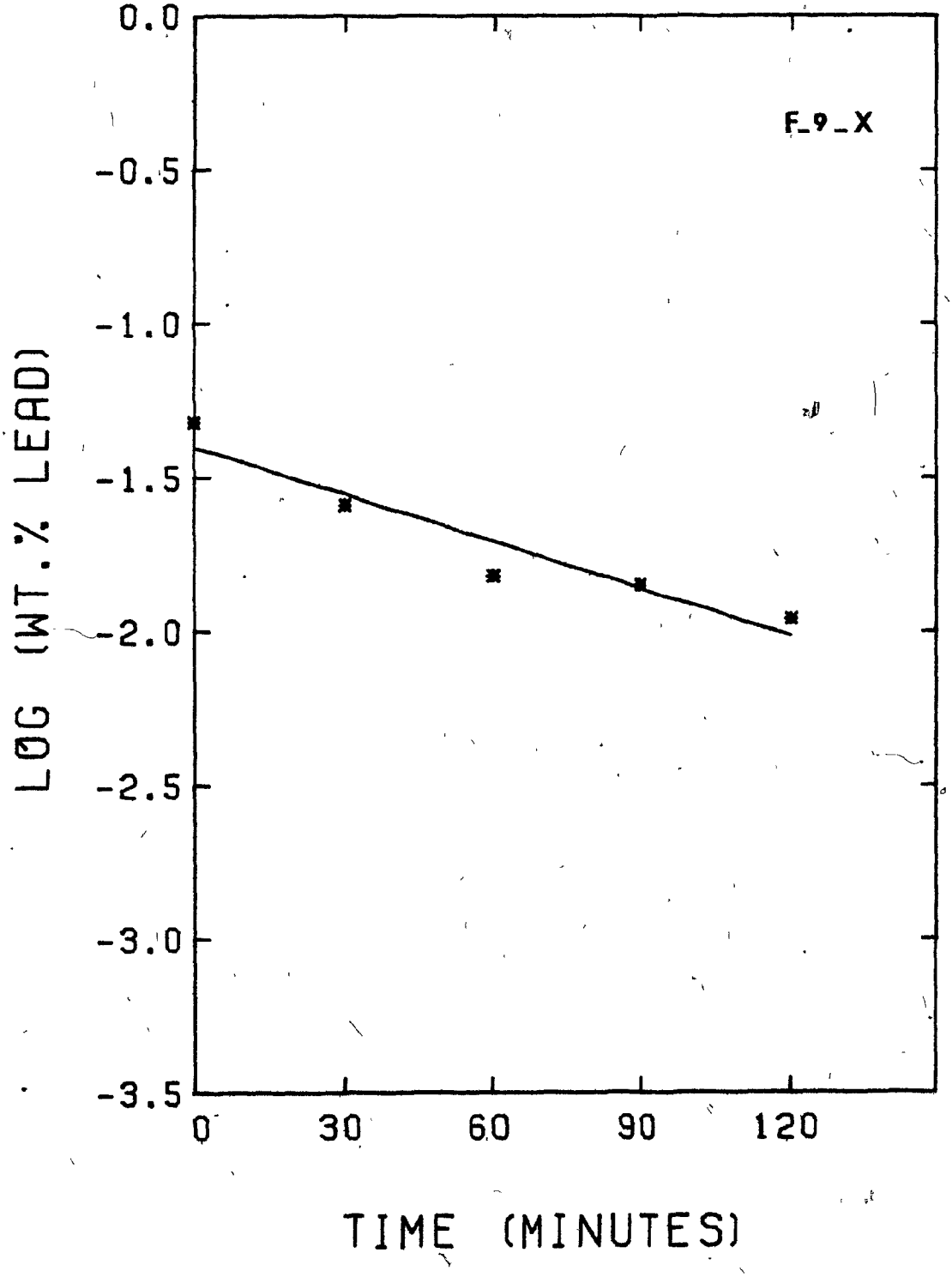
F_9_X
0.0
-0.5
-1.0
-1.5
-2.0
-2.5
-3.0
-3.5
LOG (WT.% LEAD)
0
30
60
90
120
TIME (MINUTES)

FIGURE 26

Rate of removal of bismuth and lead from copper, Test F-7 (F-10).*

	Bi	Pb
K($\times 10^{-3}$ cm.s^{-1}):	1.794	2.521
Elim'n, wt.%:	75	85

time (min.)	wt.% Bi	wt.% Pb
0	0.044	0.126
30	0.037	0.107
60	0.023	0.049
90	0.022	0.046
120	0.011	0.019

*First 120 min of test F-10 was reported as test F-7.

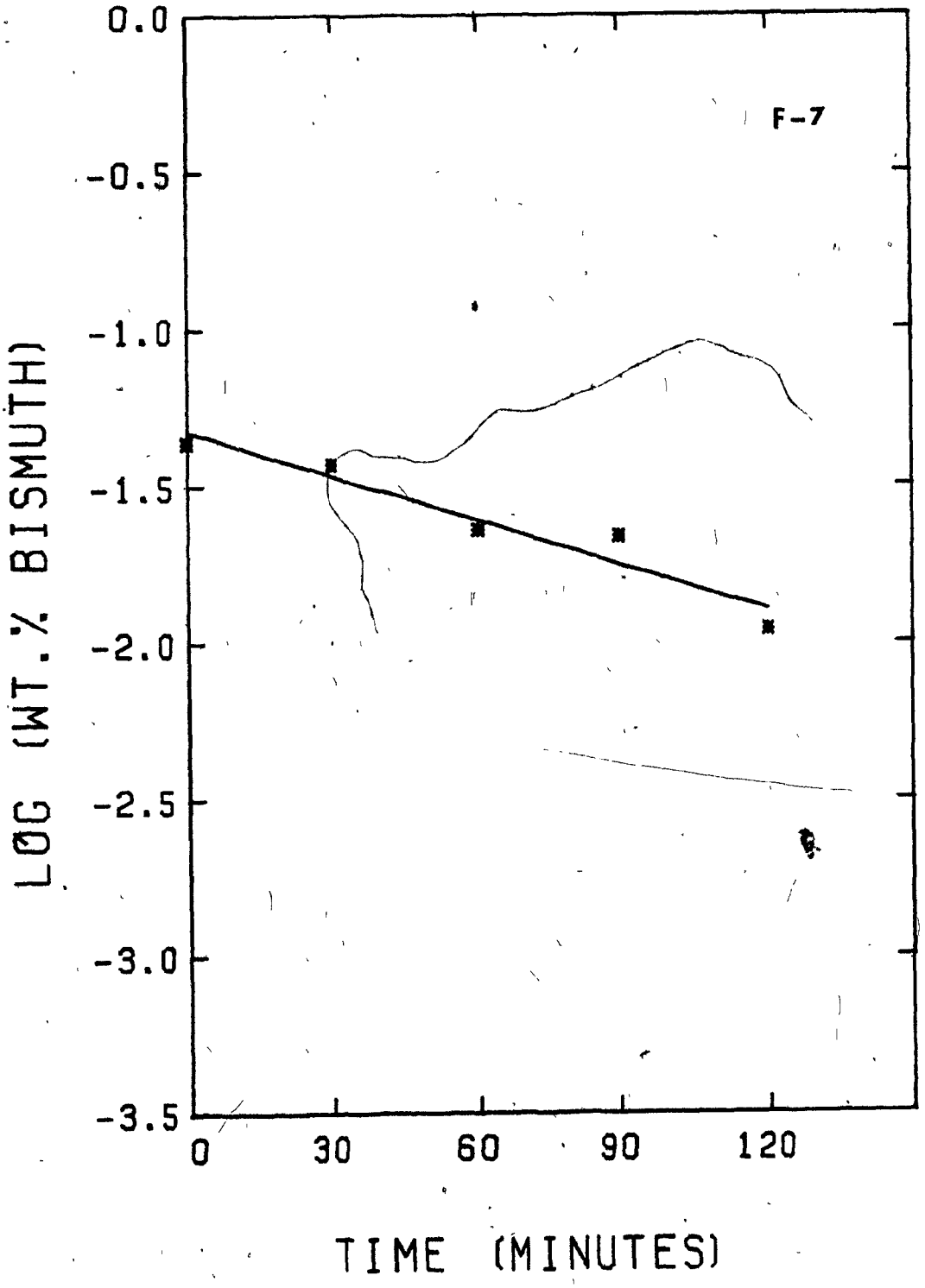
F-7
0.0
-0.5
-1.0
-1.5
-2.0
-2.5
-3.0
-3.5
LOG (WT.% BISMUTH)
0
30
60
90
120
TIME (MINUTES)

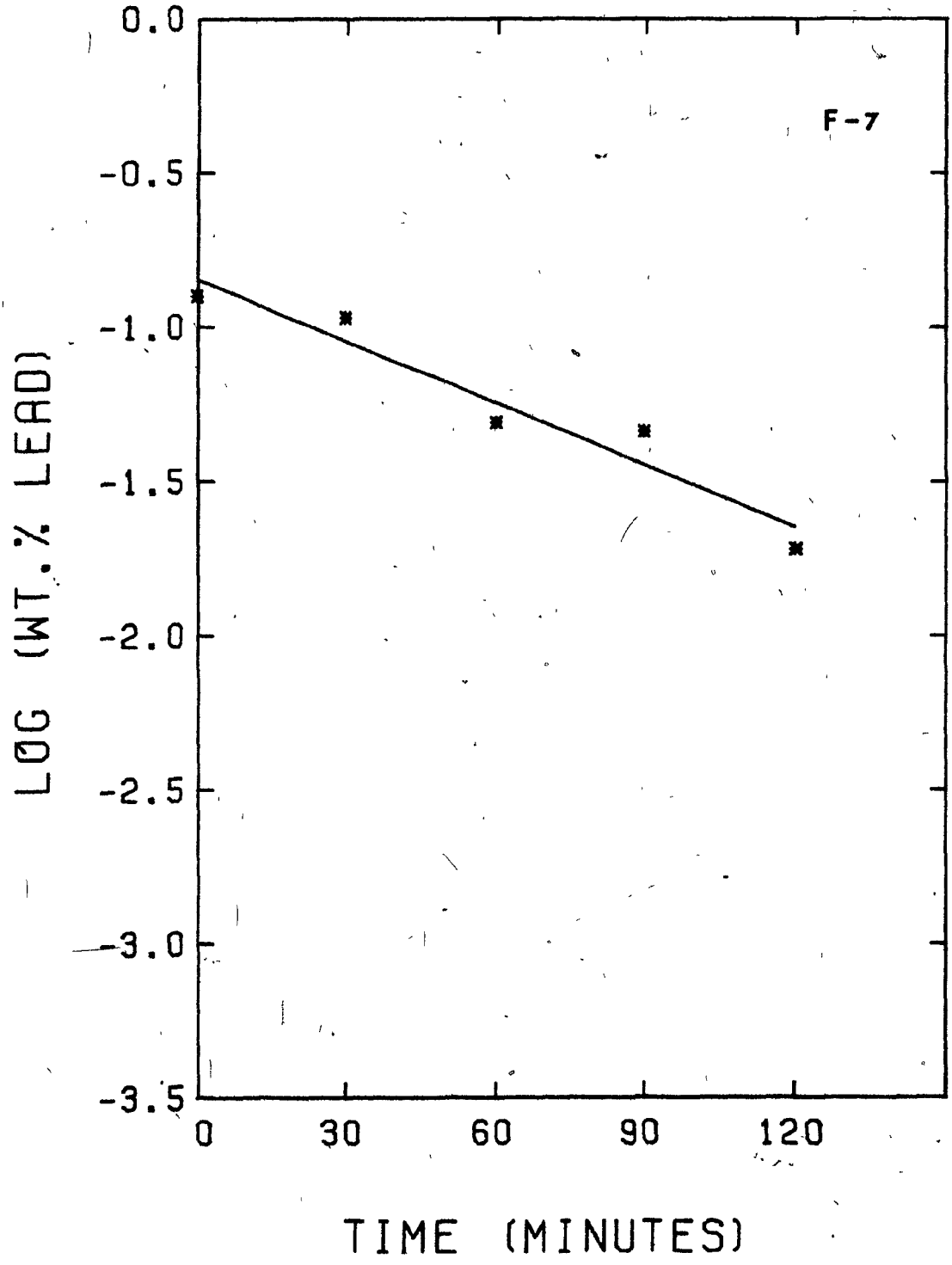
F-7
0.0
-0.5
-1.0
-1.5
-2.0
-2.5
-3.0
-3.5
LOG (WT.% LEAD)
0
30
60
90
120
TIME (MINUTES)

FIGURE 27

Rate of removal of bismuth and lead from copper, Test A-7-X.

	Bi	Pb
$K(\times 10^{-3}$ cm.s$^{-1})$:	1.874	2.505
Elim'n, wt.%:	60	75

time (min.)	wt.% Bi	wt.% Pb
0	0.025	0.047
30	0.019	0.023
60	0.014	0.015
90	0.011	0.014
120	0.010	0.012

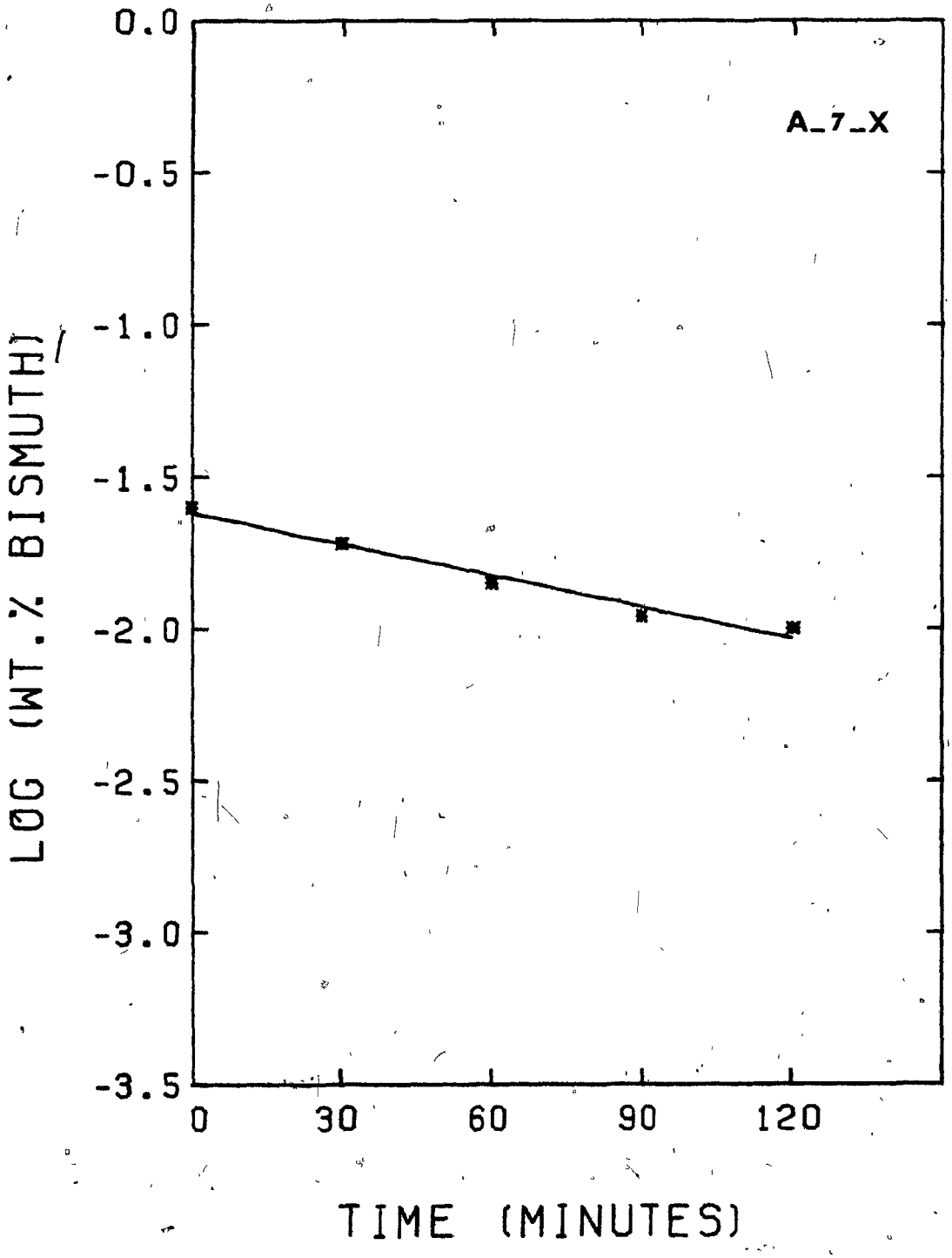
A_7_X
0.0
-0.5
-1.0
-1.5
-2.0
-2.5
-3.0
-3.5
LOG (WT.% BISMUTH)
0
30
60
90
120
TIME (MINUTES)

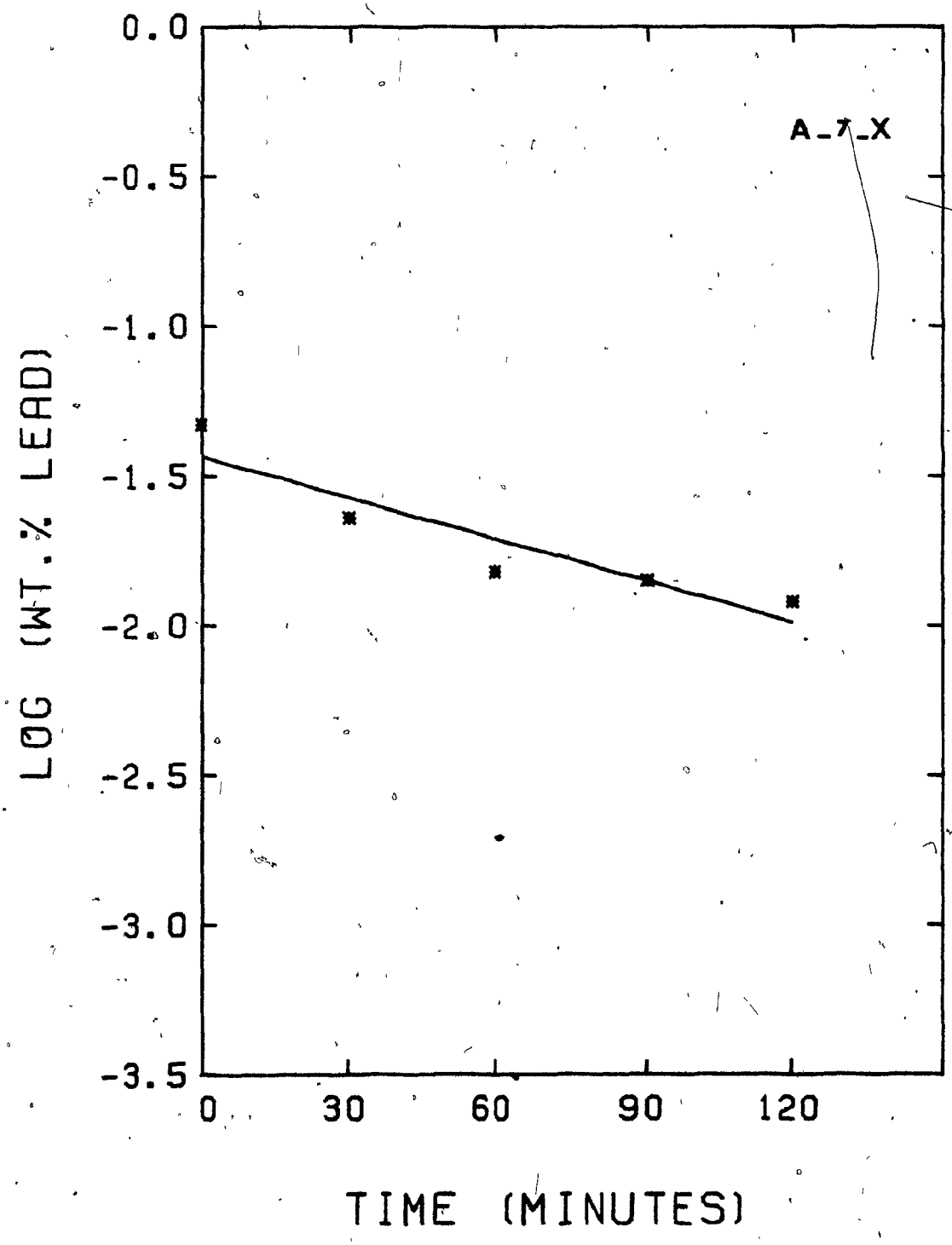
A_7_X
0.0
-0.5
-1.0
-1.5
-2.0
-2.5
-3.0
-3.5
LOG (WT.% LEAD)
0
30
60
90
120
TIME (MINUTES)

FIGURE 28

Rate of removal of bismuth and lead from copper, Test F-9.

	Bi	Pb
$K(\times 10^{-3}$ cm.s$^{-1})$:	0.753	1.631
Elim'n, wt.%:	70	92

time (min.)	wt.% Bi	wt.% Pb
0	0.020	0.048
30	0.013	0.026
60	0.011	0.015
90	0.010	0.014
120	0.008	0.011
150	0.007	0.008
180	0.007	0.006
210	0.006	0.004
240	0.006	0.004

Total copper loss = 340 gr.

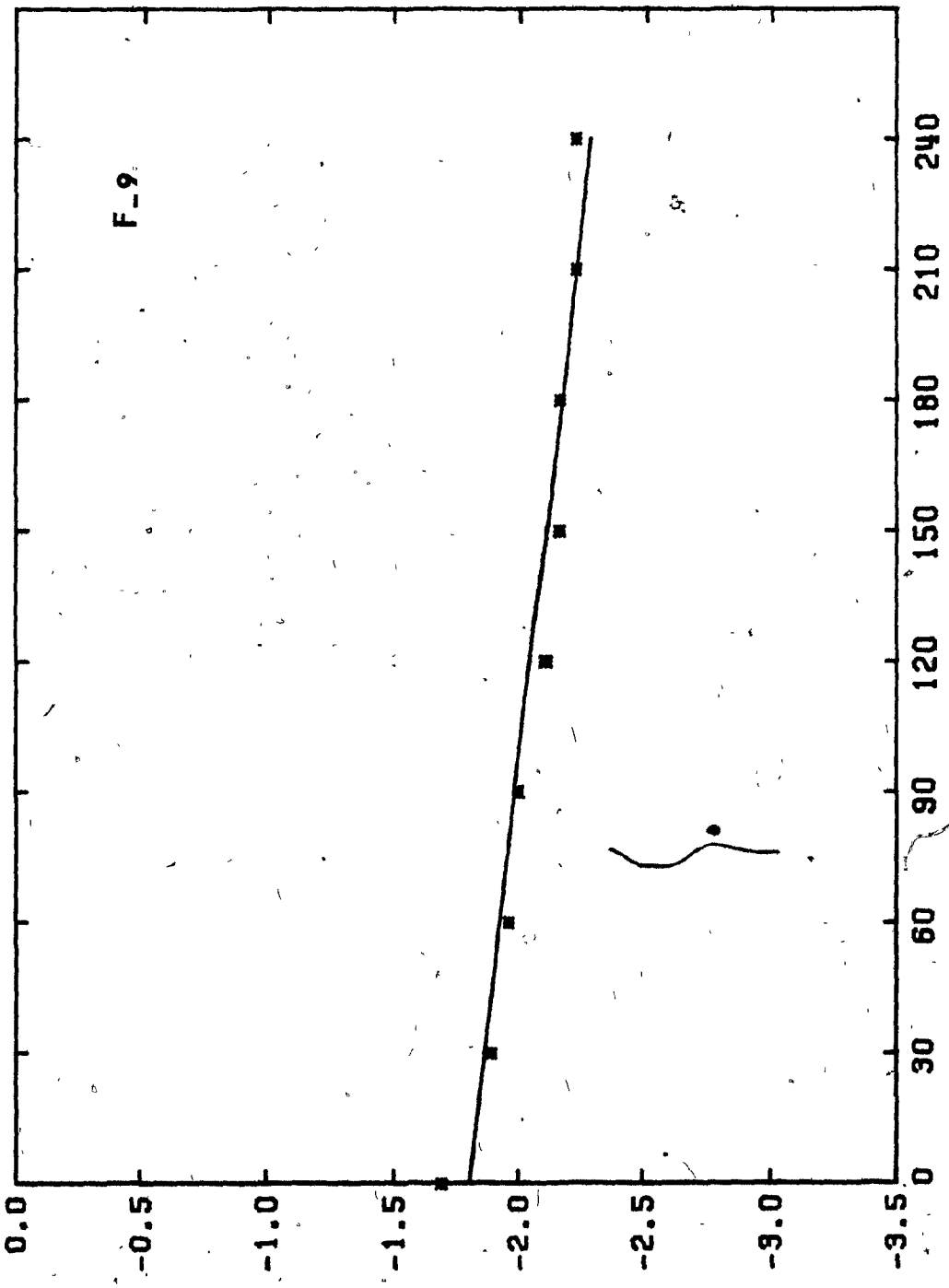
F_9
LOG (WT.% BISMUTH)
0.0
-0.5
-1.0
-1.5
-2.0
-2.5
-3.0
-3.5
0
30
60
90
120
150
180
210
240
TIME (MINUTES)

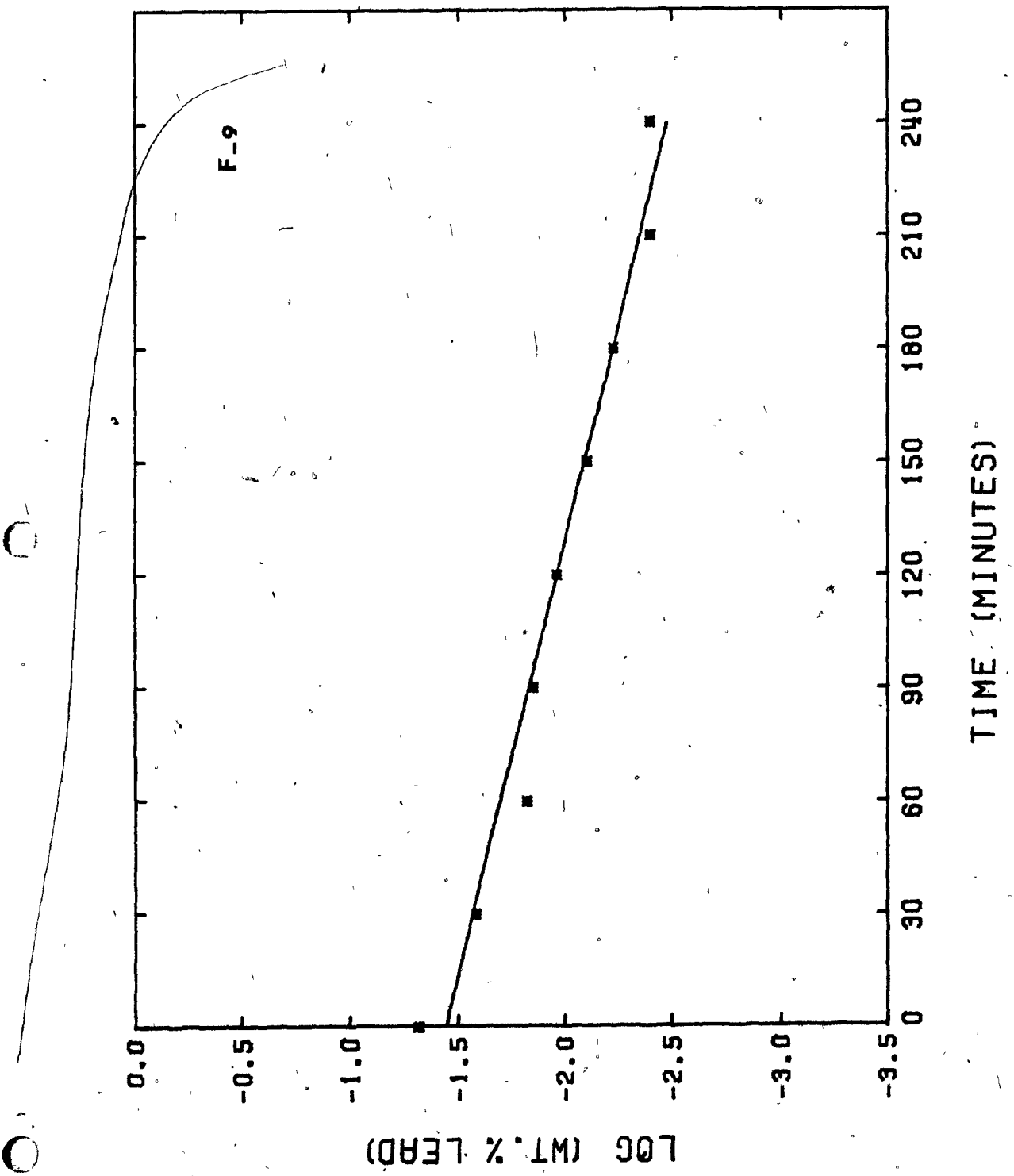
F_9
LOG (WT.% LEAD)
0.0
-0.5
-1.0
-1.5
-2.0
-2.5
-3.0
-3.5
0
30
60
90
120
150
180
210
240
TIME (MINUTES)

FIGURE 29

Rate of removal of bismuth and lead from copper, Test F-10.

	Bi	Pb
$K(\times 10^{-3}$ cm.s$^{-1})$:	1.616	2.841
Elim'n, wt.%:	89	98

time (min.)	wt.% Bi	wt.% Pb
0	0.044	0.126
30	0.037	0.107
60	0.023	0.049
90	0.022	0.046
120	0.011	0.019
150	0.010	0.015
180	0.007	0.005
210	0.005	0.003
240	0.005	0.003

Total copper loss = 360 gr.

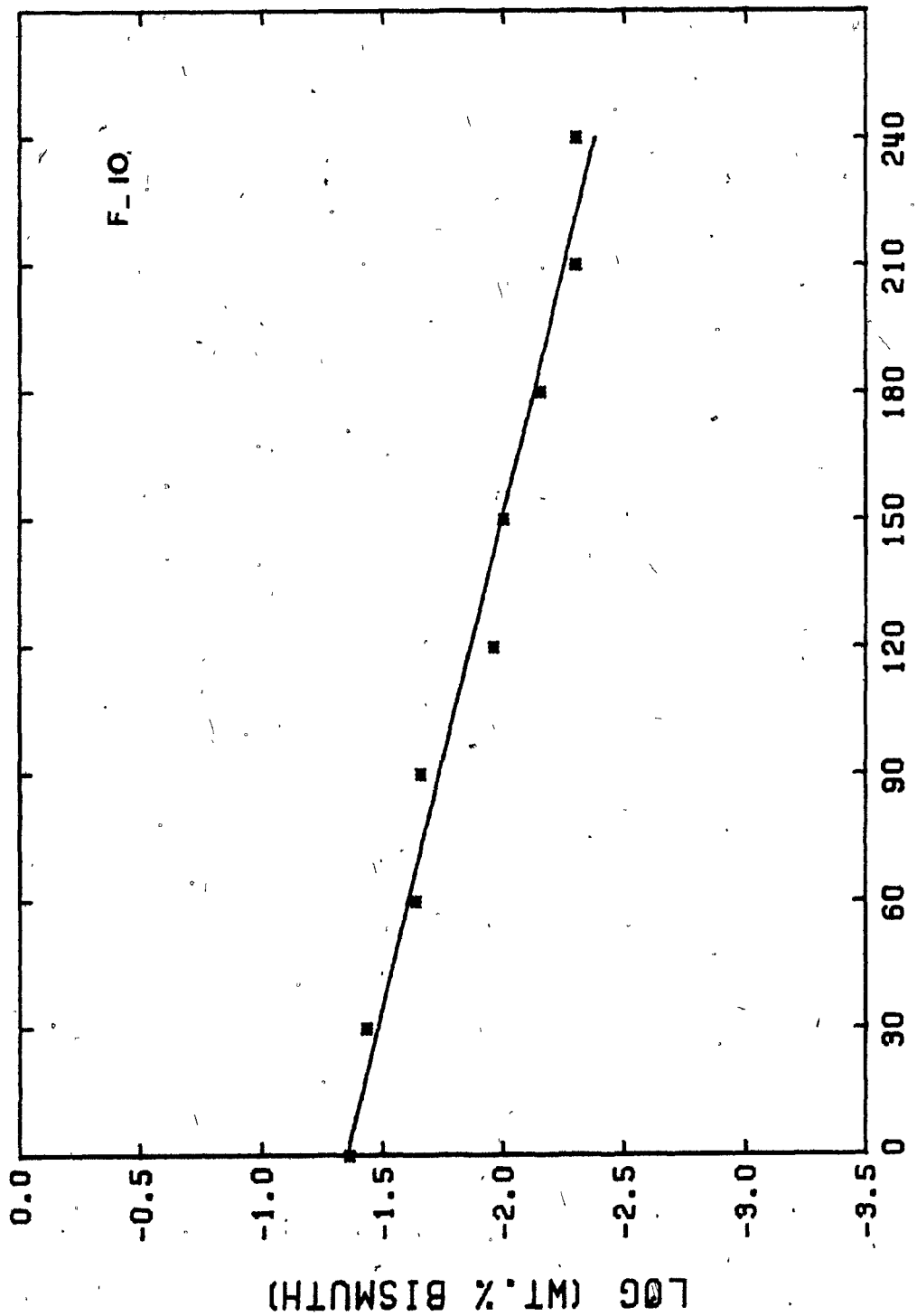
F_10
LOG (WT.% BISMUTH)
0.0
-0.5
-1.0
-1.5
-2.0
-2.5
-3.0
-3.5
0
30
60
90
120
150
180
210
240
TIME (MINUTES)

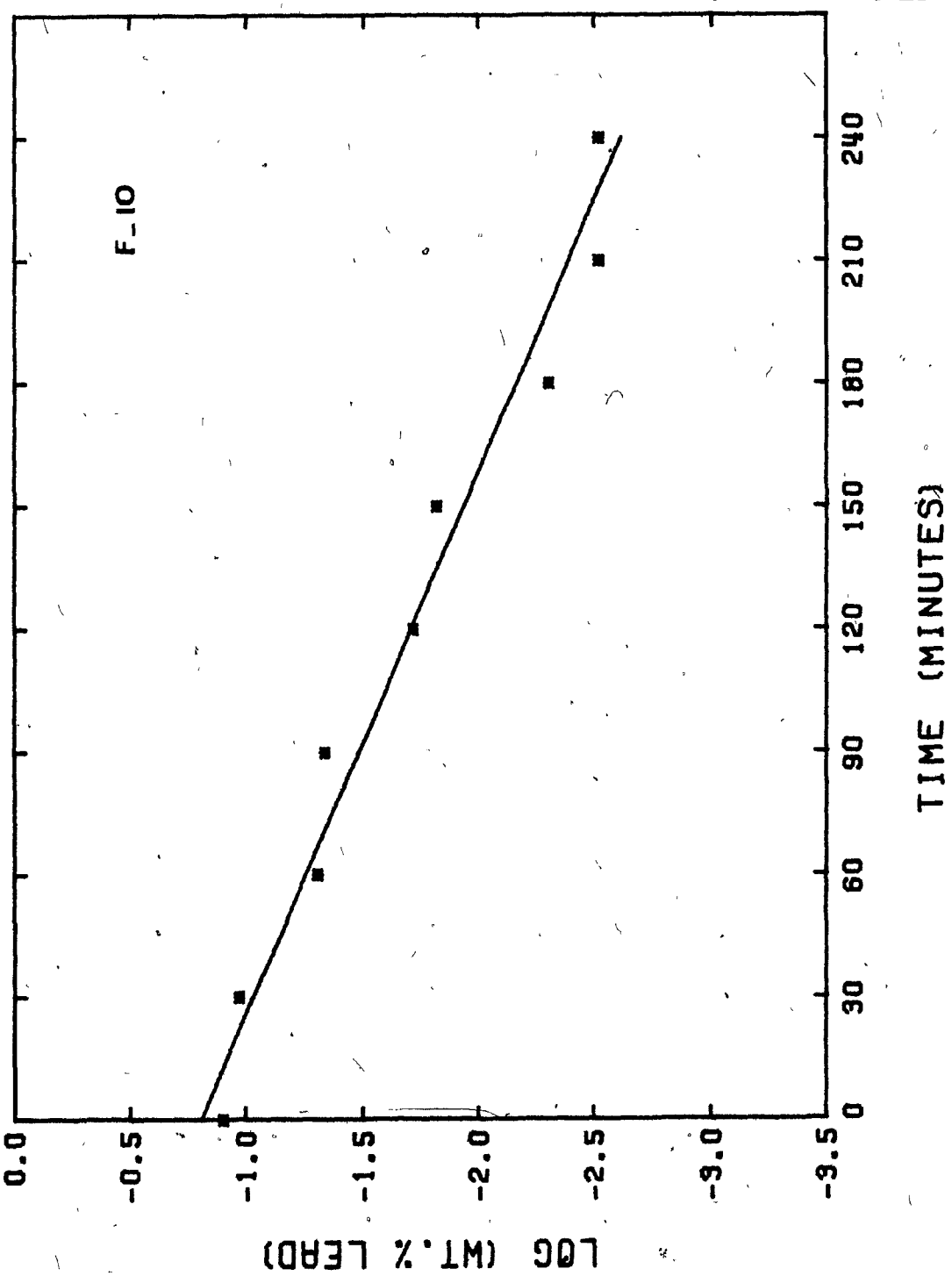
F_10
LOG (WT.% LEAD)
0.0
-0.5
-1.0
-1.5
-2.0
-2.5
-3.0
-3.5
0
30
60
90
120
150
180
210
240
TIME (MINUTES)

FIGURE 30

Rate of removal of bismuth and lead from copper, Test A-7.

	Bi	Pb
$K(\times 10^{-3}$ cm.s$^{-1})$:	1.355	2.445
Elim'n, wt.%:	76	94

time (min.)	wt.% Bi	wt.% Pb
0	0.025	0.047
30	0.019	0.023
60	0.014	0.015
90	0.011	0.014
120	0.010	0.012
150	0.008	0.007
180	0.007	0.006
210	0.007	0.004
240	0.006	0.003

Total copper loss = 330 gr.

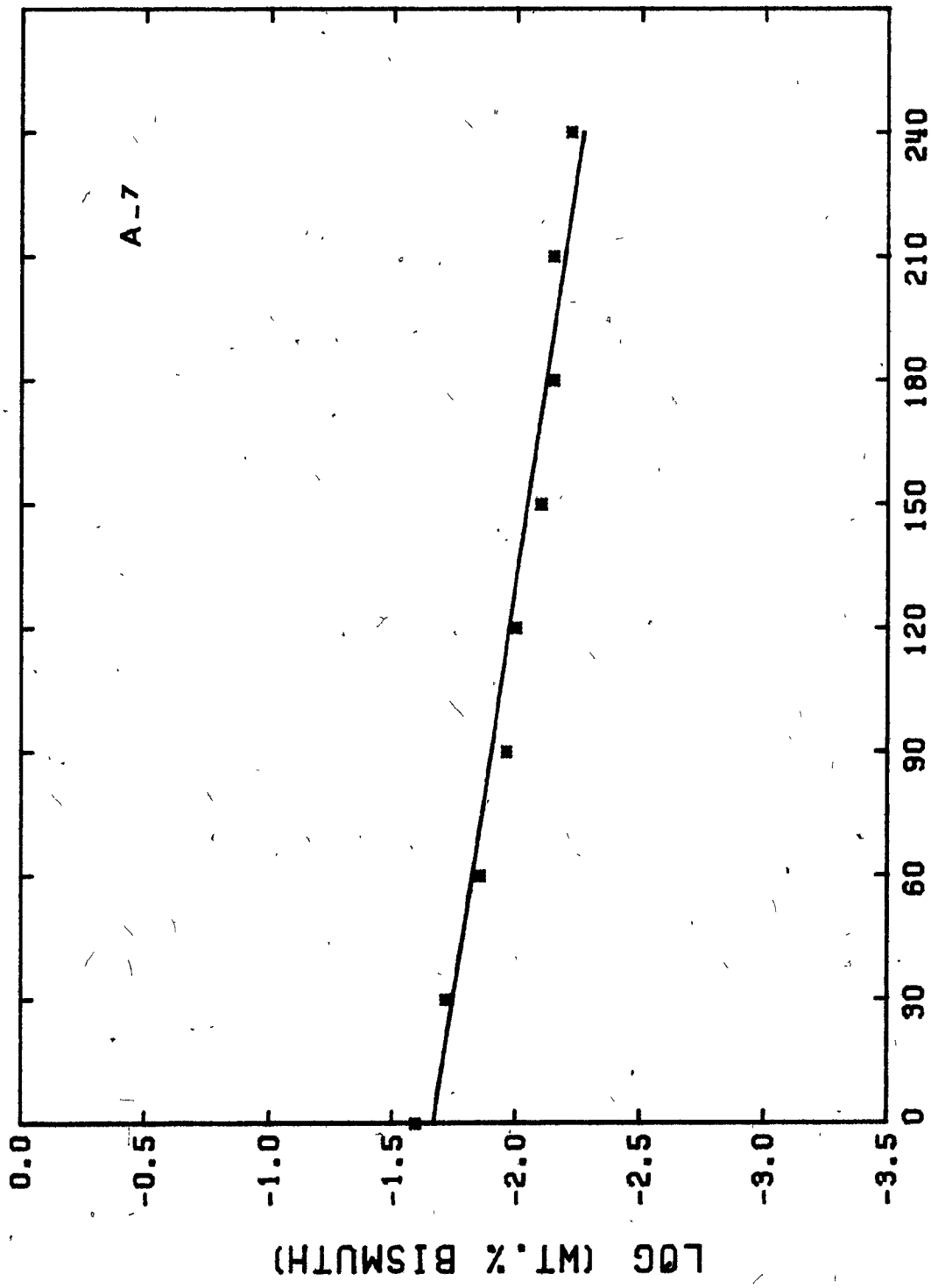
A_7
LOG (WT.% BISMUTH)
0.0
-0.5
-1.0
-1.5
-2.0
-2.5
-3.0
-3.5
0
30
60
90
120
150
180
210
240
TIME (MINUTES)

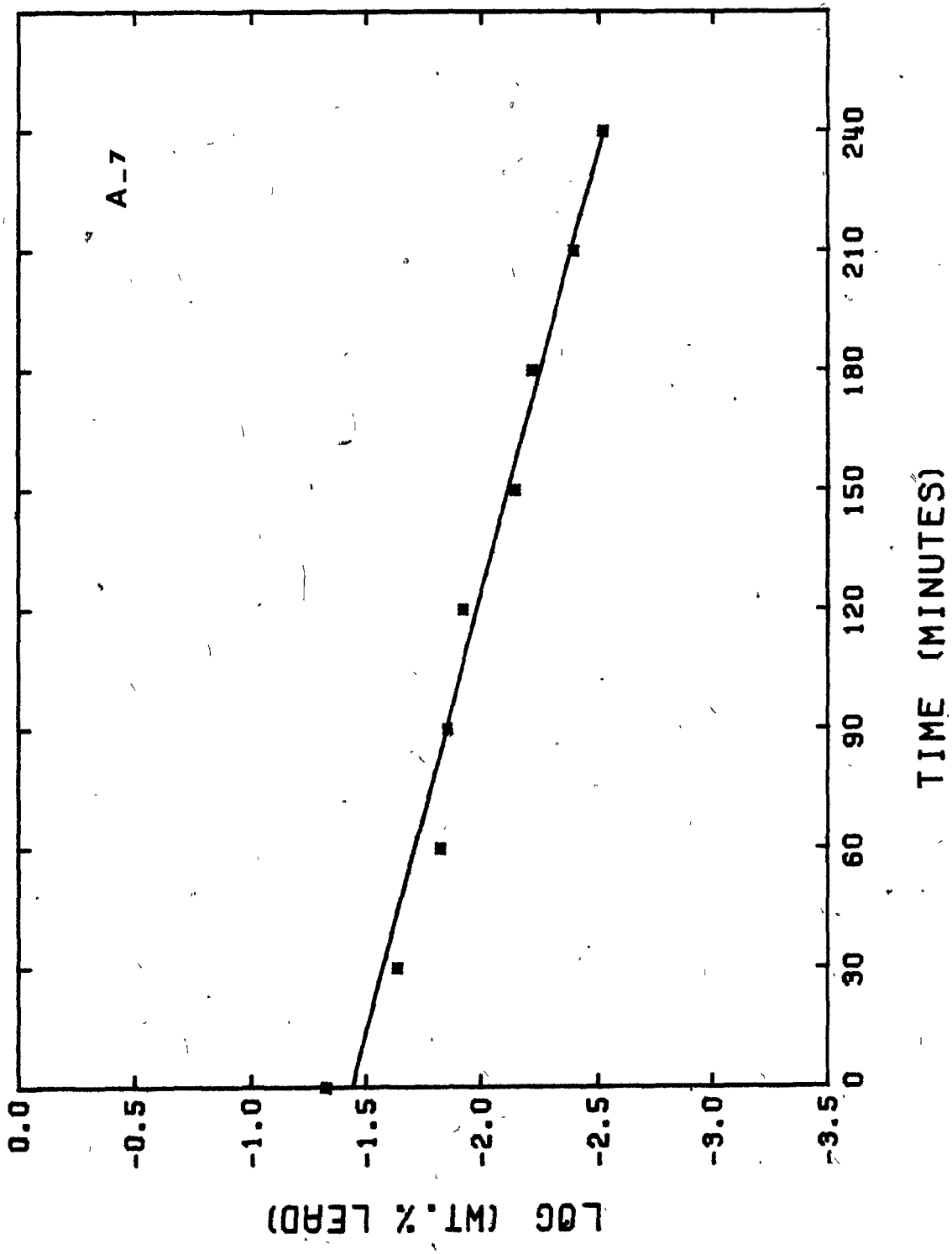
A_7
LOG (WT.% LEAD)
0.0
-0.5
-1.0
-1.5
-2.0
-2.5
-3.0
-3.5
0
30
60
90
120
150
180
210
240
TIME (MINUTES)

By applying vacuum for 240 minutes rather than 120 minutes, it was possible to obtain residual concentration of bismuth and lead below 100 parts per million. That is, weight percent elimination of both bismuth and lead at the end of 240 minutes, were approximately 15% higher compared to the eliminations obtained at the end of 120 minutes. Contrary to this, K_{Bi} and K_{Pb}, were generally lower for 240 minute treatment times compared to 120 minute treatment, except for test F-10, where K_{Pb} increased from 2.52×10^{-3} cms^{-1} to 2.84×10^{-3} cms^{-1}.

Three randomly selected experiments, two from Part I and one from Part II were repeated. Experiments with the labels of F-1-X, F-9-X and A-7-X were replicates of the experiments F-1, F-3, and A-2, respectively (Table 14). The results showed that in experiments F-1-X and F-9-X, overall mass transfer coefficients for both bismuth and lead varied in the range of ±1. to ±10.%, as compared to those for experiments F-1 and F-3. However, in experiment A-7-X, identical results with those of experiment A-2 were achieved. This was a confirmation of the reproducibility of the results and the appropriateness of estimating experimental errors as being in the range of ±5 to ±10%.

No significant effect of changing from silicon carbide-graphite crucibles (Tercod) to high purity alumina crucibles (Hycor Alumina) was observed on mass transport rates of bismuth and lead from copper.

TABLE 14. Comparison of Duplicate Experiments

Test No.	Press. μ Hg	Temp. °C	Bismuth K(10^{-3} cm/s)	Bismuth Initial wt%	Bismuth Final wt%	Bismuth Elim'n wt%	Lead K(10^{-3} cm/s)	Lead Initial wt%	Lead Final wt%	Lead Elim'n wt%
F-1	300	1150	0.61	0.037	0.028	24	0.71	0.099	0.070	29
			-8%[1]			-12%	-4%			-17%
F-1-X	300	1150	0.56	0.043	0.034	21	0.68	0.126	0.096	24
F-3	100	1250	1.34	0.039	0.020	49	2.22	0.125	0.043	66
			-7%			+18%	-10%			+14%
F-9-X	100	1250	1.24	0.020	0.008	60	1.99	0.048	0.011	77
A-2	100	1250	1.86	0.020	0.008	60	2.52	0.028	0.007	75
			+1%			0%	0%			0%
A-7-X	100	1250	1.87	0.025	0.010	60	2.51	0.047	0.012	75

1. Percent difference of duplicates from the actual experiments.

V-6. PART IV EXPERIMENTS

In two experiments, the removal of arsenic and antimony, in conjunction with bismuth and lead, were investigated. No elimination of arsenic and antimony was measured during these tests, which were carried out at 1250°C and 100 μHg (Table 16). For bismuth and lead, however, very similar rates of removal were found to those reported earlier (Table 15). Plots of the change of bismuth and lead concentrations (log wt.%) with time are given in Figures 31 and 32.

V-7. CONDENSATE ANALYSIS

A schematic diagram of the inside of the vacuum furnace is given in Figure 33, showing the locations of the condensate samples. The results of the condensate analysis are summarized in Table 17.

The condensate which collected on the bottom surface of the condenser itself formed a brittle, wafer-like layer which could be separated very easily from the condenser. It also contained metallic droplets caused by splashing. These droplets would first be separated from the bulk sample by grinding and screening.

In experiment F-10, separate condensate samples were taken from the bottom (facing the melt), the side and the top of the condenser, to investigate any variations in composition. No variability was found.

TABLE 15. Summary of Experimental Conditions[1] and Results, Bismuth and Lead Removal, Part IV Experiments

				BISMUTH							
Test No	Press. μHg	Temp. °C	K_L (10^{-3} cm/s)	Corr. Coeff.	K(10^{-3} cm/s)	K_E (10^{-3} cm/s)	K_U (10^{-3} cm/s)	K_G (cm/s)	Initial wt%	Final wt%	Elim'n wt%
A-8	100	1250	7.21	0.999	2.20	62.90	3.33	520	0.025	0.008	68
A-9	100	1250	7.21	0.990	1.51	62.90	1.98	308	0.045	0.021	53

				LEAD							
Test No	Press. μHg	Temp. °C	K_L (10^{-3} cm/s)	Corr. Coeff.	K(10^{-3} cm/s)	K_E (10^{-3} cm/s)	K_U (10^{-3} cm/s)	K_G (cm/s)	Initial wt%	Final wt%	Elim'n wt%
A-8	100	1250	7.21	0.998	2.54	97.53	4.09	413	0.067	0.018	73
A-9	100	1250	7.21	0.997	1.78	97.53	2.43	246	0.110	0.044	60

1. Copper weight = 34 kilogram, A/V = 7.1 m^{-1}, Condenser Distance > 65, time = 120 minutes.

TABLE 16. Elimination of Arsenic and Antimony

Test No.	As%		Sb%	
	Initial	Final	Initial	Final
A-8	0.33	0.31	0.15	0.15
A-9	0.39	0.40	0.24	0.25

FIGURE 31

Rate of removal of bismuth and lead from copper, Test A-8.

	Bi	Pb
K($\times 10^{-3}$ cm.s^{-1}):	2.198	2.541
Elim'n, wt.%:	68	73

time (min.)	wt.% Bi	wt.% Pb
0	0.025	0.067
30	0.018	0.045
60	0.014	0.034
90	0.011	0.024
120	0.008	0.018

Total copper loss = 210 gr.

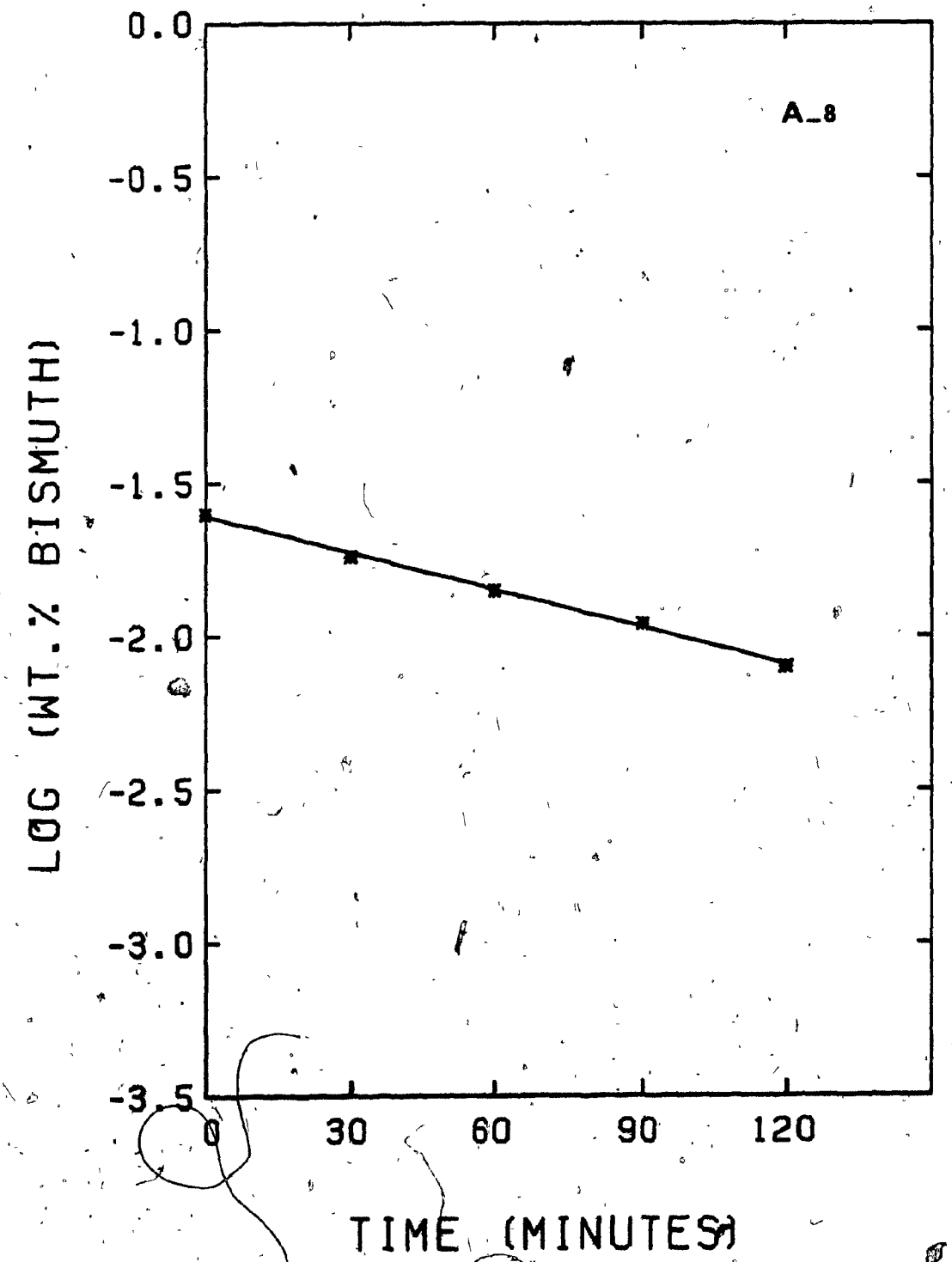
A_8
0.0
-0.5
-1.0
-1.5
-2.0
-2.5
-3.0
-3.5
LOG (WT.% BISMUTH)
0
30
60
90
120
TIME (MINUTES)

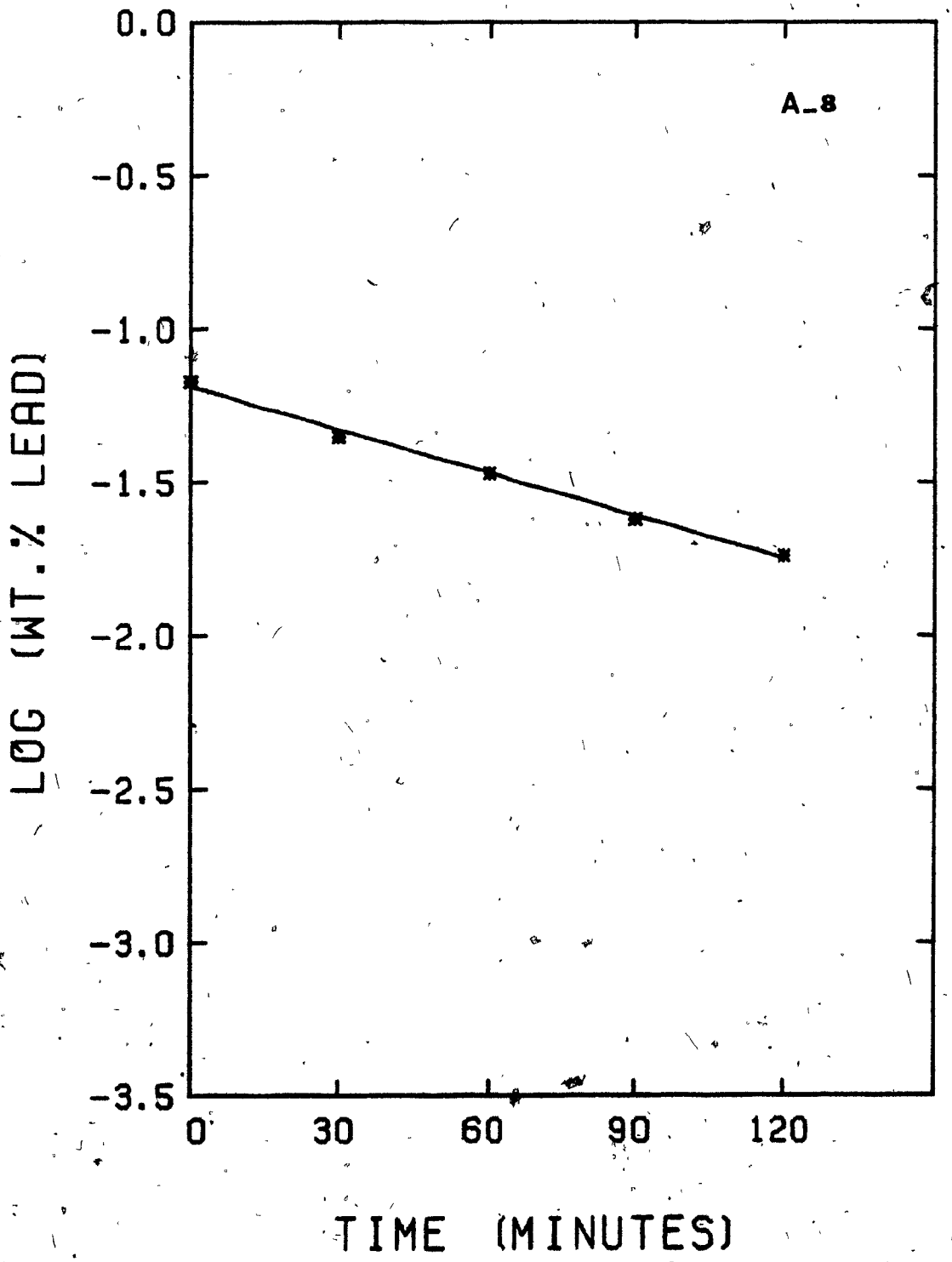
A_8
0.0
-0.5
-1.0
-1.5
-2.0
-2.5
-3.0
-3.5
LOG (WT.% LEAD)
0
30
60
90
120
TIME (MINUTES)

FIGURE 32

Rate of removal of bismuth and lead from copper, Test A-9.

	Bi	Pb
$K(\times 10^{-3}$ cm.s$^{-1})$:	1.514	1.784
Elim'n, wt.%:	53	60

time (min.)	wt.% Bi	wt.% Pb
0	0.045	0.110
30	0.038	0.081
60	0.030	0.067
90	0.023	0.053
120	0.021	0.044

Total copper loss = 220 gr.

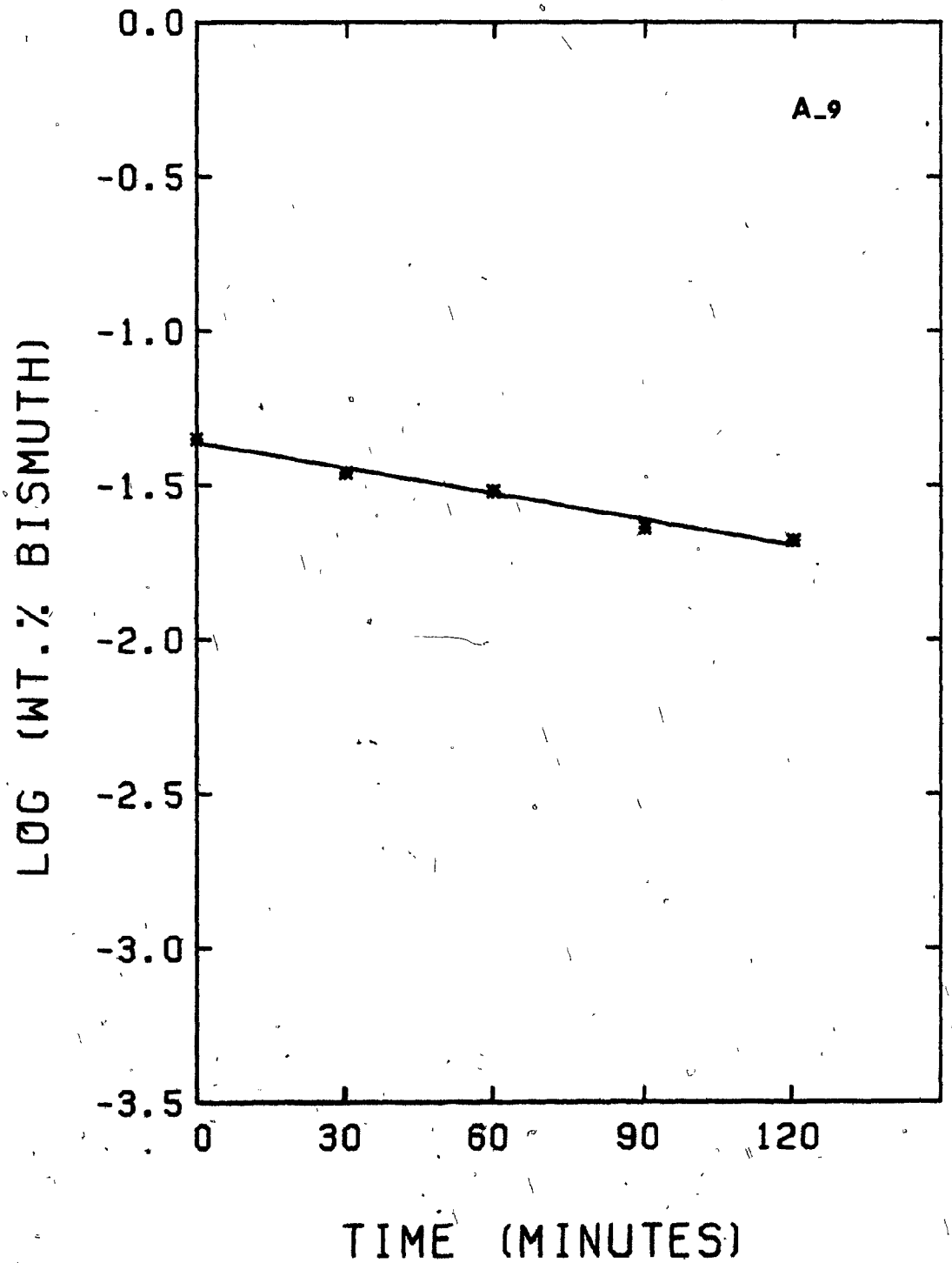
A_9
0.0
-0.5
-1.0
-1.5
-2.0
-2.5
-3.0
-3.5
LOG (WT.% BISMUTH)
0
30
60
90
120
TIME (MINUTES)

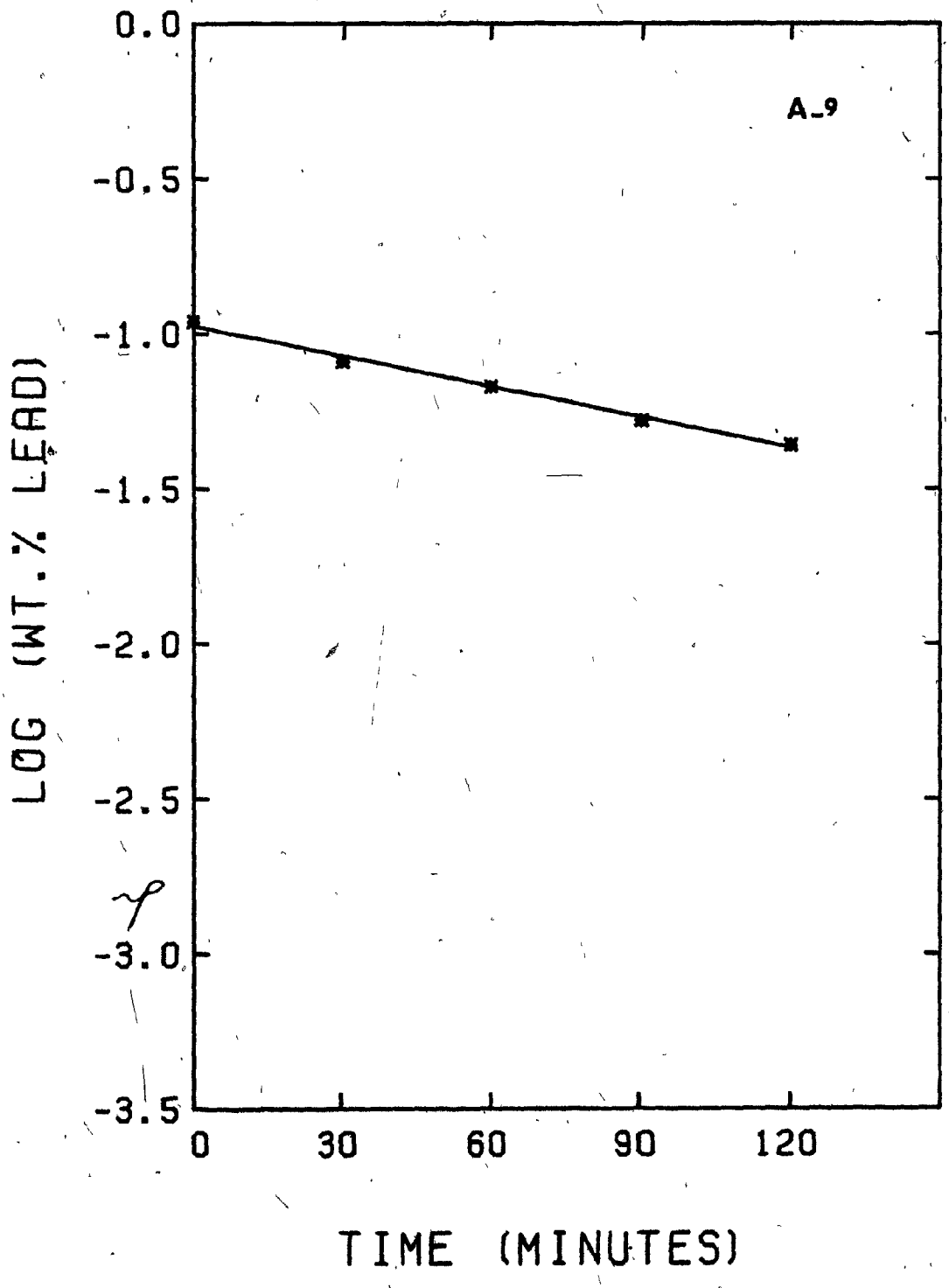
A-9
0.0
-0.5
-1.0
-1.5
-2.0
-2.5
-3.0
-3.5
LOG (WT.% LEAD)
0
30
60
90
120
TIME (MINUTES)

TABLE 17. Analysis of Condensate, wt%

Test No.	Location of Sample	Location No.	Average Distance to Melt Surface cm	Powder[1,2]			Droplets[3]	
				Bi%	Pb%	Cu%	Bi%	Pb%
F-2	Condenser	1	1.5-2.	14.5	70.8	5.3	16.7	72.0
F-4	Condenser	1	1.5-2.	13.7	68.7	12.4	3.7	12.7
F-6	Condenser	1	1.5-2.	10.7	42.9	12.4	4.5	13.1
	Around Crucible	2	25	6.5	26.2	30.0	-	-
	Filter Plate	3	80	7.3	32.8	2.4	-	-
	Chamber	4	65	7.2	31.3	3.3	-	-
	Door	5	100	7.0	29.6	4.7	-	-
F-10[4]	Condenser (Average)	1	1.5-2.	10.5	42.0	41.5	0.2	0.9
	Condenser (Bottom)	-	-	11.1	40.6	54.4	0.1	0.2
	Condenser (Side)	-	-	12.0	46.9	35.0	0.3	1.4
	Condenser (Top)	-	-	13.7	46.9	22.4	0.6	2.2
	Filter Plate	3	80	11.1	42.9	9.8	-	-
	Chamber	4	65	8.3	32.2	21.5	-	-
A-9	Filter Plate	3	80	8.5	25.2	4.9	-	-
	Chamber	4	65	5.2	16.2	2.7	-	-
	Door	5	100	2.0	4.4	2.6	-	-

1. Samples were ground and separated by -100 mesh screen.

2. The balance assumed to be oxygen.

3. The balance is not analyzed.

4. Time = 240 minutes, first 120 minutes was reported as F-7.

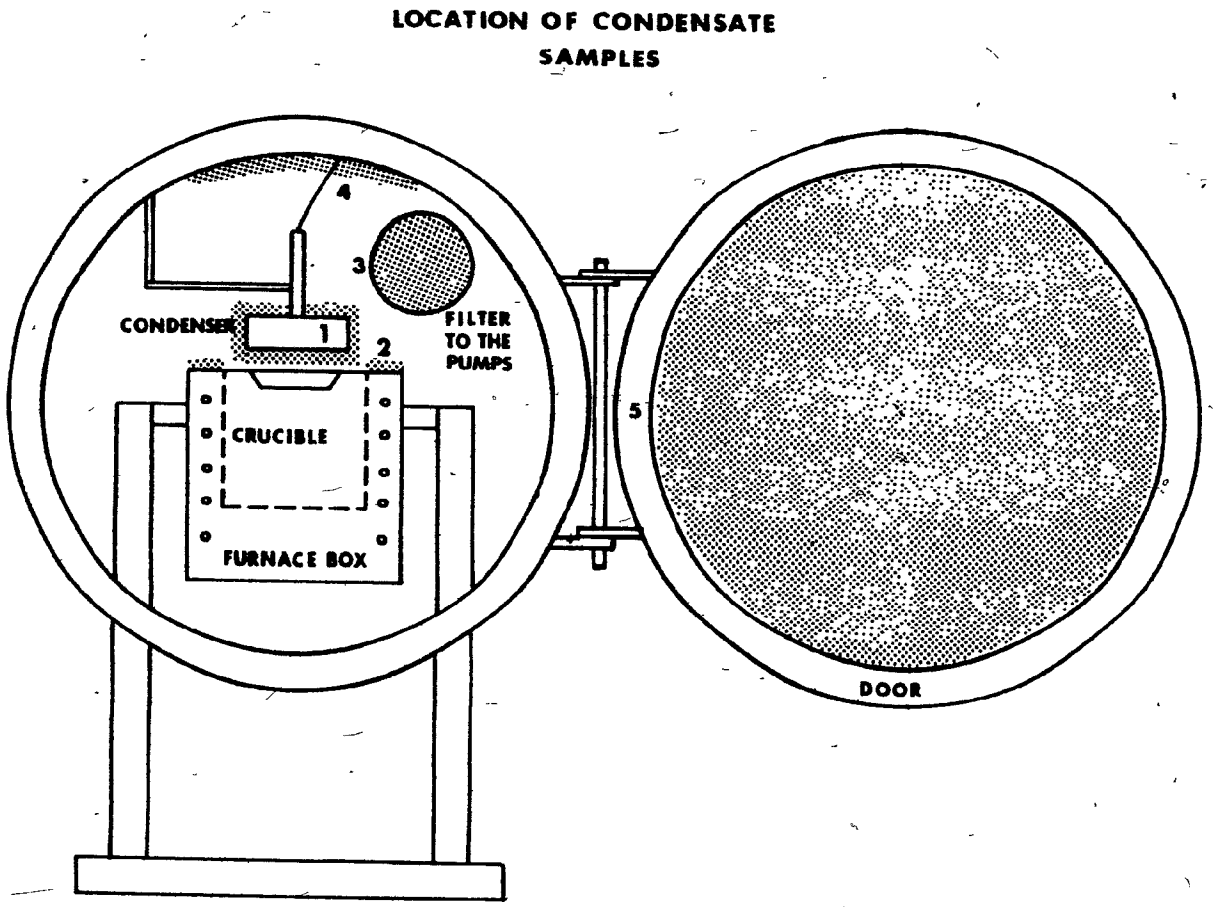

Figure 33. Location of condensate samples.

Based on the detailed analysis of the condensate accumulated on the condenser and weight percent eliminations, the ratio of solute which remained on the condenser relative to the total weight of solute evaporated from copper melts were calculated and included in Appendix V.

Samples collected from other parts of the chamber took the form of a black powder of lead and bismuth oxides. Chemical analysis showed that the bismuth content ranged between 5 and 15%, lead between 25 and 50% and copper between 3 and 25% by weight.

During experiments with hycor alumina crucibles, an accumulation of condensate occurred, which started just above the melt level on the inside surface of the crucible. It was found to comprise mainly metallic copper for the first 2-3 cm above the melt level. Above this, the condensate changed into a wafer-like deposit. The material was sectioned every 5 mm and chemically analysed for two experiments. The representative shape of the accumulation and typical chemical analyses are given in Figure 34.

V-8. STATISTICAL EVALUATION OF THE EXPERIMENTAL WORK, ACCURACY

In this study, a total of twenty experiments were carried out and of these, three experiments were duplicates which confirmed the reproducibility of the results obtained.

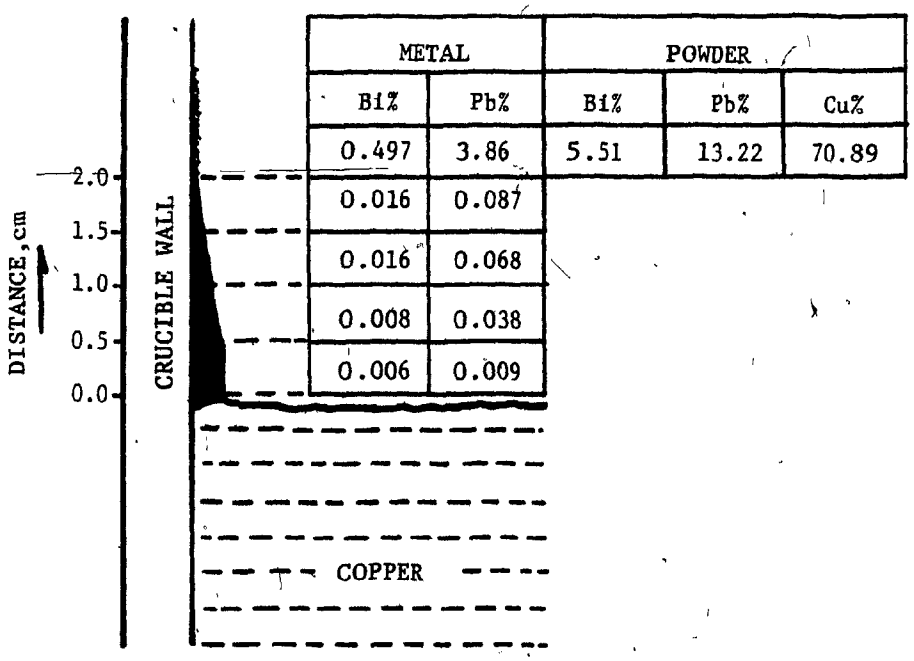

Figure 34. Crucible surface metallic accumulation, a - Test A-1; (time = 120 minutes).

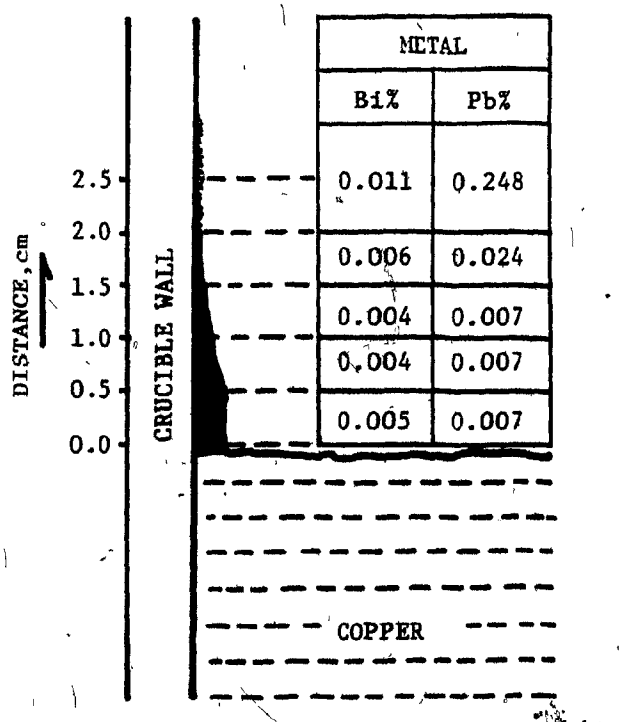

Figure 34 b - Test A-7, (time = 240 minutes).

Overall, a total of 224 samples were analysed for two elements (bismuth and lead), i.e. 448 analyses were obtained. Of these 224 samples, 36 of them were randomly selected (16% of the total) and analysed a second time for the two elements (total of 72 values). Out of these 72 values only 6 (8% of the 72 values) varied by more than ±10% compared to the original values, and variations never exceeded 20%.

Twenty-one randomly selected samples were sent to the Noranda Research Center to be analysed for bismuth, lead and some of them also for copper, arsenic and antimony. The results obtained showed that only one value varied by more than ±10% compared to the original values obtained in our laboratories.

Analyses of arsenic, antimony and copper were not included in this evaluation study, since these elements were involved in only a few samples.

The foregoing evaluation studies provide confidence in the accuracy of the results obtained in the present study.

CHAPTER VI

DISCUSSION

VI-1. INTRODUCTION

The main objectives undertaken at the beginning of the experimental program were successfully achieved. It was shown that bismuth and lead could be eliminated from copper melts under vacuum and that the main factors controlling the kinetics of this process could be defined clearly. Similarly, a sufficient amount of accurate data were obtained to enable comparisons with previous literature data available on the vacuum refining of copper.

VI-2. REMOVAL OF BISMUTH AND LEAD

VI-2.A Fractional Factorial Test Design

In the first part of the experimental work, a two-level fractional factorial test design was used. With the subsequent eight experiments, four variables could be screened. Two of these, vacuum pressure and melt temperature were identified as being the most significant factors controlling the overall rate constant for the removal of bismuth and lead from copper melts.

One indication showing the satisfactory use of fractional factorial test design is that the interactions are small compared to the main effects. This can be clearly

observed in the relatively low values for the effects of AB,CD and AC,BD interactions for both bismuth and lead data (Tables IV-1 and IV-2 in Appendix IV).

The magnitude of an interaction depends upon the ranges of the variables selected; as the ranges are decreased the interactions become smaller compared to the main effects, and when the region to be examined is sufficiently small, the interactions with few exceptions become negligible[120].

As the range becomes narrower, the magnitudes of the effects become smaller, and the more likely are they to be masked by experimental error. The ranges chosen must be such as to produce effects which are measurable but not so large as to give rise to appreciable interactions.

This may be one of the reasons why the factors melt surface area to volume ratio and condenser distance to melt surface were found to have insignificant effect on the rate of removal of bismuth and lead. The range between the levels selected for melt surface area to volume ratio (6.7 and 10.2 m^{-1}) were clearly not sufficiently different to cause any significant effects on K in the present experimental equipment.

However, high levels of melt surface area to volume ratio are hard to achieve in equivalent industrial applications since melt surface area to volume ratio would be always limited to the crucible and induction coil dimensions. Higher melt surface area to volume ratios can be provided

through by mixing the melt with inert gas bubbling or through use of a vacuum lift refining type of process. These were both considered to be beyond the scope of the present work. However, as mentioned in Section II-4.A, Kametani and Yamauchi [29,63-65] could not obtain good impurity elimination results with vacuum lift refining treatment of blister copper, in which the melt surface area to volume ratio reaches much higher values.

Similar to the effect of variable melt surface to volume ratio, one could say that the present selection of the variable condenser distance from the melt surface as 2 and 65 cm may not have been sufficiently different to obtain significant effects.

The purpose of designing the water cooled condenser and placing it as close to the melt surface as possible (1.5-2.0 cm) was to create a condensation sink for the evaporating molecules, thereby overcoming the gas phase resistance and providing enhanced vapourization. Maximum or limiting evaporation could have been achieved if the condensation sink had been located within the distance of mean free path of the evaporating atoms. However, mean free paths for all the impurities being considered were estimated as being less than one centimeter over the temperature and pressure ranges of the present experiments. (Mean free path values are included in Appendix II.)

Unfortunately, there were practical reasons why the water cooled condenser could not be placed within this

"critical distance" of the melt surface. Thus, splashes from the melt and safety considerations concerning the possibility of melting the steel jacket and causing a water-liquid metal explosion, prevented closer juxtapositioning.

Based on the present experiments, one can conclude that when a water cooled condenser is placed at distances of 2 cm or more from the melt surface, it has little effect on the rate of removal of impurities over the range of conditions studied in the present work.

One other interesting observation was that the analysis of the condensate samples from different locations of the vacuum chamber, including the water cooled condenser, showed that the condensate composition was independent of distance from the melt surface (Table 17). This may be an indication that the whole chamber acts as the condensing surface rather than only those cold surfaces nearby the melt.

It should be clarified at this point that the results of the fractional factorial test design shows that vacuum pressure and melt temperature have much more effect than A/V and condenser distance, but that the latter do play a minor role.

Actually, comparison of the results of the experiments F-7, F-9-X, A-2 and F-10, F-9 shows the favorable effects of having the condenser distance ~ 2.0 cm (Table 18) compared to ~ 65 cm. In addition, further evidence was obtained from

TABLE 18. Comparison of Results, Showing the Effect of Condenser Distance

Test No.	Press. μ Hg	Temp. °C	A/V m^{-1}	Cond. Dist. cm	Time min.	Elimination,%		K(10^{-3} cm/s)	
						Bi	Pb	Bi	Pb
F-7	100	1250	10.2	2	120	75	85	1.79	2.52
F-9-X	100	1250	10.2	65	120	60	77	1.24	1.99
A-2	100	1250	7.1	65	120	60	75	1.86	2.52
F-10	100	1250	10.2	2	240	89	98	1.62	2.84
F-9	100	1250	10.2	65	240	70	92	0.75	1.63

TABLE 19. Distribution Ratio of Impurity Removed to Condenser

Test No.	Press. μ Hg	Temp. °C	Amount of Condensate Accumulated On Condenser gram	Distribution Ratio of Impurity to Condenser[1]	
				Bi%	Pb%
F-2	100	1150	53	54	55
F-4	300	1250	73	59	61
F-6	300	1150	34	83	74
F-10[2]	100	1250	128	41	52

1. Balance was scattered to chamber surface.

2. Time = 240 minutes.

the analysis of the condensate accumulated on the water cooled condenser (Table 17). Using this data and the total amount of bismuth and lead evaporated from copper, distribution ratio of these elements settling on the condenser surface was calculated. Details of these calculations are included in Appendix V and a summary of the results provided in Table 19.

It is interesting to note that 40-80% of the bismuth or lead evaporated from copper accumulated on the water cooled condenser even though this did not reflect in any significant changes in the rate of mass transport.

The use of a fractional factorial test design proved most successful in the present work. Vacuum pressure and melt temperature were found to be the most significant factors in comparison to melt surface area to volume ratio and condenser distances.

The results obtained in Part II, confirmed that the estimation of mean square (error variances) from two factor interactions, as well as estimated experimental errors, had been carried out correctly.

VI-2.B Effects of Pressure and Temperature

Analysing of the effect of pressure and temperature variations on impurity evaporation rates, one can observe similar changes: For instance, holding the pressure constant at 60 μHg or at 100 μHg and varying the temperature from 1150°C to 1350°C, values of K_{Bi} and K_{Pb} increased by two to

two and a half times (Figures 35 and 36 and Table 20). Similarly, on holding the melt temperature constant at 1150°C, 1250°C and 1350°C respectively, and varying pressures from 300 μHg to 60 μHg, overall mass transfer coefficients, K_{Bi} and K_{Pb}, were again increased by two to two and a half times (Figure 38).

When one considers the effects of pressure and temperature in combination much improved eliminations are possible. Thus by increasing the melt temperature from 1150°C to 1350°C and decreasing the vacuum chamber pressure from 300 μHg to 60 μHg, the overall mass transfer coefficient could be increased by a factor of six for bismuth and eight times for lead.

In view of the close relationship of K_L, K_E and K_G with temperature and pressure (Section III-1) this behaviour can be anticipated: Increasing temperature causes an increase in solute vapour pressure, activity coefficient, diffusivity in the liquid and an increase in mean free path distances in the gas phase. Similarly, decreasing pressure causes an increase in mean free path values resulting in a decrease in the gas phase's resistance to evaporating solute molecules.

In Figures 37 and 39, the results for weight percent elimination of bismuth and lead at different temperatures and pressures are presented. The results show increased eliminations for temperature changes between 1150°C and 1250°C while pressure decreases from 300 μHg to 100 μHg, than for

TABLE 20. A Summary of Experimental Kinetic Data, Showing the Effect of Melt Temperature and Vacuum Pressure

				Bismuth				Lead			
Test No.	Press. μ Hg	Temp. °C	$K_L(10^{-3}$ cm/s)	$K(10^{-3}$ cm/s)	$K_E(10^{-3}$ cm/s)	$K_U(10^{-3}$ cm/s)	K_G (cm/s)	$K(10^{-3}$ cm/s)	$K_E(10^{-3}$ cm/s)	$K_U(10^{-3}$ cm/s)	K_G (cm/s)
A-6	60	1150	5.09	1.32	28.44	1.89	631	2.00	47.92	3.54	704
A-3	60	1250	7.21	2.76	62.90	4.81	750	4.04	97.53	10.13	1024
A-5	60	1350	9.78	3.15	125.40	4.84	391	4.70	180.99	9.54	536
A-1	100	1150	5.09	1.05	28.44	1.38	460	1.84	47.92	3.06	609
A-2	100	1250	7.21	1.86	62.90	2.60	406	2.52	97.53	4.04	409
A-4	100	1350	9.78	2.33	125.40	3.13	252	3.93	180.99	6.81	383
F-1	300	1150	5.15	0.61	28.44	0.71	237	0.71	47.92	0.83	166
F-8	300	1250	6.59	0.99	62.90	1.19	186	1.66	97.53	2.26	229

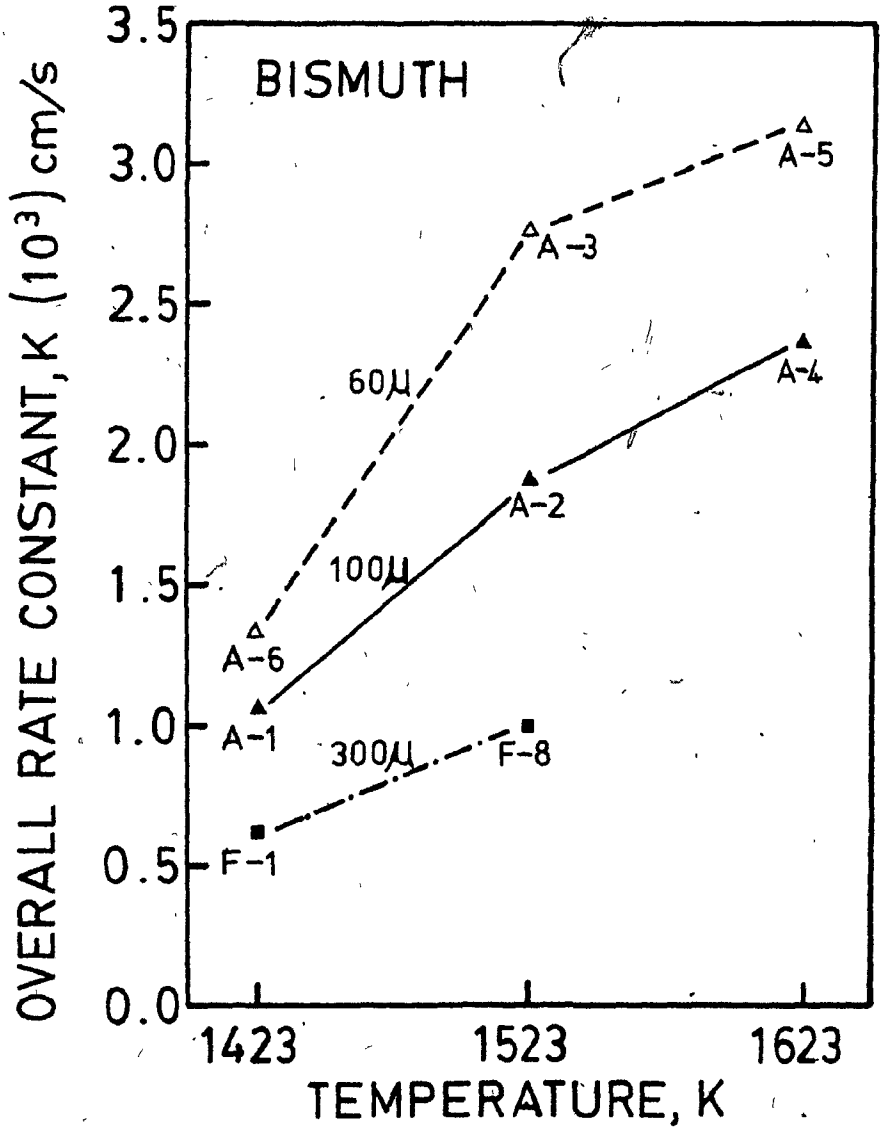

Figure 35. Overall rate constant vs. temperature, for bismuth.

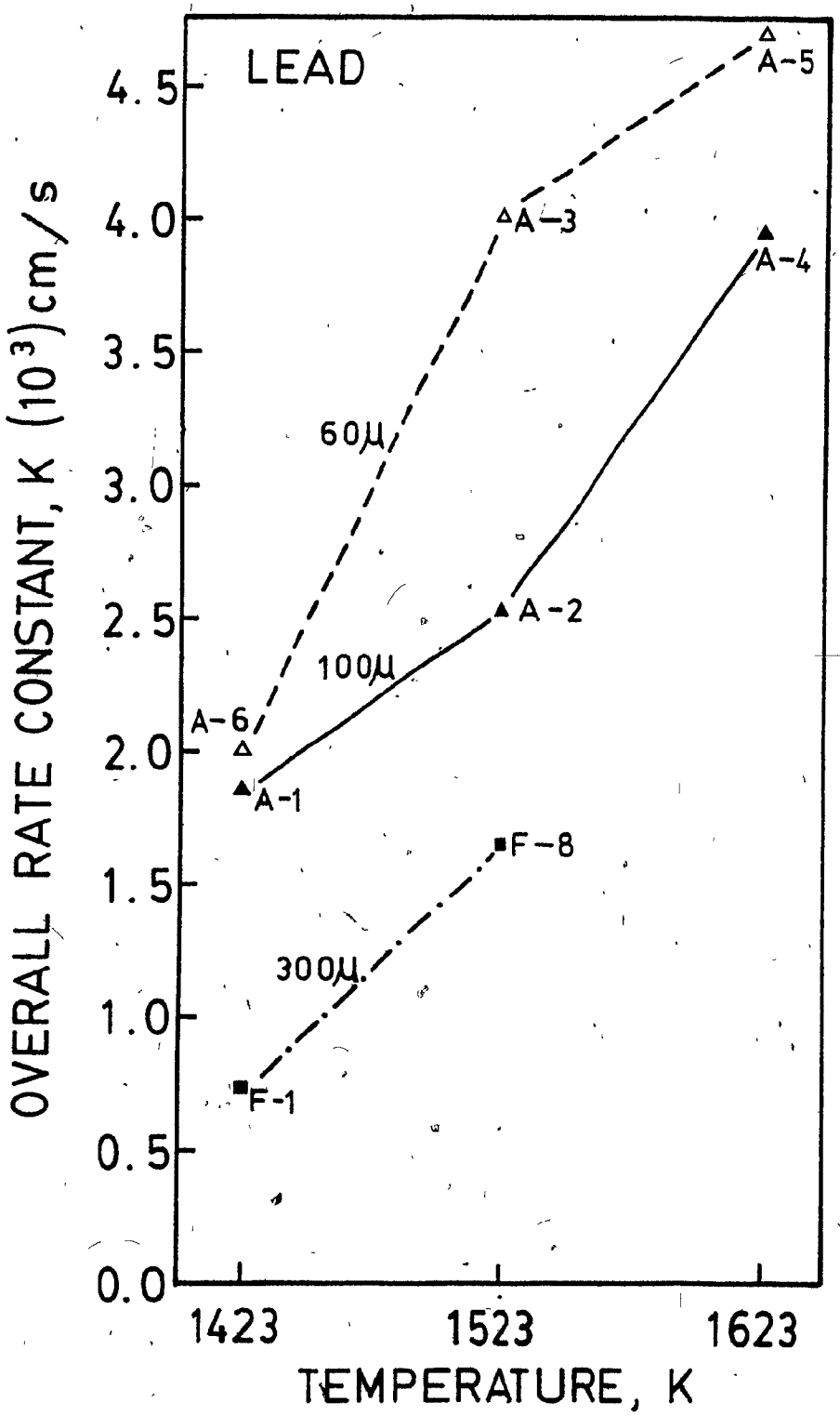

Figure 36. Overall rate constant vs. temperature, for lead.

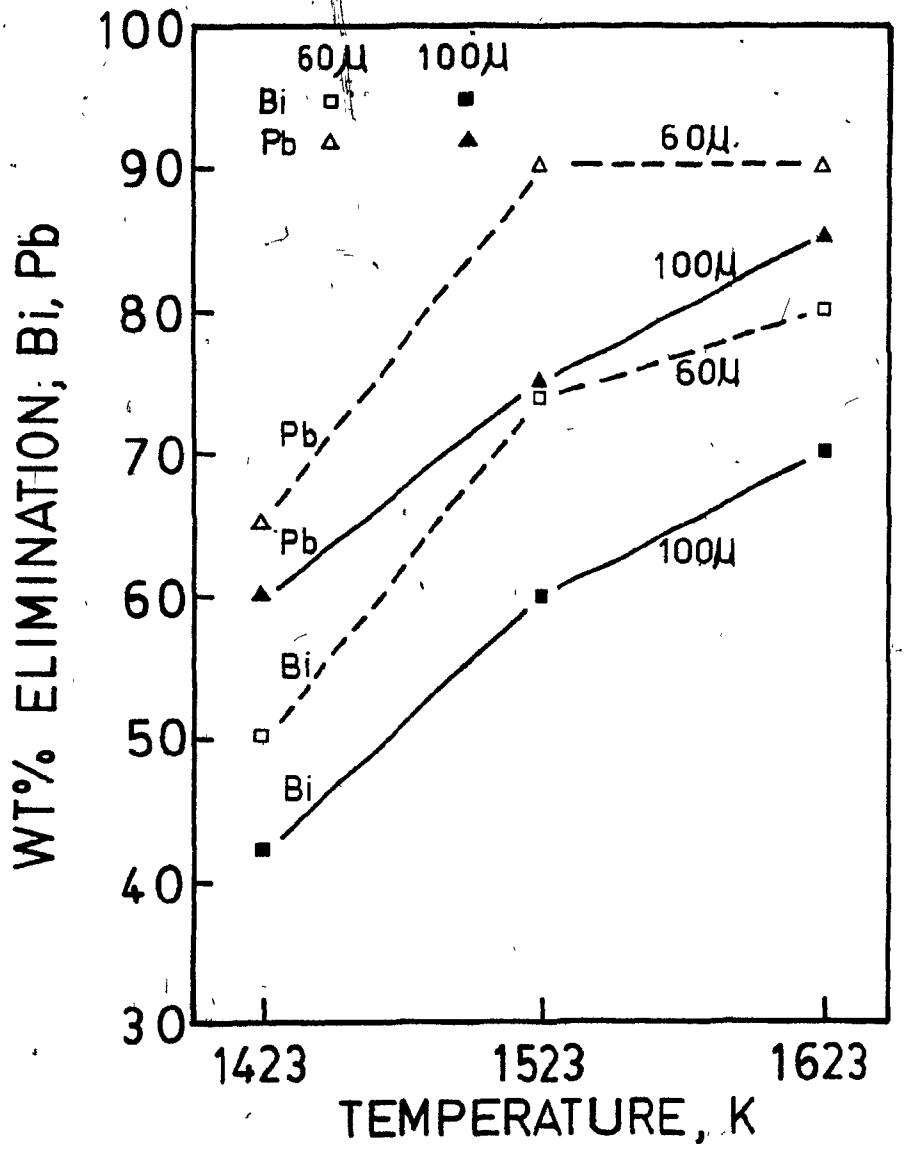

Figure 37. Wt% elimination vs. temperature, for bismuth and lead.

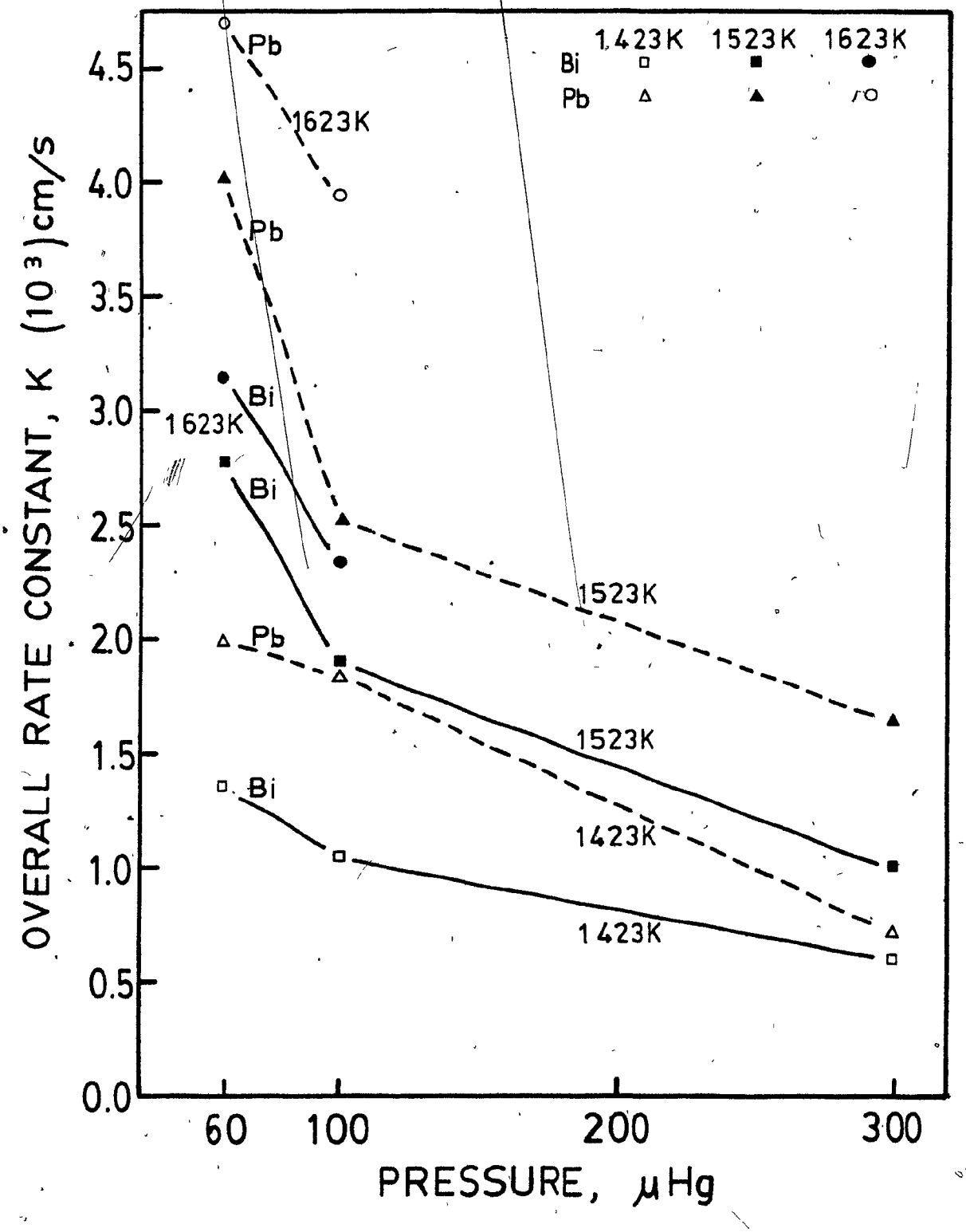

Figure 38. Overall rate constant vs. pressure, for bismuth and lead.

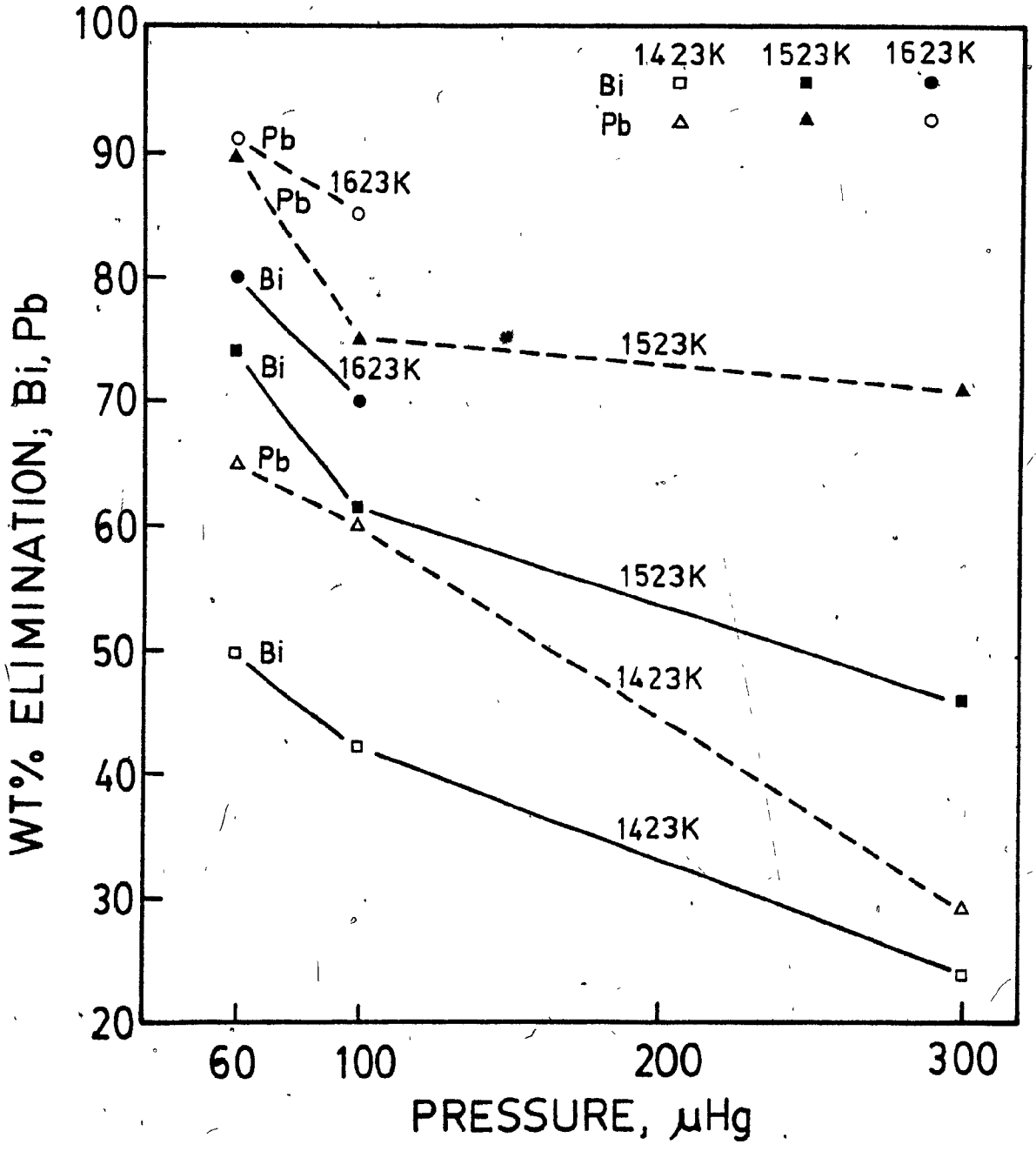

Figure 39. Wt% elimination vs. pressure, for bismuth and lead.

temperature increases between 1250°C and 1350°C and pressure decreaaes between 100 μHg and 60 μHg.

VI-2.C Processing Time and Reproducibility

By doubling the time from 120 min. to 240 min. in three experiments bismuth and lead concentrations could both be significantly reduced below the 0.010% level (Tables 12 and 13).

It was observed in these experiments that the overall mass transfer coefficient for both bismuth and lead appeared to decrease somewhat during the second 120 minute time interval. In Table 11, a comparison of the results for experiments F-9-X to F-9, F-7 to F-10 and A-7-X to A-7 clearly indicates such a behaviour.

This suggests that there may indeed be a so called "critical level of concentration of impurities" for optimum rates of removal. The level in the present study would be around 100 ppm.

Duplication of three randomly selected experiments confirmed the reproducibility of the results presented (Table 14).

VI-3. REMOVAL OF ARSENIC AND ANTIMONY

In two experiments (A-8 and A-9) carried out at 1250°C and 100 μHg vacuum pressure, no elimination of either arsenic or antimony was obtained following 120 minutes of treatment (Table 16). The explanation for this probably lies in their

extremely low activity coefficients in molten copper ($\gamma^{\circ}_{As} = 10^{-6}$ and $\gamma^{\circ}_{Sb} = 2.2 \times 10^{-2}$ at 1573°C, Appendix I). Consequently, even though their vapour pressures are high, ($P^{\circ}_{Sb} = 2.74$ mm Hg, $P^{\circ}_{As_T} = 6 \times 10^{5}$ mm Hg at 1573 K, Appendix I) their overall potential for evaporation is low.

From the data provided in Appendix I, evaporation mass transfer coefficients were estimated for arsenic and antimony by using Equations 20 and 39. The results were:

$$K_{E_{As}} = 8.29 \times 10^{-4} \text{ cm/s at } 1573 \text{ K}$$

$$K_{E_{Sb}} = 6.53 \times 10^{-5} \text{ cm/s at } 1573 \text{ K}$$

$$K_{E_{Sb_2}} = 6.40 \times 10^{-8} \text{ cm/s at } 1573 \text{ K}$$

These values are generally more than 100 times less than $K_{E_{Bi}}$ and $K_{E_{Pb}}$ at similar temperatures.

In the two experiments the rates of removal of bismuth and lead remained very similar to those obtained in earlier experiments (Table 15), confirming that any solute interactions between bismuth, lead, arsenic and antimony could be discounted over the typical industrial ranges studied.

VI-4. INFLUENCE OF THE PRESENCE OF OXYGEN AND SULPHUR IN THE SYSTEM

In the entire experimental work, oxygen and sulphur levels were lower than 0.001% in the copper prior to melting and the melt surface stayed perfectly clean and clear during

the experiments. Thus, the lowest vacuum pressure obtained was always in the range 40-50 μHg while running the pumping system at full capacity (as explained in the previous sections, chamber pressures of 60, 100 and 300 μHg were maintained by leaking nitrogen gas into the vacuum chamber). Assuming that it was all air then, the partial pressure of oxygen in the system (21% oxygen in air) was only ∿10 μHg at all times.

Thermodynamic calculations were carried out in order to estimate the stability of the common oxides of the elements which are being considered, i.e. copper, bismuth, lead, arsenic and antimony. The F.A.C.T. system facility of McGill University [123] was utilized for this purpose.

Two different approaches were used in the calculations for forming liquid metal oxides from either liquid or gaseous metal molecules with oxygen.

a) Assuming an extreme case of 500 μHg chamber pressure ($P^{\circ}_{O_2}$ = 100 μHg) the equilibrium temperatures were estimated (Table 21-a).

b) At three different temperatures (1423 K, 1523 K and 1623 K) equilibrium partial pressures of oxygen were estimated (Table 21-b).

In both cases it was assumed that activity of copper was 1.0, the activity of bismuth was 0.001 and the activities of lead, arsenic and antimony were 0.004 (again extreme cases were selected).

TABLE 21-a. Estimated Equilibrium Temperatures at which Metal Oxides would Form[1,2].

Element	Temperature, K	
	For Liquid Metal	For Metal Vapour
Cu	1139	-
Bi	938.8	1043.1
Pb	1000.1	1091.3
As	- [3]	1410.3
Sb	1339.1	1384.5

1. Activities of the elements were assumed to be:

   $a_{Cu} = 1.0$, $a_{Bi} = 0.001$, $a_{Pb} = a_{As} = a_{Sb} = 0.004$

   Chamber pressure = 500 μHg, P_{O_2} = 100 μHg

2. $nM + \frac{m}{2}O_2 \longrightarrow M_nO_m(l)$ or $nM_{(g)} + \frac{m}{2}O_{(g)} \longrightarrow M_nO_m(l)$.
   There is no data available for forming gaseous metal oxides.

3. There is no data available.

TABLE 21-b. Estimated Equilibrium Oxygen Pressures at which Metal Oxides would Form[1,2] (for certain melt temperatures)

Element	Minimum chamber pressure for oxide formation, mm Hg					
	1423 K		1523 K		1623 K	
	Liquid Metal	Metal Vapour	Liquid Metal	Metal Vapour	Liquid Metal	Metal Vapour
Cu	0.018	-	0.073	-	0.249	-
Bi	36.7	17.3	187.7	64.0	775.2	199.1
Pb	40.4	14.0	302.5	53.6	1740.4	172.5
As	-	0.014	-	0.090	-	0.454
Sb	0.001	0.023	0.007	0.137	0.061	0.646

1. Activities of the elements were assumed to be:

   $a_{Cu} = 1.0$, $a_{Bi} = 0.001$, $a_{Pb} = a_{As} = a_{Sb} = 0.004$.

2. $n\underline{M} + \frac{m}{2} O_2 \rightarrow M_n O_m(1)$ or $nM_{(g)} + \frac{m}{2} O_{(g)} \rightarrow M_n O_m(1)$.
   There is no data available for the formation of gaseous metal oxides

3. There is no data available.

The first set of calculations indicate that at the temperatures at which the experiments were carried out, it was not possible to form the metal oxides of any of the elements being considered (Table 21-a) before or during the evaporation of the elements being considered.

However, equilibrium temperatures for the formation of oxides of both arsenic and antimony (1410 K for arsenic and 1385 K for antimony) were much closer to the lowest melt temperature (1423 K) maintained during the experiments than bismuth (1043 K), lead (1091 K) and copper (1139 K).

Similarly, in the second set of calculations for bismuth and lead the estimated equilibrium oxygen pressures were much higher than the oxygen partial pressures maintained in the experiments, while for arsenic, antimony and copper equilibrium oxygen pressures were closer to the oxygen pressures (Table 21-b) maintained during the experiments.

On the basis of these thermodynamic studies one can conclude that in the experiments concerning the elimination of bismuth and lead from copper there was no possibility of metal oxide formation before or during the evaporation of the elements. One can therefore conclude that there was no effect of oxygen on the results obtained. However, this may not be the case with arsenic and antimony.

These results also show that metal oxides would form either after evaporated metal molecules condense and during cooling down of the particles or after the experiment was completed and air was let into the vacuum chamber.

There was no possibility of sulphur contamination in the system.

Consequently, the effects of oxygen and sulphur presence are considered to be negligible in the present work, except in their influence on the precipitation of bismuth and lead oxide condensates adjacent to the cooler sidewalls of the chamber.

Computer print-outs of the calculations are included in Appendix VII.

VI-5. ANALYSIS OF CONDENSATE AND COPPER LOSSES

Condensate samples collected from the chamber surface were in the form of a black powder of bismuth and lead oxides. On the basis of thermodynamic calculations dealing with the stability of these oxides, it was deduced that these particles precipitated in the gas phase, away from the melt surface, at temperatures significantly below the temperature of the copper melts (Tables 21-a and 21-b). Furthermore, at the partial pressures of oxygen and at the melt temperatures maintained during the experiments stable oxide phases of these three elements could not exist in either the liquid or gaseous form.

Analysis of the condensate showed that fine, micron sized oxide particles of bismuth and lead were scattered throughout the vacuum chamber (Figure 33 and Tables 17 and 19) and on the crucible sidewall above the melt (Figure 34-a, 34-b).

These indicate that evaporated molecules travel random distances until on arriving at cold surfaces they begin to collect. This may be an explanation again as to why, in small scale system, eliminations were found to be significantly higher than in our large pilot scale system. Thus, since metallic vapour has to travel longer distances in larger scale systems, the probability of recondensation of evaporated elements at the melt surface is relatively higher than precipitation of adjacent cold surfaces.

The observation of high levels of bismuth and lead (>1.0 wt.%) on the crucible surface presents a technological problem. Thus, when one finishes refining and starts pouring the melt into a ladle or mold, it will be possible to recontaminate the copper with this accumulated condensate on the crucible surface.

Copper levels in the condensate were generally low (Table 17). This is consistent with the difference in weight of copper before and after the experiments which was always less than 1% of the initial weight of copper. Less than 1% copper loss included splashes which occurred during samplings and after the experiment was completed during casting the molten copper into the molds. The weight of copper lost to the condensate and percentages are reported in Appendix V, Table V-3.

Considerably lower vapour pressure of copper (Appendix I) within the temperature range of 1150-1350°C accounts for these

low losses. Assuming a maximum rate of evaporation (Equation 15), the weight of copper evaporating in 120 minutes would be no more than 34-193 and 887 grams at temperatures of 1150-1250 and 1350°C respectively. This represents 0.1, 0.6 and 2.6% of the 34 kg initial charge of copper. It also indicates that copper losses should be comparatively low for industrial vacuum refining processes.

Knowing the maximum amount of copper that would be transferred to condensate within 120 minutes and assuming a typical average of 70% by weight elimination for bismuth and lead with the starting concentrations of 0.1% and 0.4% respectively, the percent composition of the condensate can be predicted as follows:

	1150°C	1250°C	1350°C
Bi	16	8	2
Pb	62	30	9
Cu	22	62	89

Since the maximum rate of evaporation is assumed for copper this would represent the most extreme case. Also, from the time copper charges were molten until the first sample was taken there was usually a 30-60 minute time gap. This was needed to adjust the melt temperature and chamber pressure levels to the desired values. Naturally, evaporation of the impurities and of copper took place during this time gap during which it was not possible to measure their rates. Therefore, comparison of predicted condensate compositions with experimental results is somewhat suspect.

VI-6. KINETIC STUDIES

As no elimination of arsenic and antimony could be detected, kinetic studies concentrated only on bismuth and lead impurities in copper.

Experimental results showed that the elimination of both bismuth and lead by vacuum induction melting followed first order kinetics over the whole range of conditions studied. For the linear relationships fitted to the logarithms of the relative changes in concentrations of bismuth and lead with time, the lowest correlation coefficients obtained were 0.940 for bismuth and 0.927 for lead out of a total of 20 independent experiments.

The conclusion is in partial accord with the results obtained by Ohno[49,50] who, at pressure below 10 μHg, found that the removal of bismuth obeyed first order kinetics while lead did not. The results of Bryan et al.[53] indicated that bismuth only obeyed first order kinetics at pressures above 200 μHg, while below that pressure, the rate of removal of bismuth deviated from first order kinetics.

In all the present experiments, the overall rate constant for lead was found to be higher than that of bismuth. This observation can be attributed to a two times higher activity coefficient of lead as compared to bismuth in copper, together with a vapour pressure of bismuth only about 1.4 times that of lead (Appendix I).

The overall rate constant, together with component coefficients for the liquid, interface and gas phase (K_L, K_E and K_G, K_U) have been plotted versus temperature (°C) for two different levels of pressure (Figures 40-a and 40-b). The estimated values of the coefficients for both bismuth and lead were always in the following order of magnitude:

$$K < K_U < K_L < K_E < K_G$$

This order shows that both bismuth and lead elimination rates were generally controlled by the term, K_U, containing the gas phase mass transfer coefficient. Figure 40 also shows that there is a tendency towards mixed control (i.e. liquid plus gas) as melt temperature was increased and pressure decreased. This tendency was stronger for lead than bismuth.

By using Equation 39, evaporation mass transfer coefficients, $K_{E_{i_2}}$, were estimated for diatomic bismuth molecules (Appendix I, Table I-1). They were always much lower than evaporation mass transfer coefficients (K_{E_i}) for monoatomic bismuth molecules (350 and 610 times lower at 1150°C and 1350°C (respectively). Therefore, it was decided to ignore the evaporation of diatomic species and base estimations only on K_{E_i}, for monoatomic bismuth metal vapour.

Due to lack of experimental data on the diffusivity of bismuth and lead in liquid copper, liquid phase mass transfer coefficient K_L values had to be estimated based on assumptions concerning D and ΔE (see Appendix III). In view of these uncertainties, numerically equivalent values of K_L for both bismuth and lead were used in the analysis.

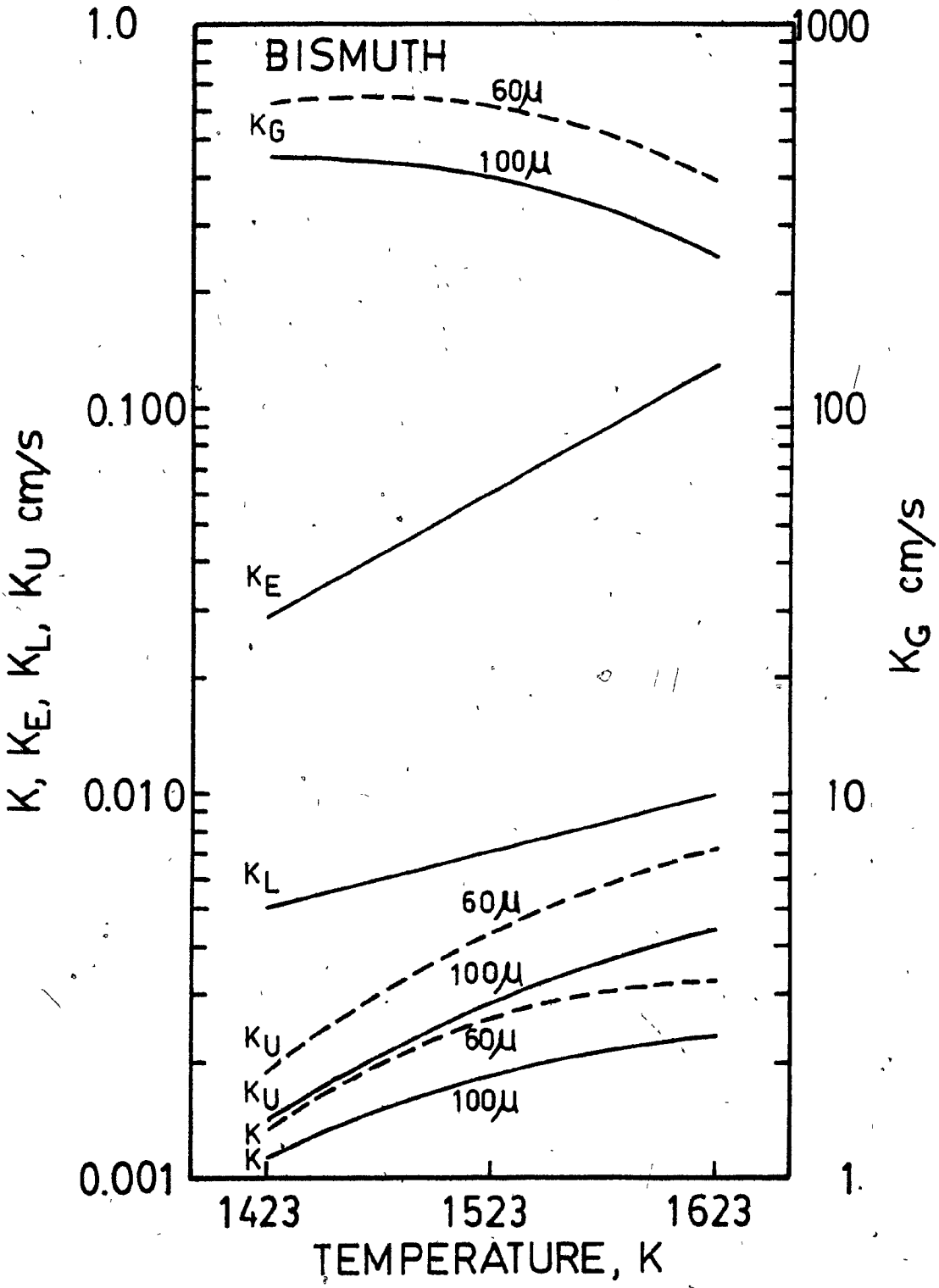

Figure 40-a. Mass transport coefficients vs. temperature, at pressures of 100 and 60 μHg, for bismuth.

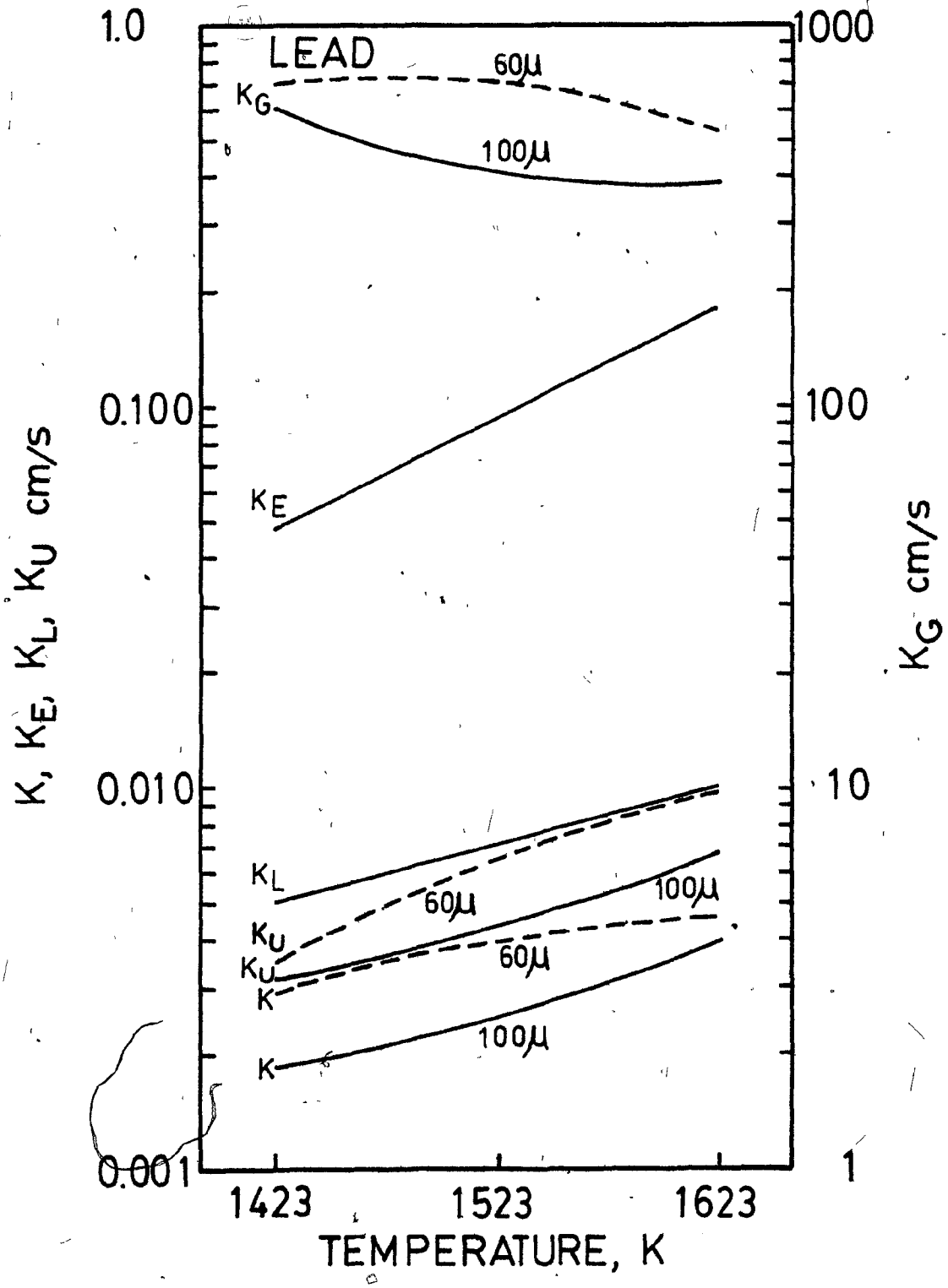

Figure 40-b. Mass transport coefficients vs. temperature, at pressures of 100 and 60 μHg, for lead.

In order to demonstrate the sensitivity of K_L to changes in the activation energy for diffusion, ΔE was decreased by 50% to 15,000 cal/mole and values of D and K_L recalculated. The results are summarized in Figure 41, where changes in the values of K_L with temperature are shown for ΔE = 15 and 30 Kcals/mole respectively.

Comparison of the two sets of values for K_L shows that a 50% decrease in ΔE could result in a 50% decrease in the value of K_L at high melt temperatures of 1650°C. With such uncertainty, a distinction between the probability of gas and liquid phases transport control becomes questionable. Over the lower temperature ranges of the present experiments, such uncertainties in ΔE are considered less critical in considering rate controlling steps and concluding that kinetics were dominated by transfer through the gas phase.

Values for the evaporation mass transfer coefficient, K_E, were also extrapolated up to 1650°C using the data in Appendix I. For bismuth and lead, the results are summarized in Figure 42.

As mentioned in Chapter III, section 1, values for K_U were deduced from Equation 31 and values for K_G then determined by Equation 28.

By using the present data obtained for K_U at 100 and 60 μHg chamber pressures and 1150, 1250 and 1350°C melt temperatures (Table 20), a two variable linear equation was determined through regression analysis for both bismuth and

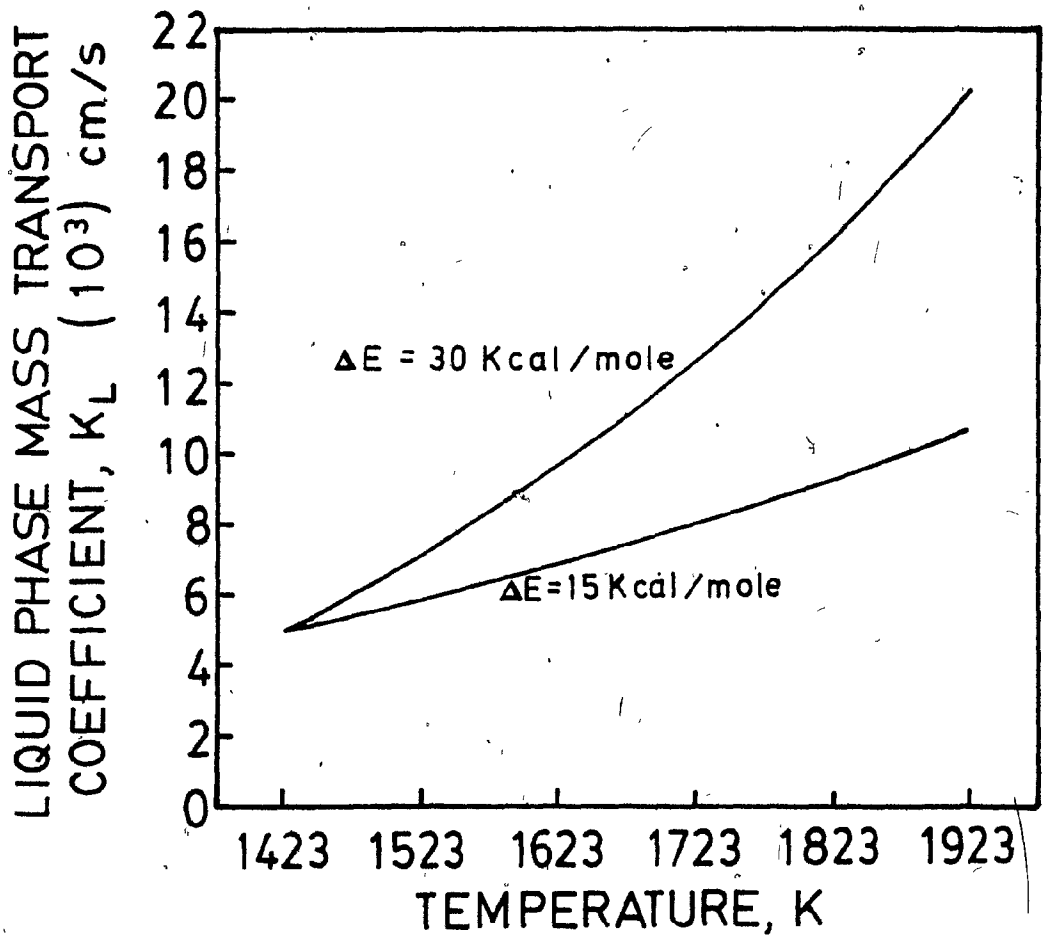

Figure 41. Liquid phase mass transport coefficient vs. temperature, for two levels of activation energy, ΔE

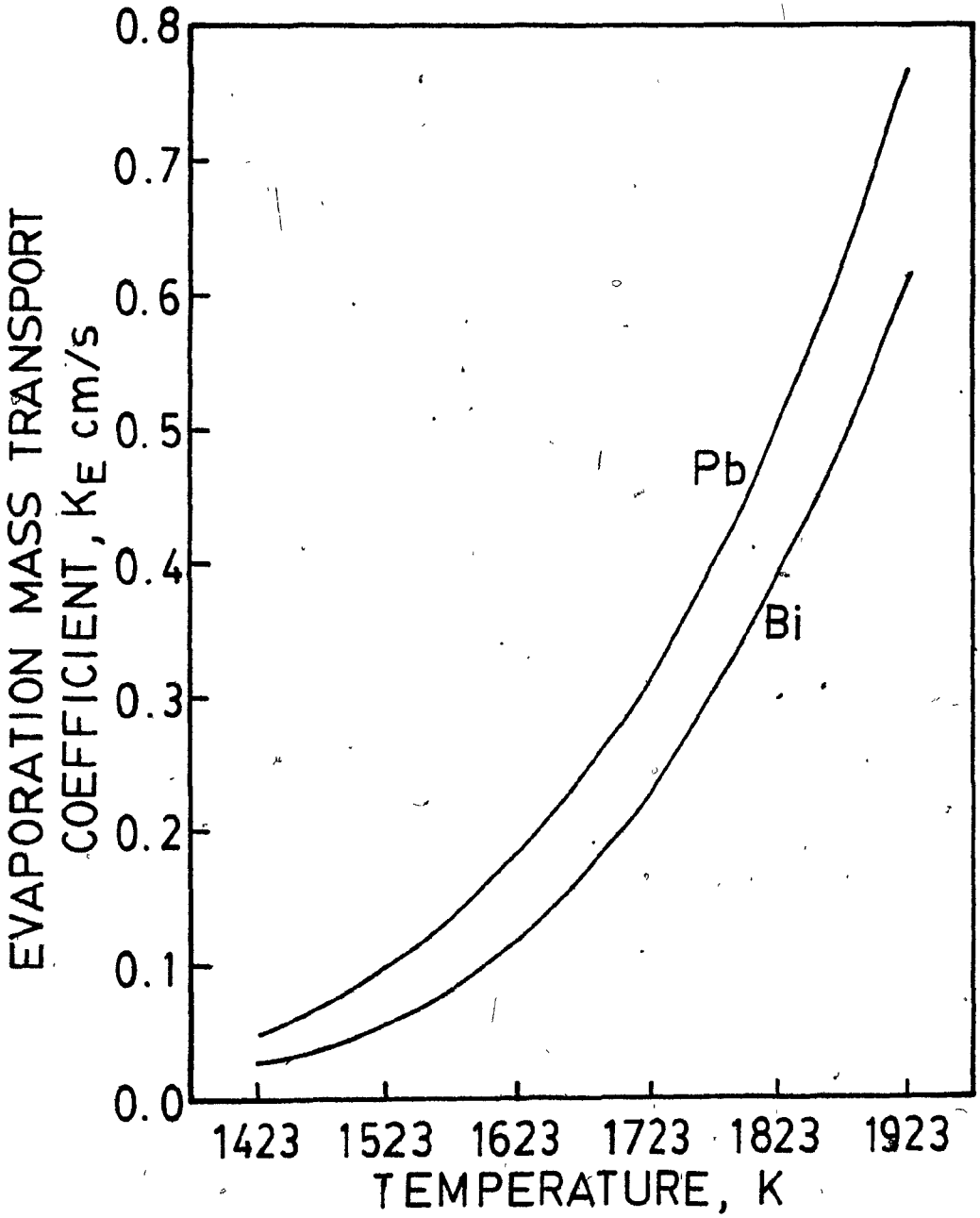

Figure 42. Evaporation mass transfer coefficient vs. temperature, for bismuth and lead.

and lead. The equations are:

$$K_{U_{Bi}} = (-14.526 + 11.75 \times 10^{-3}T + 221\ 1/p) \times 10^{-3} \quad (40)$$

Corr. Coeff. = 0.910

$$K_{U_{Pb}} = (-30.50 + 24.38 \times 10^{-3}T + 466\ 1/p) \times 10^{-3} \quad (41)$$

Corr. Coeff. = 0.915

Combining these K_U equations with those for K_E and K_L, the overall rate constant, K, could then be "predicted" as a function of chamber pressure and melt temperature. Similarly extrapolating the above equations, K_U and K_G could be estimated for temperatures of 1450, 1550 and 1650°C and pressures of 40 and 20 μHg. The results obtained are given in Tables 22 and 23 and Figures 43-46.

For comparison, Figures 43 and 44 include experimental values of K_U at pressure levels of 300, 100 and 60 μHg respectively.

Using values for K_U (as calculated from Equations 40 and 41), and those for K_L and K_E, values of the overall rate constant K could be predicted over the temperature range 1150°C to 1650°C for both bismuth and lead at pressure levels of 300, 100, 60, 40 and 20 μHg. The results are listed in Tables 22 and 23 and plotted against temperature in Figures 47 and 48.

Extrapolated predictions suggest that at 1150°C, decreasing the pressure from 100 μHg to 20 μHg could increase

TABLE 22. Predicted Mass Transfer Coefficients for Bismuth

			300 μ			100 μ			60 μ			40 μ			20 μ		
Temp °C	$K_L(10^{-3}$ cm/s)	$K_E(10^{-3}$ cm/s)	$K_U(10^{-3}$ cm/s)	K_G (cm/s)	$K(10^{-3}$ cm/s)	$K_U(10^{-3}$ cm/s)	K_G (cm/s)	$K(10^{-3}$ cm/s)	$K_U(10^{-3}$ cm/s)	K_G (cm/s)	$K(10^{-3}$ cm/s)	$K_U(10^{-3}$ cm/s)	K_G (cm/s)	$K(10^{-3}$ cm/s)	$K_U(10^{-3}$ cm/s)	K_G (cm/s)	$K(10^{-3}$ cm/s)
1150	5.09	28.4	-0.28	-	-	1.19	397	0.93	2.67	890	1.65	4.51	1504	2.21	10.03	3345	3.02
1250	7.21	62.9	0.90	140	0.79	2.37	370	1.73	3.85	601	2.41	5.69	888	3.03	11.21	1749	4.10
1350	9.78	125.4	2.07	167	1.69	3.54	286	2.55	5.02	406	3.23	6.86	554	3.91	12.38	1000	5.24
1450	12.80	229.5	3.25	148	2.56	4.72	215	3.40	6.20	282	4.10	8.04	366	4.83	13.56	617	6.42
1550	16.28	392.7	4.42	121	3.45	5.89	161	4.28	7.37	202	5.01	9.21	252	5.80	14.73	403	7.58
1650	20.19	616.0	5.60	98	4.35	7.07	124	5.19	8.55	149	5.95	10.39	182	6.78	15.91	278	8.77

TABLE 23. Predicted Mass Transfer Coefficients for Lead

			300 μ			100 μ			60 μ			40 μ			20 μ		
Temp °C	K_L (10^{-3} cm/s)	K_E (10^{-3} cm/s)	K_U (10^{-3} cm/s)	K_G (cm/s)	K (10^{-3} cm/s)	K_U (10^{-3} cm/s)	K_G (cm/s)	K (10^{-3} cm/s)	K_U (10^{-3} cm/s)	K_G (cm/s)	K (10^{-3} cm/s)	K_U (10^{-3} cm/s)	K_G (cm/s)	K (10^{-3} cm/s)	K_U (10^{-3} cm/s)	K_G (cm/s)	K (10^{-3} cm/s)
1150	5.09	47.9	-0.91	-	-	2.26	437	1.49	5.31	1055	2.47	9.19	1826	3.07	20.84	4141	3.77
1250	7.21	97.5	1.53	155	1.25	4.64	469	2.74	7.75	783	3.60	11.63	1175	4.26	23.28	2353	5.21
1350	9.78	181.0	3.97	223	2.78	7.07	397	4.01	10.18	572	4.85	14.06	790	5.59	25.71	1444	6.82
1450	12.80	311.6	6.40	216	4.21	9.51	320	5.36	12.62	425	6.23	16.50	556	7.05	28.15	948	8.56
1550	16.28	503.9	8.84	189	5.66	11.95	256	6.80	15.06	322	7.70	18.94	405	8.61	30.59	655	10.41
1650	20.19	769.1	11.28	163	7.17	14.39	207	8.31	17.50	252	9.26	21.38	308	10.25	33.03	476	12.33

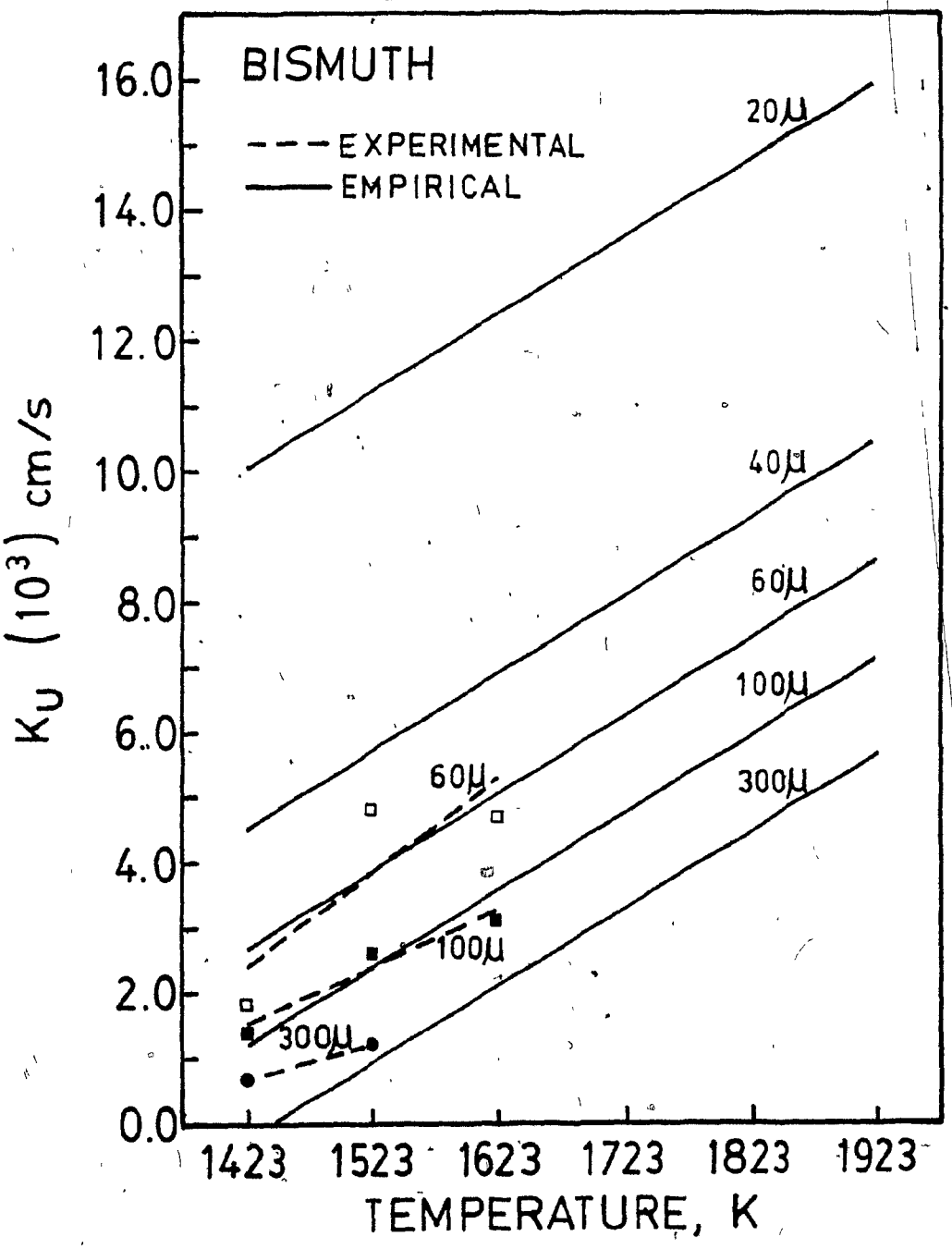

Figure 43. K_U vs. temperature, at different chamber pressures, for bismuth.

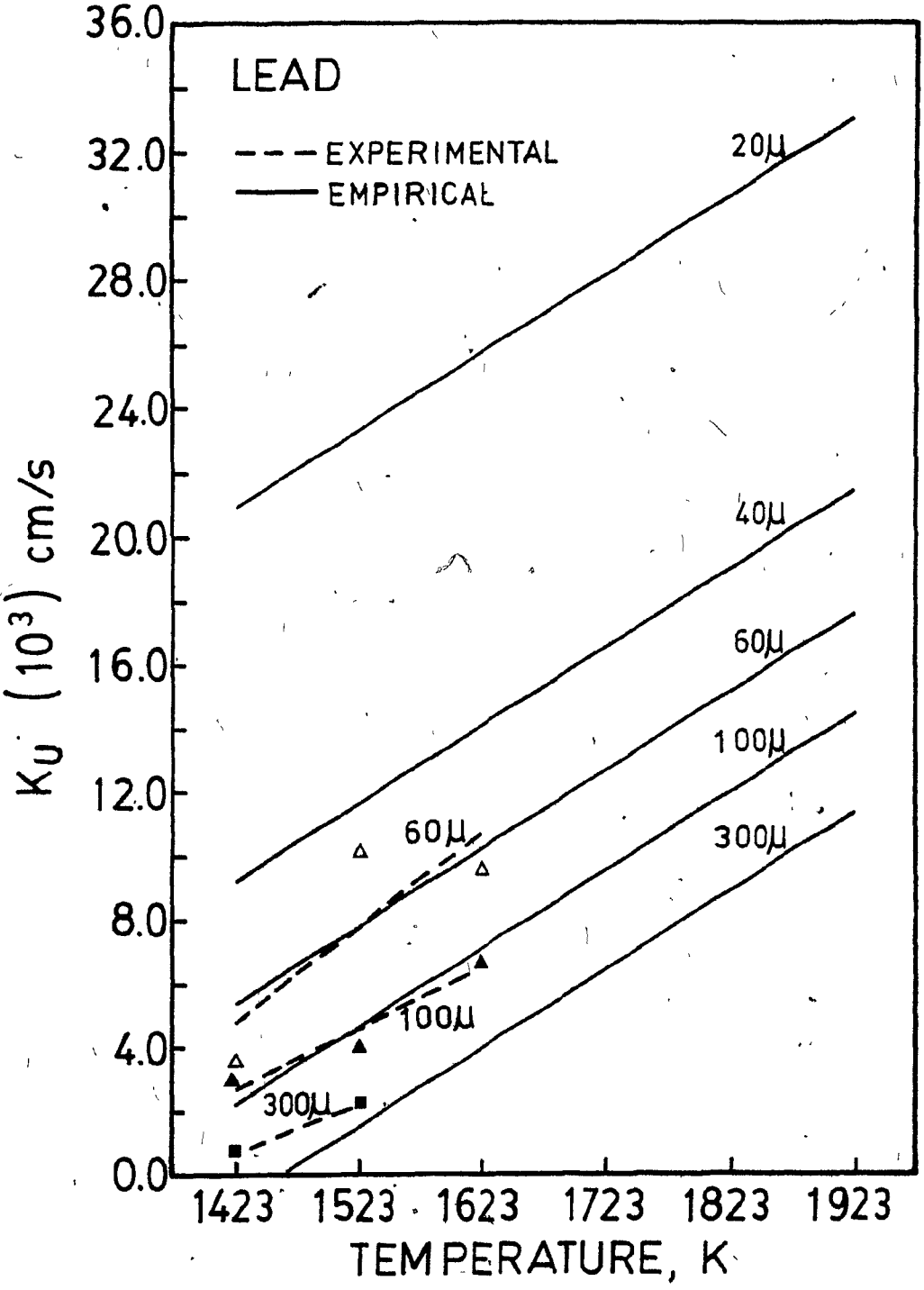

Figure 44. K_U vs. temperature, at different chamber pressures, for lead.

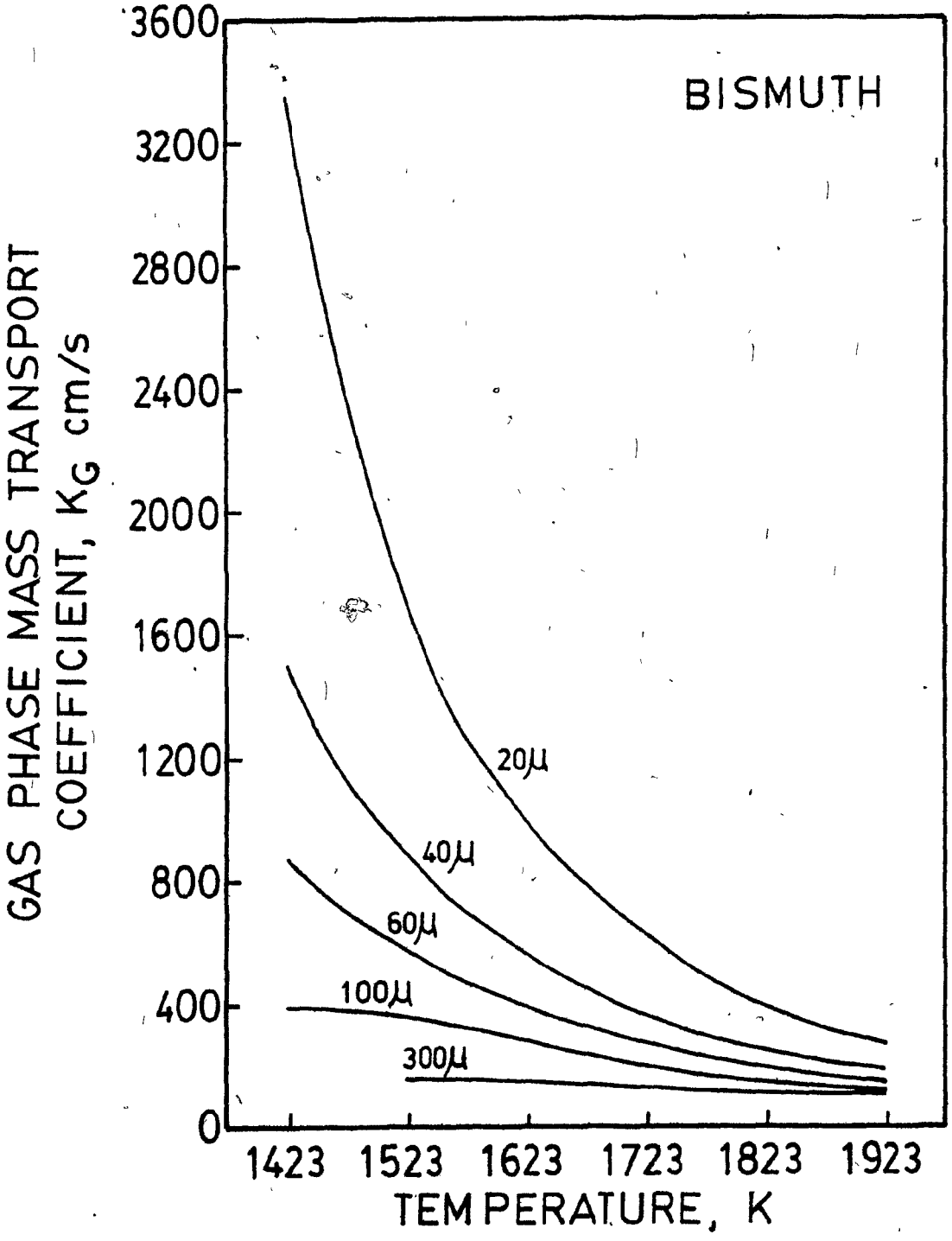

Figure 45. Predicted gas phase mass transport coefficient vs. temperature, at different chamber pressures, for bismuth.

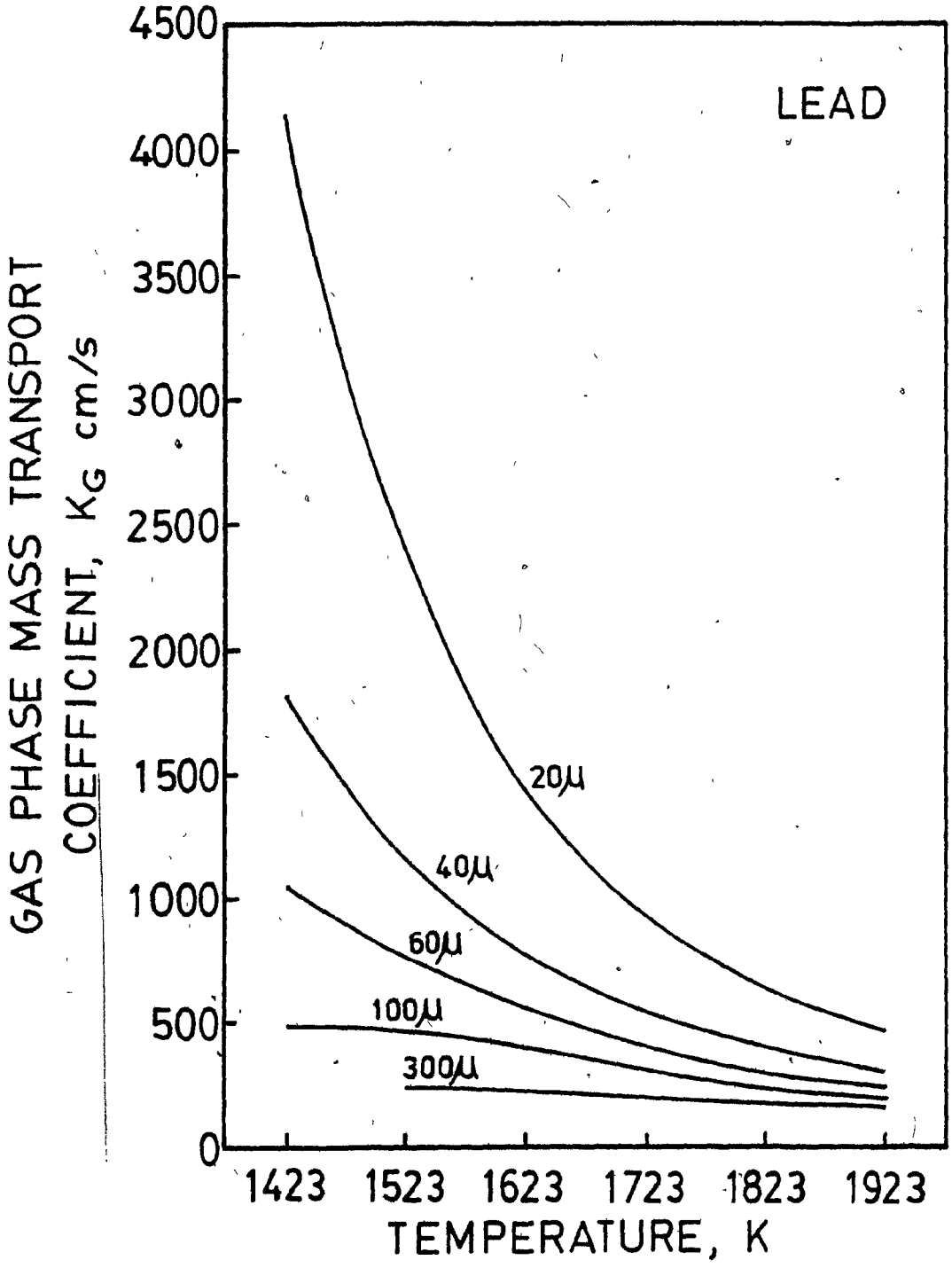

Figure 46. Predicted gas phase mass transport coefficient vs. temperature, at different chamber pressures, for lead.

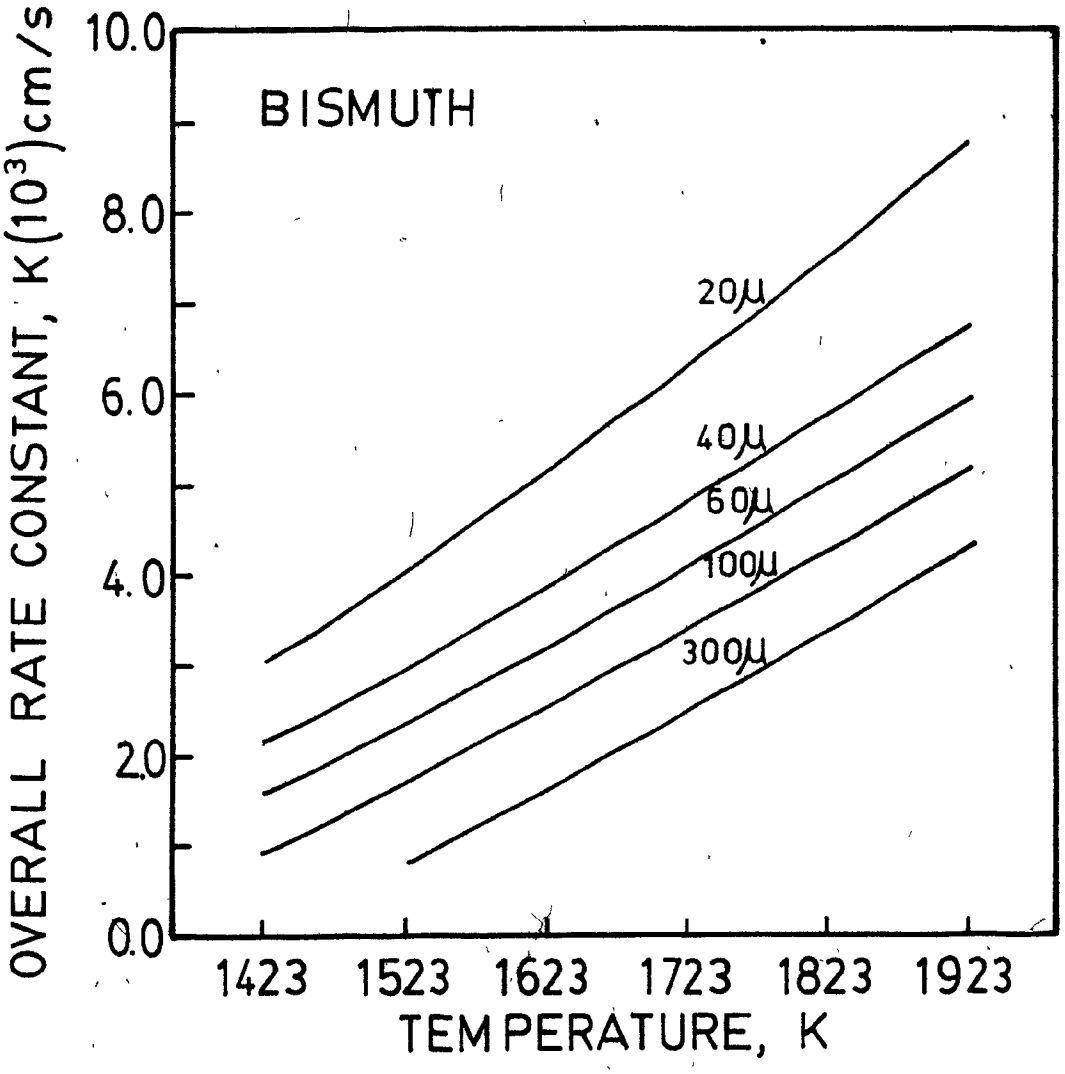

Figure 47. Predicted overall rate constant vs. temperature, at different chamber pressures, for bismuth.

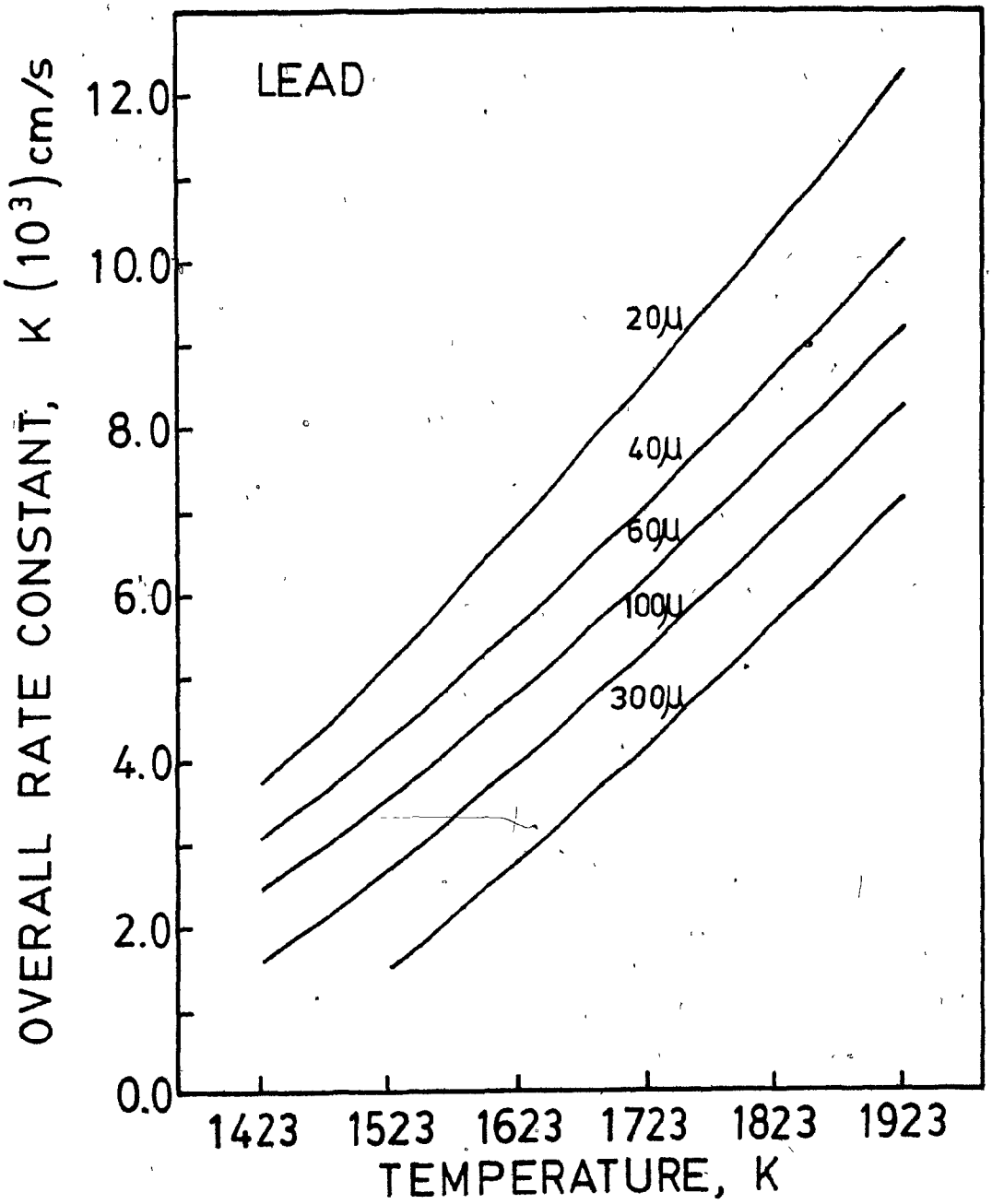

Figure 48. Predicted overall rate constant vs. temperature, at different chamber pressures, for lead.

K_{Bi} by 3.3 times and K_{Pb} 2.5 times. By comparison, at 100 μ Hg, increasing the temperature from 1150°C to 1650°C should increase both K_{Bi} and K_{Pb} by 5.6 times, while the increase is only 2.9 times for K_{Bi} and 3.3 times for K_{Pb} at 20 μ Hg. By increasing the temperature from 1150 to 1650 and decreasing the pressure from 100 μ Hg to 20 μ Hg, it is predicted that K_{Bi} and K_{Pb} should increase by 9.4 and 8.3 times respectively. This would mean the level of weight percent elimination that could be obtained for bismuth and lead at 1150°C and 100 μ Hg in 120 minutes should be obtained within 13-15 minutes at 1650°C and 20 μ Hg.

Based on the experimental results obtained at 100 and 60 μ Hg chamber pressures and 1150, 1250 and 1350°C melt temperatures for overall rate constant, K, (Table 20) a two variable-temperature and pressure-linear equation was also determined for both bismuth and lead through regression analysis as follows:

$$K_{Bi} = (-8.967 + 7.78 \times 10^{-3} T + 99.5\ 1/p) \times 10^{-3} \quad (42)$$

Corr. Coeff. = 0.958

$$K_{Pb} = (-13.43 + 11.98 \times 10^{-3} T + 122.5\ 1/p) \times 10^{-3} \quad (43)$$

Corr. Coeff. = 0.959

With these equations it is again possible to extrapolate the values of K up to 1650°C and decreasing the pressure to 40 and 20 μ Hg. The results are summarized in Table 24 and in Figures 49 and 50 for bismuth and lead respectively. In Figures 49 and 50 experimental K values were also plotted against temperature at 300, 100 and 60 μ Hg.

TABLE 24. Extrapolation of Overall Experimental Rate Constant for Bismuth and Lead

Temp. °C	Bismuth K(10^{-3}cm/s)					Lead K(10^{-3}cm/s)				
	300μ	100μ	60μ	40μ	20μ	300μ	100μ	60μ	40μ	20μ
1150	0.31	0.98	1.64	2.47	4.96	0.76	1.57	2.39	3.41	6.47
1250	1.09	1.75	2.42	3.25	5.73	1.95	2.77	3.59	4.61	7.67
1350	1.87	2.53	3.19	4.02	6.51	3.15	3.97	4.79	5.81	8.87
1450	2.65	3.31	3.97	4.80	7.29	4.35	5.17	5.98	7.00	10.07
1550	3.42	4.09	4.75	5.58	8.07	5.55	6.36	7.18	8.20	11.26
1650	4.20	4.87	5.53	6.36	8.85	6.75	7.56	8.38	9.40	12.46

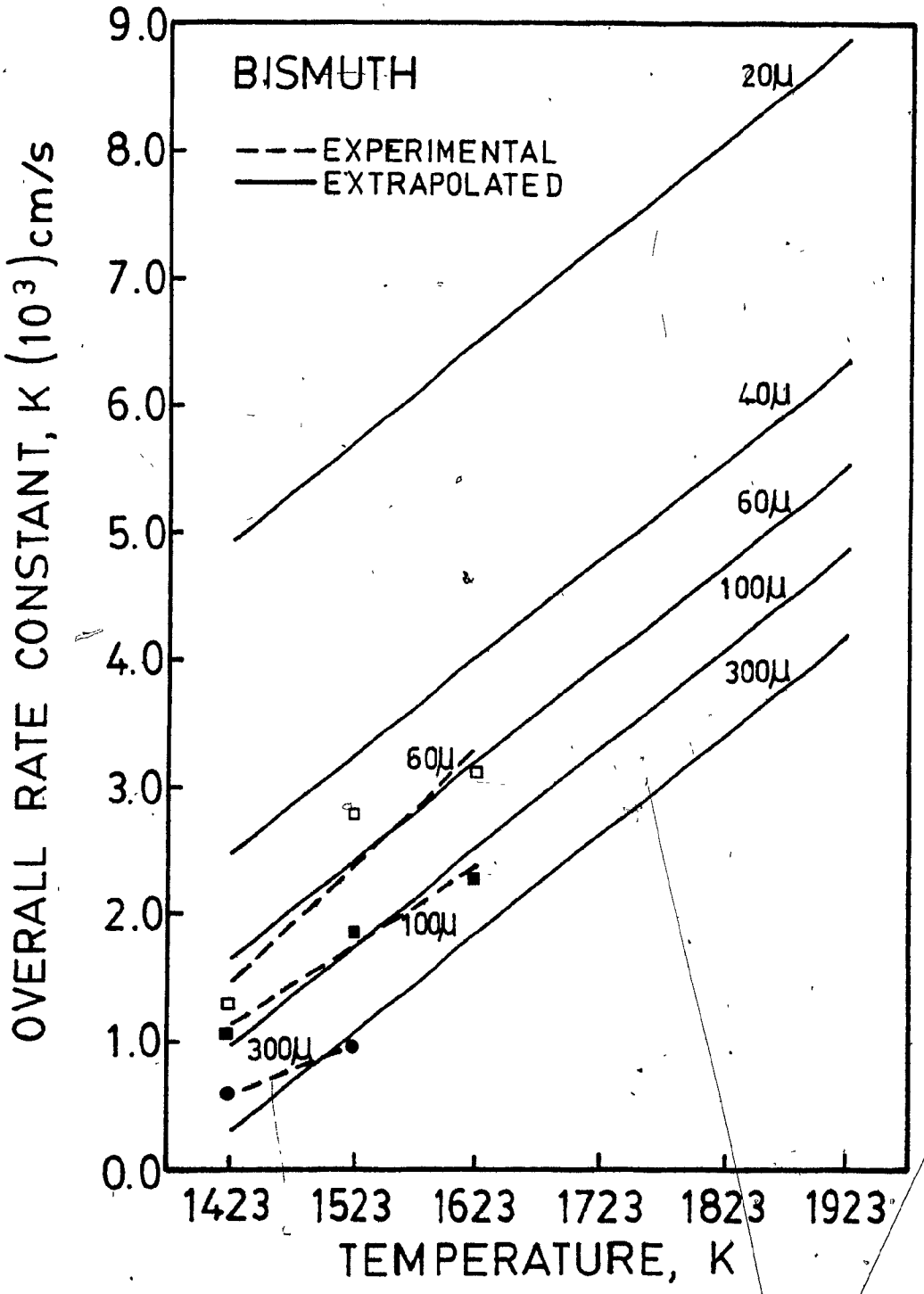

Figure 49. Extrapolated overall rate constant vs. temperature, at different chamber pressures, for bismuth.

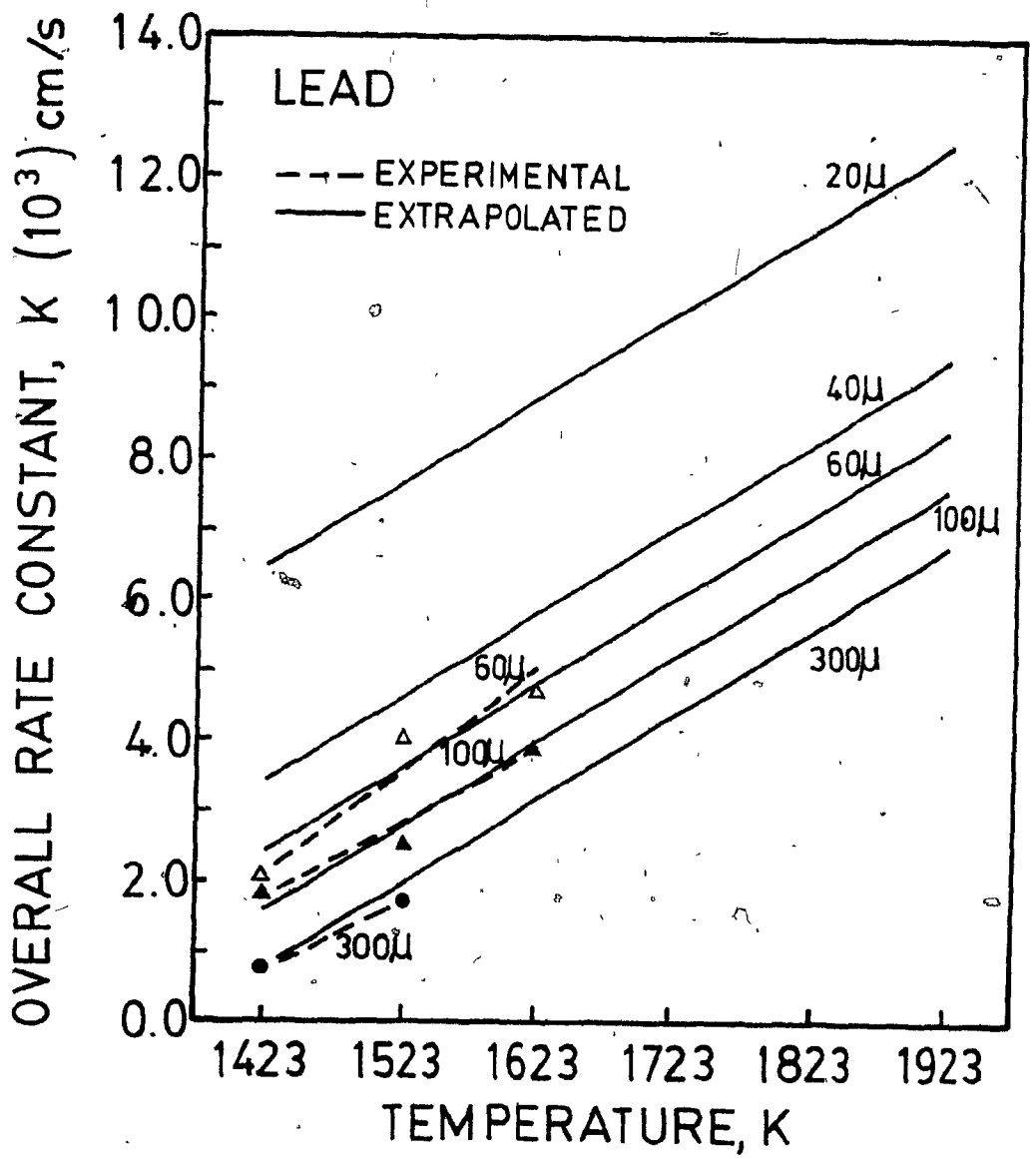

Figure 50. Extrapolated overall rate constant vs. temperature, at different chamber pressures, for lead.

Overall rate constants obtained from linear equations (Equations 42 and 43) are in good agreement with the values predicted from K_L, K_E and K_U on the semi empirical basis previously described for both bismuth and lead. Both sets of values are also in excellent agreement with the experimental results, as shown in Table 25.

Of these two sets of correlations, it was decided to select Equations 42 and 43 as most appropriate to the present work since they were directly related with the experimental results.

As implied in the previous discussion, it was expected and supposed that the gas phase mass transport coefficient, K_G, was inversely proportional to chamber pressure [47,48] in line with equivalent variations in gas diffusivities with ambient pressure. In present work this could not be demonstrated clearly as the chamber pressure could not be reduced to the 1 μHg range. Similarly, insufficient knowledge of transport in the gas phase, and the role of trace amounts of oxygen precluded the quantitative prediction of gas phase mass transfer coefficients.

Other Considerations:

As mentioned in Chapter III, in the present study, the possible effects of gases present in the gas phase, of surface active elements which may be present at the interface, of heat transfer on the condenser surface and finally pumping rate were

TABLE 25. Comparison of Experimental Results with "Predicted" Overall Rate Constants, $K(10^{-3}cm/s)$

		$K(10^{-3}cm/s)$					
		BISMUTH			LEAD		
Press. μHg	Temp. °C	Experimental Results	"Predicted" from K_L, K_E and K_U[1.]	Best Fitted[2.]	Experimental Results	"Predicted from K_L, K_E and K_U[1.]	Best Fitted[2.]
60	1150	1.32	1.65	1.64	2.00	2.47	2.39
60	1250	2.76	2.41	2.42	4.04	3.60	3.59
60	1350	3.15	3.23	3.19	4.70	4.85	4.79
100	1150	1.05	0.93	0.98	1.84	1.49	1.57
100	1250	1.86	1.73	1.75	2.54	2.74	2.77
100	1350	2.33	2.55	2.53	3.93	4.01	3.97

1. As calculated from Equations 40 and 41.

2. As calculated from Equations 42 and 43.

not determined. These effects, whether or not important, were incorporated in the values of K_U, this being calculated from the difference of K and $(K_L + K_E)$. During the course of experiments, it was observed that the melt surface always remained clean and shiny, and there was no obvious oxide layer present.

VI-7. COMPARISON OF RESULTS WITH PREVIOUS WORK

A study of the kinetic data available in the literature showed that in most cases information regarding certain variables were incomplete (e.g. especially melt surface area to volume ratio), so that a thorough comparison of the results reported by various investigators and present results was not possible. Consequently, only the range of results available in the literature could be compared with the range of the present results.

A summary of work up to this date by various scientists (Table 3) is combined with the present results and included in Table 26.

The comparison shows that the weight percent eliminations obtained for bismuth and lead in the present study were generally lower than those reported by previous researchers. This was the case even after 240 minutes of treatment (Table 11). This discrepancy has been attributed to the higher pressures and lower A/V ratios applied in the present study relative to other experimental conditions. Also, since the weight of the

TABLE 26. Comparison of the Present Results with the Results Available in Literature

Source	Copper Weight kg	Press. μHg	Temp. °C	Time min	A/V m^{-1}	Elimination, wt% Bi	Pb	As	Sb	K(10^{-3} cm/s) Bi	Pb	Ref. #
Present	34.0	60-100	1150-1350	120	6.7-10.2	40-80	50-90	0	0	1.0-3.0	1.5-4.5	-
Kameda	0.03	100	1100	60	-	50-80	+90	10-30	50-55	-	-	26
Kameda	0.03	100	1200	60	-	+90	+95	40-70	30-40	-	-	26
Ohno	0.15	1-8	1200-1300	5-20	60	+95	+95	-	-	8-30	10-30	54,55
Bryan	0.02	80	1170	60	-	99	-	-	-	-	-	58
Bryan[1]	4.00	20-200	1200-1300	50-60	-	80-95[2]	-	-	-	-	-	58
Komarova	0.03	10	1200	120	-	50-80	50-90	50-80	50-75	-	-	59
Golovko	-	100-500	1200	5-15	-	93	100	20	20	-	-	62
Kim	-	-	-	-	-	-	75	30-50	40	-	-	60
Kametani	0.6-6.0	1000-2000	1200	Vacuum Lift Refining		10	60-80	10-20	20	-	-	29
Taubenblat	25	<0.1	1150-1300	30	-	50	50	-	-	Cathode Copper		85

1. Overall rate constants were reported in different unit and could not be compared with the present values.

2. Estimated from the graphs.

in the present pilot scale study was 200-1000 times larger than those used by previous investigators, there is good reason to suppose that the present results are more representative of kinetic mechanisms one would expect to observe in large scale systems.

Ohno[54,55] and Bryan et al.[58] were the only investigators who carried out kinetic studies and reported overall mass transfer coefficient values. They reported different rate constants, Ohno using units of "kg m^{-2} s^{-1}" while Bryan et al. used "cm^{-2} s^{-1}". From the information given in Ohno's data, it is possible to convert his data to allow comparison with the present work.

$$K(\text{present study}) = \frac{1}{10\ \mathring{Cu}} \times K_{(\text{ohno})}$$

This was not possible for the data of Bryan et al., since neither crucible radius, melt density nor type of copper melted was reported.

It was found that in the present study K_{Bi} was ≈10 times and K_{Pb} was ≈7 times lower than the values reported by Ohno[54,55] This was attributed to higher chamber pressure, lower A/V ratios, and the larger scale experiments in the present study.

Concurrent work in the same equipment, work on vacuum refining processes in steel and cast iron melts by Harris[122] and Bernhurst and Gruzleski[124] respectively have also indicated that refining processes can operate at very different rates in large (pilot scale) as compared to small (laboratory

scale) vacuum systems. It is therefore clear that special care should be directed towards understanding the causes for such changes in mechanisms in any scale-up (or scale-down) studies.

In Table 25, the results of vacuum lift refining studies carried out by Kametani and Yamauchi as an alternative to vacuum induction melting[29] are included. The percentage eliminations were generally much lower than these by vacuum induction melting. The results obtained by Taubenblat et al.[85] are also included in the same table as being representative of the recent work on the refining of cathode (rather than anode or blister) copper. These were mainly degassification experiments and, as we would expect, starting levels of metallic impurities were much lower than the blister or anode type copper being considered in the present study. Good degassification, but low elimination of metallic impurities, were obtained.

As shown in Table 26, zero elimination of either arsenic or antimony in the present study contradicts the results of Kameda and Yazawa[26], Komerova[59] and Golovko[62]. Further studies need to be carried out to investigate the mechanism of their rate of removal in more detail, i.e. the possible effects of oxygen and/or sulphur concentrations in the melt.

These comparisons reveal that the present study contains by far the most detailed consideration into the kinetic mechanisms of impurity elimination from copper so far reported.

In terms of claims to originality, the placement of a water-cooled condenser as close as 1.5 - 2 cm to the melt surface was novel and unique to this work. Similarly, the concentration-time data was significantly more extensive in comparison with the three data point per experiment obtained by Ohno[54,55]. Finally, a detailed analysis of condensate composition was again unique to this work.

CHAPTER VII

CONCLUSIONS

Based on the results and discussions presented in previous chapters, the following conclusions can be drawn:

1. In the absence of oxygen and sulphur, bismuth and lead could be eliminated by up to 80% and 90% respectively from copper by vacuum induction melting, while removal of arsenic and antimony was negligible.

2. The rate of removal of bismuth and lead increased by about 5 and 7 times respectively as the chamber pressure was lowered from 300 to 60 μHg and the melt temperature increased from 1150 to 1350°C.

3. The melt surface area to volume ratio and the distance of the condenser to melt surface did not have significant effects on the rate constants governing the rate of removal of impurities.

4. The rate of elimination of bismuth and lead over the range 1150 - 1350°C and 300 - 60 μHg, followed first order kinetics.

5. Elimination rates were largely controlled by mass transport in the gas phase. However, as melt temperature increased above 1350°C and pressure decreased below 60 μHg, kinetic analysis indicated that the rate of eliminations were controlled by a combination of both liquid and gas phase mass transport.

6. It is predicted that a lowering of chamber pressure to 20 μHg and a melt temperature of 1650°C would generate overall rate constants of $9.x10^{-3}$ cms^{-1} and $12.x10^{-3}$ cms^{-1} for bismuth and lead respectively.

7. The rate of elimination of impurities in the present pilot plant scale equipment were significantly lower than laboratory scale results.

8. Total copper losses to the condensate in vacuum induction melting were found to be low. In the range of 1150-1350°C and 300 - 60 μHg it is not more than 1-2%.

9. Vacuum induction melting would appear to give better results than vacuum lift refining.

10. There are no known commercial installations for the vacuum refining of copper.

Claim to Originality:

The following aspects of the present work are considered to be original:

a) A study of the vacuum refining of copper at a pilot plant scale;

b) A study of the effects of a water cooled condenser on the evaporation of impurities;

c) A detailed analysis of condensate samples;

d) Detailed kinetic studies and calculations;

e) The development of equipment and techniques for frequent sampling during vacuum refining experiments.

Suggestions for Future Work:

The possible effect of oxygen and sulphur concentration levels on the rate of removal of impurities from copper should be investigated since the vapour pressures of oxides and sulphides are generally much higher than pure elements.

Similarly, the simultaneous presence of oxygen and sulphur and possible nucleation of sulphur dioxide in the copper should be investigated as this could possibly increase melt surface area to volume ratios to higher levels.

The conditions necessary for improving the elimination of arsenic and antimony should be determined.

A feasibility study of vacuum induction refining and a full comparison with the existing pyrometallurgical copper refining processes should be prepared.

REFERENCES

1. Hsu, Y.T. and O'Reilly, B., Impurity Effects in High-Conductivity Copper, J. Metals, 21-24, (Dec. 1977).
2. Phillips, A.J., The Worlds Most Complex Metallurgy - copper, lead and zinc -, Trans. of the Metallurgical Society of AIME, 224, 657-668, (August 1962).
3. Davenport, W.G. and Biswas, A.K., Extractive Metallurgy of Copper, Pergamon Press, 1976.
4. Jeffes, J.H.E. and Jacob, K.T., The Physical Chemistry of Fire Refining Copper, NPL 1971 Symposium on Metallurgical Chemistry, 513-525, (1972).
5. McKerrow, G.C. and Pannel, D.G., Gaseous Deoxidation of Anode Copper at the Noranda Smelter, Can. Met. Quarterly, 11 (4), 629-633, (1972).
6. Yazawa, A., Thermodynamic Considerations of Copper Smelting, Can. Met. Quarterly, 13 (3), 443-453, (1974).
7. Yazawa, A. and Azakami, T., Thermodynamics of Removing Impurities During Copper Smelting, Can. Met. Quarterly, 8 (3), 257-261, 1969.
8. Basagoitia, A., Arsenic and Antimony Removal from Blister Copper by Fire Refining, The Future of Copper Pyrometallurgy, Proceedings of First Latin American Congress of Min. and Ext. Met., Santiago, Chile; 219-231, (August 1973).

9. Nagamori, M., Mackey, P.J., and Tarassoff, P., Copper Solubility in $FeO-Fe_2O_3-SiO_2-Al_2O_3$ Slag and Distribution Equilibria of Pb, Bi, Sb and As Between Slag and Metallic Copper, Metallurgical Trans. 6B, 295-301, (June 1975).

10. Nagamori, M. and Mackey, P.J., Thermodynamics of Copper Matte Converting, Metallurgical Trans. 9B, 567-579, (Dec. 1978).

11. Mackey, P.J., McKerrow, G.C. and Tarassoff, P., Minor Elements in the Noranda Process, 104th AIME Annual Meeting, New York, N.Y.; (Feb. 1975).

12. Mackey, P.J., The Noranda Process - A Review of Metallurgy, Professional Development Seminars, Dept. Min. & Met. Eng., McGill Univ., (Jan. 1977).

13. Mackey, P.J. and Bailey, J.W.B., The Noranda Process, Professional Development Seminars, Dept. Min. & Met. Eng., McGill Univ., (Jan. 1978).

14. Suzuki, T. and Shibasaki, T., Behavior of Impurities in Mitsubishi Cont. Copper Smelting and Converting Process, 104th AIME Annual Meeting, New York, N.Y.; A75-40, (Feb. 1975).

15. Mackey, P.J. and Balfour, G.C., Pyrometallurgy, J. Metals, 36-39, (April 1978).

16. Yazawa, A., Kubota, Y. and Ujiie, H., Refining of Crude Copper by Addition of Chlorides, Bul. Research Inst. of Min. Dressing and Met., Tohoku Univ., 27 (1,2), 209-216, (Oct. 1971).

17. Miller, H.J., The Fire Refining of Copper, The Refining of Non-Ferrous Metals - Proceedings, London, England; 145-184, (July 1949).

18. Fritze, H.W., U.S. Patent 3,262,773.

19. De Bie, E., Canadian Patent 922,902.

20. Bell, M.C.E. and Pargeter, K., U.S. Patent 3,767,383.

21. Bunshah, R.F., The Last Ten Years and the Next Five Years in Vacuum Metallurgy, Trans. of the International Vac. Met. Conference 1967, 1-14, 1967.

22. Barraclough, K.C., The Applications of Vacuum Technology to Steelmaking, Vacuum, 22 (3), 91-102, 1972.

23. Holden, C., Developments in the Processing of Liquid Steel, Jour. of the Iron and Steel Inst., 806-825, (June 1969).

24. Chesters, J.H., Refractories for Iron and Steelmaking, The Metals Society, London, 322-357, 1974.

25. Darmara, F.N., Huntington, J.S. and Machlin, E.S., Vacuum Induction Melting, Jour. of the Iron & Steel Inst., 266-275, (March 1959).

26. Kameda, M. and Yazawa, A., Refining of Crude Copper by Vacuum Melting, Tohoku Daigaku Senko Seiren Kenkyusho Iho, 19 (1), 57-68, 1963.

27. Roth, A., Vacuum Technology, North-Holland Publishing Comp., 1976.

28. Belk, J.A., Vacuum Techniques in Metallurgy, Pergamon Press, 1963.

29. Kametani, H. and Yamauchi, C., Vacuum Lift Refining in Copper Smelting, Trans. of NRI for Metals, 20 (1), 22-59, 1978.

30. Winkler, O. and Bakish, R., Vacuum Metallurgy, Elsevier Pub. Comp., 1974.

31. Servi, I.S., High-Vacuum Induction Melting, Western Metal Congress, Los Angeles, 103-111, (March 1961).

32. Nisbet, J.D., Progress of Vacuum Metallurgy in North America, Trans. of the International Vac. Met. Conference 1967, 15-36, 1967.

33. Knacke, O. and Stranski, I.N., The Mechanism of Evaporation, Progress in Metal Physics-6, edited by B. Chalmers and R. King, Pergamon Press, 181-235, 1956.

34. Davey, T.R.A., Distillation under Moderately High Vacuum, Vacuum, 12 (2), 83-95, 1962.

35. Davey, T.R.A., Discussion, Vacuum, 14, 227-230, 1964.

36. Davey, T.R.A., Vacuum Dezincing of Desilverized Lead Bullion, J. of Metals, 991-997, (August 1953).

37. Stauffer, R.A., Fox, K. and DiPietro, O.W., Vacuum Melting and Casting of Copper, Industrial and Eng. Chem., 40 (5), 820-825, (1948).

38. Hultgren, R., et. al., Selected Values of the Thermodynamic Properties of the Elements, ASM, 1973.

39. Olette, M., Vacuum Distillation of Minor Elements from Liquid Ferrous Alloys, Physical Chemistry of Process Metallurgy, edited by G. St. Pierre, 8 (2), 1065-1087, 1961.

40. Pehlke, R.D., Unit Processes of Extractive Metallurgy, American Elsevier Pub. Comp., 130-141, 1973.

41. Ohno, R. and Ishida, T., Rate of Evaporation of Mn, Cu, Sn, Cr and S from Molten Iron under Vacuum, J. of the Iron & Steel Inst., 904-908, (Sept. 1968).

42. Ward, R.G., Evaporative Losses During Vacuum Induction Melting of Steel, J. of the Iron & Steel Inst., 11-15, (Jan. 1963).

43. Ward, R.G. and Aurini, T.D., Mechanism of Alloying Element Evaporating During the Vacuum Induction Melting of Steel, J. of the Iron & Steel Inst., 920-923, (Sept. 1966).

44. Ohno, R., Kinetics of Evaporation of Mn, Cu and S from Iron Alloys in Vacuum Induction Melting, Trans. ISIJ, 17, 732-741, 1977.

45. Kinsman, G.J.M., Hazeldean, G.S.F. and Davies, M.W., Physicochemical Factors Affecting the Vacuum Deoxidation of Steels, J. of the Iron & Steel Inst., 1463-1478, (Nov. 1969).

46. Machlin, E.S., Kinetics of Vacuum Induction Refining Theory, Trans. of Met. Society of AIME, 218, 314-326, (April 1960).

47. Geiger, G.H. and Poirier, D.R., Transport Phenomena in Metallurgy, Addison-Wesley Pub. Comp., 547-571, 1973.

48. Higbie, R., Trans. AICHEJ, 31, 365, (1935).

49. Irons, G.A., Chang, C.W., Guthrie, R.I.L. and Szekely, J., The Measurement and Prediction of the Vaporization of Magnesium from an Inductively Stirred Melt, Met. Trans. B, 9B, 151-154, March 1978.

50. Bradshaw, A.V. and Richardson, F.D., Thermodynamic and Kinetic Aspects of Vacuum Degassing, Vacuum Degassing of Steel, Special Report 92, The Iron & Steel Inst., 1965.

51. Ohno, R., Kinetics of Evaporation of Various Elements from Liq. Iron Alloys Under Vacuum, Liquid Metals - Chemistry &

Physics, edited by S.Z. Beer, Marcel Dekher Inc., New York, Chapter 2, 1972.

52. Richardson, F.D., Physical Chemistry of Melts in Metallurgy, Vol. 1 & 2, Academic Press, 483-493, 1974.

53. Sherwood, T.K. and Cooke, N.E., Mass Transfer at Low Pressure, A.I.Ch.E. Journal, 3 (1), 37-42, (March 1957).

54. Ohno, R., Rates of Evaporation of Ag, Pb and Bi from Copper Alloys in Vacuum Induction Melting, Met. Trans. AIME, 7B, 647-653, (Dec. 1976).

55. Ohno, R., Rates of Evaporation of Ag, Pb, Bi and S from Molten Copper Alloys Stirred at Different Speeds under Reduced Pressure, Tran. JIM, 18, 232-238, 1977.

56. Salomon-de-Friedberg, H. and Davenport, W.G., Vacuum Removal of Copper From Melted Steel Scrap, The Metallurgical Society of CIM, Annual Volume, 1977.

57. Inoue, M., Yoshii, I. and Ohno, R., Rates of Evaporation of Ag from Liquid Cu-Ag Alloys in High Frequency Vacuum Induction Melting, Jap. Inst. Metals J. 37 (9), 953-963, (1973).

58. Bryan, R., Pollard, D.M. and Willis, G.M., Removal of Bismuth from Copper by Vacuum Refining, Extractive Metallurgy Symposium, The Univ. of N.S. Wales, Australia, (Nov. 1977).

59. Komorova, L., Vacuum Refining Technique for Removal of Impurities from Copper, Hutnicke Listy, (Czech), 8, 577-582, (1973). Translation BISI 12425, The Metals Soc., London, U.K.

60. Kim, G.V., Kvyatkovskii, A.N., et. al., Vacuum Processing of Crude Copper, Tr. Altaisk Gorno-Met. Nauchn.-Issled. Inst., Akad. Nauk Kaz. SSR, 14, 86-89, (1963).

61. Novoshiliv, A.B., Vacuum Refining of Copper, Tr. Inst. Met. Obogashch., Akad. Nauk Kaz. SSR, 31, 23-30, (1968).

62. Golovko, V.V. and Isakova, R.A., Removal of Impurities from Binary Alloys and Crude Copper by a Vacuum Method, Tr. Inst. Met. i Obogashch., Akad. Nauk Kaz. SSR, 13, 32-37, (1965).

63. Kametani, H., and Yamauchi, C., A Fundamental Study on Vacuum Lift Refining of Molten Copper, Trans. of Jap. Inst. Metals, 13 (1), 13-20, (1972).

64. Kametani, H. and Yamauchi, C., Vacuum Lift Refining of Molten Copper Removal of S and O, J. Min. Metall. Inst. Japan, 88, 347-352, (1972),

65. Yamauchi, C. and Kametani, H., Removal of S, O and Other Impurities by Vacuum Lift Refining of Molten Blister Copper, J. Min. Metall. Inst. Japan, 89, 45-50, (1973).

66. Greater Purity for Oxygen-Free Copper, Metal Progress, 124, (Dec. 1963).

67. Gupta, V.K., Madhav Rao, V.N. and Tamhankar, R.V., Oxygen-Free High Conductivity Copper by Vacuum Melting, Trans. Indian Inst. Metals, 25 (2), 33-39, (1972).

68. Stauffer, R.A., Fox, K. and DiPietro, O.W., Vacuum Melting and Casting of Copper, Industrial and Eng. Chem., 40 (5), 820-825, (1948).

69. Nikolaev, A.K., Vodyanaya, T.A. and Revina, N.I., Vacuum Induction Melting of Copper, Tr., Gos. Nauch.-Issled. Proekt. Inst. Splavov Obrab. Tsvet. Metal., 32, 41-48, (1969).

70. Blank, H.A., Fabricating OFHC Copper, Metal Ind., 768-770, (June 1964).

71. Militsyn, K.N., Zolotoi, A.L., and Saramutin, V.I., Effect of Vacuum-Melting on Gas Content and Porosity of Copper, Tr. Mosk. Inst. Radiotekh., Electron. Avtom., 41, 209-213, (1973).

72. Winkler, O., The Degassing Process of Metallic Melts in Vacuo, Vakuum Tech., 3 (5), 87-96, (1954).

73. Golonka, J. and Legowski, F., Physical-Chemical Phenomena in the Production of Oxygen-Free Copper Melted in Vacuo, Pr. Inst. Hutn. Poland, 20 (4), 221-227, (1968).

74. Zyazev, V.L., Spevak, N.D., et. al., Vacuum Treatment of Liquid Copper, Tsvetn. Metal., 35 (7), 32-37, (1962).

75. Aleksandrov, B.N. and Udovikov, B.I., Impurity Behavior During Vacuum Heating of Copper at High Temperatures, Fiz. Kondens. Sostoyaniya, 16, 114-121, (1971).

76. Zelenov, A.N., Ivanova, N.T., et. al., Effect of Vacuum Remelting on Gas Content of Copper, Tsvet. Metal., 39 (11), 92-93, (1966).

77. Zelenov, A.N., Ivanova, N.T., et. al., Content of Gases in Cast Copper Produced by Vacuum Melting, Tsvetn. Metal., 40 (5), 84-85, (1967).

78. Strel'tsov, F.N., Fridlyanskii, R.M. and Moldavskii, O.D., Behaviour of Gases in Copper and Copper Alloys During Vacuum Furnace Melting, Tsvetn. Metal., 44 (9), 81-85, (1971).

79. Belen'kii, L. Ya., Nam, B.P., et. al., Deoxidation of Copper During Vacuum Induction Melting, Tsvetn. Metal., (2), 67-68, (1976).

80. Strel'tsov, F.N., et. al., Removal of Impurities from Copper During Vacuum Furnace Melting, Tsvetn, Metal., (8), 40-43, (1973).

81. Moldavskii, O.D., Nonmetallic Inclusions in Copper Alloys Melted in Open and Vacuum Induction Furnaces, Tsvetn. Metal., (12), 42-44, (1973).

82. Aleksandrov, B.N., Study on the Behaviour of Impurities During Vacuum Distillation (or Initial Heating) and Zone Melting of 9 Easily Fusible Metals and Copper, Fiz. Kondens. Sostoyaniya, 31, 92-104, (1974).

83. Clark Peres, A.E., Pitella, C.F., et. al., Aspects of Vacuum Refining of Copper-Zinc Alloys, Portuguese Met. AMB., 25 (138), 351-360, (1969).

84. Dimitrieva, G.S., Osokin, N.G., et. al., Copper and Nickel Loss During Vacuum Melting, Tr. Nauch.-Issled. Proekt. Inst. Splavov Obrab. Tsvet. Metal., (35), 13-19, (1971).

85. Taubenblat, P.W., Brockup, F.H., et. al., Vacuum Melting and Casting of Copper, Vacuum Metallurgy, Edited by R.C. Krutenat, Proceedings of 1977 Vacuum Met. Conference, Pittsburgh, Penn., 543-568, (June 1977).

86. Militsyn, K.N., Zolotoi, A.L. and Saramutin, V.I., Determination of the Castability of Copper and Copper Alloys in Vacuo, Tr. Mosk. Inst. Radiotekh., Electron. Aveom., 41, 171-174, (1973).

87. Zyazev, V.L. and Tanutrov, I.N., Effect of Vacuum Treatment on the Properties of Copper in Ingots. Mekhan. Svoistva. Litogo Metal., Akad. Nauk SSSR, Inst. Mashinoved., Tr.

Vosmogo Soveshch. Po. Teorii Liteinykh Protsessov, 297-302, (1963).

88. Clites, P.G., Vacuum Arc Melting and Casting of Copper, Bureau of Mines R.I. 6254, U.S. Dept. of Interior, Washington D.C., (1963).

89. Kametani, H. Yamauchi, C., et. al., A Fundamental Study on the Vacuum Treatment of Molten Matte and White Metal., Trans. Jap. Inst. Metals., 14 (3), 218-223, (1973).

90. Yamauchi, C. and Kametani, H., EMF of an Oxygen Concentration Cell and Magnetite Measurements in Connection with the Vacuum Treatment of Molten Matte and White Metal., Trans. Jap. Inst. Metals. 14 (4) 261-266, (1973).

91. Yamauchi, C., Kametani, H., et. al., Removal of Impurities in Molten Mattes and White Metals by the Vacuum Lift Refining, J. Min. Metall. Inst. Japan, 89, 669-674, (1973).

92. Yamauchi, C., and Kametani, H., A Model on Vacuum Lift Refining of Molten Matte, J. Min. Metall. Inst. Japan, 89, 737-742, (1973).

93. Kametani, H., Yamauchi, C., et. al., Elimination of Impurities in Molten Matte and White Metal by Purge Gas Blowing, J. Min. Metall. Inst. Japan, 90, 103-108, (1974).

94. Player, R.L., Removal of Impurities from Copper Matte by Vacuum Treatment, Proceedings, 6th International Vacuum Metallurgy Conference on Special Melting and Metallurgical Coatings, San Diego, April 23-27, 1979.

95. De Bie, E. and Tougarinoff B., German Patent 1,912,936 (U.K. 1,248,556, Canadian 907,341).

96. Sickbert, A., and Stick, W., U.S. Patent 3,367,396.

97. Hart, T.G., Canadian Patent 874,351.

98. Hart, T.G., U.S. Patent 3,575,399.

99. Hart, T.G., U.S. Patent 3,607,231.

100. Tsuda, N., Japan Kokai, 73-71,321.

101. Gutov, L.A., Postnov, L.M., et. al., U.S.S.R. Patent 248,224.

102. Miklossy, K., Czeck. Patent, 128,049.

103. Bell, M.C.E., and Pargeter, J.K., U.S. Patent 3,767,383 (Canadian 973,720).

104. Von Der Crone, G., and Fricke, H., German Patent 2,024,302 (U.K. 1,289,265).

105. Suvorov, A.I., Sokolov, V.I., et. al., U.S.S.R. Patent 334,269.

106. Shima, M., and Nakao, S., Japan Patent 112044/1970, (Canadian 953,923).

107. Edwards, J.B., Huche, E.E. and Martin, J.J., Diffusion in Binary Liquid-Metal Systems, Metallurgical Reviews, Review 120, Part I, 13, 1968.

108. Edwards, J.B., Huche, E.E. and Martin, J.J., Diffusion in Binary Liquid-Metal Systems, Metallurgical Reviews, Review 120, Part II, 13, 1968.

109. Walls, H.A. and Upthegrove, W.R., Theory of Liquid Diffusion Phenomena, Acta Metallurgica, 12, 461-471, (May, 1964).

110. Solar, M.Y., Kinetics of Hydrogen and Carbon Monoxide Absorption by Stagnant Molten Iron, Ph.D. Thesis, McGill Univ., 1971.

111. Gourtsoyannis, L. Kinetics of Compound Gas Absorption by Liquid Iron and Nickel, Ph.D. Thesis, McGill Univ., 1978.

112. Szekely, J. and Chang, C.W., Melt Velocities, Temperature Profiles, Tracer Dispersion Rates and Scrap Melting Kinetics in Vacuum Induction Melting, Vacuum Metallurgy, Edited by R.C. Krutenat, Proceedings of 1977 Vac. Met. Conference, Pittsburgh, Penn., 15-48, (June 1977).

113. Tarapore, E.D. and Evans, J.W., Fluid Velocities in Induction Melting Furnaces: Part I. Theory and Laboratory Experiments, Metallurgical Trans. B., 7B, 343-351, (Sept. 1976).

114. Tarapore, E.D., Evans, J.W. and Langfeldt, J., Fluid Velocities in Induction Melting Furnaces: Part II. Large Scale Measurements and Predictions, Metallurgical Trans., 8B, 179-184, (March 1977).

115. Turkdogan, E.T., Grieveson, P. and Darken, L.S., Enhancement of Diffusion-Limited Rates of Vaporization of Metals, J. Phys. Chem., 67, 1647-1654, (Aug. 1963).

116. Distin, P.A. and Whiteway, S.G., Kinetics of Vapourization and Oxidation of Liq. Iron Levitated in Flowing Helium-Oxygen, Can. Met. Quarterly, 9 (2), 419-426, 1970.

117. Saito, T., Absorption and Evolution of Gases by and from Molten Iron Alloys, Proceedings of 4th Inter. Conf. in Vac. Met., Tokyo, Japan, 3-7, (June 1973).

118. Parker, R.H., An Introduction to Chemical Metallurgy, Pergamon P., Second Ed., 258-261, 1978.

119. Szekely, J. and Poveromo, J.J., Heat and Mass Transfer Considerations in Vapour Deposition, Proceedings of 4th Inter. Conf. on Vac. Met., Tokyo, Japan, 204-208, (June 1973).

120. Davies, O.L., Editor, The Design and Analysis of Industrial Experiments, Hafner Pub. Co., New York, Chapters 7 and 10, 1963.

121. Salomon-De-Friedberg, H., Residual Copper in Steel, Significance, Vacuum Removal; M. Eng. Thesis, McGill Univ., 1976.

122. Harris, R., Vacuum Removal of Copper from Liquid Steel, M. Eng. Thesis, McGill Univ., 1978.

123. Bale, C.W., Pelton, A.D., Thompson, W.T., F.A.C.T. User's Guide, First Edition, McGill Univ. and Ecole Polytechnique, June 1970.

124. Barnhurst, R.J. and Gruzleski, J.E., Vacuum Refinement of Cast Iron Melts, Proceedings, 6th International Vacuum Metallurgy Conference on Special Melting and Metallurgical Coatings, San Diego, April 23-27, 1979.

125. Kubaschewski , O., Evans, E.LL. and Alcock, C.B., Metallurgical Thermochemistry, Pergamon P., Fourth Edition, 1974.

126. Gomez, M., et. al., Densities of Molten Copper and Molten Bismuth-Copper Alloys, Z. Metallkde, 67, 131-134, 1976.

127. Iida, S., Ohno, K., et. al., "Tables of Physical Constants - Butsuri Josu-hyo", Asakura, Tokyo, Japan, 1969.

APPENDIX I

THERMODYNAMIC DATA

I-1. Vapour Pressure of Pure Elements:

Cu: $\log P^\circ = -17520T^{-1} - 1.21 \log T + 13.21$ mm Hg [125]

Bi: $\log P^\circ = -10400T^{-1} - 1.26 \log T + 12.35$ mm Hg [125]

Bi_2: $\log P^\circ = -10730T^{-1} - 3.02 \log T + 18.10$ mm Hg [125]

Pb: $\log P^\circ = -10130T^{-1} - 0.985 \log T + 11.16$ mm Hg [125]

Sb: $P^\circ_{Sb} = 2.74$ mm Hg at 1573 K [38]

$P^\circ_{Sb_2} = 66.12$ mm Hg at 1573 K [38]

As: $P^\circ_{As_T} = P_{As} + P_{As_2} + P_{As_4} \simeq 784$ atm $= 6 \times 10^5$ mm Hg at 1523 K [59]

I-2. Activity Coefficients:

$\log \gamma^\circ_{Bi} = 1900T^{-1} - 0.885$ [9]

$\log \gamma^\circ_{Pb} = 2587T^{-1} - 1.010$ [9]

$\gamma^\circ_{Sb} \simeq 2.2 \times 10^{-2}$ at 1573 K [9]

$\gamma^\circ_{As} \simeq 10^{-6}$ at 1573 K [9]

I-3. Density of Copper:

$\rho_{Cu} = 7.936 - 7.862 \times 10^{-4} (T-1356)$ g/cm^3 [126]

T = temperature, K

$\rho_{Cu} = 7.88$ g/cm^3 at 1423 K

$\rho_{Cu} = 7.81$ g/cm^3 at 1523 K

$\rho_{Cu} = 7.73$ g/cm^3 at 1623 K

$\rho_{Cu} = 7.65$ g/cm^3 at 1723 K

$\rho_{Cu} = 7.57$ g/cm^3 at 1823 K

$\rho_{Cu} = 7.49$ g/cm^3 at 1923 K

I-4. Molecular Weights:

M_{Cu} = 63.54

M_{Bi} = 209.00

M_{Bi_2} = 418.00

M_{Pb} = 207.21

M_{Sb} = 121.76

M_{As} = 74.91

I-5. Crucible Dimensions:

#30 Crucible: r = 9.6 cm A/V = 0.067 cm^{-1}

#50 Crucible: r = 11.8 cm A/V = 0.102 cm^{-1}

Alumina Crucible: r = 9.9 cm A/V = 0.071 cm^{-1}

I-6. Pressure Convertion:

1 atm = 760 mm Hg = 1.01325 x 10^5 pascal

μ	1	10	60	100	300	1000
pascal	0.13	1.33	8.00	13.33	40.00	133.32

Table I-1. Values of Activity Coefficient, Vapour Pressure and Evaporation Mass Transfer Coefficient

Temp. K	γ			P, mm Hg			$K_E(10^{-3})$ cm/s		
	Bi	Bi_2	Pb	Bi	Bi_2	Pb	Bi	Bi_2	Pb
1423	2.82	2.82	6.43	17.71	10.89	8.62	28.4	0.080	47.9
1523	2.30	2.30	4.88	32.45	27.73	23.64	62.9	0.133	97.5
1623	1.93	1.93	3.84	78.91	62.18	57.06	125.4	0.205	181.0
1723	1.65	1.65	3.10	172.30	125.58	123.87	229.5	0.297	311.6
1823	1.44	1.44	2.57	343.97	232.55	246.24	392.7	0.411	503.9
1923	1.27	1.27	2.16	636.75	400.46	454.43	616.0	0.542	769.1

APPENDIX II

MEAN FREE PATH CALCULATIONS

II-1. Mean Free Path Calculations:

$$\lambda = \frac{kT}{\sqrt{2}\,\pi\varepsilon^2 P} = 2.33 \times 10^{-20}\,\frac{T}{\varepsilon^2 P}\ \text{cm} \quad [27]$$

λ = mean free path, cm

T = temperature, K

ε = molecular diameter, cm

P = ambient pressure, torr

k = Boltzman Constant

Temperatures: 1423 K, 1523 K, 1623 K

Pressures: 60 μHg, 100 μHg, 300 μHg

80 pascal, 13.33 pascal, 40.0 pascal

Molecular Diameter: ($\text{Å} = 10^{-8}$ cm) [127]

Cu: 2.56 x A; Bi: 3.40 x A; Pb: 3.50 x A,

As: 2.78 x A; Sb: 3.18 x A

Table II-1. Predicted Mean Free Paths, λ(cm)

Copper:

Pressure/ Temperature	1423	1523	1623
8.0	0.843	0.903	0.962
13.3	0.506	0.541	0.577
40.0	0.169	0.180	0.192

Arsenic:

Pressure/ Temperature	1423	1523	1623
8.0	0.715	0.765	0.816
13.3	0.429	0.459	0.489
40.0	0.143	0.153	0.163

Bismuth:

Pressure/ Temperature	1423	1523	1623
8.0	0.478	0.512	0.545
13.3	0.287	0.307	0.327
40.0	0.096	0.102	0.109

Antimony:

Pressure/ Temperature	1423	1523	1623
8.0	0.546	0.585	0.623
13.3	0.328	0.351	0.374
40.0	0.109	0.117	0.125

Lead:

Pressure/ Temperature	1423	1523	1623
8.0	0.451	0.483	0.515
13.3	0.271	0.290	0.309
40.0	0.090	0.097	0.103

APPENDIX III

ESTIMATION OF DIFFUSION AND MASS TRANSPORT COEFFICIENTS IN LIQUID PHASE

III-1. ESTIMATION OF DIFFUSION IN LIQUID PHASE

III-1.1. Empirical Equations:

In order to estimate the diffusion in liquid copper, empirical equations studied are as follows:

(i) Equation of Walls and Upthegrove for Henrian Solutions [52].

$$D_{AB} = \frac{k_B T}{2\pi r_A (2b+1)\mu_B} \qquad \text{(III-1.)}$$

(ii) Equation of Sutherland for $r_A \gg r_B$ [52]

$$D_{AB} = \frac{k_B T}{4\pi r_A \mu_B} \qquad \text{(III-2.)}$$

(iii) Equation of Stokes-Einstein for $r_A > r_B$ [52]

$$D_{AB} = \frac{k_B T}{6\pi r_A \mu_B} \qquad \text{(III-3.)}$$

(iv) Arrhenius Equation [52]

$$D = D_o^{-\Delta E/RT} \qquad \text{(III-4.)}$$

D, $D_{A,B}$ = diffusion (of solute A in solvent B), $cm^2 s^{-1}$

k_B = Boltzman constant, 1.38062×10^{-23} joule K^{-1}

T = temperature, K

r_A = radius of solute molecule, Å 10^{-8} cm

r_B = radius of solvent molecule, Å 10^{-8} cm

b = ratio of r_A to solvent interatomic spacing

μ_B = liquid solvent viscosity (poise) gm $cm^{-1} s^{-1}$

Do = diffusion coefficient, $cm^2 s^{-1}$

ΔE = activation energy for diffusion cal $gmole^{-1}$

R = gas constant, 8.31432 x 10^7 $gmole^{-1}$ g cm^2 s^{-2} K^{-1}

III-1.2. Data Available:

Data used in the computations are listed below and the results are tabulated in Table III-1.

(a) Radius of molecules: [127]

r_{Cu} = 1.28 Å, r_{Bi} = 1.70 Å, r_{Pb} = 1.75 Å

(b) Interatomic spacing for copper: [127]

2.55 Å

(c) Viscosity of liquid copper: [47]

μ_{Cu} = 3cP = 3 x 10^{-9} joule·s·cm^{-3}

(d) Activation energy for diffusion: [52]

ΔE = 30 kcal·$mole^{-1}$

III-1.3. Estimation of Diffusion by Arrhenius Equation:

It is assumed that D = 1. x 10^{-5} cm^2/s at 1423K and ΔE = 30 kcal/mole at all temperatures. Then by ratio of D 1423 to D 1523, D at 1523 can also be determined:

$$\frac{D\ 1423}{D\ 1523} = e^{-\Delta E/R\ \left(\frac{1}{1423} - \frac{1}{1523}\right)}$$

By using the ratio method, diffusions are estimated up to 1923 K and included in Table III-2. Sensitivity of diffusion to decreasing ΔE to 15 kcal/mole is also checked and included in Table III-2.

TABLE III-1. Estimated Diffusivities of Bismuth and Lead in Liquid Copper

Temp. °C	Walls & Upthe. (10^{-5} cm^2/s)		Stokes & Ein. (10^{-5} cm^2/s)		Sutherland (10^{-5} cm^2/s)	
	Bi	Pb	Bi	Pb	Bi	Pb
1150	2.63	2.51	2.05	1.39	3.07	2.98
1250	2.81	2.69	2.19	2.13	3.28	3.19
1350	3.00	2.86	2.33	2.27	3.50	3.40

TABLE III-2. Estimated Diffusivity and Liquid Phase Mass Transport Coefficient Values for Two Levels of Activation Energy[1].

Temp. °C	ΔE = 30 kcal/mole		ΔE = 15 kcal/mole	
	D (10^{-5} cm^2/s)	K_L (10^{-3} cm/s)	D (10^{-5} cm^2/s)	K_L (10^{-3} cm/s)
1150	1.0	5.09	1.0	5.09
1250	2.0	7.21	1.42	6.06
1350	3.70	9.78	1.92	7.05
1450	6.34	12.80	2.52	8.07
1550	10.25	16.28	3.20	9.10
1650	15.77	20.19	3.97	10.13

1. Crucible radius = 9.85 cm

III-2. ESTIMATION OF LIQUID PHASE MASS TRANSPORT COEFFICIENT

Based on the estimated diffusion values, liquid phase mass transport coefficients, K_L* were calculated at different temperatures and for the three different diameters of the crucibles used in the experiments. These values which were used in the kinetic studies are included in Table III-3.

* Equation for predicting K_L is given by Equation 14.

TABLE III-3. Estimated Liquid Phase Mass Transport Coefficient Values for Different Crucible Radius[1].

Temp. °C	K_L (10^{-3} cm/s)		
	Crucible radius, cm		
	9.60	11.80	9.85
1150	5.15	4.65	5.09
1250	7.30	6.59	7.21
1350	9.91	8.94	9.78

1. ΔE = 30 kcal/mole

APPENDIX IV

EVALUATION OF 2-LEVEL FRACTIONAL FACTORIAL TEST DESIGN

IV-1. CALCULATION OF EFFECTS AND MEAN SQUARES

In order to analyse the effects of four factors on overall mass transfer coefficient, K, the first step was to calculate the effects measured and the mean squares from the data obtained.[120] Yates' Method[120] was used for this purpose and the results obtained including the stepwise calculation columns are tabulated in Tables IV-1 and IV-2 for bismuth and lead respectively. This calculation provides the seven effects (A, B, C, D, AB or CD, AC or BD, BC or AD) involving seven independent comparisons between the eight responses. Thus, in this test design, since every effect is based on one degree of freedom, the sums of squares also denote the mean squares.

IV-2. INTERPRETATION OF RESULTS

In order to carry out a comparison of the effects measured using statistical testing methods, the experimental error variance need to be established. Since there was one set of experimental data, there was no direct estimate of the experimental error variance by which the significance of the effects might be judged. In non-replicated fractional factorial test designs such as this, the interaction mean squares can be used to give an estimate of the error variance.[120] Or, as an alternative, the error variance can be estimated from the variance obtained by duplicating a few randomly selected experiments from the test design.

Method a.

In Table IV-3-a calculations for the mean sum of squares (estimate of error variance) from two factor interactions for both bismuth and lead are

shown. Using these values, F-tests were carried out for one and three degrees of freedom to determine the significant effects (Table IV-3-b).

At 5 and 10% levels of F-tests, melt temperature and vacuum pressure were defined as the most significant factors effecting mass transport coefficient of bismuth and lead.[120]

Method b.

In Table IV-4-a estimation of error variance from duplicated experiments (Experiment F-1 was duplicated in experiment F-1-X and experiment F-3 was duplicated in test F-9-X) is tabulated. Using these values, again F-tests were carried out for one and two degrees of freedom to determine the significant effects (Table IV-4-b) for both bismuth and lead. Similar results to "Method a" were obtained and significance levels were much higher. Factors:- melt temperature and vacuum pressure, were determined as significantly effecting the overall mass transport coefficients of both bismuth and lead at the 1% level of F-test.

Also at 5 and 10% levels of F-test the interaction effects of BC and AD were found to be significant (Table IV-4-b). The effects of interactions were further analyzed by the two-way table of total effects[120] (Table IV-5). The interaction effect of AD seems to be slightly higher than BC, 1.461 compared to 1.393 for Bi and 2.158 compared to 2.089 for Pb. Since the difference is so small it is difficult to separate the interaction effects of AD and BC from each other. Table IV-5 indicates that combined effects of decreasing vacuum pressure and decreasing condenser distance to melt surface thus again combined effects of increasing melt temperature and increasing A/V can have positive effects on K_{Bi} and K_{Pb}.

TABLE IV-1. Calculation of Effects and Mean Squares by Yates' Method - Bismuth

Experiment Number	Responses $K(10^{-3}$ cm/s)	(1)	(2)	(3)	Mean Effect (Col.3)/4	Sum of Squares* $(Col.3)^2/8$	Effects Measured	Total Effect	Degrees of Freedom
F-2	1.127	1.738	4.183	8.009	-	-	-	-	-
F-1	0.611	2.445	3.826	-1.811	-0.453	0.410	A	-1.811	1
F-3	1.337	1.041	-0.745	2.451	0.613	0.751	B	2.451	1
F-4	1.108	2.785	-1.066	-0.253	-0.063	0.008	AB,CD	-0.253	1
F-5	0.652	-0.516	0.707	-0.357	-0.089	0.016	C	-0.357	1
F-6	0.389	-0.229	1.744	-0.321	-0.080	0.013	AC,BD	-0.321	1
F-7	1.794	-0.263	0.287	1.037	0.257	0.134	BC,AD	1.037	1
F-8	0.991	-0.803	-0.540	-0.827	-0.207	0.085	D	-0.827	1
Total	8.009	-	-	-	-	1.417	-	-	7

*Arithmetic Check:

$$\text{Sum of Squares} = (1.127)^2 + (0.611)^2 + (1.337)^2 + (1.108)^2 + (0.652)^2 + (0.389)^2 + (1.794)^2 + (0.991)^2 - \frac{(8.009)^2}{8} = 1.418$$

TABLE IV-2. Calculation of Effects and Mean Squares by Yates' Method - Lead

Experiment Number	Responses $K(10^{-3}cm/s)$	(1)	(2)	(3)	Mean Effect (Col.3)/4	Sum of Squares* $(Col.3)^2/8$	Effects Measured	Total Effect	Degrees of Freedom
F-2	1.795	2.502	6.149	12.032	-	-	-	-	-
F-1	0.707	3.647	5.883	-3.262	-0.861	1.330	A	-3.262	1
F-3	2.215	1.706	-1.871	3.616	0.904	1.634	B	3.616	1
F-4	1.432	4.177	-1.391	-0.034	-0.009	0.0002	AB,CD	-0.034	1
F-5	1.116	-1.088	1.145	-0.266	-0.067	0.009	C	-0.266	1
F-6	0.590	-0.783	2.471	0.480	0.120	0.029	AC,BD	0.480	1
F-7	2.521	-0.526	0.305	1.326	0.332	0.220	BC,AD	1.326	1
F-8	1.656	-0.865	-0.339	-0.644	-0.161	0.052	D	-0.644	1
Total	12.032	-	-	-	-	3.274	-	-	7

*Arithmetic Check:

$$\text{Sum of Squares} = (1.795)^2 + (0.707)^2 + (2.215)^2 + (1.432)^2 + (1.116)^2 + (0.590)^2 + (2.521)^2 + (1.656)^2 - \frac{(12.032)^2}{8} = 3.274$$

TABLE IV-3-a. Estimation of Mean Square from Two Factor Interactions

Interactions	Bi	Pb
AB,CD	0.008	0.0002
AC,BD	0.013	0.029
BC,AD	0.134	0.220
Total sum of squares	0.155	0.249
Number of sum of squares	3	3
Mean sum of squares	0.052	0.083

TABLE IV-3-b. Analysis of Variance Based on Interactions (Determination of Significant Effects, F-test for 1, 3 degrees of freedom)

Bismuth:

% Level	F-value		Mean Squ.		Significance Level	Significant Effects
10	5.54	x	0.052	=	0.288	B,A
5	10.10	x	0.052	=	0.525	B
2.5	17.40	x	0.052	=	0.905	-
1	34.10	x	0.052	=	1.773	-

Lead:

% Level	F-value		Mean Squ.		Significance Level	Significant Effects
10	5.54	x	0.083	=	0.460	B,A
5	10.10	x	0.083	=	0.838	B,A
2.5	17.40	x	0.083	=	1.444	B
1	34.10	x	0.083	=	2.830	-

TABLE IV-4-a. Estimation of Error Variance From Duplicated Experiments

		Original/ $K(10^{-3}$ cm/s)	Duplicate/ $K(10^{-3}$ cm/s)	Difference	$(Dif)^2/2$	Error Variance (I+II)/2
Bi	I	F-1 0.61	F-1-X 0.56	0.05	1.25×10^{-3}	3.125×10^{-3}
	II	F-3 1.34	F-9-X 1.24	0.10	5.0×10^{-3}	
Pb	I	F-1 0.71	F-1-X 0.68	0.03	0.45×10^{-3}	13.45×10^{-3}
	II	F-3 2.22	F-9-X 1.99	0.23	26.45×10^{-3}	

TABLE IV-4-b. Analysis of Variance Based on Estimated Error Variance, F-Test for 1, 2 Degrees of Freedom

	% Level	F-value		Error Variance		Significance Level	Significant Effects
Bi	10.0	8.53	x	3.125×10^{-3}	=	26.66×10^{-3}	B,A,BC-AD
	5.0	18.50	x	3.125×10^{-3}	=	57.81×10^{-3}	B,A,BC-AD
	2.5	38.50	x	3.125×10^{-3}	=	120.31×10^{-3}	B,A
	1.0	98.50	x	3.125×10^{-3}	=	307.81×10^{-3}	B,A
Pb	10.0	8.53	x	13.45×10^{-3}	=	0.115	B,A,BC-AD
	5.0	18.50	x	13.45×10^{-3}	=	0.249	B,A
	2.5	38.50	x	13.45×10^{-3}	=	0.518	B,A
	1.0	98.50	x	13.45×10^{-3}	=	1.325	B

TABLE IV-5. Analysis of Interactions BC and AD

B / C	6.70 m^{-1} (-)		10.20 m^{-1} (+)	
1150°C (-)	1.127 0.611 1.738	0.869	0.652 0.389 1.041	0.521
1250°C (+)	1.337 1.108 2.445	1.223	1.794 0.991 2.785	1.393

A / D	<2 cm (-)		>67 cm (+)	
100μHg (-)	1.127 1.794 2.921	1.461	1.337 0.652 1.989	0.995
300μHg (+)	1.108 0.389 1.497	0.749	0.611 0.911 1.602	0.801

Lead

B / C	6.70 m^{-1} (-)		10.20 m^{-1} (+)	
1150°C (-)	1.795 0.707 2.502	1.251	1.116 0.590 1.706	0.853
1250°C (+)	2.215 1.432 3.647	1.824	2.521 1.656 4.177	2.089

A / D	<2 cm (-)		>67 cm (+)	
100μHg (-)	1.795 2.521 4.316	2.158	2.215 1.116 3.331	1.666
300μHg (+)	1.432 0.590 2.022	1.011	0.707 1.656 2.363	1.182

APPENDIX V

ANALYSIS OF CONDENSATE AND COPPER LOSSES

V-1. ANALYSIS OF CONDENSATE

Water cooled condenser was used in four experiments and this was held within a distance of 1.5-2 cm above the melt surface. After the experiments, condensate accumulated on the condenser was removed, weighed and ground. Metallic droplets were separated from -100 mesh size powder by screening, weighed again, and chemically analyzed separately. Using the chemical analysis, the amount of bismuth and lead in the condensate were calculated. Then from the initial and final contents of bismuth and lead in the copper, the total amount of element evaporated was determined. Finally, the ratio of amount of element accumulated on the condenser to the amount of element evaporated was calculated. The details of calculations are given in Tables V-1 and V-2.

V-2. COPPER LOSSES

The amount of copper charge used was weighed before and after each experiment and recorded. Then the ratio of the weight difference to initial copper weight was determined and tabulated as approximate copper loss weight % in Table V-3. The reason it was called approximate was because it contained the splashes and the amount of impurities evaporated.

TABLE V-1. Analyses of Condensate Accumulated on Condenser

Test No.	Press. μHg	Temp. °C	Amount of Condensate Accumulated On Condenser gram	-100 Mesh Powder gram	-100 Mesh Powder wt% Bi	-100 Mesh Powder wt% Pb	-100 Mesh Powder weight, gram Bi_I	-100 Mesh Powder weight, gram Pb_{II}	Metallic Droplets gram	Metallic Droplets wt% Bi	Metallic Droplets wt% Pb	Metallic Droplets weight, gram Bi_{III}	Metallic Droplets weight, gram Pb_{IV}	Total weight gram Bi I+III	Total weight gram Pb II+IV
F-2	100	1150	53	34	14.5	70.8	4.93	24.07	19	16.7	72.2	3.17	13.72	8.10	37.79
F-4	300	1250	73	27	13.7	68.6	3.70	18.52	46	3.7	12.7	1.70	5.84	5.40	24.36
F-6	300	1150	34	7	10.7	42.9	0.75	3.00	27	4.5	13.1	1.22	3.54	1.97	6.54
F-10[1]	100	1250	128	50	10.5	42.0	5.25	21.00	78	0.2	0.9	0.16	0.70	5.41	21.70

1. Time = 240 min.

TABLE V-2. Distribution Ratio to Condenser

Test No.	Bismuth Initial, wt%	Bismuth Final, wt%	Bismuth Eliminated weight, gram V	Lead Initial, wt%	Lead Final, wt%	Lead Eliminated weight, gram VI	Distribution Ratio to Condenser, wt% Bi (I+III)/V	Distribution Ratio to Condenser, wt% Pb (II+IV)/VI
F-2	0.090	0.046	14.96	0.333	0.130	69.02	54	55
F-4	0.060	0.033	9.18	0.215	0.098	39.78	59	61
F-6	0.032	0.025	2.38	0.080	0.054	8.84	83	74
F-10[1]	0.044	0.005	13.26	0.126	0.003	41.82	41	52

1. Time = 240 min.

TABLE V-3. Copper Losses

Test No.	Difference in Initial and Final Weight of Copper, gram	Ratio of Difference to Initial Copper Weight, %
F-1	150	0.44
F-2	220	0.65
F-3	210	0.62
F-4	230	0.68
F-5	190	0.56
F-6	130	0.38
F-8	260	0.76
F-9[1.]	400	1.17
F-10[1.]	420	1.23
A-1	220	0.65
A-2	300	0.88
A-3	320	0.94
A-4	310	0.91
A-5	340	1.00
A-6	320	0.94
A-7[1.]	400	1.17
A-8	300	0.88
A-9	280	0.82

1. Time = 240 minutes

APPENDIX VI

COMPUTER PROGRAM

```
C
C   LISTING OF THE COMPUTER PROGRAM "MASS TRANSFER COEFFICIENTS"
C      A-0 BI
C
       DIMENSION  X1(20),Y1(20)
       REAL  M,KL,KE,PVAP,PVAP1,MIMP,GAMA,MCU,KU,KGAS,K,RGAS,RAD,  RCU
       CALL PLOTON
       DO  10  I=1,20
C
C   READ THE DATA OF CHANGE OF WEIGHT PERCENT OF IMPURITIES BY TIME
C
       READ(5,*) X1(I),Y1(I)
       IF(Y1(I).EQ.0.0)GO TO 15
  10   CONTINUE
C
C   PLOT  LOG OF CHANGE OF WEIGHT PERCENT OF IMPURITY BY TIME
C
  15   I=I-1
       X1(I+1)=0.0
       X1(I+2)=30.0
        Y1(I+1)=-3.5
       Y1(I+2)=0.5
        CALL PLOT(1.0,2.0,-3)
       X=1.0
       Y=0.0
       DO 20 N=1,5
       CALL PLOT(X,0.0,2)
        CALL PLOT(X,0.1,2)
       CALL PLOT(X,0.0,3)
       X=X+1.0
 20    CONTINUE
        CALL PLOT(5.0,0.0,3)
       Y=1.0
        X=5.0
        DO 25 N=1,7
         CALL PLOT(X,Y,2)
        CALL PLOT(X-0.1,Y,2)
        CALL PLOT(X,Y,3)
       Y=Y+1.0
 25    CONTINUE
       CALL PLOT(5.0,7.0,3)
        X=4.0
       Y=7.0
       DO 30 N=1,5
        CALL PLOT(X,Y,2)
        CALL PLOT(X,Y-0.1,2)
       CALL PLOT(X,Y,3)
       X=X-1.0
 30    CONTINUE
       CALL PLOT(0.0,7.0,3)
       X=0.0
       Y=6.0
       DO 35 N=1,7
       CALL PLOT(X,Y,2)
       CALL PLOT(X+0.1,Y,2)
      CALL PLOT(X,Y,3)
         Y=Y-1.0
 35    CONTINUE
        X=0.0
      Y=-0.3
       F=0.0
         DO 40 N=1,5
        IF(F.EQ.30.0)X=X-0.15
```

```
      IF(F.EQ.120.0)X=X-0.075
       CALL NUMBER(X,Y,0.15,F,0.0,-1)
       X=X+1.0
      F=F+30.0
40    CONTINUE
       X=-0.65
        Y=-0.075
      F=-3.5
       DO 45 N=1,8
      IF(F.EQ.0.0)X=-0.5
      CALL NUMBER(X,Y,0.15,F,0.0,1)
      Y=Y+1.0
       F=F+0.5
45    CONTINUE
      CALL SYMBOL(1.0,-1.0,0.20,14HTIME (MINUTES),0.0,14)
      CALL SYMBOL(-1.0,1.5,0.20,18HLOG (WT.% BISMUTH),90.0,18)
      CALL PLINE(X1,Y1,I,1,-1,11)
C
C   DO THE LINEAR REGRESSION
C
     XY=0.0
      X=0.0
        Y=0.0
       XX=0.0
      YY=0.0
      DO 50 N=1,I
      XY=XY+X1(N)*Y1(N)
      X=X+X1(N)
      Y=Y+Y1(N)
        XX=XX+X1(N)*X1(N)
      YY=YY+Y1(N)*Y1(N)
50    CONTINUE
C
C   DEFINE THE SLOPE OF THE LINE= B
C
      C=I*XY-X*Y
      D=I*XX-X*X
      B=C/D
C
C   DEFINE THE INTERCEPT OF THE LINE= A
C
       A=(Y-B*X)/I
C
C   CALCULATE THE CORRELATION COEFF= R
C
      C1=I*XY-X*Y
      F1=(I*XX-X*X)**(0.5)
      F2=(I*YY-Y*Y)**(0.5)
      R=C1/(F1*F2)
        XX1=0
        YY1=(3.5+A)/0.5
       XX2=4.0
       YY2=(3.5+(A+B*120.0))/(0.5)
        WRITE(6,90)XY,X,Y,XX,YY
90      FORMAT(5F15.4)
        WRITE(6,90)C,D,B,A,C1
          WRITE(6,90)R,F1,F2,YY1,YY2
      CALL DASH(XX1,YY1,XX2,YY2,0.0)
C
C   ADJUSTMENT FOR DEFINING THE OVERALL MASS TRANSFER COEFF.= K
C
        M=-1.8498
        K=B/M
C
```

```
C    CALCULATE THE MASS TRANSFER COEFF. IN LIQUID PHASE= KL
C
        RAD=9.85
        KL=0.016*((1/RAD)**0.5)
         MCU=63.54
        TEMP=1523.
C
C    CALCULATE THE DENSITY OF COPPER= RCU
C
        RCU=7.936-0.7682*0.001*(TEMP-1358.)
C
C    CALCULATE THE ACTIVITY COEFF. OF IMPURITY= GAMA
C
          T1=(1800./TEMP)-0.885
        GAMA=10.0**T1
C
C    CALCULATE THE VAPOUR PRESSURE OF IMPURITY= PVAP
C
        PVAP1=(-10400./TEMP)-1.28*ALOG10(TEMP)+12.35
         PVAP=10.0**PVAP1
        EX=1.0
            MIMP=209.0
C
C    CALCULATE THE MASS TRANSFER COEFF. OF EVAPORATION= KE
C
        F1=(GAMA*MCU)/RCU
         F1=F1**EX
         F2=(MIMP*TEMP)**0.5
        F3=0.0583*PVAP/F2
        KE=F3*F1
C
C    CALCULATE THE MASS TRANSFER COEFF. IN THE GAS PHASE FROM K,KL,KE
C
         Z=K*KL*KE
        Z1=(KL*KE)-K*(KE+KL)
           KU=Z/Z1
        RGAS=82362.53
        Z2=RCU/(GAMA*MCU)
        Z3=Z2**EX
        Z4=KU*TEMP*RGAS*Z3
         KGAS=Z4/PVAP
        WRITE(6,100) B,A,K,KL,KE,KU,KGAS,RAD,TEMP,RCU,PVAP,GAMA,A
100     FORMAT('1',///,10X,'B=',F13.7,/,10X,'A=',F13.7,/,10X,'K=',F13.7,
     1'CM/SEC',/,10X,'KL=',F13.7,'CM/SEC',/,10X,'KE=',F13.7,'CM/SEC',/,
     110X,'KU=',F13.7,'CM/SEC',/,10X,'KGAS=',F13.7,'CM/SEC',/,10X,
     2'RAD=',F13.7,'CM',/,10X,'TEMP=',F13.7,'K',/,10X,'RCU=',F13.7,
     1 'GM/CC',/,10X,'PVAP=',F13.7,'MM',/,10X,'GAMA=',F13.7,
     1/,10X,'A=',F13.7)
        CALL ENDPLT
        STOP
         END
```

APPENDIX VII

THERMODYNAMIC CALCULATIONS WITH F.A.C.T. SYSTEM

VII-1. ESTIMATION OF EQUILIBRIUM TEMPERATURES AT WHICH METAL OXIDES FORM

```
XXXXXXXXXXXXXXXXXXXXXXXXXXXXXXXXXXXXXXXXXXXXXXXXXXXXXXXXXXXXXXXXXXXXXXXXXXXXXXXXXXX

  2CU              +          .502          =          CU2O
 (T,.000658,L)        (T,.000658,G,.0001316)          (T,.000658,L)

        CALCULATIONS ARE BASED ON THE INDICATED NUMBER OF GRAM MOLES

*********************************************************************************
   (T)       DELTA H      DELTA G      DELTA V      DELTA S      DELTA U      DELTA A
   (K)        (CAL)        (CAL)         (L)        (CAL/K)      (CAL)        (CAL)
*********************************************************************************
?
    *            *           0
 1139.1     -32294.7          0.0   -0.710E+05      28.351      31162.8       1131.9
?


/d

XXXXXXXXXXXXXXXXXXXXXXXXXXXXXXXXXXXXXXXXXXXXXXXXXXXXXXXXXXXXXXXXXXXXXXXXXXXXXXXXXXX

YOU DO (1) OR YOU DO NOT (2) WISH TO EXAMINE PHASES AND TEMPERATURE RANGES
?
```

```
XXXXXXXXXXXXXXXXXXXXXXXXXXXXXXXXXXXXXXXXXXXXXXXXXXXXXXXXXXXXXXXXXXXXXXXXXXXXXXXXXX

  2BI                  +          1.502                    =          BI2O3
 (T,.000658,L,.001)  (T,.000658,G,.0001316)               (T,.000658,L)

         CALCULATIONS ARE BASED ON THE INDICATED NUMBER OF GRAM MOLES

**********************************************************************************
   (T)       DELTA H      DELTA G     DELTA V      DELTA S      DELTA U       DELTA A
   (K)        (CAL)        (CAL)        (L)        (CAL/K)       (CAL)         (CAL)
**********************************************************************************
?
   *          *             0
  938.8   -111138.0        -0.1   -0.176E+06    -118.379    -108339.3       2798.5
?

/d

XXXXXXXXXXXXXXXXXXXXXXXXXXXXXXXXXXXXXXXXXXXXXXXXXXXXXXXXXXXXXXXXXXXXXXXXXXXXXXXXXX

YOU DO (1) OR YOU DO NOT (2) WISH TO EXAMINE PHASES AND TEMPERATURE RANGES
?
```

XXXXXXXXXXXXXXXXXXXXXXXXXXXXXXXXXXXXXXXXXXXXXXXXXXXXXXXXXXXXXXXXXXXXXXXXXXXXXXXX

2BI	+	1.502	=	BI2O3
(T,.000658,G,.001)		(T,.000658,G,.0001316)		(T,.000658,L)

CALCULATIONS ARE BASED ON THE INDICATED NUMBER OF GRAM MOLES

(T) (K)	DELTA H (CAL)	DELTA G (CAL)	DELTA V (L)	DELTA S (CAL/K)	DELTA U (CAL)	DELTA A (CAL)
1043.1	-202820.2	0.0	-0.455E+06	-194.431	195561.5	7255.8

?

/d

XXXXXXXXXXXXXXXXXXXXXXXXXXXXXXXXXXXXXXXXXXXXXXXXXXXXXXXXXXXXXXXXXXXXXXXXXXXXXXXX

YOU DO (1) OR YOU DO NOT (2) WISH TO EXAMINE PHASES AND TEMPERATURE RANGES
?

```
XXXXXXXXXXXXXXXXXXXXXXXXXXXXXXXXXXXXXXXXXXXXXXXXXXXXXXXXXXXXXXXXXXXXXXXXXXXXXXX


     PB                +           .502                   =             PBYO
  (T,.000658,L,.004)   (T,.000658,G,.0001316)          (T,.000658,L)


          CALCULATIONS ARE BASED ON THE INDICATED NUMBER OF GRAM MOLES  .

*******************************************************************************
   (T)        DELTA H      DELTA G     DELTA V      DELTA S      DELTA U      DELTA A
   (K)         (CAL)        (CAL)        (L)        (CAL/K)       (CAL)        (CAL)
*******************************************************************************
?
  *           *            0
 1000.1    -45371.6          0.0  -0.624E+05    -45.366     -44377.9        993.8
?

/d


XXXXXXXXXXXXXXXXXXXXXXXXXXXXXXXXXXXXXXXXXXXXXXXXXXXXXXXXXXXXXXXXXXXXXXXXXXXXXXX


YOU DO (1) OR YOU DO NOT (2) WISH TO EXAMINE PHASES AND TEMPERATURE RANGES
?
```

XXXXXXXXXXXXXXXXXXXXXXXXXXXXXXXXXXXXXXXXXXXXXXXXXXXXXXXXXXXXXXXXXXXXXXXXXXXXXXXXXXXXXX

```
   PB                +         .502          -          =            PB*O
 (T,.000658,G,.004)    (T,.000658,G,.0001316)                   (T,.000658,L)
```

CALCULATIONS ARE BASED ON THE INDICATED NUMBER OF GRAM MOLES

```
*************************************************************************************
   (T)       DELTA H      DELTA G     DELTA V      DELTA S      DELTA U      DELTA A
   (K)        (CAL)        (CAL)        (L)        (CAL/K)       (CAL)        (CAL)
*************************************************************************************
?
  *            *             O
 1091.3     -88992.4          0.0  -0.204E+06     -81.548     -85739.2      3253.2
?

/d
```

XXXXXXXXXXXXXXXXXXXXXXXXXXXXXXXXXXXXXXXXXXXXXXXXXXXXXXXXXXXXXXXXXXXXXXXXXXXXXXXXXXXXXX

YOU DO (1) OR YOU DO NOT (2) WISH TO EXAMINE PHASES AND TEMPERATURE RANGES
?

McGill University Computing Centre

```
XXXXXXXXXXXXXXXXXXXXXXXXXXXXXXXXXXXXXXXXXXXXXXXXXXXXXXXXXXXXXXXXXXXXXXXXXXXXXXXX


   2AS                  +                  1.502               =            AS203
 (T,.000658,G,.004)   (T,.000658,G,.0001316)     (T,.000658,L)


         CALCULATIONS ARE BASED ON THE INDICATED NUMBER OF GRAM MOLES

********************************************************************************
    (T)        DELTA H      DELTA G     DELTA V      DELTA S      DELTA U      DELTA A
    (K)         (CAL)        (CAL)        (L)        (CAL/K)       (CAL)        (CAL)
********************************************************************************
?
  *         *         0
 1410.3   -280722.1          0.0  -0.616E+06    -199.049     270912.3       9809.7
?
/3


XXXXXXXXXXXXXXXXXXXXXXXXXXXXXXXXXXXXXXXXXXXXXXXXXXXXXXXXXXXXXXXXXXXXXXXXXXXXXXXX


YOU DO (1) OR YOU DO NOT (2) WISH TO EXAMINE PHASES AND TEMPERATURE RANGES
?
```

```
XXXXXXXXXXXXXXXXXXXXXXXXXXXXXXXXXXXXXXXXXXXXXXXXXXXXXXXXXXXXXXXXXXXXXXXXXXXXXXX


2SB                    +          1.502              =        SB2O3
(T,.000658,L,.004)        (T,.000658,G,.0001316)           (T,.000658,L)


        *CALCULATIONS ARE BASED ON THE INDICATED NUMBER OF GRAM MOLES

*********************************************************************************
   (T)       DELTA H      DELTA G      DELTA V      DELTA S      DELTA U      DELTA A
   (K)        (CAL)        (CAL)         (L)       (CAL/K)       (CAL)        (CAL)
*********************************************************************************
?
  *            *            0
 1339.1    -157172.0          0.0   -0.250E+06    -117.369     153180.0      3991.9
?


/d


XXXXXXXXXXXXXXXXXXXXXXXXXXXXXXXXXXXXXXXXXXXXXXXXXXXXXXXXXXXXXXXXXXXXXXXXXXXXXXX


YOU DO (1) OR YOU DO NOT (2) WISH TO EXAMINE PHASES AND TEMPERATURE RANGES
?
2
```

```
XXXXXXXXXXXXXXXXXXXXXXXXXXXXXXXXXXXXXXXXXXXXXXXXXXXXXXXXXXXXXXXXXXXXXXXXXX


2SB                   +           1.502              =        SB2O3
(T,.000658,G,.004)       (T,.000658,G,.0001316)       (T,.000658,L)


        CALCULATIONS ARE BASED ON THE INDICATED NUMBER OF GRAM MOLES

**************************************************************************
   (T)      DELTA H     DELTA G    DELTA V     DELTA S     DELTA U     DELTA A
   (K)       (CAL)       (CAL)       (L)       (CAL/K)      (CAL)       (CAL)
**************************************************************************
?
   *          *           0
 1384.5   -269308.7         0.0  -0.604E+06  -194.523   259678.8      9629.8
?


/d


XXXXXXXXXXXXXXXXXXXXXXXXXXXXXXXXXXXXXXXXXXXXXXXXXXXXXXXXXXXXXXXXXXXXXXXXXX


YOU DO (1) OR YOU DO NOT (2) WISH TO EXAMINE PHASES AND TEMPERATURE RANGES
?
```

VII-2. ESTIMATION OF EQUILIBRIUM OXYGEN PRESSURES AT WHICH METAL OXIDES FORM

XXXXXXXXXXXXXXXXXXXXXXXXXXXXXXXXXXXXXXXXXXXXXXXXXXXXXXXXXXXXXXXXXXXXXXXXXXXXXX

2CU	+	.5O2	=	CU2O
(T,P,L)		(T,P,G)		(T,P,L)

CALCULATIONS ARE BASED ON THE INDICATED NUMBER OF GRAM MOLES

(T) (K)	(P) (ATM)	DELTA H (CAL)	DELTA G (CAL)	DELTA V (L)	DELTA S (CAL/K)	DELTA U (CAL)
?						
1423	*	*	0			
1423.0	0.230E-04	-30934.3	0.0	0.254E+07	21.739	29520.3
?						
1523	*	*	0			
1523.0	0.957E-04	-30465.0	0.0	0.653E+06	20.003	-28951.7
?						
1623	*	*	0			
1623.0	0.328E-03	-30000.9	0.0	0.203E+06	18.485	-28388.1

?
/d

UNDECODEABLE CHARACTER "/"

?
/d

XXXXXXXXXXXXXXXXXXXXXXXXXXXXXXXXXXXXXXXXXXXXXXXXXXXXXXXXXXXXXXXXXXXXXXXXXXXXXX

YOU DO (1) OR YOU DO NOT (2) WISH TO EXAMINE PHASES AND TEMPERATURE RANGES-
?

```
XXXXXXXXXXXXXXXXXXXXXXXXXXXXXXXXXXXXXXXXXXXXXXXXXXXXXXXXXXXXXXXXXXXXXXXXXXXXXXXXXX


 2BI                 !          1.5O2           -        =         B12O3
 (T,P,L,.OO1)                  (T,P,G)                            (T,P,L)


          CALCULATIONS ARE BASED ON THE INDICATED NUMBER OF GRAM MOLES

**********************************************************************************
   (T)        (P)         DELTA H      DELTA G     DELTA V     DELTA S     DELTA U
   (K)       (ATM)         (CAL)        (CAL)        (L)       (CAL/K)      (CAL)
**********************************************************************************
?
 1423          *            *             O
 1423.O   O.483E 01    -105818.4        -O.1    O.363E+O4     74.363     101576.4
?
1523           *            *             O
 1523.O   O.247E+OO    -10476O.5         O.1   -O.76OE+O3     68.786    -10022O.4
?
1623           *            *             O
 1623.O   O.1O2E+O1    -103717.9         O.O   -O.197E+O3     63.9O5     -98879.9
?

/d


XXXXXXXXXXXXXXXXXXXXXXXXXXXXXXXXXXXXXXXXXXXXXXXXXXXXXXXXXXXXXXXXXXXXXXXXXXXXXXXXXX


YOU DO (1) OR YOU DO NOT (2) WISH TO EXAMINE PHASES AND TEMPERATURE RANGES
?
```

```
XXXXXXXXXXXXXXXXXXXXXXXXXXXXXXXXXXXXXXXXXXXXXXXXXXXXXXXXXXXXXXXXXXXXXXXXXXXXXXXXXXXXXXX


  2BI            +        1,502                =          BI203
 (T,P,G,.001)             (T,P,G)                        (T,P,L)


        CALCULATIONS ARE BASED ON THE INDICATED NUMBER OF GRAM MOLES

*********************************************************************************************
   (T)        (P)          DELTA H       DELTA G      DELTA V       DELTA S       DELTA U
  (K)        (ATM)          (CAL)         (CAL)         (L)         (CAL/K)       (CAL)
*********************************************************************************************
?
 1423          *              *              0
 1423.0   0.228E-01     -197496.9            0.0    -0.179E+05     -138.789     -187598.9
?
 1523          *              *              0
 1523.0   0.842E-01     -196133.2            0.0    -0.520E+04     -128.781     -185539.7
?
 1623          *              *              0
 1623.0   0.262E+00     -194785.6            0.0    -0.178E+04      120.016     -183496.9
?

/d


XXXXXXXXXXXXXXXXXXXXXXXXXXXXXXXXXXXXXXXXXXXXXXXXXXXXXXXXXXXXXXXXXXXXXXXXXXXXXXXXXXXXXXX


YOU DO (1) OR YOU DO NOT (2) WISH TO EXAMINE PHASES AND TEMPERATURE RANGES
?
```

```
XXXXXXXXXXXXXXXXXXXXXXXXXXXXXXXXXXXXXXXXXXXXXXXXXXXXXXXXXXXXXXXXXXXXXXXXXXXXXXX

     PB               +       .502              =              PB*O
  (T,P,L,.004)               (T,P,G)                          (T,P,L)

          CALCULATIONS ARE BASED ON THE INDICATED NUMBER OF GRAM MOLES

*******************************************************************************
   (T)       (P)        DELTA H      DELTA G     DELTA V     DELTA S     DELTA U
   (K)      (ATM)        (CAL)        (CAL)        (L)       (CAL/K)      (CAL)
*******************************************************************************
?
1423         *            *            0
 1423.0  0.532E-01    -43546.9        0.0   -0.110E+04    30.602     42132.9
?
1523         *            *            0
 1523.0  0.398E+00    -43124.0        0.0    0.157E+03    28.315     41610.8
?
1623         *            *            0
 1623.0  0.229E+01    -42708.4        0.0    0.291E+02    26.314     41096.2
?

/d

XXXXXXXXXXXXXXXXXXXXXXXXXXXXXXXXXXXXXXXXXXXXXXXXXXXXXXXXXXXXXXXXXXXXXXXXXXXXXXX

YOU DO (1) OR YOU DO NOT (2) WISH TO EXAMINE PHASES AND TEMPERATURE RANGES
?
```

```
XXXXXXXXXXXXXXXXXXXXXXXXXXXXXXXXXXXXXXXXXXXXXXXXXXXXXXXXXXXXXXXXXXXXXXXXXXXXXXX


   PB                 +        .5O2                     =            PB*O
 (T,P,G,.004)                (T,P,G)                                (T,P,L)


        CALCULATIONS ARE BASED ON THE INDICATED NUMBER OF GRAM MOLES

*******************************************************************************
    (T)         (P)         DELTA H      DELTA G     DELTA V      DELTA S      DELTA U
    (K)        (ATM)         (CAL)        (CAL)        (L)        (CAL/K)       (CAL)
*******************************************************************************
?
1423            *              *             0
 1423.0   0.184E-01      -86948.5           0.0   0.951E+01    -61.102      82706.5
?
1523            *              *             0
 1523.0   0.705E-01      -86358.5           0.0  -0.266E+04     56.703      81813.4
?
1623             *             *              0
 1623.0   0.227E+00      -85783.7           0.0  -0.881E+03     52.855      80945.7
?

/d


XXXXXXXXXXXXXXXXXXXXXXXXXXXXXXXXXXXXXXXXXXXXXXXXXXXXXXXXXXXXXXXXXXXXXXXXXXXXXXX


YOU DO (1) OR YOU DO NOT (2) WISH TO EXAMINE PHASES AND TEMPERATURE RANGES
?
```

```
XXXXXXXXXXXXXXXXXXXXXXXXXXXXXXXXXXXXXXXXXXXXXXXXXXXXXXXXXXXXXXXXXXXXXXXXXXXXXXXX


   2AS                 +             1.502                   =            AS203
(T,P,G,.004)                       (T,P,G)                              (T,P,L)



        CALCULATIONS ARE BASED ON THE INDICATED NUMBER OF GRAM MOLES

********************************************************************************
   (T)        (P)          DELTA H      DELTA G     DELTA V      DELTA S      DELTA U
   (K)       (ATM)          (CAL)        (CAL)        (L)        (CAL/K)       (CAL)
********************************************************************************
?
1423       *              *             0
 1423.0  0.184E-04    -280548.0          0.0    0.222E+08     197.152     270650.0
?
1523          *           *             0
 1523.0  0.118E-03    -279183.8          0.0   -0.370E+07     183.312     268590.2
?
1623          *           *             0
 1623.0  0.597E-03    -277834.9          0.0   -0.781E+06     171.186     266545.7
?
/d


XXXXXXXXXXXXXXXXXXXXXXXXXXXXXXXXXXXXXXXXXXXXXXXXXXXXXXXXXXXXXXXXXXXXXXXXXXXXXXXX


YOU DO (1) OR YOU DO NOT (2) WISH TO EXAMINE PHASES AND TEMPERATURE RANGES
?
```

XXXXXXXXXXXXXXXXXXXXXXXXXXXXXXXXXXXXXXXXXXXXXXXXXXXXXXXXXXXXXXXXXXXXXXXXXXX

2SB + 1.502 = SB203
(T,P,L,.004) (T,P,G) (T,P,L)

CALCULATIONS ARE BASED ON THE INDICATED NUMBER OF GRAM MOLES

(T) (K)	(P) (ATM)	DELTA H (CAL)	DELTA G (CAL)	DELTA V (L)	DELTA S (CAL/K)	DELTA U (CAL)
?						
1423	*	*	0			
1423.0	0.877E-06	-156356.7	0.0	-0.200E+09	109.878	-152114.7
?						
1523	*	*	0			
1523.0	0.980E-05	-155398.9	0.0	0.191E+08	102.035	150858.9
?						
1623	*	*	0			
1623.0	0.802E-04	-154456.5	0.0	-0.249E+07	95.167	149618.2
?						

/d

XXXXXXXXXXXXXXXXXXXXXXXXXXXXXXXXXXXXXXXXXXXXXXXXXXXXXXXXXXXXXXXXXXXXXXXXXXX

YOU DO (1) OR YOU DO NOT (2) WISH TO EXAMINE PHASES AND TEMPERATURE RANGES
?

```
XXXXXXXXXXXXXXXXXXXXXXXXXXXXXXXXXXXXXXXXXXXXXXXXXXXXXXXXXXXXXXXXXXXXXXXXXXXXXXX

2SB                  +              1.502              -        SB2O3
(T,P,G,.004)              (T,P,G)                        (T,P,L)


        CALCULATIONS ARE BASED ON THE INDICATED NUMBER OF GRAM MOLES

**********************************************************************************
   (T)       (P)          DELTA H      DELTA G     DELTA V      DELTA S      DELTA U
   (K)      (ATM)          (CAL)        (CAL)        (L)        (CAL/K)      (CAL)
**********************************************************************************
?
1423         *              *             0
 1423.0   0.305E-04    -268744.1          0.0   -0.134E+08     188.857    -258846.1
?
1523         *              *             0
 1523.0   0.180E-03    -267294.3         -0.1   -0.243E+07    -175.505     256700.7
?
1623         *              *             0
 1623.0   0.850E-03    -265866.1         -0.1   -0.548E+06     163.812    -254576.9
?



/d


XXXXXXXXXXXXXXXXXXXXXXXXXXXXXXXXXXXXXXXXXXXXXXXXXXXXXXXXXXXXXXXXXXXXXXXXXXXXXXX


YOU DO (1) OR YOU DO NOT (2) WISH TO EXAMINE PHASES AND TEMPERATURE RANGES
?
```

VII-3. DATA

FORMULA: CU

NAME: COPPER

FORMULA WEIGHT: 63.546

PHASE	NAME	RANGE (K)	
S1	SOLID	298.0 - 1357.0	D H TRANS (1356.60 K) = 3.170 (KCAL)
L1	LIQUID	1357.0 - 2848.0	D H TRANS (2848.00 K) = 72.743 (KCAL)
G1	GAS	2848.0 - 3400.0	

CP = A + 1.0E-3*B*T(K) + 1.0E5*C*T(K)** 2 + 1.0E 6*D*T(K)**2

PHASE	D H298 (KCAL)	S298 (CAL/K)	DENSITY (G/CM**3)	A	B	C	D
					(CAL/K)		
S1	0.0	7.913	8.920	5.910	0.905	0.332	-0.0
L1	2.224	8.666	8.920	7.500	0.0	0.0	0.0
G1	79.200	37.954	IDEAL	5.810	0.0	0.0	0.0

REFERENCE: "THERMOCHEMICAL PROPERTIES OF INORGANIC SUBSTANCES",
I. BARIN, O. KNACKE, AND O. KUBASCHEWSKI,
SPRINGER-VERLAG, BERLIN, 1977.

PRESS "RETURN" WHEN READY FOR DISPLAY
?

FORMULA: BI

NAME: BISMUTH

FORMULA WEIGHT: 208.981

PHASE	NAME	RANGE (K)	
S1	SOLID	298.0 - 544.0	D H TRANS (544.00 K) - 2.700 (KCAL)
L1	LIQUID	544.0 - 1200.0	
L1	LIQUID	1200.0 - 1837.0	
G1	GAS	298.0 - 1200.0	
G1	GAS	1200.0 - 1500.0	
G1	GAS	1500.0 - 1837.0	
G1	GAS	1837.0 - 2000.0	

CP = A + 1.0E-3*B*T(K) + 1.0E5*C*T(K)** 2 + 1.0E 6*D*T(K)**2

PHASE	D H298 (KCAL)	S298 (CAL/K)	DENSITY (G/CM**3)	A	B	C	D
					-(CAL/K)		
S1	0.0	13.560	9.800	2.832	7.282	0.981	0.0
L1	2.216	17.208	9.800	4.515	2.479	4.957	0.951
L1	2.838	18.695	9.800	6.500	0.0	0.0	0.0
G1	50.400	44.670	IDEAL	4.968	0.0	0.0	0.0
G1	50.106	44.681	IDEAL	4.952	0.013	0.0	0.0
G1	50.137	44.734	IDEAL	4.886	0.057	0.0	0.0
G1	50.508	44.842	IDEAL	4.776	0.117	0.0	0.0

REFERENCE: "THERMOCHEMICAL PROPERTIES OF INORGANIC SUBSTANCES",
I. BARIN, O. KNACKE, AND O. KUBASCHEWSKI,
SPRINGER VERLAG, BERLIN, 1977.

FORMULA: PB

NAME: LEAD

FORMULA WEIGHT: 207.200

PHASE	NAME	RANGE (K)	
S1	SOLID	298.0 - 600.0	D H TRANS (600.58 K) = 1.141 (KCAL)
L1	LIQUID	600.0 - 1200.0	
L1	LIQUID	1200.0 - 1400.0	
L1	LIQUID	1400.0 - 1700.0	
L1	LIQUID	1700.0 - 2026.0	D H TRANS (2026.00 K) = 42.530 (KCAL)
G1	GAS	2026.0 - 3000.0	

CP = A + 1.0E-3*B*T(K) + 1.0E5*C*T(K)** 2 + 1.0E 6*D*T(K)**2

PHASE	D H298 (KCAL)	S298 (CAL/K)	DENSITY (G/CM**3)	A	B	C (CAL/K)	D
S1	0.0	15.484	11.344	5.789	2.082	0.0	0.0
L1	0.927	16.853	11.344	7.765	0.738	0.0	0.0
L1	1.151	17.275	11.344	7.110	0.195	0.0	0.0
L1	1.420	17.747	11.344	6.491	0.246	0.0	0.0
L1	1.618	18.062	11.344	6.143	0.453	0.0	0.0
G1	46.315	40.826	IDEAL	4.846	0.846	2.945	0.666

REFERENCE: "THERMOCHEMICAL PROPERTIES OF INORGANIC SUBSTANCES",
I. BARIN, O. KNACKE, AND O. KUBASCHEWSKI,
SPRINGER-VERLAG, BERLIN, 1977.

PRESS "RETURN" WHEN READY FOR DISPLAY

FORMULA: AS

NAME: ARSENIC

FORMULA WEIGHT: 74.922

PHASE	NAME	RANGE (K)
S1	SOLID	298.0 - 800.0
G1	GAS	298.0 - 1200.0

CP = A + 1.0E-3*B*T(K) + 1.0E5*C*T(K)**-2 + 1.0E-6*D*T(K)**2

PHASE	D H298 (KCAL)	S298 (CAL/K)	DENSITY (G/CM**3)	A	B	C (CAL/K)	D
S1	0.0	8.534	5.727	5.504	1.373	0.0	0.0
G1	72.120	41.611	IDEAL	4.968	0.0	0.0	0.0

REFERENCE: "THERMOCHEMICAL PROPERTIES OF INORGANIC SUBSTANCES",
I. BARIN, O. KNACKE, AND O. KUBASCHEWSKI,
SPRINGER VERLAG, BERLIN, 1977.

PRESS "RETURN" WHEN READY FOR DISPLAY.
?

FORMULA: SB

NAME: ANTIMONY

FORMULA WEIGHT: 121.750

PHASE	NAME	RANGE (K)	
S1	SOLID	298.0 - 904.0	D H TRANS (904.00 K) = 4.750 (KCAL)
L1	LIQUID	904.0 - 1860.0	
G1	GAS	298.0 - 800.0	
G1	GAS	800.0 - 2000.0	

CP = A + 1.0E-3*B*T(K) + 1.0E5*C*T(K)**-2 + 1.0E-6*D*T(K)**2

PHASE	D H298 (KCAL)	S298 (CAL/K)	DENSITY (G/CM**3)	A	B	C	D
					(CAL/K)		
S1	0.0	10.880	6.684	7.283	3.677	0.478	4.287
L1	4.190	14.988	6.684	7.500	0.0	0.0	0.0
G1	63.230	43.053	IDEAL	4.968	0.0	0.0	0.0
G1	62.973	42.407	IDEAL	4.261	0.456	2.313	0.0

REFERENCE: "THERMOCHEMICAL PROPERTIES OF INORGANIC SUBSTANCES",
I. BARIN, O. KNACKE, AND O. KUBASCHEWSKI,
SPRINGER-VERLAG, BERLIN, 1977.

PRESS "RETURN" WHEN READY FOR DISPLAY
?

FORMULA: O2

NAME: OXYGEN

FORMULA WEIGHT: 31.999

PHASE	NAME	RANGE (K)
G1	GAS	298.0 - 3000.0

CP = A + 1.0E-3*B*T(K) + 1.0E5*C*T(K)**-2 + 1.0E-6*D*T(K)**2

PHASE	D H298 (KCAL)	S298 (CAL/K)	DENSITY (G/CM**3)	A	B	C (CAL/K)	D
G1	0.0	49.005	IDEAL	7.160	1.000	-0.400	0.0

REFERENCE: "THERMOCHEMICAL PROPERTIES OF INORGANIC SUBSTANCES",
I. BARIN, O. KNACKE, AND O. KUBASCHEWSKI,
SPRINGER-VERLAG, BERLIN, 1977.

DO YOU WISH TO FIND (1) PARTICULAR COMPOUND(S), OR (2) GROUP OF COMPOUNDS?
?

FORMULA: CU2O

NAME: COPPER(I) OXIDE

FORMULA WEIGHT: 143.091

PHASE	NAME	RANGE (K)	
S1	CUPRITE	298.0 - 1509.0	D H TRANS (1509.00 K) - 13.580 (KCAL)
L1	LIQUID	1509.0 - 2000.0	

CP = A + 1.0E-3*B*T(K) + 1.0E5*C*T(K)**-2 + 1.0E-6*D*T(K)**2

PHASE	D H298 (KCAL)	S298 (CAL/K)	DENSITY (G/CM**3)	A	B	C	D
					(CAL/K)		
S1	-40.700	22.210	6.000	13.520	7.000	0.0	0.0
L1	-32.151	22.691	6.000	24.000	0.0	0.0	0.0

REFERENCE: "THERMOCHEMICAL PROPERTIES OF INORGANIC SUBSTANCES",
I. BARIN, O. KNACKE, AND O. KUBASCHEWSKI,
SPRINGER-VERLAG, BERLIN, 1977.

PRESS "RETURN" WHEN READY FOR DISPLAY
?

FORMULA: BI2O3

NAME: BISMUTH TRIOXIDE

FORMULA WEIGHT: 465.959

PHASE	NAME	RANGE (K)	
S1	SOLID-A	298.0 - 978.0	D H TRANS (978.00 K) = 13.600 (KCAL)
S2	SOLID-B	978.0 - 1097.0	D H TRANS (1097.00 K) = 14.300 (KCAL)
L1	LIQUID	1097.0 - 1800.0	

CP = A + 1.0E-3*B*T(K) + 1.0E5*C*T(K)**-2 + 1.0E-6*D*T(K)**2

PHASE	D H298 (KCAL)	S298 (CAL/K)	DENSITY (G/CM**3)	A	B	C	D
				(CAL/K)			
S1	-136.400	36.200	8.200	24.740	8.000	0.0	0.0
S2	-126.305	43.357	8.550	35.000	0.0	0.0	0.0
L1	-113.203	54.439	8.550	36.500	0.0	0.0	0.0

REFERENCE: "THERMOCHEMICAL PROPERTIES OF INORGANIC SUBSTANCES",
I. BARIN, O. KNACKE, AND O. KUBASCHEWSKI,
SPRINGER-VERLAG, BERLIN, 1977.

PRESS "RETURN" WHEN READY FOR DISPLAY
?

FORMULA: PB*O

NAME: LEAD MONOXIDE

FORMULA WEIGHT: 223.199

PHASE	NAME	RANGE (K)	
S1	LITHARGE	298.0 - 762.0	D H TRANS (762.00 K) = 0.394 (KCAL)
S2	MASSICOT	762.0 - 1158.0	D H TRANS (1158.00 K) = 6.570 (KCAL)
L1	LIQUID	1158.0 - 1400.0	
G1	GAS	298.0 - 2000.0	

CP = A + 1.0E-3*B*T(K) + 1.0E5*C*T(K)**-2 + 1.0E-6*D*T(K)**2

PHASE	D H298 (KCAL)	S298 (CAL/K)	DENSITY (G/CM**3)	A	B	C	D
				---------- (CAL/K) ----------			
S1	-52.410	15.600	9.530	9.908	3.664	0.0	0.0
S2	-52.458	15.232	8.000	10.712	3.946	0.0	0.0
L1	-47.439	17.954	8.000	15.388	0.0	0.0	0.0
G1	11.480	57.346	IDEAL	8.731	0.186	0.935	0.0

REFERENCE: "THERMOCHEMICAL PROPERTIES OF INORGANIC SUBSTANCES",
I. BARIN, O. KNACKE, AND O. KUBASCHEWSKI,
SPRINGER-VERLAG, BERLIN, 1977.

PRESS "RETURN" WHEN READY FOR DISPLAY
?

FORMULA: AS203

NAME: ARSENIC TRIOXIDE

FORMULA WEIGHT: 197.841

PHASE	NAME	RANGE (K)	
S1	CLAUDETITE	298.0 - 582.0	D H TRANS (582.00 K) = 4.400 (KCAL)
L1	LIQUID	582.0 - 734.0	
S2	ARSENOLITE	298.0 - 548.0	

CP = A + 1.0E-3*B*T(K) + 1.0E5*C*T(K)** 2 + 1.0E 6*D*T(K)**2

PHASE	D H298 (KCAL)	S298 (CAL/K)	DENSITY (G/CM**3)	A	B	C	D
					(CAL/K)		
S1	-156.160	29.330	4.150	14.300	42.000	0.0	0.0
L1	-152.815	33.963	4.150	36.500	0.0	0.0	0.0
S2	-157.000	25.980	3.865	30.370	48.600	0.0	0.0

REFERENCE: "THERMOCHEMICAL PROPERTIES OF INORGANIC SUBSTANCES",
I. BARIN, O. KNACKE, AND O. KUBASCHEWSKI,
SPRINGER-VERLAG, BERLIN, 1977.

PRESS "RETURN" WHEN READY FOR DISPLAY

FORMULA: SB2O3

NAME: ANTIMONY OXIDE

FORMULA WEIGHT: 291.498

PHASE	NAME	RANGE (K)	
S1	SENARMO.TE	298.0 - 845.0	D H TRANS (845.00 K) = 1.600 (KCAL)
S2	VALEN.ITE	845.0 - 929.0	D H TRANS (929.00 K) = 13.150 (KCAL)
L1	LIQUID	929.0 - 1729.0	

CP = A + 1.0E-3*B*T(K) + 1.0E5*C*T(K)**-2 + 1.0E-6*D*T(K)**2

PHASE	D H298 (KCAL)	S298 (CAL/K)	DENSITY (G/CM**3)	A	B	C	D
					(CAL/K)		
S1	-171.000	31.700	5.200	22.000	15.800	0.0	0.0
S2	-169.400	33.593	5.670	22.000	15.800	0.0	0.0
L1	-159.912	40.100	5.670	37.500	0.0	0.0	0.0

REFERENCE: "THERMOCHEMICAL PROPERTIES OF INORGANIC SUBSTANCES",
I. BARIN, O. KNACKE, AND O. KUBASCHEWSKI,
SPRINGER-VERLAG, BERLIN, 1977.

DO YOU WISH TO FIND (1) PARTICULAR COMPOUND(S), OR (2) GROUP OF COMPOUNDS?
?